
Doctoral Dissertations

Student Theses and Dissertations

1968

An experimental determination of the homogeneous nucleation rate of water vapor in argon and helium

Louis Benton Allen

Follow this and additional works at: https://scholarsmine.mst.edu/doctoral_dissertations



Part of the [Physics Commons](#)

Department: Physics

Recommended Citation

Allen, Louis Benton, "An experimental determination of the homogeneous nucleation rate of water vapor in argon and helium" (1968). *Doctoral Dissertations*. 2126.

https://scholarsmine.mst.edu/doctoral_dissertations/2126

This thesis is brought to you by Scholars' Mine, a service of the Missouri S&T Library and Learning Resources. This work is protected by U. S. Copyright Law. Unauthorized use including reproduction for redistribution requires the permission of the copyright holder. For more information, please contact scholarsmine@mst.edu.

AN EXPERIMENTAL DETERMINATION OF THE
HOMOGENEOUS NUCLEATION RATE OF WATER VAPOR
IN ARGON AND HELIUM

by

LOUIS BENTON ALLEN, JR.

A DISSERTATION

Presented to the Faculty of the Graduate School of the
UNIVERSITY OF MISSOURI AT ROLLA

In Partial Fulfillment of the Requirements for the Degree
DOCTOR OF PHILOSOPHY

in

Physics

1968

James L. Kasser, Jr.

Grant L. Dackow

Charles E. Tuttle

Charles E. McFarland

J. Ruess

Amos W. Gund

Don C. Hopkins

PLEASE NOTE: Not original
copy. Several pages are
blurred and indistinct.
Filmed in the best possible
way.

UNIVERSITY MICROFILMS

AN EXPERIMENTAL DETERMINATION OF THE
HOMOGENEOUS NUCLEATION RATE OF WATER VAPOR
IN ARGON AND HELIUM

An Abstract of a Dissertation
Presented to
the Faculty of the Graduate School
University of Missouri at Rolla

In Partial Fulfillment
of the Requirements for the Degree
Doctor of Philosophy

by
Louis Benton Allen, Jr.

May 1968

AN EXPERIMENTAL DETERMINATION OF THE
HOMOGENEOUS NUCLEATION RATE OF WATER VAPOR
IN ARGON AND HELIUM

Abstract

An expansion type cloud chamber was used to measure the nucleation rate of water vapor in an atmosphere of helium and argon. A careful study was made of the thermodynamic characteristics during the expansion so that the nucleation data could be interpreted with reasonable accuracy and consistency.

A fine wire thermocouple was used to measure the gas temperature during the course of an isentropic expansion in the dry chamber. When the finite heat capacity of the thermocouple is accounted for, it is found that there is almost perfect agreement with the temperature calculated from the equation of state and the pressure measurement. This establishes the expansion cloud chamber as the instrument with the most accurately known thermodynamic characteristics and the one where the supersaturation may be calculated with the greatest precision.

The homogeneous nucleation rate of water vapor in a helium atmosphere was measured as a function of temperature, supersaturation and sensitive time. It was found that there exists a form of heterogeneous nucleation occurring above the *ion limit* at about the *critical supersaturation* predicted by the classical Becker-Doring theory for homogeneous nucleation. This form of heterogeneous nucleation appears to occur upon chemically bonded centers whose concentration is very low and depends upon the vapor pressure before the expansion. The consistency of the number of these nucleating centers indicates that they may be a

neutral product of the action of natural radioactivity and cosmic rays.

A semiphenomenological theory was developed along the lines of the classical theory but which includes the chemical bond energy of the heterogeneous nucleating center. The *theory* predicts a different temperature dependence for the heterogeneous and homogeneous nucleation rates and at least qualitatively explains the essential features of the experimental data.

A considerable disparity in the temperature dependence of the critical supersaturation limit has existed for many years. The variation in the temperature dependence with nucleation rate as determined by the author's data shows: (a) that a large part of the disparity is due mainly to the interpretation of the experiments and (b) that the different temperature dependence of the heterogeneous and homogeneous nucleation rates is responsible for the different temperature dependences reported by the various experimenters.

It was definitely established that the nucleation rate of water vapor is higher in an argon atmosphere than in a helium atmosphere. This may be due to a disruption factor related to the higher velocity of the *light* helium atoms. It is, however, more likely due to the hydration of the argon atom into the critical cluster with a resultant increased stability in the critical clusters.

AN EXPERIMENTAL DETERMINATION OF THE
HOMOGENEOUS NUCLEATION RATE OF WATER VAPOR
IN ARGON AND HELIUM

A Dissertation
Presented to
the Faculty of the Graduate School
University of Missouri at Rolla

In Partial Fulfillment
of the Requirements for the Degree
Doctor of Philosophy

by

Louis Benton Allen, Jr.

May 1968

James L. Kassner, Jr., Dissertation Supervisor

ACKNOWLEDGMENTS

The author would like to express his gratitude to Dr. James L. Kassner, Jr., Professor Physics, for his advice and assistance during the course of this research.

Thanks are also due to the author's co-researchers, John Carstens, Micheal Eastburn, Theodore Moore, Raymond Schmitt, Micheal Vietti, Daniel White and Paul Yue. Especial thanks are due Arthur Piermann, Ronald Dawbarn and Donald Packwood who in the course of this research willingly gave advice, encouragement and labor beyond the call of duty. Thanks are also due to the many other students, both graduate and undergraduate who provided vital assistance at one time or another.

The author is especially grateful to the Computer Science Center for allowing free use of the computer facilities. The author also thanks Lee Anderson for his fine machine work.

The author thanks his parents for converting much of the raw data to usable form. Especial thanks are due to the author's wife, Barbara, for the continued encouragement during all our years in school. She assisted in nearly all of the data reduction and preparation of this manuscript.

The author is indebted to the Department of Health, Education and Welfare and the National Science Foundation for support during most of his program.

TABLE OF CONTENTS

	PAGE
ABSTRACT	ii
ACKNOWLEDGMENTS	v
LIST OF FIGURES	ix
LIST OF TABLES	xii
LIST OF PLATES	xiii
CHAPTER	
I. STATEMENT OF THE PROBLEM	1
1-1. Instruments for measuring the nucleation rate.	3
II. EXPERIMENTAL TECHNIQUE	8
2-1. Temperature control.	8
2-2. Pressure regulation.	12
2-3. The pressure measuring system.	15
2-4. Pressure calibration.	17
2-5. Photographic technique.	21
2-5-1. Film and development.	30
2-6. The mechanical Brake.	32
2-7. Program board.	32
2-8. Purification of the water.	34
2-9. Preparation of the chamber.	46
2-10. The cloud chamber program.	47
III. CLOUD CHAMBER THERMODYNAMICS	50
3-1. Measuring temperature directly.	52
3-2. Reliability of volume measurements.	52
3-3. Method of Richarz.	56
3-4. Temperature-entropy diagram method.	57

CHAPTER	PAGE
3-5. Comparison of methods of temperature determination.	58
3-6. Experimental test of equations of state and measuring techniques.	62
3-6-1. Obtaining a pure atmosphere.	64
3-7. Thermal characteristics of fine wire thermocouples.	69
IV. NUCLEATION MEASUREMENTS	78
4-1. Theory.	90
V. DROPLET GROWTH	99
5-1. Droplet growth equations.	101
5-2. Solution of the droplet growth equations.	108
5-3. Dead space calculation.	109
5-4. The computer solution.	111
VI. SUMMARY	119
BIBLIOGRAPHY	122
APPENDIX	
I. VARIATION OF PHYSICAL PARAMETERS	127
I-1. Equilibrium vapor pressure of water.	127
I-2. Surface tension of water.	127
I-3. Latent heat of vaporization of water.	130
I-4. Heat capacity and compressibility of water vapor.	130
I-5. Thermal conductivity of Helium.	135
I-6. Heat capacity and compressibility of Helium, Argon, Nitrogen and Air.	135
I-7. Diffusion coefficient for water vapor in helium	141

APPENDIX	PAGE
II. COMPUTER SOLUTION OF THE HEAT FLOW EQUATION FOR A CYLINDRICAL WIRE	142
II-1. Computer program for calculation of the thermal lag of the thermocouple.	148
III. COMPUTER SOLUTION OF THE DROPLET GROWTH EQUATIONS. .	151
IV. NUCLEATION DATA	157
VITA	195

LIST OF FIGURES

FIGURE		PAGE
1	The cloud chamber used for measuring homogeneous nucleation rates.	9
2	Arrangement of the cloud chamber heaters.	11
3	Block diagram of the pressure regulation system.	14
4	Block diagram of the pressure measuring system.	16
5	Sample of visicorder data. Galvanometer sensitivity 9.0mm/in, chart speed 10in/sec.	18
6	Sample of visicorder data. Galvanometer sensitivity 9.0mm/in, chart speed 40in/sec.	19
7	Sample of visicorder data. Galvanometer sensitivity 9.0mm/in, chart speed 40in/sec.	20
8	Flash tube light source.	22
9	Lamp number 1: collimated July 18, 1967.	23
10	Lamp number 2: collimated July 19, 1967.	24
11	First stage still showing method of continuous filling	37
12	Method of rinsing glassware. The flask is rinsed with pure water from condensing steam.	39
13	The steam generator.	41
14	Third stage still.	44
15	Typical cloud chamber cycle.	48
16	Creation of supersaturation in helium and water vapor by means of an adiabatic expansion.	51
17	Temperature diffusion profiles in a finite cylindrical cloud chamber.	54
18	Vapor diffusion profiles in a finite cylindrical cloud chamber.	55
19	Determination of the true temperature from the temperature-pressure-entropy diagram.	60
20	Determination of the true temperature by the entropy method.	61

FIGURE		PAGE
21	Thermocouple used for measuring the gas temperature.	66
22	The cloud chamber used for measuring gas temperature with a thermocouple.	67
23	Block diagram of the temperature measuring system. .	70
24	Measured temperature and pressure in dry argon.	75
25	Temperature difference for the expansion shown in Fig. 24.	76
26	Data of Israel and Nix.	77
27	Comparison of the nucleation rate in argon and helium.	79
28	The arrangement of hydrogen bonds for twenty water molecules in a dodecahedral configuration.	81
29	The arrangement of hydrogen bonds for twenty-four water molecules in a tetrakaidecahedral configuration.	81
30	Data of Parungo and Lodge.	82
31	Number of droplets nucleated as a function of peak supersaturation.	83
32	Data of Schuster.	85
33	Temperature dependence of the nucleation rate. . . .	86
34	Nucleation rate as a function of time.	88
35	Gibbs free energy vs. radius.	92
36	Distribution of clusters.	94
37	Comparison of homogeneous and heterogeneous nucleation rates.	97
38	Choosing the radius of the impermeable sphere. . . .	104
39	Pressure vs. time.	112
40	Temperature vs. time for the expansion of Fig. 39. .	113
41	Supersaturation vs. time for the expansion of Fig. 39	114

FIGURE		PAGE
42	Radius vs. time for the expansion of Fig. 39.	115
43	Number vs. radius for the expansion of Fig. 39.	116
44	Vapor pressure vs. time for the expansion of Fig. 39.	117
45	Dead space for the expansion of Fig. 39.	118
46	Equilibrium vapor pressure of water.	128
47	Surface tension of water.	129
48	Latent heat of vaporization of water.	131
49	Heat capacity of water vapor.	133
50	Heat capacity of water vapor.	134
51	Compressibility of water vapor.	136
52	Thermal conductivity of Helium.	137
53	Mesh used for thermocouple heat flow calculation.	145
54	Temperature profile around the thermocouple.	147

LIST OF TABLES

TABLE		PAGE
I	Power Input to Cloud Chamber Heaters	11
II	The heat capacity of water vapor	132
III	Compressibility, heat capacity and adiabatic constant of Argon.	138
IV	Compressibility, heat capacity and adiabatic constant of nitrogen.	159
V	Compressibility, heat capacity and adiabatic constant of air.	140
VI	Possible values of h and k for Argon	144
VII	Output of thermocouple heat flow computer program	150
VIII	Output of the droplet growth computer program	156
IX	Helium data	157
X	Argon data	190

LIST OF PLATES

PLATE		PAGE
1	Grid used for calibrating the camera magnification.	26
2	Nucleation.	27
3	Nucleation.	28
4	Diffraction from small droplets.	29
5	Static.	31
6	Program board.	33
7	First stage still.	38
8	Corning still.	43
9	Third stage still.	45

CHAPTER I

STATEMENT OF THE PROBLEM

Man has long been studying the atmosphere, yet it is only in the last few years that technology has advanced to the point where a true understanding of atmospheric processes is possible. This understanding must be turned to useful ends if we are ever to forget the fear of storms, make the deserts bloom or to continue to have clean air to breathe. Of all the problems facing atmospheric scientists, perhaps the most fascinating is that of the action of water vapor in the atmosphere. Water vapor content determines the stability of atmospheric layers and exerts control on the energy balance in the atmosphere¹. The details of the processes by which the size distribution of droplets in a cloud changes with time is not well understood.^{2,3}

Before an understanding of complex processes may be attained, the most elementary and basic processes must be comprehended. Nucleation, the formation of new droplets, is not the simple process that it was once thought to be. Nucleation on particulate matter is a form of heterogeneous nucleation. Atmospheric nuclei serve to lower the energy barrier for condensation. Ions also serve to reduce the free energy of formation of clusters. In the absence of condensation nuclei and ions, droplets begin to form as a result of chance fluctuations at a supersaturation of 4.8 and higher. The latter has been termed homogeneous nucleation. Early experimental results,^{4,5,6,7,8} observing the so-called critical limit for heterogeneous nucleation

on smoke particles, dust particles, ions and homogeneous nucleation, showed that at least a qualitative explanation was provided by classical theory⁹. Classical theory is based on the idea that a barrier to nucleation exists and that statistical fluctuations carry the embryos over the barrier. A critical size of embryo is associated with the peak height of the free energy barrier. It now appears that a full understanding of homogeneous nucleation is required before the various forms of heterogeneous nucleation may be comprehended. Heterogeneous nucleation, which is the dominant form of nucleation found in nature, encompasses the features of homogeneous nucleation with the addition of extra interfacial energies which greatly complicate the problem.¹⁰

The semiphenomenological classical theory, developed by Farkas¹¹, Becker and Doring¹², Zeldovich¹³, Frenkel¹⁴ and others for the homogeneous nucleation of liquid drops, seemed at first to predict nucleation rates which showed good agreement with experiment. More definitive experimental data on the nucleation of water drops from the vapor by various groups, namely Volmer and Flood¹⁵ and Powell¹⁶, exhibit self consistency within themselves but display considerable disparity when intercompared. Attempts to compare results comprehensively^{17,18,19,20} have only emphasized the peculiar nature of homogeneous nucleation in water vapor.

The extent of renewed interest in nucleation phenomena is evidenced by the amount of recent theoretical activity²¹⁻³⁵. This renewed interest also indicates a general lack of confidence in the classical nucleation theory. Moreover, there has been a resurgence of interest in the experimental measurement of homogeneous nucleation rates.^{19,20,36-40}

Most experimental studies have observed the critical supersaturation limit only. The critical supersaturation limit is usually taken as that point where noticeable droplet formation occurs in the expansion chamber. This may be for nucleation rates of from one to one million droplets per cubic centimeter per second, depending upon the details of the observation system and the sensitive time of the apparatus. Due to the nature of most of the experiments where sensitive times and droplet densities are estimated only to an order of magnitude, a given experiment may be interpreted differently by different authors.^{20,36} Since both the estimates of sensitive times and drop densities are usually consistent for a given investigator, the temperature dependence is adequately determined but the nucleation rate to which it belongs is somewhat ambiguous.

Definitive experimental work must be done so that a comprehensive picture of the homogeneous nucleation process may be constructed for comparison with theory. It is the purpose of this study to provide a set of data overlapping that of several other experimenters and to provide the most extensive measurements possible, utilizing the capabilities of the highly automated and instrumented cloud chamber of this laboratory. The investigation undertaken by the author will experimentally determine the homogeneous nucleation rate as a function of sensitive time, supersaturation and temperature.

1-1. Instruments for measuring the nucleation rate. Nucleation theory specifically predicts the rate of formation of droplets as a function of supersaturation and temperature. It is the function of experimentation to verify the essential features of the theory. The nucleation rate is such an exceedingly steep function of increasing supersaturation

that, in a rather crude manner of speaking, it exhibits a supersaturation at which the nucleation rate first becomes observable. This has become known as the *critical supersaturation*. Early work directed toward the confirmation of nucleation theory was done with the expansion cloud chamber which was used to measure the aforementioned critical supersaturation. This technique involved an estimation of droplet concentration. Moreover, it was necessary to estimate the nucleation period or sensitive time of the cloud chamber in order to convert the observations to a nucleation rate. Little advance in technique has been reported until recent years. It is improbable that any major developments in nucleation theory will evolve until more definitive experimental measurements are forthcoming. It is to this end that work in this Laboratory has been directed.

Several experimental techniques are useful for studying nucleation phenomena. Each possesses its own characteristic advantages and disadvantages. All achieve a state of supersaturation either by adiabatic cooling or by nonisothermal vapor diffusion. The expansion cloud chamber employs the nonisothermal diffusion of vapor to produce supersaturation.

Nucleation phenomena have been studied by means of expansion nozzle techniques by Ruedy⁴¹, Wegener⁴² and Pouring⁴³. The nozzle method has the advantage of providing a steady state observation. Pressure is measured as a function of position in the flow stream. Deviations from the characteristic isentropic flow indicate the presence of condensation. The complete removal of dust and ions is impractical, but under conditions of rapid production of the condition of supersaturation such high nucleation rates are achieved that any contribution due to heterogeneous nucleation is obscured. Because very high nucleation rates

are associated with very small critical cluster sizes, it is improbable that nozzle experiments will be of value in evaluating a nucleation theory which is essentially a precatastropic theory. Moreover, it is likely that the liquid drop model breaks down for such small cluster sizes.

The diffusion chamber was invented in 1939 by Langsdorf⁴⁴, but it was not fully developed until the early 1950's.^{45,46,47} The gas in the upper part of the chamber must be less dense than the gas in the lower part of the chamber in order to prevent convection currents. Most thermal diffusion chambers operate with the upper plate at the higher temperature. Franc and Herz⁴⁸ first described an inverted diffusion cloud chamber, a chamber with water vapor diffusing up from the bottom. A very light gas such as hydrogen or helium must be used for the atmosphere in order to maintain the stability of the system. Katz and Ostermier³⁹ have used the inverted diffusion chamber to measure the temperature dependence of the critical supersaturation ratio for a number of vapors. Since the determination of the supersaturation is dependent upon an accurate knowledge of the diffusion coefficients for the vapor through the non-condensable gas, they have resorted to measuring the diffusion coefficients over a wide range of temperatures themselves.

The primary advantage of the thermal diffusion chamber lies in the fact that it is a steady state device. However, the fact that the thermodynamic coordinates are changing continuously as a function of position between the parallel chamber plates presents a problem in the determination of the state of supersaturation. Moreover, only a thin layer of the chamber exists at a state of high supersaturation. The thermal diffusion chamber suffers from the disadvantage that it can

measure only very small nucleation rates or the so-called critical supersaturation. It is most useful for measuring the temperature dependence of the critical supersaturation.

The expansion cloud chamber is the oldest device used for measuring nucleation rates. It was highly developed by nuclear physicists for the detection of ionizing particles. Moreover, it has undergone additional development in this laboratory as a tool for investigating nucleation and condensation phenomena.⁴⁷⁻⁵² Extensive studies of the thermodynamic characteristics of the expansion cloud chamber in this laboratory and in other laboratories make it the best understood of all devices available for studying nucleation phenomena. It can yield more information than any of the above mentioned instruments.

Expansion cloud chamber experiments have been customarily designed to yield only a measurement of the critical supersaturation, this is the simplest experiment which can be performed. The definition of the critical supersaturation, as it is used by a given investigator, is obviously influenced by the geometry of the observation system. Droplet densities have either been estimated visually or determined by light scattering techniques. Nucleation rates are estimated by making an educated guess for the sensitive time of the chamber, i.e. that time during which the bulk of the nucleation occurs.

The major advances made in this laboratory are the continuous measurement of the pressure throughout the expansion and the development of techniques for maintaining almost complete control over the expansion cycle. With proper instrumentation and automation, the expansion cloud chamber has an overwhelming advantage over other experimental methods in that nucleation measurements may be undertaken as a function

of supersaturation, temperature and sensitive time. No other instrument has been used to measure the dependence of the nucleation rate upon either supersaturation or time. Such diversity of information makes it possible to distinguish more clearly between different types of nucleation schemes. For this reason, the expansion cloud chamber has been selected for this work.

CHAPTER II
EXPERIMENTAL TECHNIQUE

The cloud chamber used in this work was first put into operation in March, 1962 and has undergone continuous improvement since that time, Fig. 1. Great strides were made in regulating the temperature of the cloud chamber. A servo pressure regulation control system was developed which made possible more accurate control over the starting pressure, thereby insuring accurate saturation at the starting temperature. A mechanical brake was added to the piston guide for damping out piston oscillations during the expansion. A program board was installed to facilitate the interconnection of the programming circuitry to the operating devices such as valves, lights, recorder, etc. These improvements were initiated in whole or in part by the author and contributed substantially to the success of the measurements made during the course of this work.

2-1. Temperature control. Allard⁴⁹ used a top to bottom gradient of one Centigrade degree in order to eliminate condensation on the top glass and side walls of the cloud chamber. It was felt that such a large gradient should not be necessary and that a gradient of several hundredths of a degree should suffice. Packwood⁵⁰, Schmitt⁵¹, Dawbarn⁵², Smith⁵³ and White⁵⁴ all attempted to reduce the magnitude of the gradient without much success. Before the problem could be properly assessed, a set of thermocouples was constructed and mounted inside the cloud chamber. They were spaced one inch apart up the side wall and

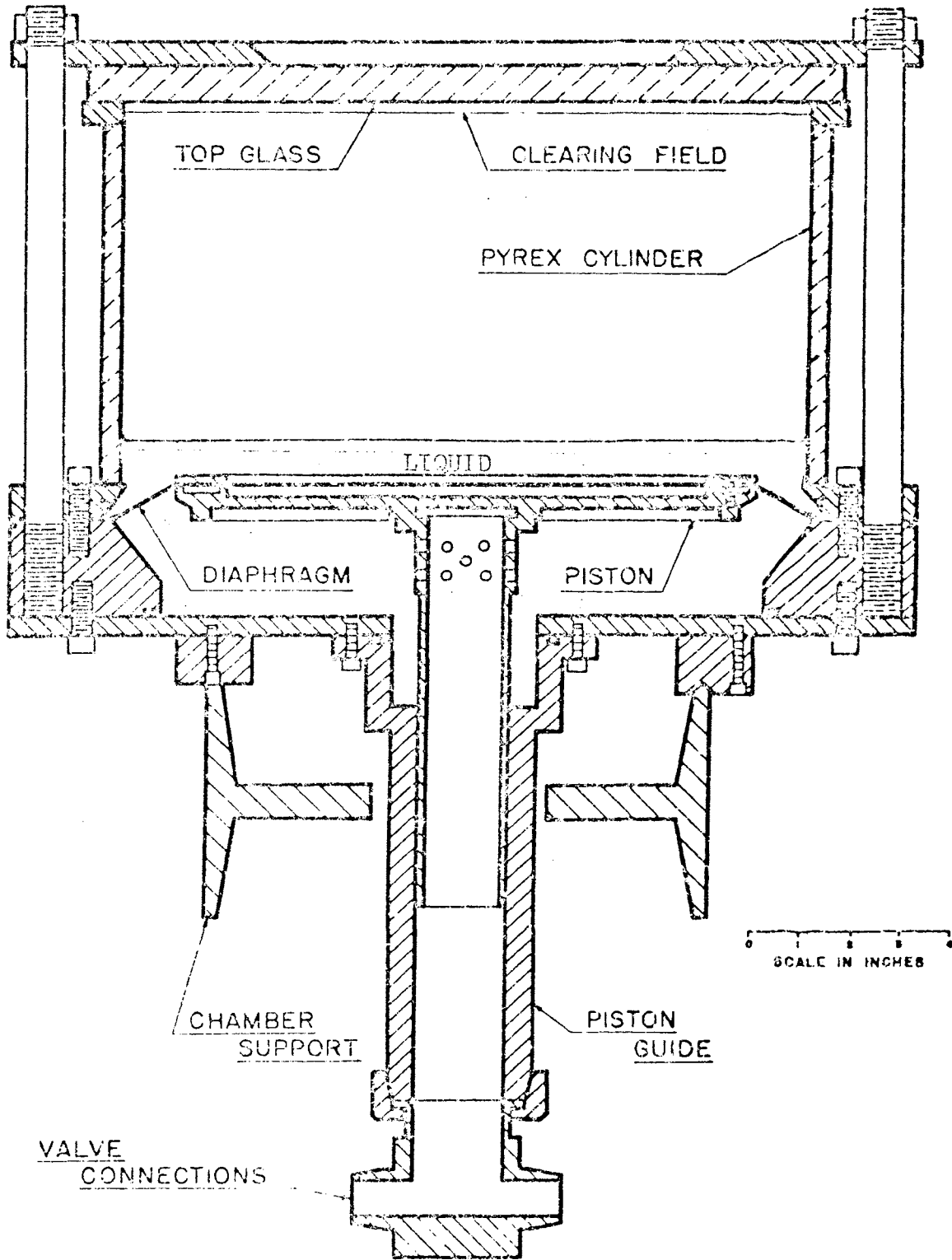


Fig. 1. The cloud chamber used for measuring homogeneous nucleation rates.

across the top. Comparison of temperatures on both sides of the top glass immediately indicated that there was more than one-half degree gradient through the glass. Moreover, about one-half degree difference in temperature existed between the center and the edge of the viewing window, see Fig. 2. The addition of another glass plate on top of the cloud chamber for added insulation did not remedy the problem. Fine heater wires were stretched across the viewing window for independent temperature control of the center of the top glass. One-half watt of heater power sufficed to eliminate the temperature variation across the top glass.

The vertical temperature gradient had to be reduced drastically. It was evident that the top half of the cylindrical wall was too cool. This allowed condensation to occur on the walls where the light beam from the flash lamps passed through the cylinder. This was very undesirable because the condensation scattered the light beam. Heater tapes were mounted just above the light beam. This tape nearly filled the space between the clearing field ring and the light beam. After a week of adjusting the voltages on the three side heaters and two top heaters, good temperature control of the interior chamber was achieved.

As the gradient was brought to less than one-tenth degree, uneven condensation occurred at various parts of the chamber top and sides. This indicated that there were gradients across the chamber which were not previously recognized. Before this problem was solved: (a) the convection currents from the air conditioner had to be completely baffled from the chamber by draping one-quarter inch rubber sheet around the chamber frame and associated plumbing, (b) extra foam rubber was added around each of the four sides of the chamber and (c) four separate

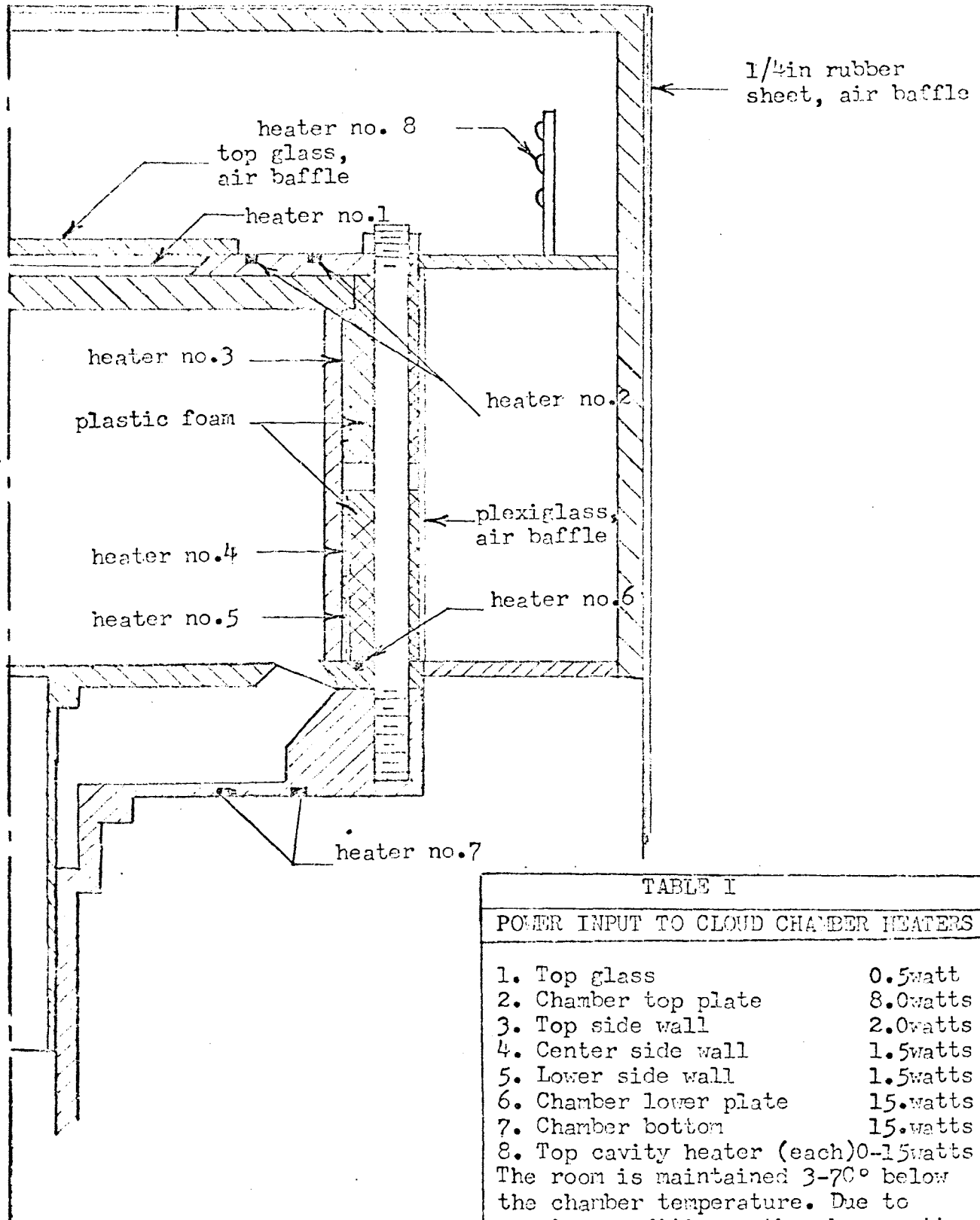


Fig. 2. Arrangement of the cloud chamber heaters.

heaters were added in the top cavity, one on each of the four sides. Temperature gradients across the top cavity due to the forced air convection currents from the room air conditioner are eliminated by individually adjusting the power input to each of the four heaters. Elimination of the cross gradients is best accomplished by lowering the gradient and allowing slight condensation to take place on the top glass and sides. Observation of the condensation tells the location of the cooler areas.

During the regular cycling of the chamber, the temperature of the bottom of the chamber drifted out of control. This was due to the heat pumping action of the cycle. Elimination of this problem consisted of installing new heaters in the aluminum plate under the piston and controlling the temperature of the air coming into the manifold system.

The temperature control during the periods of data taking was not quite as good as the temperature control during the time when the thermocouples were installed in the chamber. Temperature control did not prove dependable enough to use a gradient under 0.05°C and a gradient of about 0.1°C was finally used for convenience. The temperature of the central volume of the cloud chamber in which measurements were being made was therefore known to within the same accuracy as the water temperature, $\pm 0.05^{\circ}\text{C}$.

2-2. Pressure regulation. Leaks always occur in the plumbing under the cloud chamber. These leaks must be counteracted by letting excess air into the manifold system at a rate which exactly compensates for the leaks. Up to the time of this series of experiments, there had been no need for the initial pressure regulating system to be adjustable. The pressure regulator described by Allard consisted of a

mercury manometer with platinum wire contacts which controlled a regulator valve. This system was naturally oscillatory; the best regulation possible after careful adjustment gave pressure oscillations of about 2 mmHg.

In the new control system a pressure transducer takes the place of the mercury manometer and a servo motor attached to a variable orifice valve, Fig. 3, does the regulating. A trickle of air is continuously leaked into the manifold system as with the earlier system and the servo motor controls the valve opening so that the proper leak rate is established to maintain a constant pressure.

Some difficulty was encountered when trying to get the servo system to work. When the servo valve was allowed to pass by the completely "open position" and on to the completely "closed position" or vice versa, an oscillating condition occurred. With this arrangement control could only be established when the system pressure was nearly regulated beforehand. Installation of a clutch and stops at the fully opened and fully closed positions eliminated this problem so that the servo system could bring the pressure to regulation from an expansion or compression configuration very quickly without disrupting the sense of the servo control.

It was also found that the location of the pressure transducer controlling the servo motor is critical. It must be located in the same pressure line as the servo valve and be very close to the orifice in order to avoid pressure oscillations. The same biasing technique is used with this transducer as with the pressure transducer in the sensitive volume. The starting pressure may now be held to within one mmHg with practically any volume of trickle air leaking into the manifold

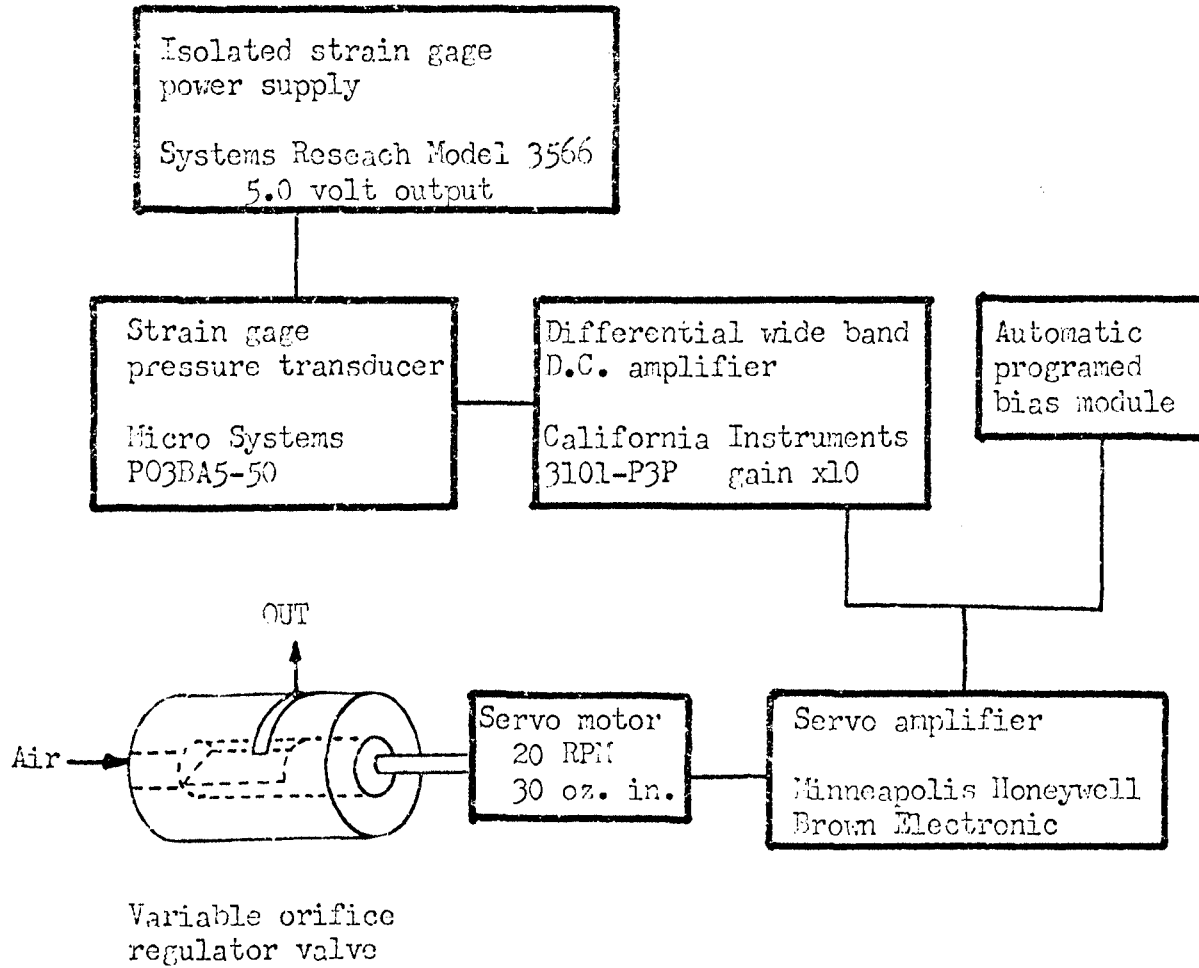


Fig. 3. Block diagram of the pressure regulation system.

system. Recovery is so good that recovery times of less than ten seconds are required to establish any given pressure. The regulating ability of this system seems to be limited only by the capability of the pressure transducer.

2-3. The pressure measuring system. The precision measurement of the pressure in the sensitive volume throughout the expansion is the most critical part of a nucleation experiment. If the supersaturation is to be determined within one percent accuracy, the pressure must be measured to within one mmHg. This requires much better resolution than can be obtained with an ordinary recording system. The stability of all components in the pressure measuring system must be of the order of 0.01 percent. The pressure measuring system employed in this work was essentially the same as that described by Packwood⁵⁰. A block diagram of the pressure measuring system is shown in Fig. 4.

The pressure transducer is a one-quarter inch diameter, flush diaphragm, strain gauge type pressure transducer. Its diaphragm is mounted nearly flush with the inside cylindrical wall of the sensitive volume. It reads absolute pressure. The transducer is excited by a highly isolated transducer power supply which possesses 0.1 micromicrofarad capacitance between its output and power line sides. This specification is necessary to keep the common mode signal to the California Instruments wide band D.C. amplifier at a low level. Triply shielded twisted pair lead wires are used to interconnect all the units. Three separate mutually insulated shields are necessary to keep the A.C. noise level to a minimum. It was also necessary to mount the amplifier and the isolated power supply as close to the pressure transducer as possible.

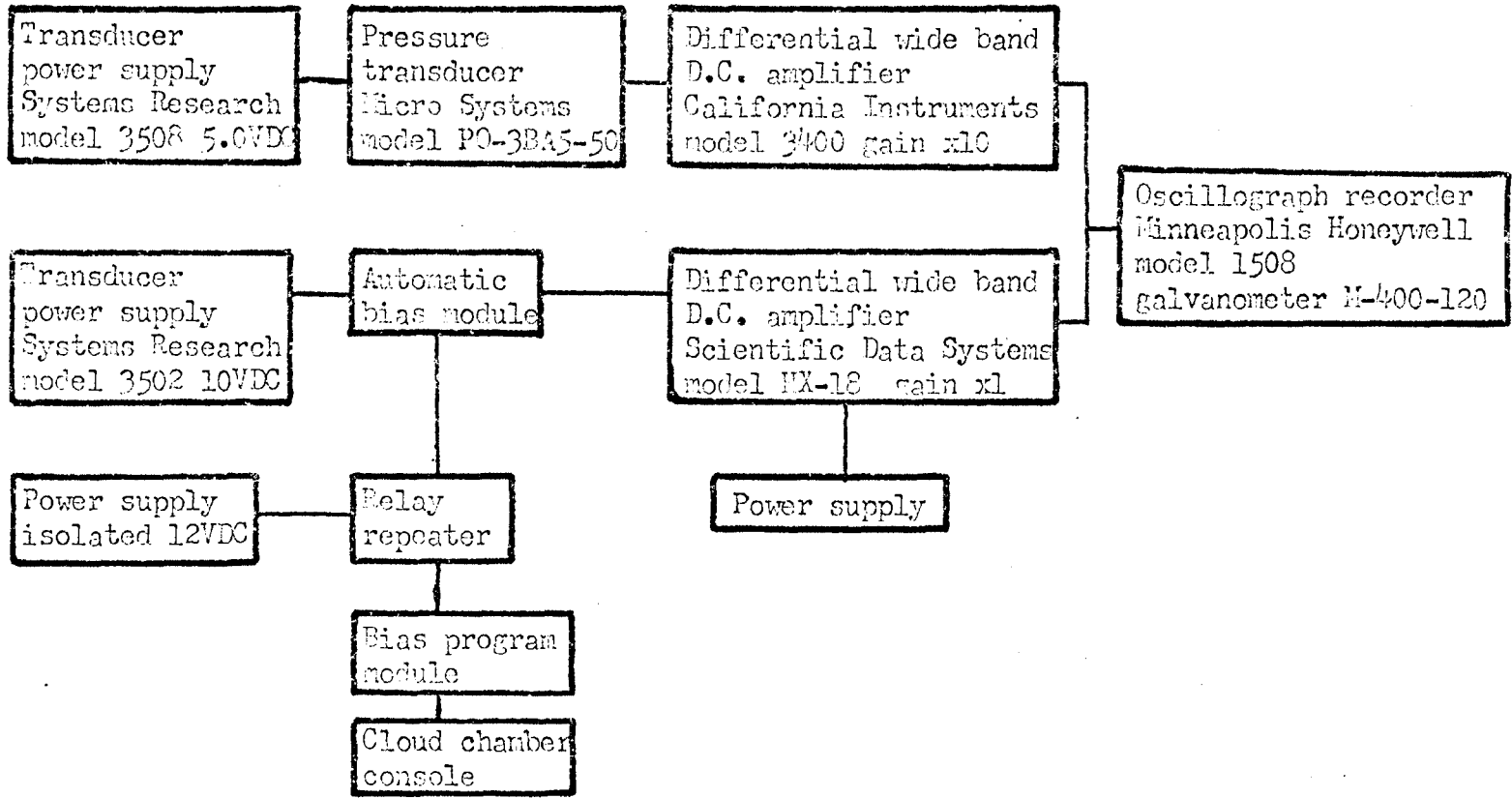


Fig. 4. Block diagram of the pressure measuring system.

In order to obtain the desired accuracy in the recorded pressure signal, a type of scale expansion system was employed. Approximately 1.2 volts D.C. signal emerges from the California Instruments amplifier. Most of this signal is biased out by a constant D.C. voltage from the automatic bias module, having a 0.01 ohm impedance. The remaining 40 millivolts signal is recorded by a light beam oscillograph. Four different bias levels are provided by the automatic bias module. The automatic bias module's circuitry maintains a high level of isolation from both power line and chassis ground. The peak to peak noise level in the recorded signal corresponds to about 0.5 mmHg. Figs. 5-7 show typical data output from the oscillogram.

2-4. Pressure calibration. Pressure calibration was greatly facilitated by the addition of a Texas Instruments Model 145 Pressure gage with a precision servo nulling readout. This type of gage uses a quartz spiral bourdon tube which exhibits no measureable hysteresis and retains its calibration indefinitely. The servo readout follows pressure changes automatically, allowing instant comparison of recorder and pressure gage readings. Hysteresis in the cloud chamber pressure transducer and in the recorder galvanometers presented a problem. The calibration of the pressure transducer had to be accomplished by approaching the desired calibration point in the same manner that the cloud chamber would reach that same point in a normal data taking cycle. Approximately the same magnitude of pressure excursion was used in the calibration procedure as in the data taking cycle. It is probable that some of the difficulties encountered by Allard⁴⁹ and Schmitt⁵¹ resulted from improper calibration procedure.

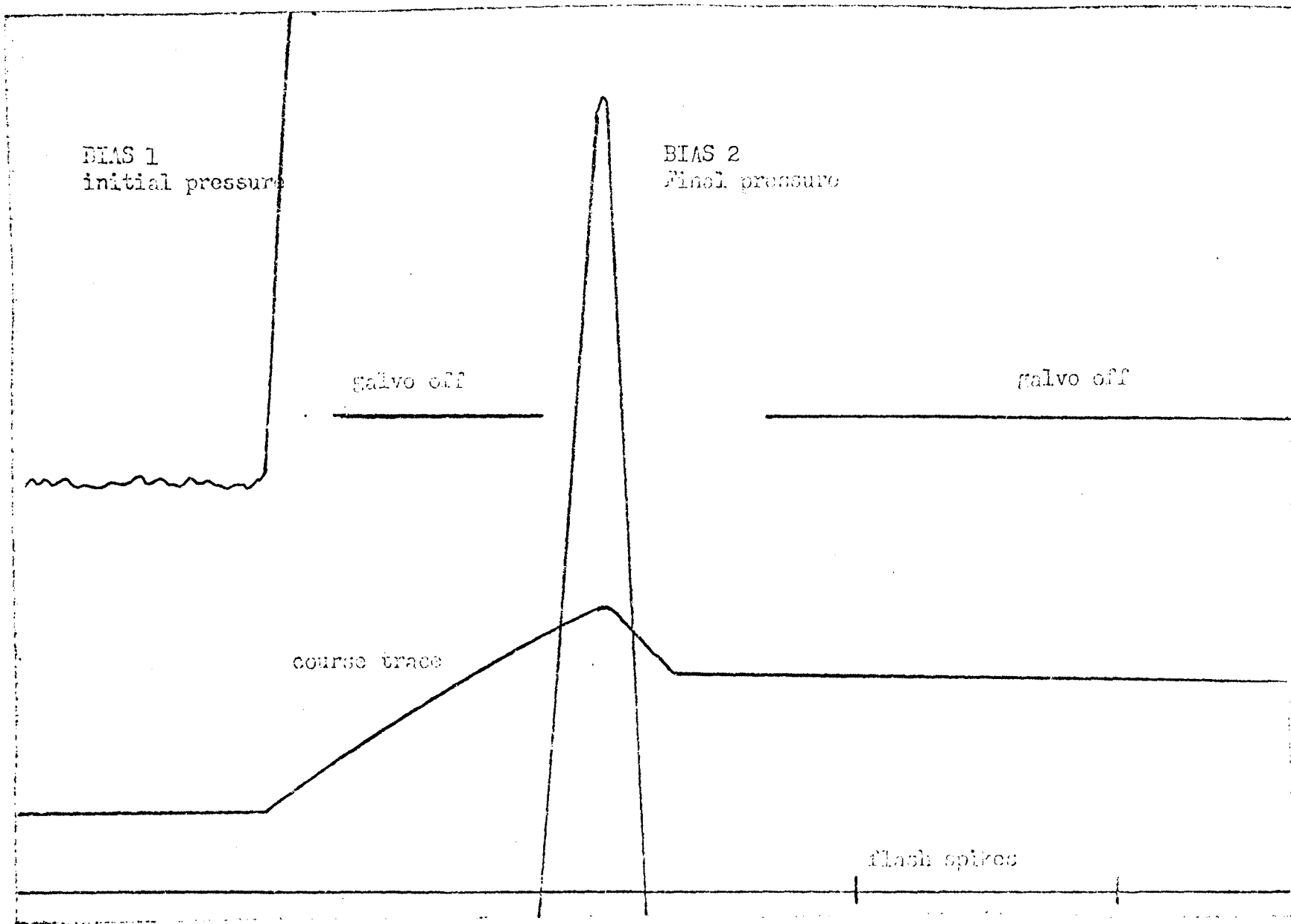


Fig. 5. Sample of visicorder data. Galvanometer sensitivity 9.0mm/in, chart speed 10in/sec.

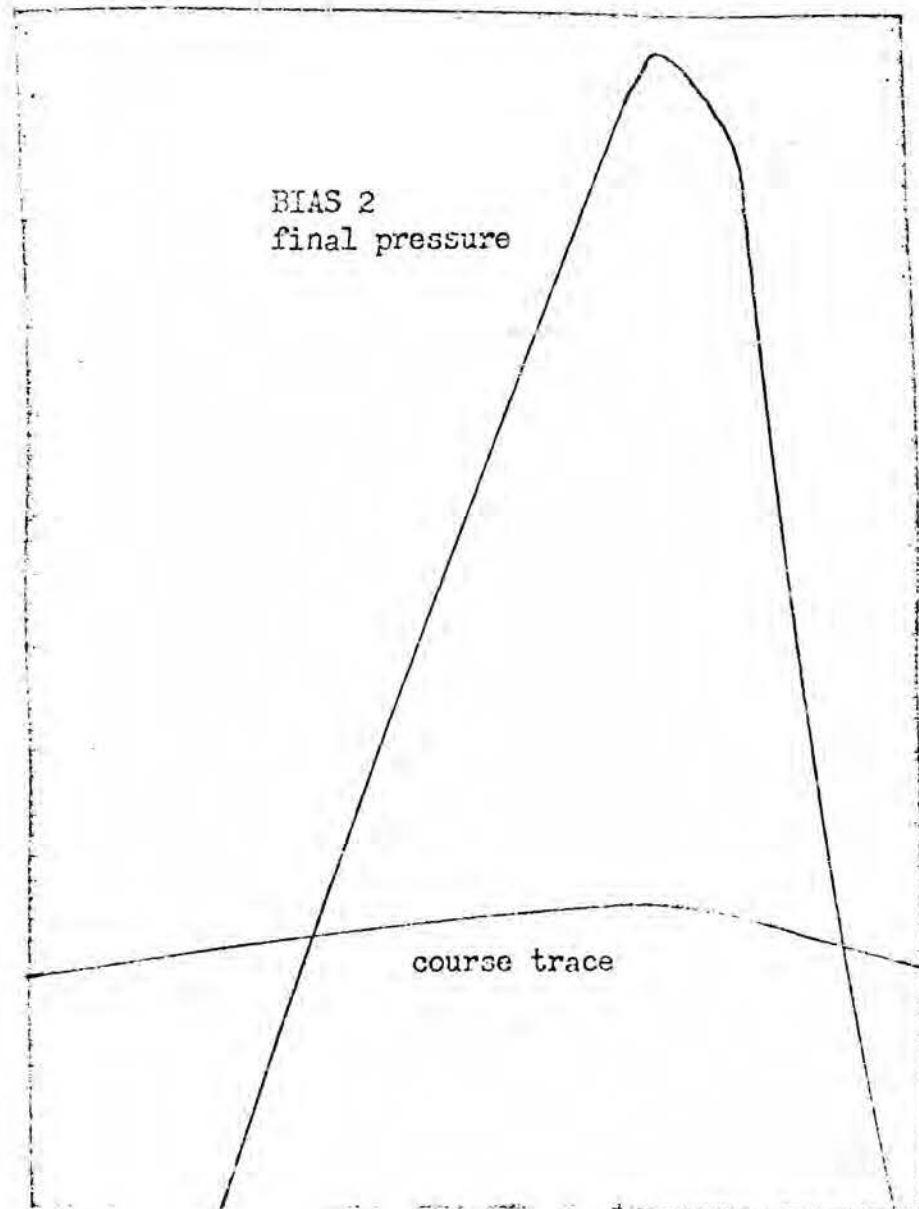
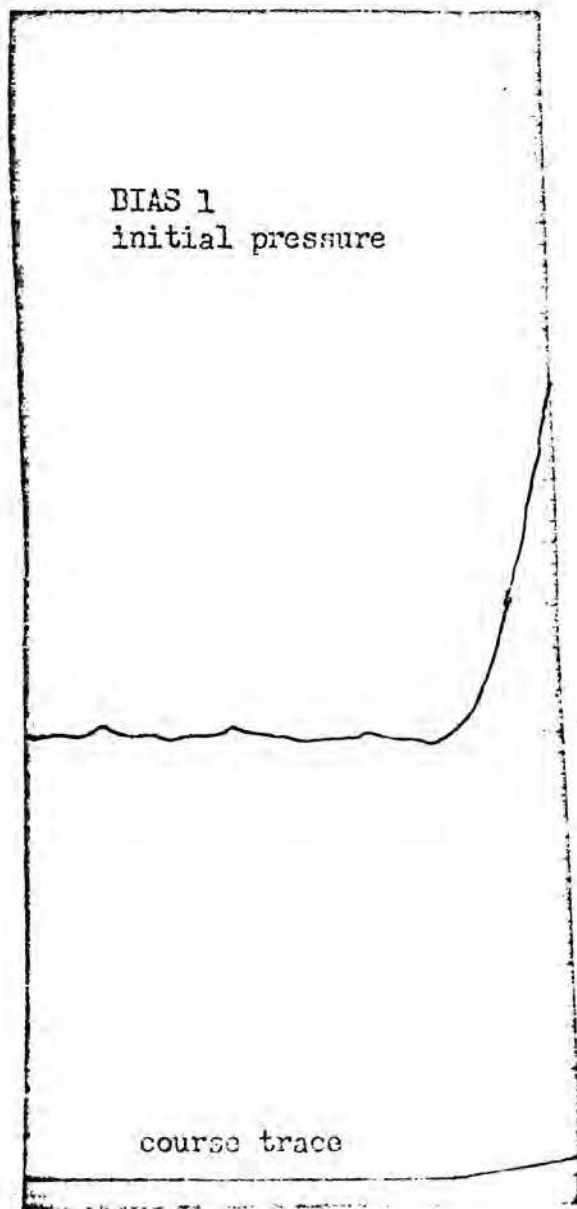


Fig. 6. Sample of visicorder data. Galvanometer sensitivity 9.0mm/in, chart speed 40in/sec.

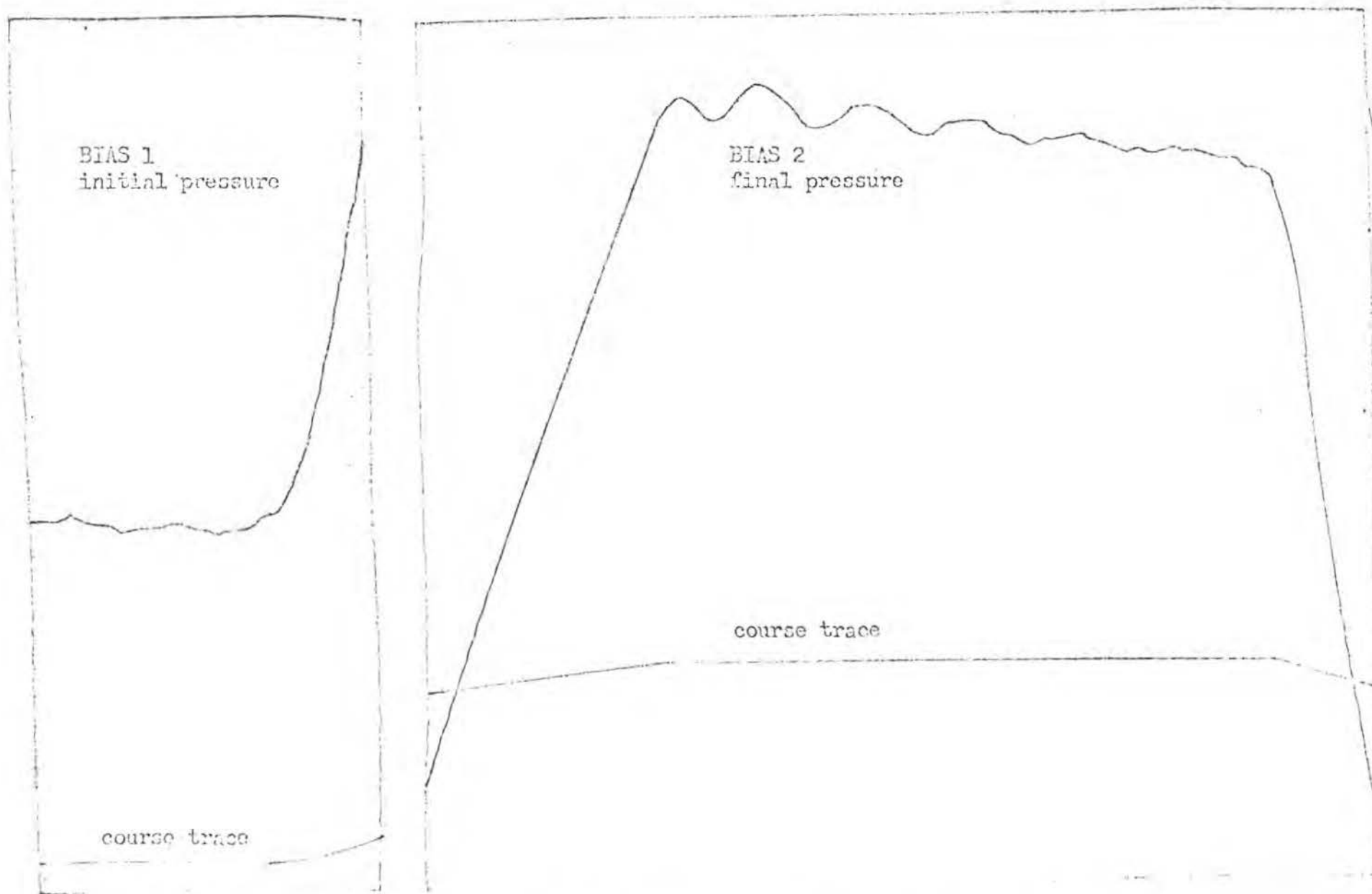


Fig. 7. Sample of visicorder data. Galvanometer sensitivity 9.0mm/in, chart speed 40in/sec.

As the chamber began cycling, the zero offset drifted for about an hour. It is believed that this is the result of the establishment of a slightly different operating temperature brought about by the heat pumping characteristics of the cloud chamber. Calibrations were run every fifteen minutes until three consecutive calibrations, identical to within 0.3 mmHg., were obtained. Thereafter, the calibration was repeated every half hour. Note that by judicious choice of cycle parameters this heat pumping can be almost eliminated.⁵⁶

Since the pressure transducer used a semiconductor strain gage element, it is quite sensitive to changes in its ambient temperature. It was found that the equilibrium temperature of the strain gage element was dependent upon the thermal conductivity of the gas used in the cloud chamber. The calibrations for different gases differ slightly in their zero offset. However, the heat capacity of the pressure transducer was sufficiently large so that temperature changes during the expansion had a negligible effect on the transducer's calibration.

2-5. Photographic technique. In order to determine the nucleation rate, the number of droplets per cubic centimeter must be determined with considerable precision after the expansion. The necessity for imaging individual droplets places strict requirements on the illumination system and photographic technique. Conditions are accurately known only within the central region of the sensitive volume so only this portion is illuminated by means of a horizontal sheet of light whose vertical thickness is about one centimeter, see Fig. 8. Figs. 9 and 10 show the quality of the collimation of the light beam used in this work. The top and bottom edges of the beam exhibited a sharp cutoff in intensity. The droplets have diameters from ten to fifteen microns at the time

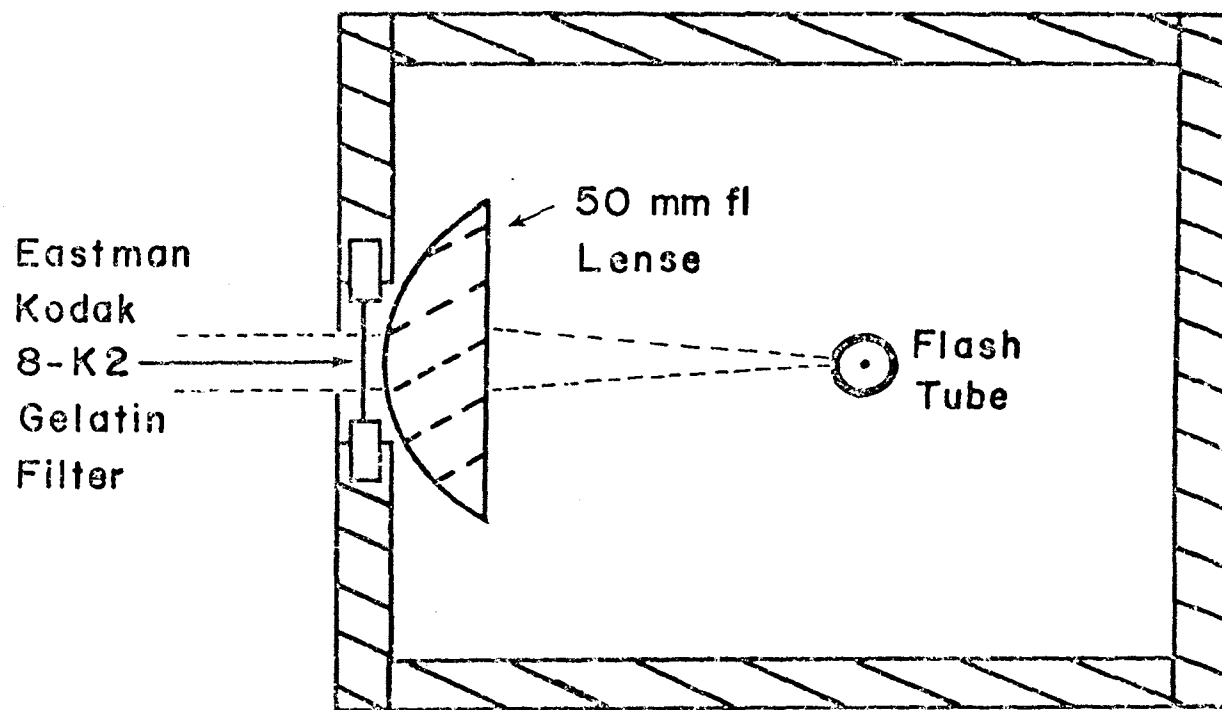


Fig. 3 Flash Tube Light Source

Lamp number 1: collimated July 18, 1967 Louis Allen
Don Hoffman

LAMP NUMBER 1

6" from lamp



8" from lamp



10" from lamp



8" from lamp Sensitive paper (Kodak F-4)



Fig. 9.

Lamp number 2; collimated July 19, 1967 by Louis Allen

LAMP NUMBER 2

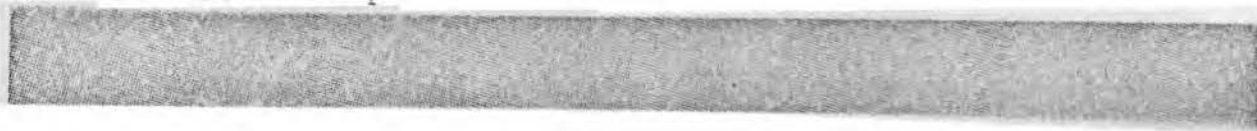
6" from lamp



8" from lamp



10" from lamp



8" from lamp Sensitive paper (Kodak F-4)

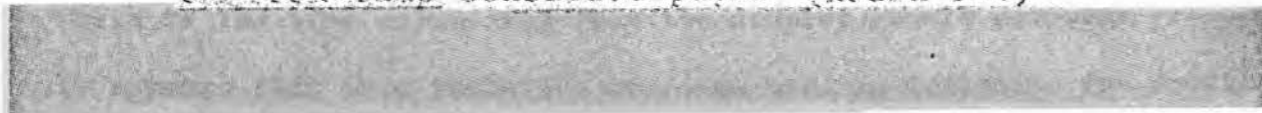


Fig. 10.

they are photographed. It was found that one lamp does not give sufficient illumination. Two lamps were flashed simultaneously on opposite sides of the cloud chamber. The total energy input to the lamps is about 800 joules. The camera was set eighteen inches above the beam. Sufficient intensity and depth of field were obtained with an f-stop setting of 3.5. A grid of wires spaced at one centimeter intervals was photographed and used for calibration of the field of view of the projected film. see Plate 1.

There is an optimum time for photographing the droplets after they are nucleated. Droplet growth is dependent upon several factors which were varied during the course of the experiment, namely supersaturation and the transport characteristics of the inert gas. The optimum time for photographing the droplets was experimentally determined in each case. Growth times varied from 0.05 second in helium at high temperatures to nearly half a second in argon at low temperatures. Plates 2 and 3 show typical homogeneous nucleation for several different droplet densities.

An anomaly showed up in the photographs which was not expected. Droplets photographed at precisely the time they are coming into visible size form rather large diffraction rings on the photograph. Pictures taken slightly later have sharply focused images. This is probably a case of Fraunhofer diffraction through the lens. A calculation assuming Fraunhofer diffraction gives droplet size of the order of ten microns which is the size calculated from the droplet growth computer program. It appears that this technique could be used to determine the droplet growth rate for an accurate verification of the droplet growth law, see Plate 4.

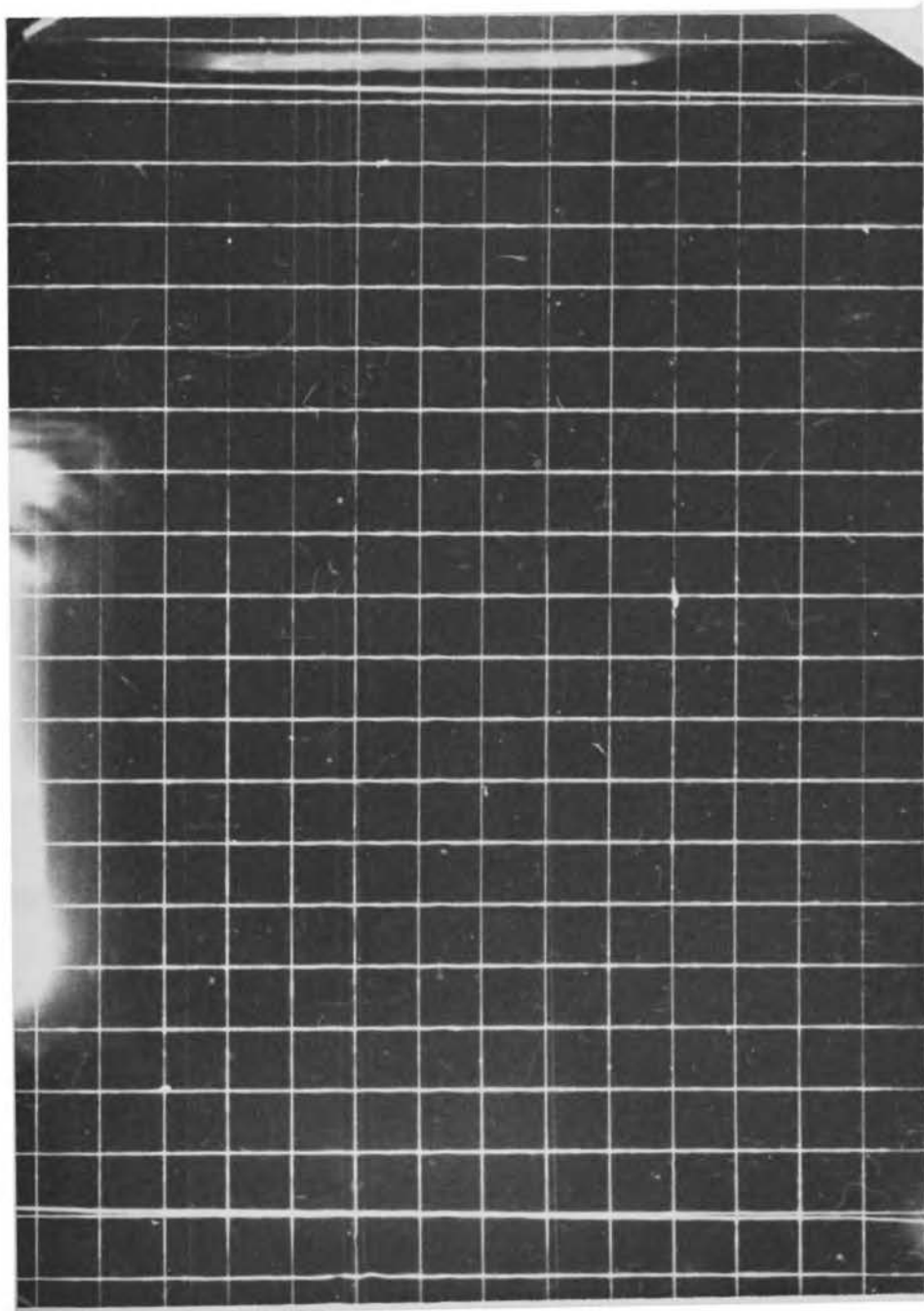


Plate 1. Grid used for calibrating the camera magnification. A 1 cm. grid made from .4 mil tungsten wire is placed in the sensitive volume of the chamber and photographed.

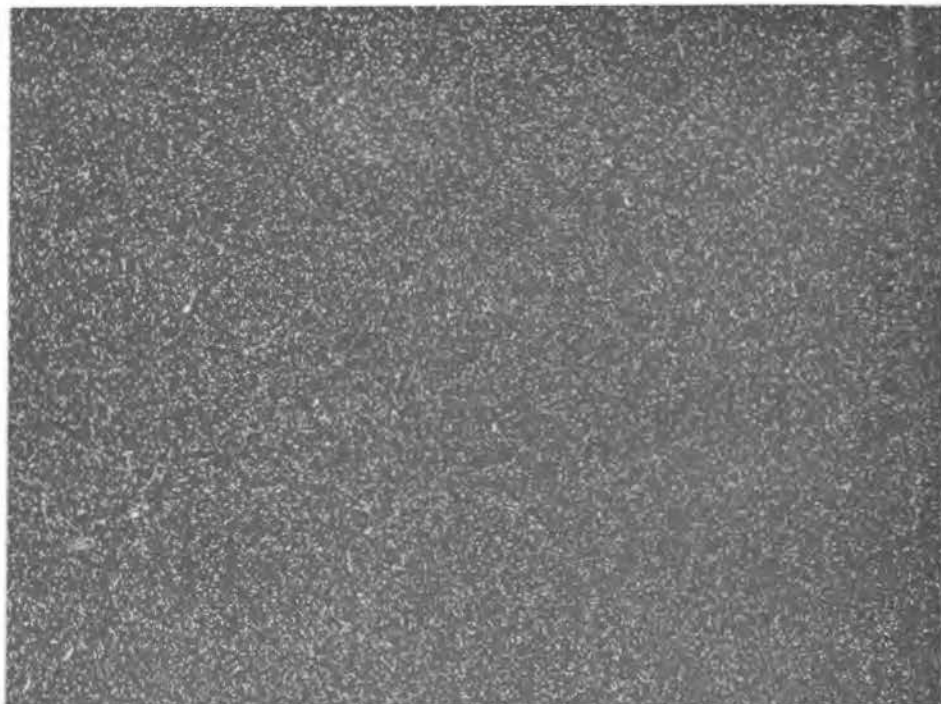
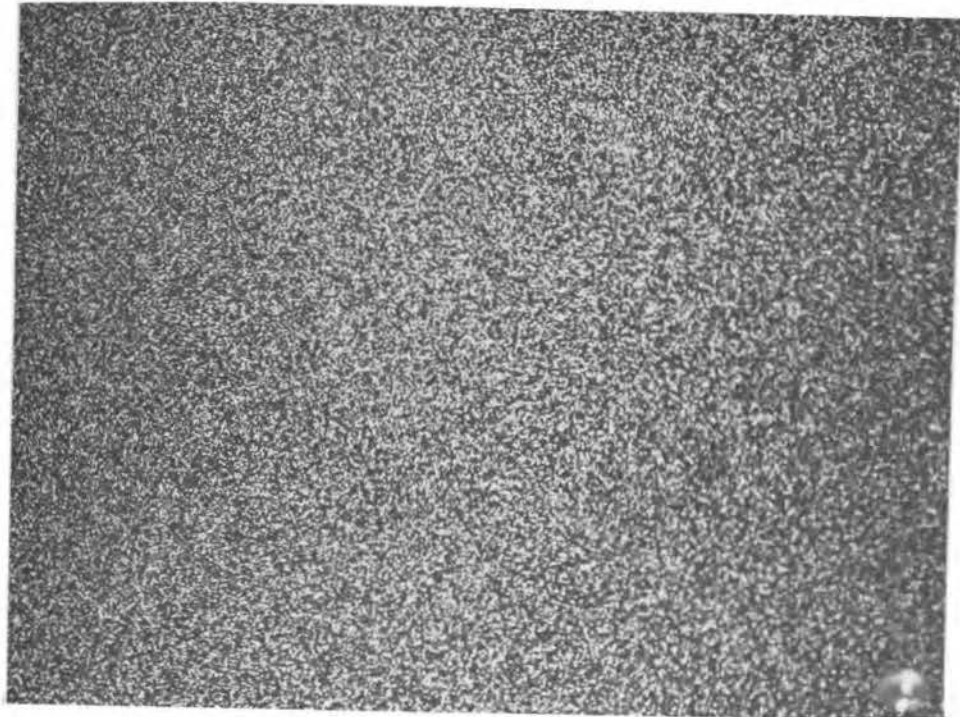


Plate 2. Nucleation. Examples of typical data are shown with the same magnification as the grid in Plate 1. Upper 250 drops/cm³, lower 140 drops/cm³.

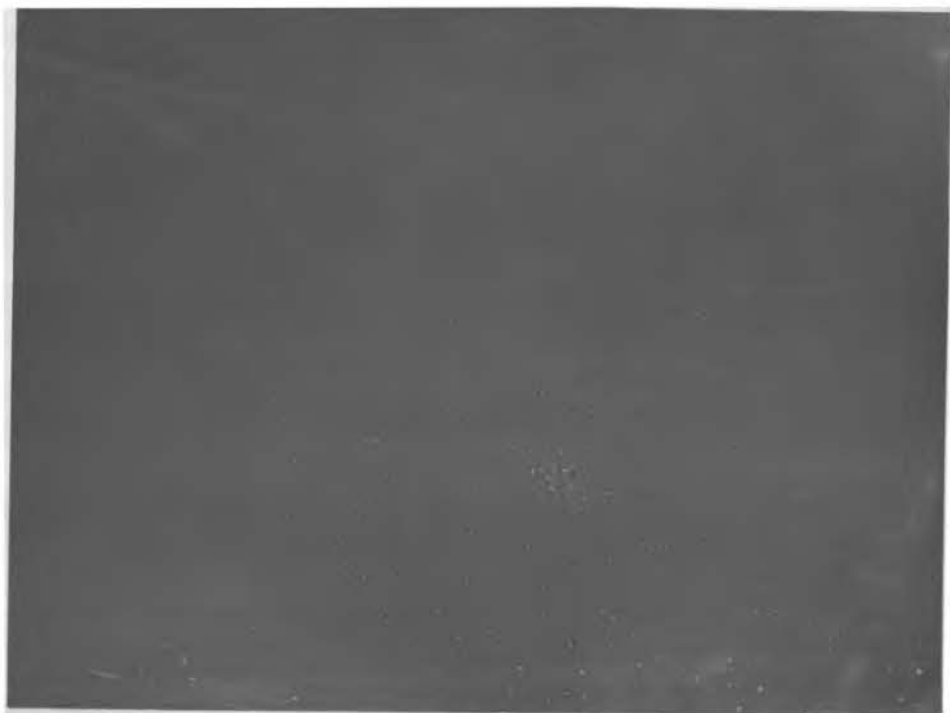


Plate 3. Nucleation. Examples of typical data are shown with the same magnification as the grid in Plate 1. Upper 42 drops/cm³, lower 2.5 drops/cm³.

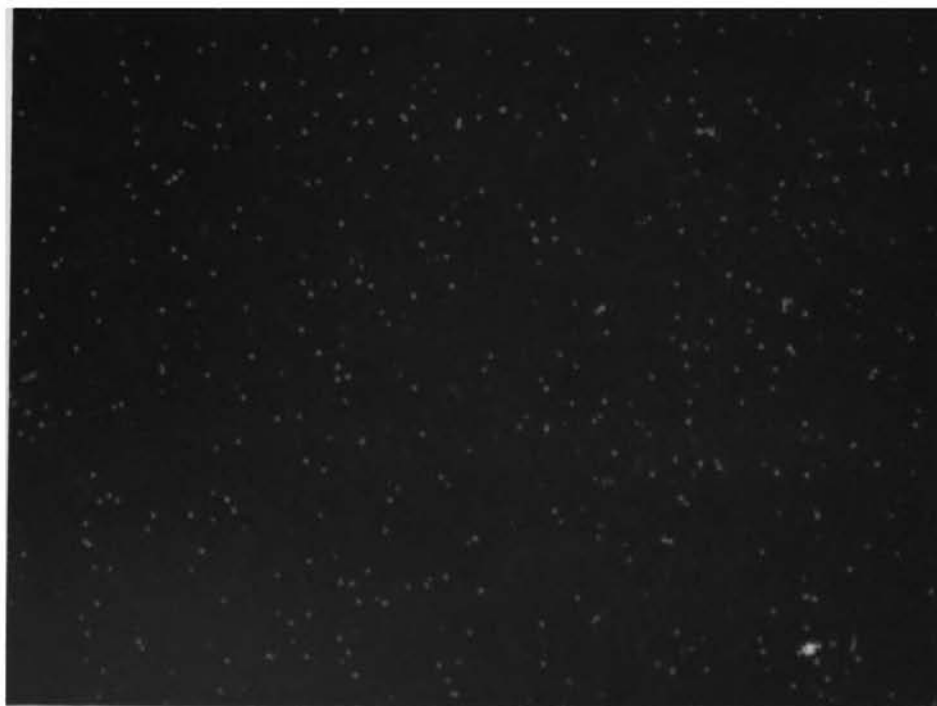
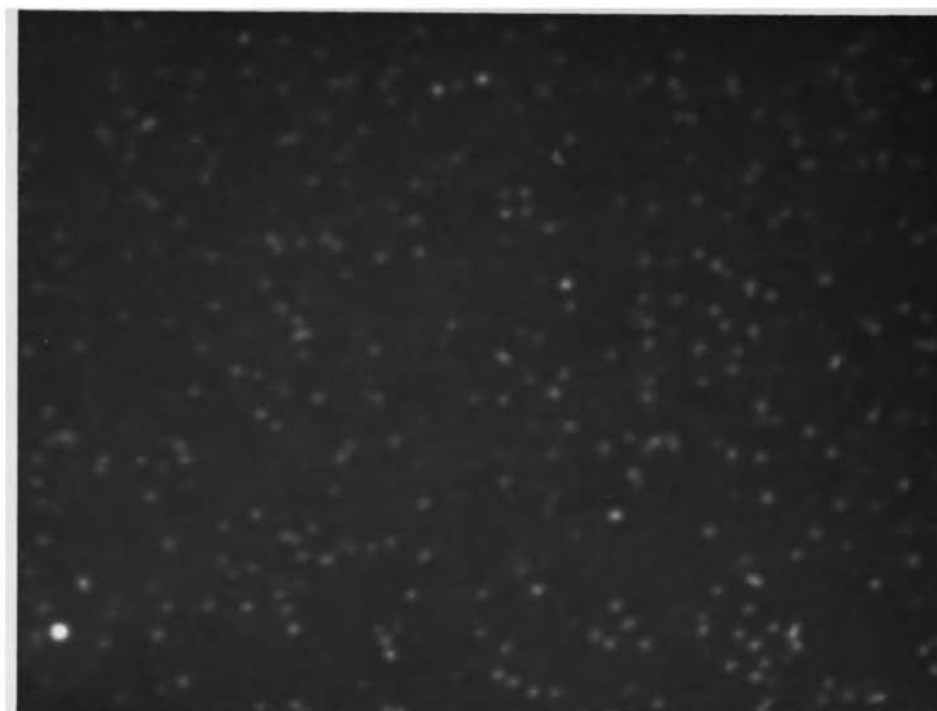


Plate 4. Diffraction from small droplets. The upper picture shows droplets as they appear when small enough to give noticeable diffraction rings on the film. The lower picture shows the same droplets 0.1 sec later.

Another strange effect showed up on the film developed on Feb. 8, 1968. Between some of the frames where the camera stopped, lines of static electricity or something similar sensitized the film. There is no shutter in the camera and the lines seem to have been catalyzed by light reflected onto the film. The static electricity itself was probably the result of strains induced into the emulsion by the motion of the film. During this particular data run the room and consequently the camera was maintained at 40°F. The atmosphere in the room was very dry. This particular combination of physical conditions is probably responsible for the effect. A developed print of this effect is shown compared with a normal print in Plate 5.

2-5.1. Film and development. Due to the very small area of the images, much denser blackening is required than in the case of ordinary photography. Moreover, grays are of no interest so that a fast, high contrast film can be employed. A degree of over development materially increases contrast and thereby the effective film speed. A wide range of results can be obtained with different film and developer combinations. Film and developer combinations which yield high speed and high contrast tend to yield a large grain size in the developed film. If the grain size becomes too large, the effective image diameter is increased.

Virtually all interesting film and developer combinations have been investigated in this laboratory, carefully noting the effective relative speeds and the maximum obtainable resolution. It was found that Eastman Kodak Linograph Shellburst film developed in Acufine film developer made by Baumann Photo-Chemical Corp. gives the greatest relative speed as well as a fine grain size. Eastman Kodak Tri-X is not quite as fast and gives considerably larger grain size.

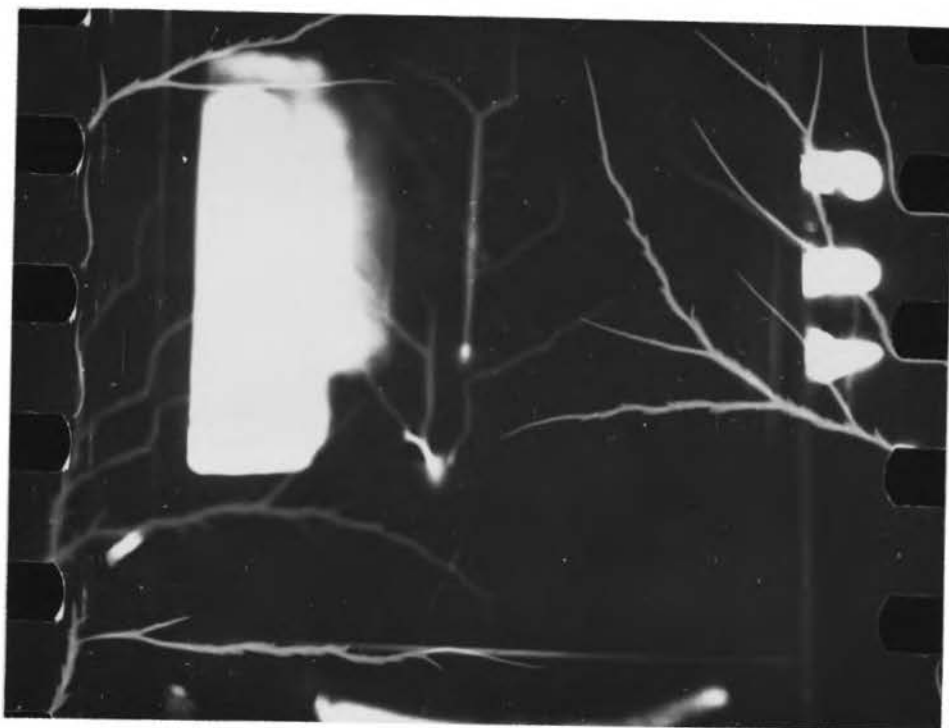


Plate 5. Static. Stresses in the emulsion of the film under certain conditions when developed display a lightning like effect which seems to be catalyzed by light. These are frames exposed during the waiting interval between expansions. This effect is shown compared to a normal frame.

A seven minute developing time is used in full strength developer at 20°C. An 18 minute developing time is used in half strength developer at 20°C when the Nikor developing machine is used.

2-6. The mechanical Brake. During the normal operation of the cloud chamber, the piston is in free suspension between the upper and lower gas volumes. Such a system is oscillatory. The original design of the cloud chamber used a hole plate suspended in the water volume for damping the piston oscillations. Although the hole plate did reduce the waves in the surface of the liquid pool, it was inefficient as a damping mechanism. A solenoid operated brake was connected to the guide cylinder. It was originally designed so that the braking action could be electrically controlled. However, it was found that it could be adjusted for a constant slight drag which was sufficient to critically damp the piston. Small oscillations in the rubber diaphragm were unavoidable. The remaining oscillations were so small, however, as to be insignificant.

2-7. Program board. A programming patch board was added to the cloud chamber in order to facilitate the programming of different experiments, see Plate 6. It was hoped that this would reduce the down time required for reprogramming and add to programming versatility. The program board contains 1632 contacts. These are used to interconnect the timing units with the control apparatus of the cloud chamber. A sequencing unit was installed in conjunction with the program board. This allows a sequence of up to ten expansions, each of which can be different. Moreover, a numbering system for the photographs is provided. The entire installation consists of more than 10,000 connections and three miles of wire.

A patchboard is wired for each type of experiment. As long as the patchboard remains intact, the experiment may be repeated at any time.

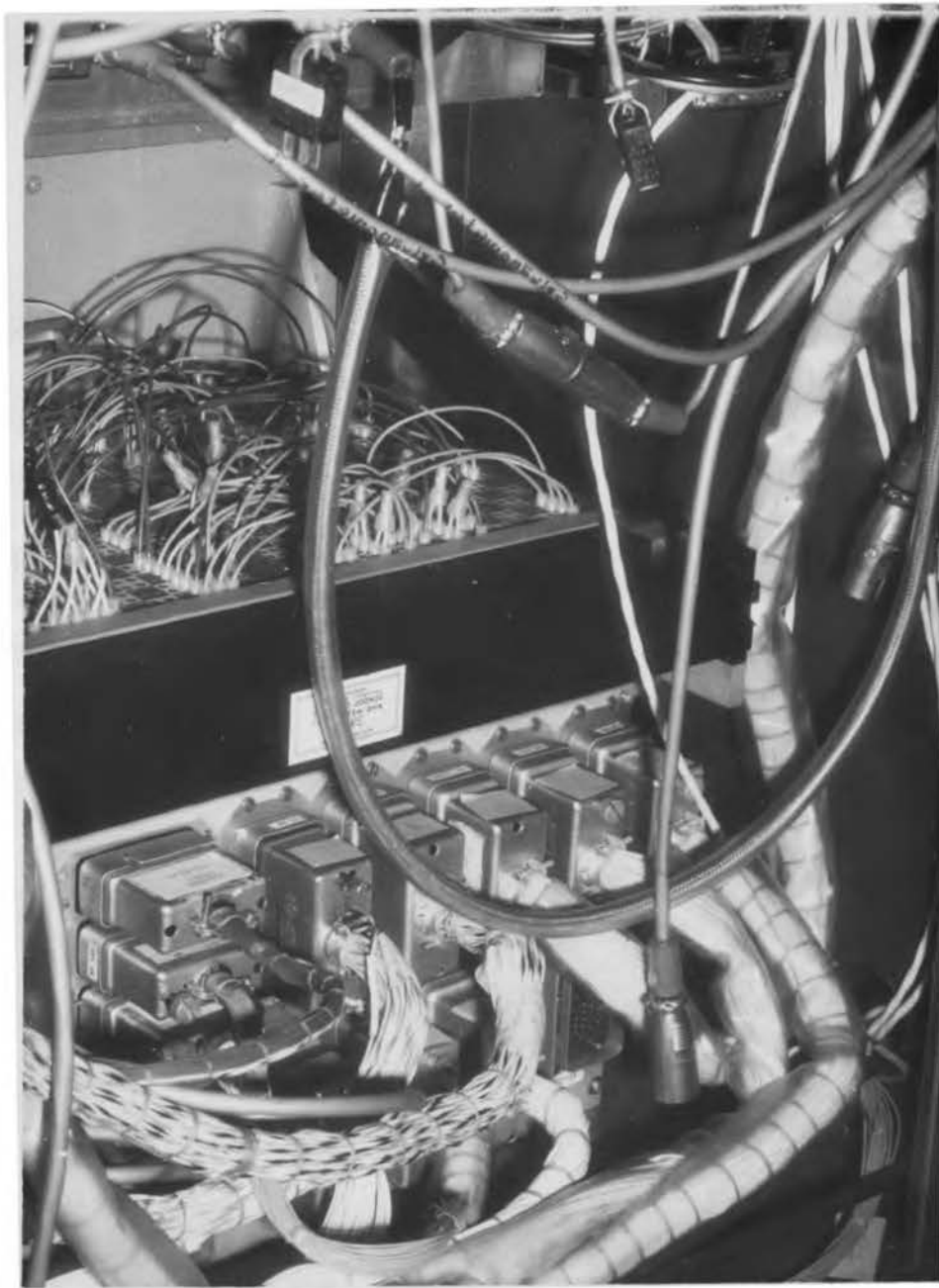


Plate 6. Program board. A rear view of the program board is shown. The patchboard used for the author's data is in place.

If two different experiments can use the same cloud chamber configuration, the appropriate program board may be installed and in a matter of minutes that experiment can be underway. This system makes more efficient use of the cloud chamber facility. It is also possible for several different cloud chambers to be run at alternate times using the same electronic control system and data processing equipment.

2-8. Purification of the water. For homogeneous nucleation rate measurements from supersaturated vapor, every effort must be made to obtain the purest possible vapor so that one may be reasonably assured that the nucleation is indeed homogeneous and not influenced by impurities. The purification of water is hampered by the fact that it is an almost "perfect" solvent. Under normal conditions water is saturated with silicates, various metal ions, and all atmospheric gases including carbon dioxide. Water has such an affinity for impurities that freshly distilled water left open to the atmosphere for a few minutes will not pass conductivity tests for purity. This is due mainly to dissolved gases.

Since the nucleation rate studies were to be done with water vapor in an atmosphere of a pure rare gas, a special purification procedure had to be devised to provide pure water free from not only dissolved solids and liquids, but free from contaminating gases. These gases might affect either the vapor pressure or bonding characteristics of the vapor molecules and modify the nucleation rate.

Various methods of purification were considered, including ion exchange techniques in conjunction with distillation. The final conclusion reached was that distillation is the most effective means of obtaining very pure water, provided that several stages are used with each stage performing a different function.

General distillation procedure was worked out with the aid of Dr. James L. Kassner, Sr., an expert in the field.

The first operations were devoted to eliminating organic compounds since these impurities were deemed to be the least desirable, the most likely to contaminate the vapor and the hardest to remove. One should keep in mind that the amount of a substance present doesn't have to be large in order to have a great number of molecules present. For instance, a tolerably good vacuum of 10^{-6} torr still has ten billion molecules per cubic centimeter. Compared to normal operating pressure, this level of impurity represents about 1×10^{-7} per cent at a total pressure of one atmosphere and only one impurity atom for each 10^7 water molecules. Keeping impurity levels down to just a few molecules per critical embryo becomes impossible and one must settle for the greatest dilution of impurities possible.

Ordinary distilled water contains some organic matter. Tap water was used as the starting water since it requires no less treatment for purification than ordinary distilled water. Potassium permanganate (ten grams per liter) with enough potassium hydroxide to assure an alkaline solution (PH of about 8 or 9) was added to the water and left standing in five gallon glass stoppered jugs for a few days. This solution was then cooked for twelve hours and refluxed for twelve hours (that is boiled and recondensed into the same flask) in such a way that any volatile gases had ample opportunity to escape. Cooking and refluxing are done so that all of the organic compounds are broken up either into volatile gases which escape or else into nonvolatile compounds which are removable by distillation. Carbon ends up as potassium carbonate provided there is sufficient potassium hydroxide in the solution.

This liquid was then distilled through a two stage continuously running still at about one-fourth liter per hour, see Fig. 11 and Plate 7.

It should be noted that the water was taken through the distillation apparatus beginning with twenty gallon batches. The first few liters as well as the last few liters, from each batch at each stage were discarded in the sense that the water was not kept as pure water but used for cleaning bottles and flasks, see Fig 12, and other such procedures necessary to the successful operation of the stills. This technique requires that four gallons of water start through the still to get one gallon of pure water out.

This permanganate solution was distilled and redistilled immediately after refluxing. Both stills were then dismantled and thoroughly cleaned so that the second stage of purification could begin. A very small amount of phosphoric acid (ten ml in 3000 ml) was added to the first still and the entire batch run through the stills in the same manner that the permanganate solutions was run through the still. Phosphoric acid was added to form insoluable phosphates of the heavier elements present and to make the solution acid.

It is not commonly known, but very pure water has a tendency to superheat. Boiling beads of many different materials were tried. Without a single exception, either the substance did not aid the boiling or interacted with the water and dissolved. Substances tried included ceramic beads, glass beads, carbon chips, various stainless steels covar metal alloy and other materials. Covar worked nicely but dissolved very quickly. Pure nitrogen works very well as a nucleating agent when slowly bubbled through the liquid in the boiling flask. This method was prohibited in this experiment, however, since the purification had to eliminate gaseous impurities as well as dissolved liquids and solids. In fact,

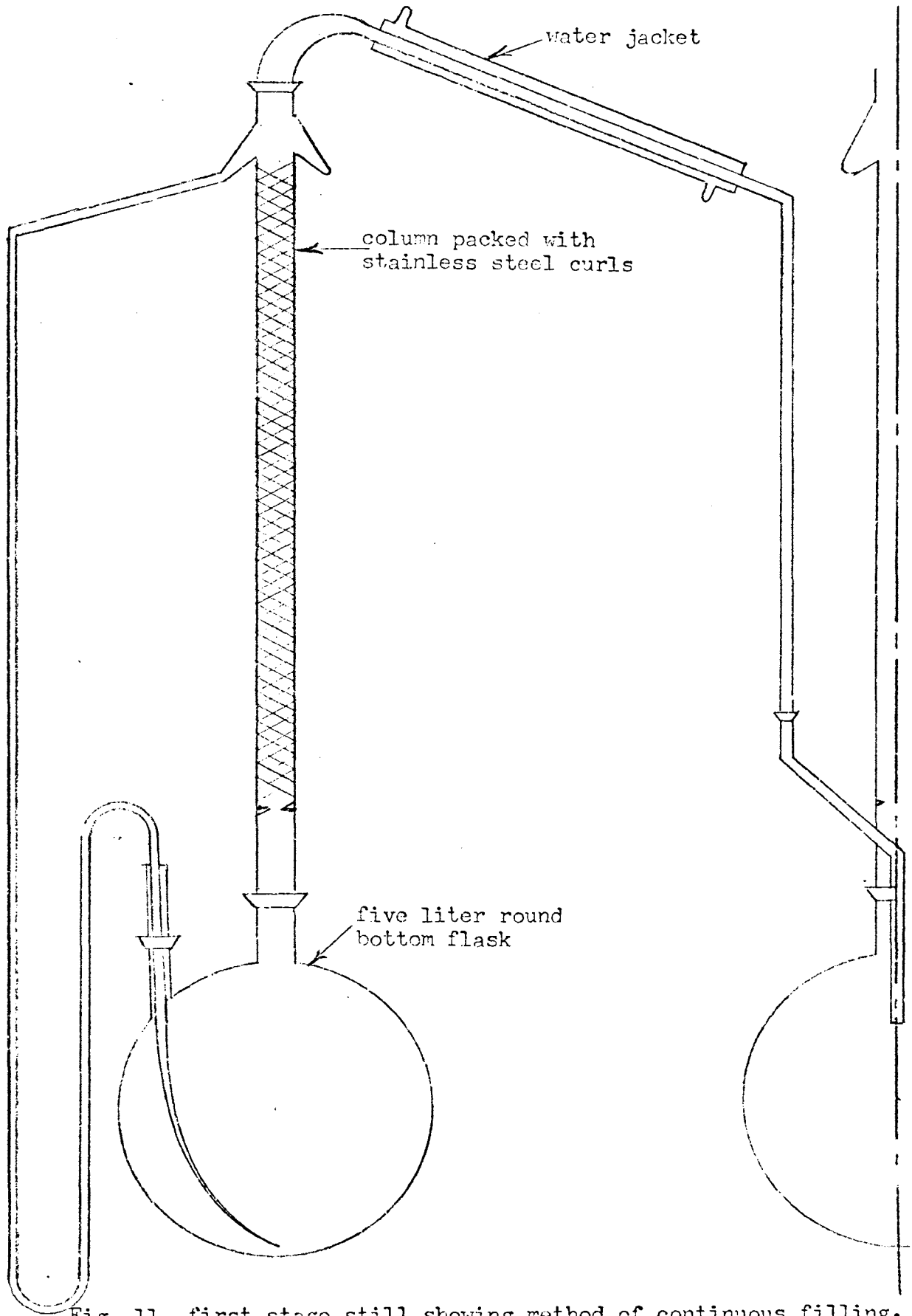


Fig. 11. first stage still showing method of continuous filling.

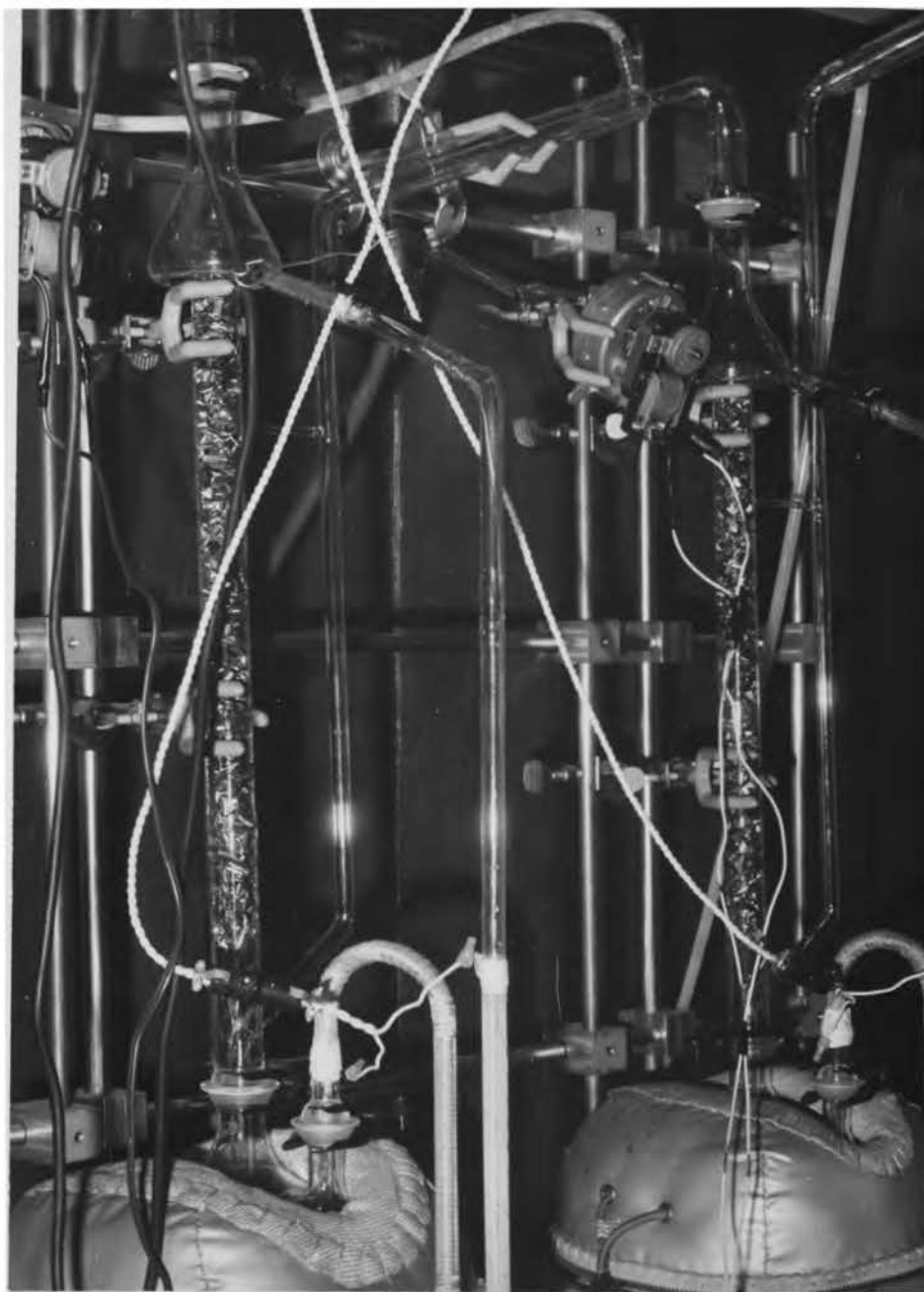


Plate 7. First stage still. The arrangement of the first stage still is shown. Water enters on the right and emerges on the left.

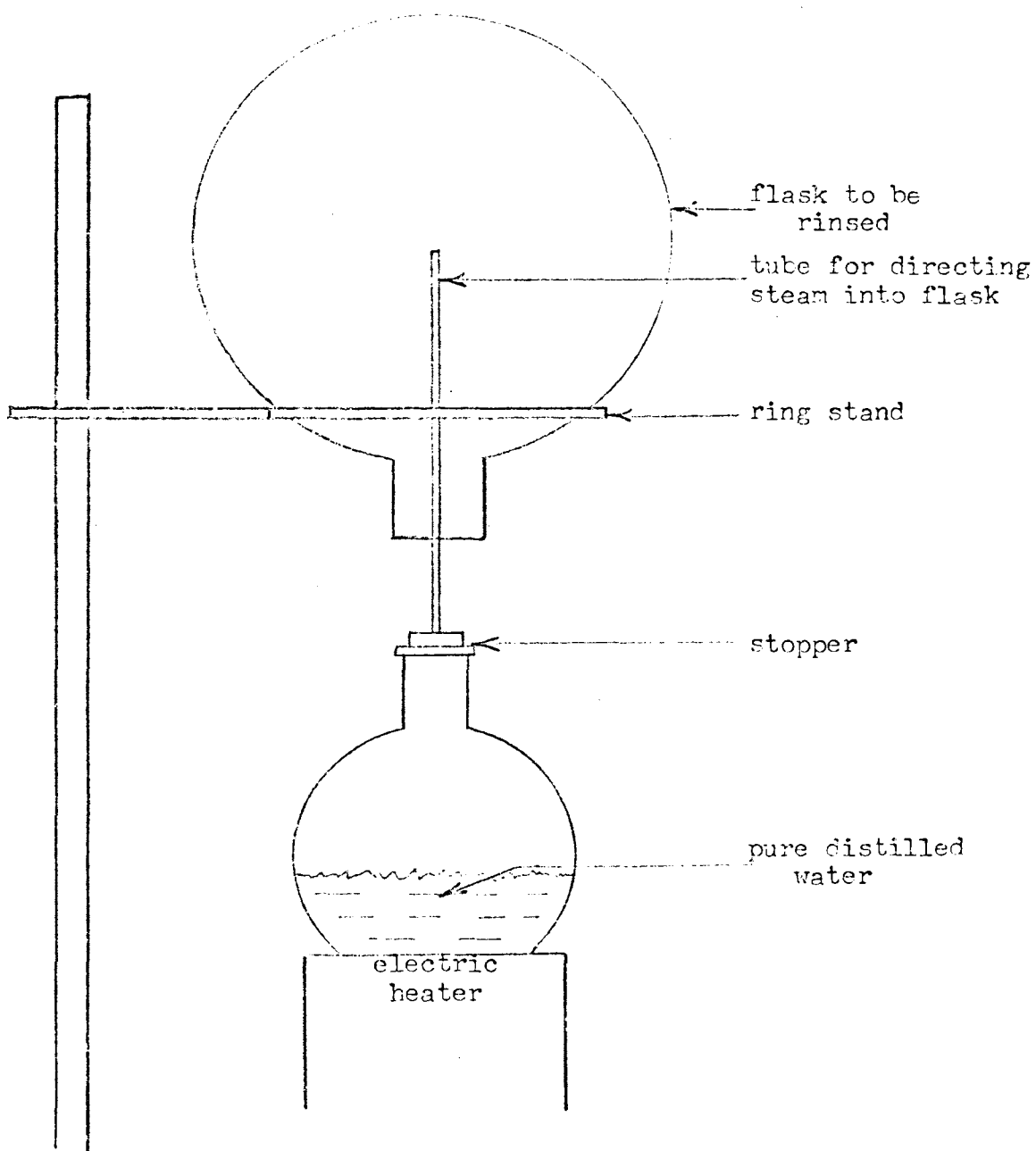


Fig. 12. Method of rinsing glassware. The flask is rinsed with pure water from condensing steam.

a system of steam generators had to be devised to keep the water in the stills agitated with superheated steam in order that purification beyond the first stage could be used with any degree of success, see Fig. 13.

The steam generator is simply a glass tube inserted in the boiling flask, drawn out to a point, bent into a double U shape and wrapped with a nichrome heater. A head of water is kept on the generator by condensing a small amount of water into the generator tube before it gets to the condensing column. This head is kept from flowing into the boiling flask by the nichrome heater which is adjusted so that about 200°C steam only enters the boiling flask.

No steam generator ever failed in service and they were kept in continuous operation for a period of two months which attests to the dependability of the steam generators. When distilling in the final stages of distillation, the need for the steam generators can be dramatically demonstrated by shutting off one and watching the temperature in the boiling flask rise degree by degree with no boiling. This is a dangerous procedure because the great amount of energy stored in the water is released with explosive force when boiling does begin again.

When a bubble of steam comes to the surface in the boiling flask, it bursts and sprays tiny water droplets in all directions, some of which are light enough to be carried into the condensing column. Smith⁵³ has shown that evaporating droplets do not evaporate completely. This is probably due to surface active materials which are concentrated in the surface. Thus, small re-evaporation nuclei which form as the result of the evaporation of sprays can effectively transport low vapor pressure organic materials through a still. This action effectively cancels part of any purification which might be effected by the distillation.

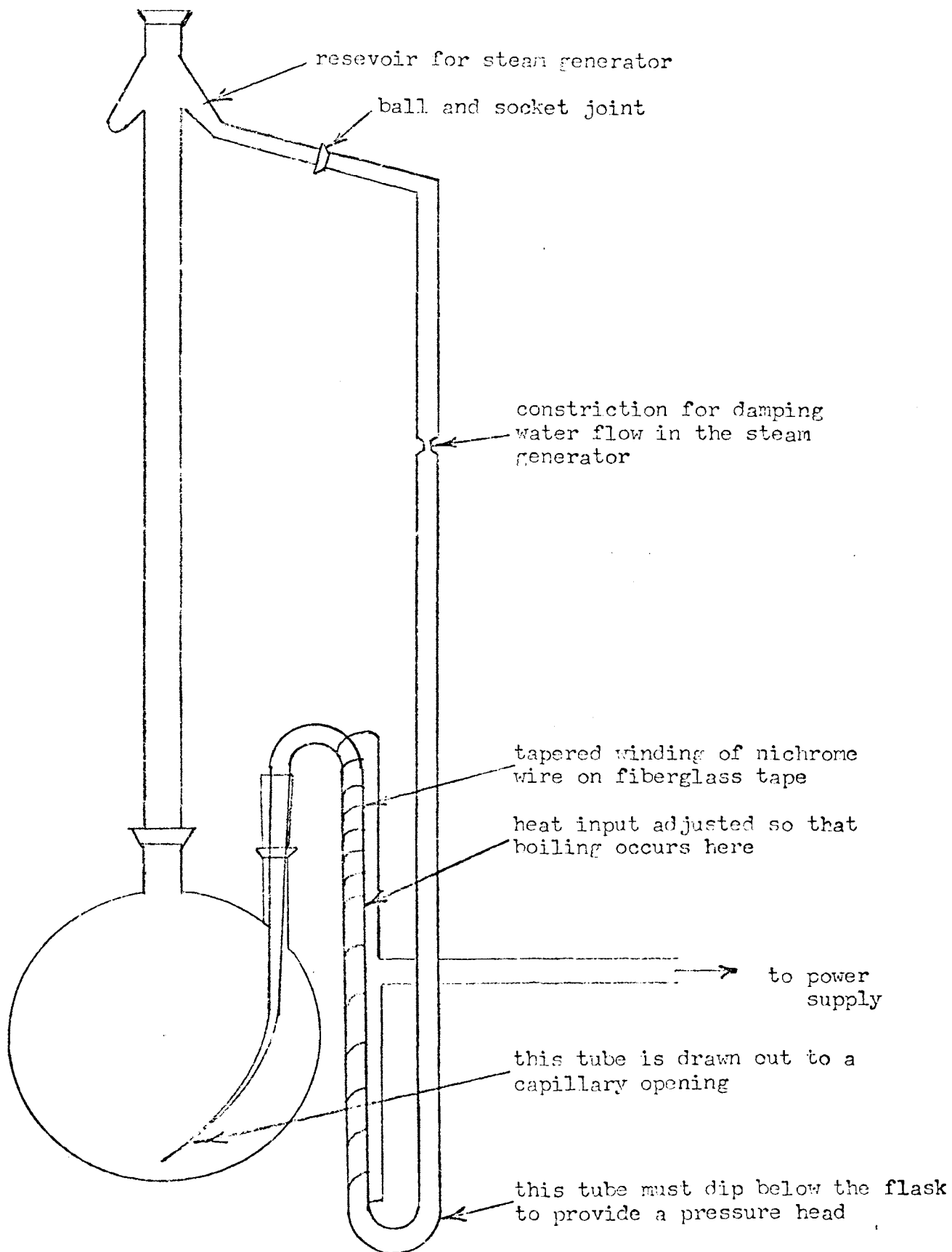


Fig. 13. The steam generator.

It was found that this problem could be effectively overcome by using small stainless steel chips closely packed in an 18 inch column above the boiling flask.

This method is especially effective when enough cooling is provided on the column containing the stainless steel chips so that sufficient water is condensed on the chips to continuously wash them clean. Resultant distillation rates are consequently lowered. The nuclei leaving the boiling pot are taken out by the chips of the column packing by both impaction and diffusion. Impaction requires a finite flow velocity and sharp edged plates while diffusion requires time and a small diffusion distance. The distillation rate was about one-fourth liter per hour.

A commercial Corning still was modified for use as an intermediate distillation unit before the water was put into the final stage, see Plate 8. The final stage is designed to remove the last traces of atmospheric gases. This intermediate distillation was considered necessary because the water was of necessity kept in ordinary glass jugs after the first two distillation stages.

The final stage of the distillation is not a continuous operation but a batch operation. This stage has a five gallon flask, so that a reasonable batch may be processed, see Plate 9. A single batch of this size suffices for any cloud chamber experiment yet devised in this laboratory. Water is continuously boiled and recondensed in the final stage while maintaining the pressure at five to ten pounds above atmospheric pressure. Gases dissolved in the water are released as the temperature rises and are allowed to leak out through a small capillary leak. This action is continued for two or three days or until about one-fourth of the water is lost to the atmosphere. For an operation of this



Plate 8. Corning still. A front view of the modified corning still is shown.

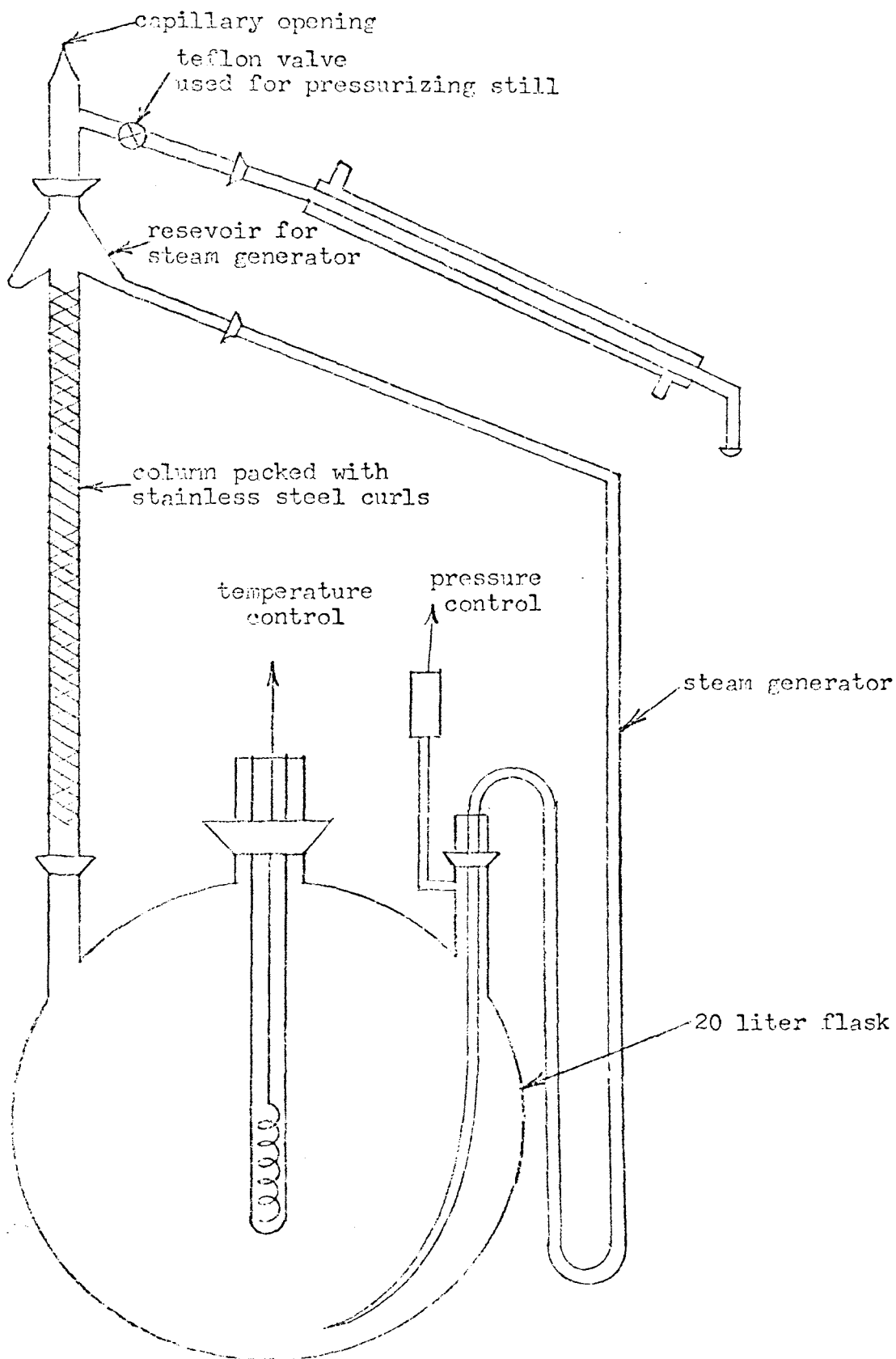


Fig. 14. Third stage still.

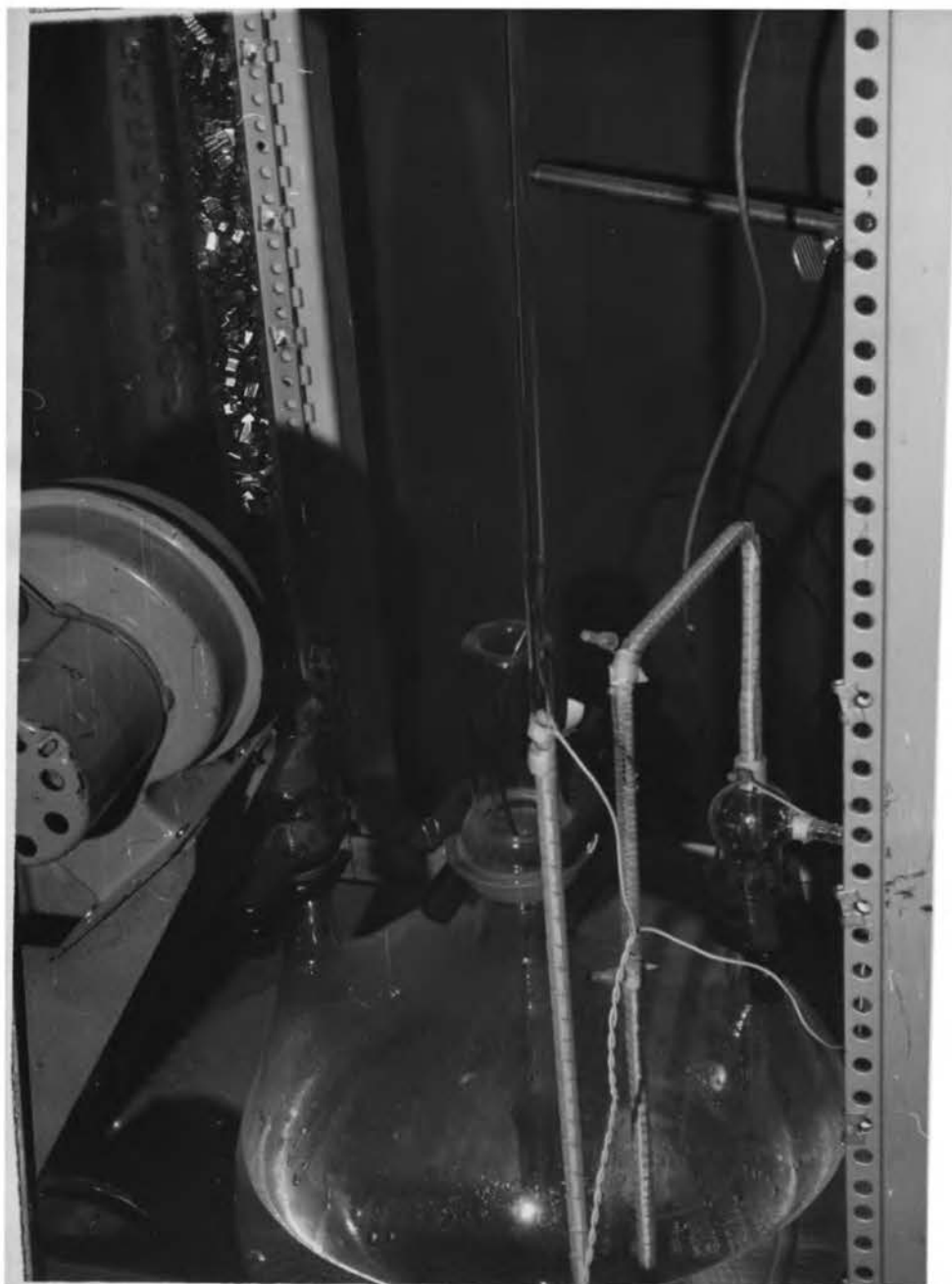


Plate 9. Third stage still. The lower part of the third stage still is shown. The packed column is on the left, the temperature sensor is in the center and the pressure sensor is out of the picture on the right.

type, continuous automatic pressure and temperature sensing are required to maintain safe operation. The pressure stays fairly constant because the temperature is held to a preset value of approximately 103°C.

Distillation from the final stage was done directly into a five gallon jug containing a helium atmosphere. There is no reason, however, the distillation could not be done directly into a vacuum bottle so that all gases are eliminated and the purest possible water obtained. Since the final distillation occurs in the cloud chamber, the materials dissolved from the glass are not troublesome. If the glass jugs are used for the same purpose for some time they may eventually become very clean.

A system of more automatic operation of the first stages than had been used is currently being incorporated into the system. Improvements include automatic filling and temperature control of the first stage stills. Other improvements include continuous conductivity and periodic mass spectographic checks of purity. There is every reason to believe that this distillation system is very effective.

2-9. Preparation of the chamber. The process of readying the cloud chamber for a particular data run begins several days in advance of the data taking process itself. Assuming that all equipment is in operating condition, the chamber is thermostated at the desired temperature. Room temperature must be kept five to ten Fahrenheit degrees below the chamber temperature for proper thermal regulation. Air tanks must be maintained at a temperature near that of the cloud chamber. Otherwise too much heat is pumped into or out of the lower drive chamber for good temperature stability. Some adjustment of heater controls is usually required to maintain proper heat input. The constant temperature bath which is

used as a thermocouple reference is usually maintained within one-half degree of the cloud chamber temperature. These thermocouples are used to thermostat the cloud chamber.

In order to assure gas purity, the cloud chamber is flushed several times immediately before each data run. This procedure eliminated gaseous impurities which may have diffused from the glass walls or the water. If a change in the gas type was made, flushing was done on two consecutive days prior to operation of the chamber. This allowed time for the former gas to diffuse out of the water pool in the chamber.

Even though it would have been desirable to use new water for each set of data, this was not possible because of the difficulty in changing the water in the chamber. No check was made of water purity after the water was in the cloud chamber, but because of the close agreement of the data taken at widely spaced intervals, it is believed that neither water purity or gas purity affected the nucleation rates measurably during the course of the entire experiment. As discussed in the section on water purification, there is little hope of having an atmosphere which is completely free of gaseous impurities. Since the author's data corresponded so well with that of the other researchers in this laboratory who used various means of water purification, it is felt that water purity is not a problem in these experiments.

2-10. The cloud chamber program. For the measurement of homogeneous nucleation rates, the cloud chamber is programmed as shown in Fig. 15. Expansion AB requires about 0.2 sec. The interval BC can be varied from 0.01 sec. to about 1. sec. The slight compression CD reduces the supersaturation by an amount sufficient to stop all subsequent nucleation.

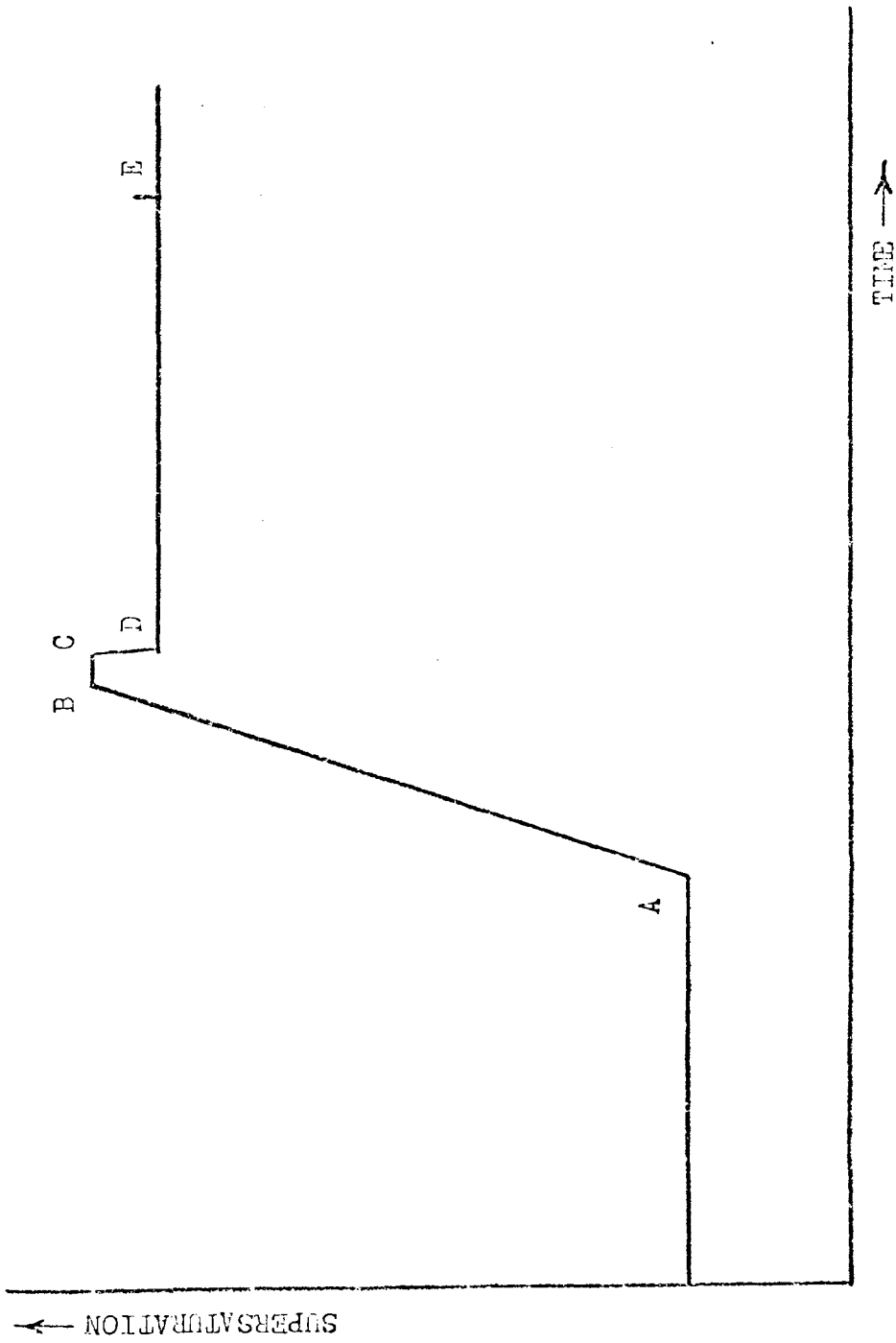


Fig. 15. Typical cloud chamber cycle.

After the droplets have had ample time to grow to photographable size, the xenon flash is triggered and the droplet density is photographed.

An electrostatic clearing field of 80 volts per cm. is used to sweep out ions which are produced in the cloud chamber between expansions. The clearing field is turned *off* just prior to the onset of condensation. Any tracks which are formed during the sensitive time of the chamber appear as easily recognizable ion tracks. Such tracks are carefully avoided when drop counts are made. Therefore, the data presented in the course of this work is not biased by the presence of ions.

Two cleaning expansions were used between data expansions to insure that re-evaporation nuclei had been eliminated. The second cleaning expansion was photographed in order to determine the background level. Except for additional sophistication in the experimental technique, the method employed is basically the same as that employed by Allard⁴⁹.

CHAPTER III

CLOUD CHAMBER THERMODYNAMICS

The most important piece of information to be extracted from the data for a cloud chamber expansion is the state of supersaturation of the atmosphere as a function of time during those parts of the cloud chamber cycle when nucleation is taking place. When the cloud chamber was used as a particle detector for high energy nuclear physics, the supersaturation needed to be controlled with only moderate accuracy so that drop formation occurred only on ions and an exact knowledge of the state of supersaturation was not necessary. In addition, it was useful to know for what period of time the cloud chamber was actually sensitive to the ions. Experiments measuring homogeneous nucleation rates and droplet growth are critically dependent upon an exact knowledge of the supersaturation as a function of time during the cloud chamber cycle.

There is no way to directly measure the water vapor content of the cloud chamber atmosphere during an expansion. The cloud chamber establishes a state of supersaturation by means of an adiabatic expansion as shown in Fig. 16. In the initial condition a noncondensable gas is saturated with water vapor at temperature T_1 . The dashed line shows the course taken by an adiabatic expansion. At a representative time the water vapor pressure has been reduced from P_1 to P_2 by the expansion itself. The temperature has dropped from T_1 to T_2 . The equilibrium vapor pressure corresponding to T_2 is P_2' so that the supersaturation ratio established by the expansion is P_2/P_2' .

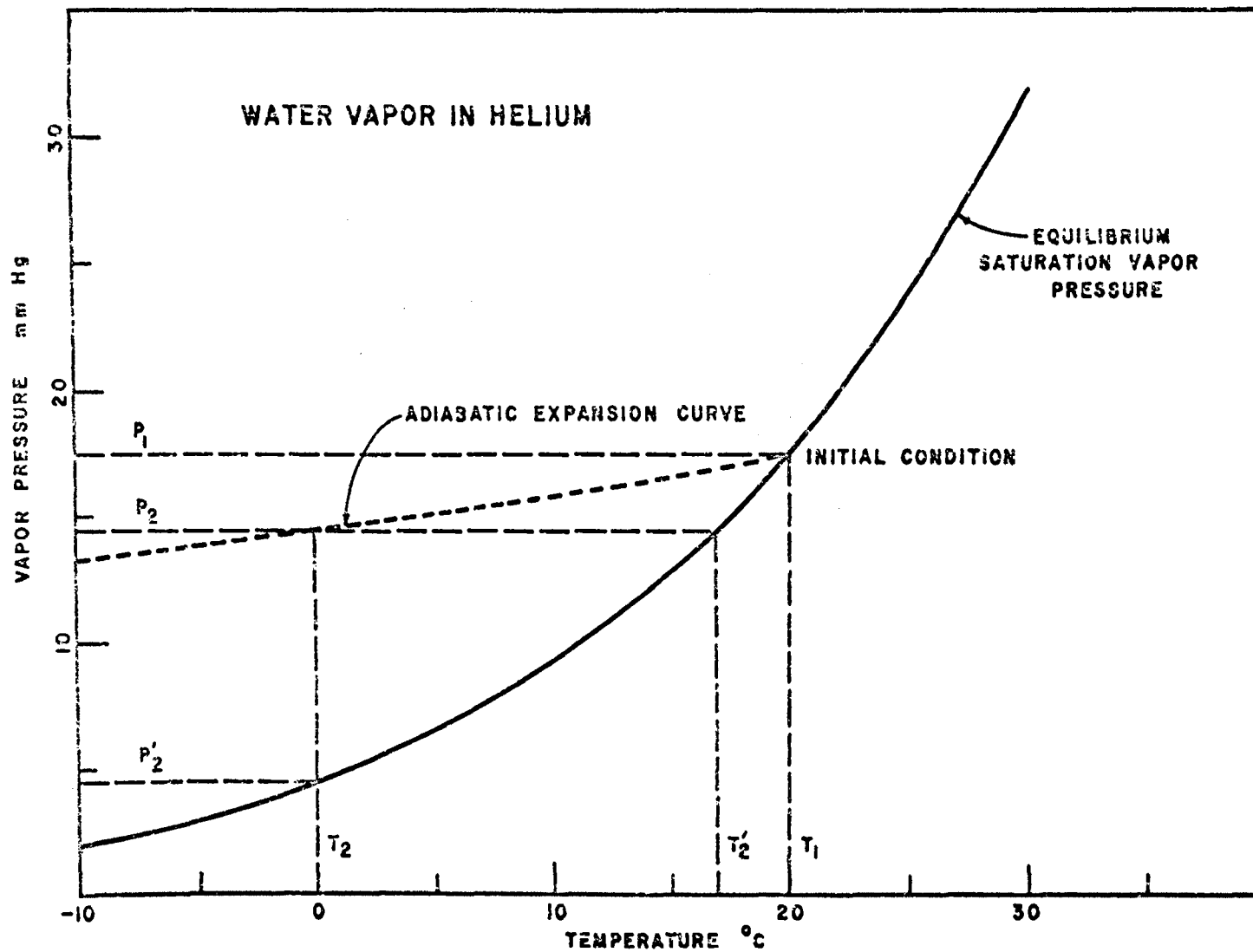


Fig. 16. Creation of supersaturation in helium and water vapor by means of an adiabatic expansion.

3-1. Measuring temperature directly. It had been hoped that an instrument could be developed which would measure temperature with sufficient speed and accuracy to permit its use in the cloud chamber. In recent years fine wire bolometers and fine wire thermocouples have been available which are seemingly fast enough to measure temperature accurately in an expanding gas. However, in a moist gas condensation occurs on the thermocouple, liberating the latent heat of condensation. The wet thermocouple tends to approach the equilibrium temperature T_2 shown in Fig. 16. The exact temperature of the thermocouple will depend upon the rate of change of conditions in the cloud chamber and upon the surface properties of the water film on the thermocouple. Moreover, surface conditions do not reproduce nicely and even this condensation does not take place reproducibly. The prospects for overcoming these effects are not favorable so that all temperature data must be obtained from other sources when the cloud chamber is in a supersaturated state.

3-2. Reliability of volume measurements. Packwood⁵⁰ has shown that calculations of temperature made from volume expansion ratios give erroneous results. This can be readily understood in terms of the thermodynamic processes taking place in the cloud chamber. During the expansion the walls of the apparatus remain at temperature T_1 , Fig. 16. Since the interior gas is at a much lower temperature, T_2 , and since the wet cloud chamber walls would have to be at temperature T_2' in order to be in equilibrium with the existing vapor density, P_2 , the rapid diffusion of both heat and vapor takes place from the wet chamber surfaces while only the diffusion of heat takes place from the dry chamber surfaces. The net effect is that boundary layers (affected by diffusion processes) expand and thereby produce a compressive effect at the interior of the chamber.

The sensitive volume of the cloud chamber as a whole is nonuniform and it makes no sense to talk about the adiabaticity of the whole volume. In fact, volume measurements are useless because the computational complexity of dealing with the real nonuniform gas situation is unduly great.

If the expansion process is slow enough so that shock waves are not created, the pressure throughout the system will everywhere be the same. Moreover, diffusion processes are inherently slow so that a finite time is required for the central regions of the cloud chamber to be sensibly affected, Figs. 17 and 18. Even though the compressive effect has been active, the center of the chamber remains truly isentropic until actual diffusion reaches these regions in perceptible magnitude.

Ordinarily, the final temperature is calculated from one of the ideal gas relationships for a constant entropy process.

$$\begin{aligned} TV^{\gamma-1} &= \text{constant} \\ PV^{\gamma} &= \text{constant} \\ TP^{(1-\gamma)/\gamma} &= \text{constant} \end{aligned} \tag{3-1}$$

The first two involve the volume and are not useful where great accuracy is required. Before using the last equation, however, an appropriate gamma for the equation must be known. Since the cloud chamber operates with a gas mixture, the difficulty in finding an appropriate gamma is magnified even more than for a single component gas system, Packwood⁵⁰ does a thorough analysis of error propagation and concludes that an error of 0.06 in the supersaturation (at a supersaturation of 5.0) produces an error of 100% in the nucleation rate. This can be caused by an error of only 0.005 in the composite gamma used in the ideal gas relationship.

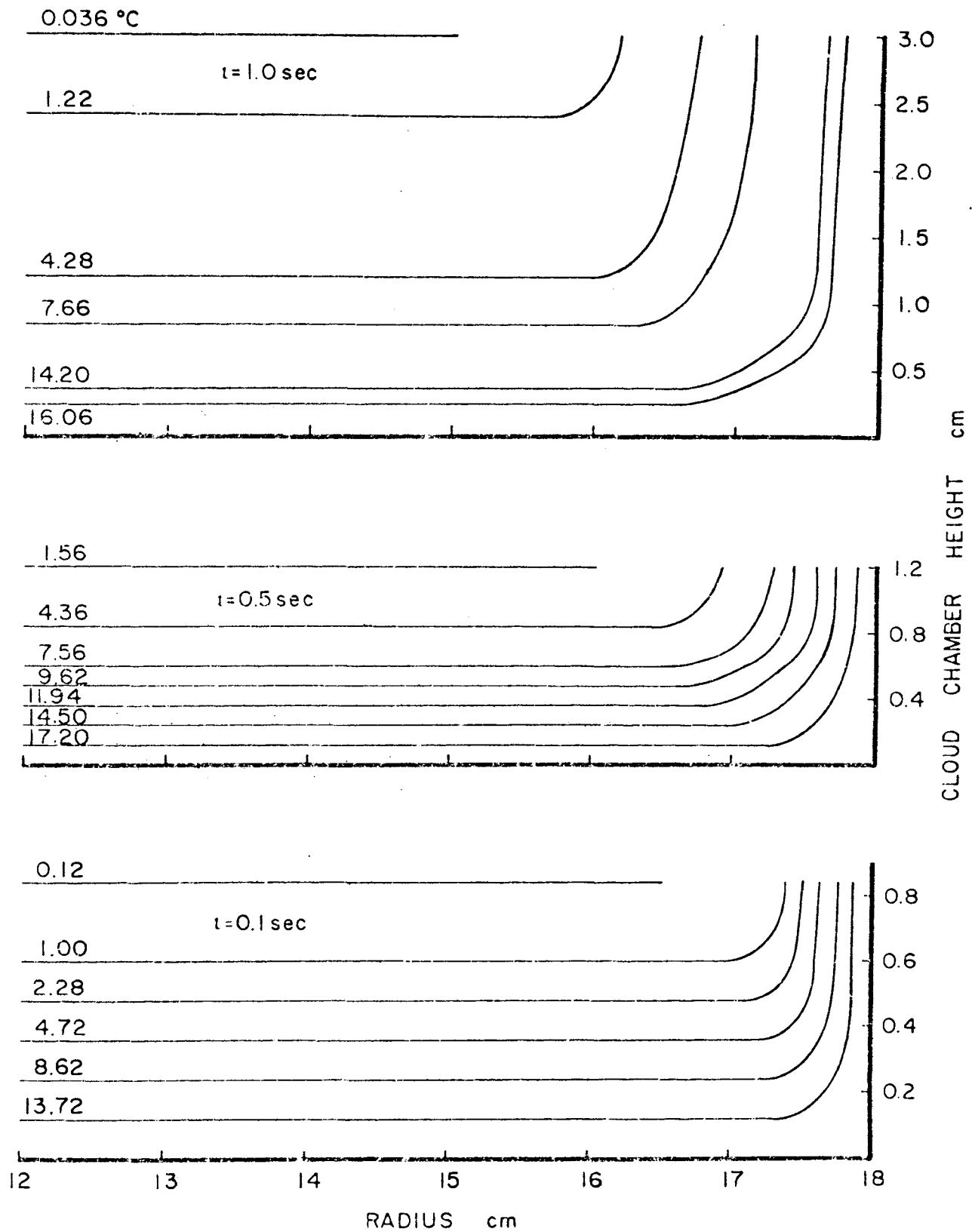


Fig. 17. Temperature Diffusion Profiles in a Finite Cylindrical Cloud Chamber.

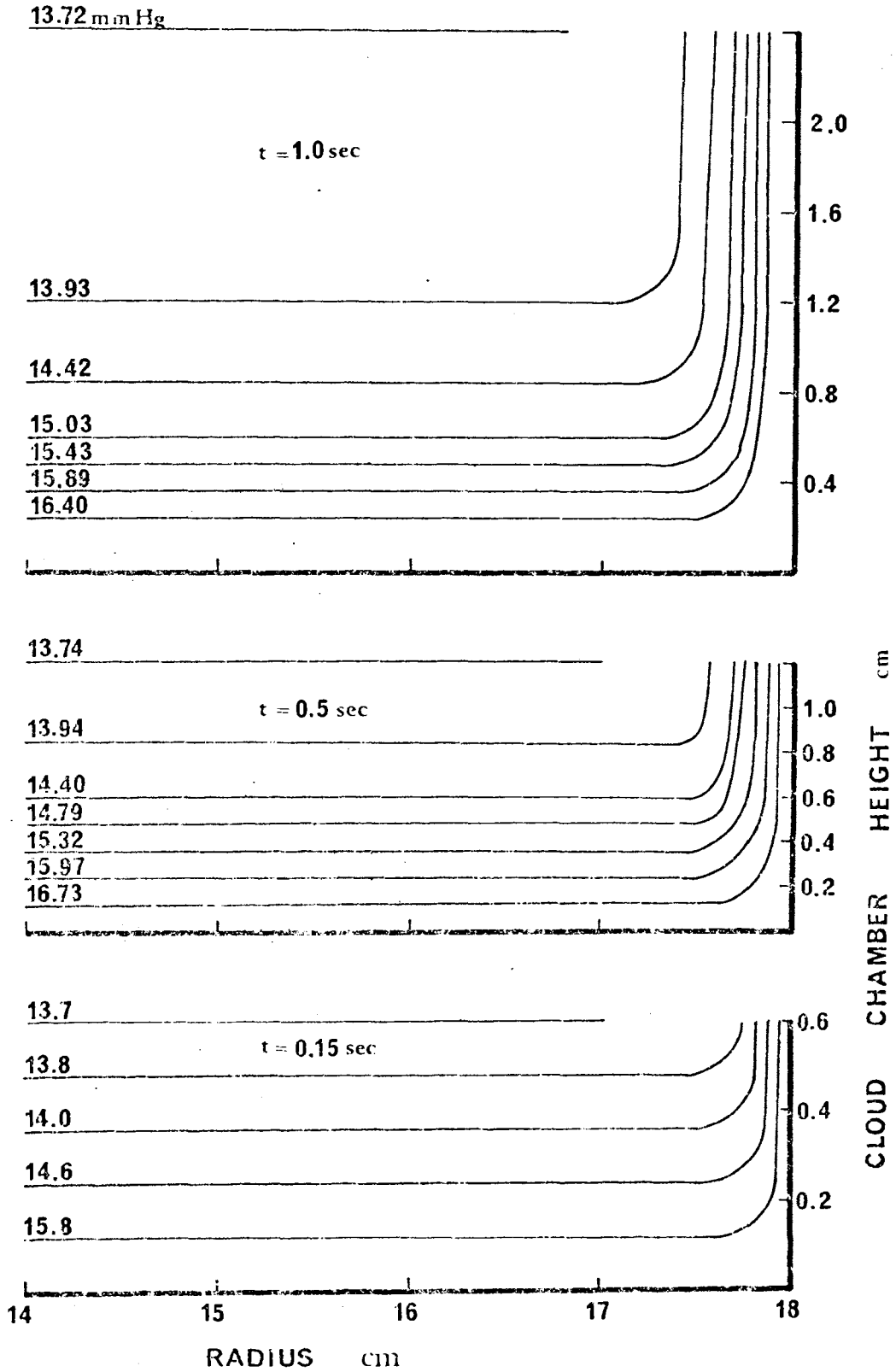


Fig. 18. Vapor Diffusion Profiles in a Finite Cylindrical Cloud Chamber.

3-3. Method of Richarz. Therefore, if the third of Eqs. (3-1) is to be employed, a gamma which is averaged over the range of thermodynamic coordinates must be employed. Methods for surmounting this difficulty are discussed in the following section. Richarz⁵⁵ derived a relationship for determining the composite gamma of a system of two noninteracting gases when the respective partial pressures and gammas are known. The following is a variation of the translation of his procedure as given by Laby⁷.

Assign a mass of 1 to the mixture so that each component is $1-\mu$ and μ respectively. Let the densities be ρ, ρ', ρ'' which are understood to be measured under standard conditions. The specific heats at constant volume are C_V, C'_V, C''_V , and the ratio of the specific heats γ, γ' and γ'' .

Conservation of energy requires

$$C_V = C'_V(1-\mu) + \mu C''_V = C'_V + \mu(C''_V - C'_V) \quad (3-2)$$

The specific volume of the mixture is

$$\frac{1}{\rho} = \frac{1}{\rho'}(1-\mu) + \mu \frac{1}{\rho''} = \frac{1}{\rho'} + \mu \left(\frac{1}{\rho''} - \frac{1}{\rho'} \right) \quad (3-3)$$

Let C_p, C'_p, C''_p be the specific heats at constant pressure

$$C_p - C_V = \frac{R}{JM} = \frac{1}{\rho} K \quad (K = \text{constant}) \quad (3-4)$$

since M is proportional to ρ , and R and J are constant

$$\text{whence} \quad \frac{1}{\gamma-1} = C_V K, \quad \frac{1}{\gamma'-1} = \rho' C'_V K', \quad \frac{1}{\gamma''-1} = \rho'' C''_V K'' \quad (3-5)$$

Now eliminate μ in Eqs. (3-2) and (3-3)

$$C_V(\rho''-\rho') = (\rho-\rho')\rho''C_V'' + (\rho''-\rho)\rho'C_V' \quad (3-6)$$

and by Eq. (3-5)

$$\frac{1}{\gamma-1} = \frac{\rho-\rho'}{\rho''-\rho'} \frac{1}{\gamma''-1} + \frac{\rho''-\rho}{\rho''-\rho'} \frac{1}{\gamma'-1} \quad (3-7)$$

This equation looks at first sight to be most adaptable to the conditions of cloud chamber work. The problem which arises is that gamma (even for the most ideal gas, helium) is a function of the thermodynamic co-ordinates to such an extent that it is not constant over the range of even a typical 30° expansion.

3-4. Temperature-entropy diagram method. Accurate temperature calculations have been made using a method devised by Schmitt⁵¹ and Dawbarn⁵². This method makes use of the temperature-pressure-entropy diagrams for the individual components of the gas. The expected temperature change during the expansion is determined by interpolating between isobars on a line of constant entropy. This temperature change allows one to calculate a gamma which is automatically averaged over the thermodynamic co-ordinates (sometimes referred to as an effective adiabatic index). The formula of Richarz is then used to calculate the composite adiabatic index. This procedure neglects the entropy of mixing and the exchange of energy between the component gases. As a result the method gives good results only when one of the gases is the dominant species.

Another method which should be even more accurate involves making a composite entropy diagram for the gas mixture and finding the temperature directly from the diagram. This latter method has the serious

drawback in that these composite entropy diagrams are very cumbersome to make and a new diagram is needed every time the initial temperature is changed since the mole fraction of vapor changes with temperature. In addition, this method is not adaptable for use with a high speed digital computer so all work has to be done by hand.

3-5. Comparison of methods of temperature determination. All temperature calculations ultimately come from an equation of state for the gas. Equations of state use three variables to completely describe the gas. Cloud chamber expansions are adiabatic so one of the variables used must be entropy. It may be set equal to a constant during the calculation. Derivations of these equations are given in standard thermodynamics texts.^{57,58} Pressure, temperature and entropy are the variables chosen when pressure is measured during the cloud chamber expansion.

The most accurate method is that which integrates directly the equation

$$ds = C_p \frac{dT}{T} - \left(\frac{\partial V}{\partial T} \right)_p dP \quad (3-8)$$

This equation refers to one mole of a single gas. For a gas mixture the mole fractions n_1 and n_2 are used where $n_1+n_2=1$ and the total entropy change is the sum of the individual entropy changes.

$$ds = n_1 ds_1 + n_2 ds_2 \quad (3-9)$$

During an expansion

$$ds = 0 = n_1 ds_1 + n_2 ds_2 \quad (3-10)$$

A numerical solution of this equation including the most accurate values of the heat capacities and compressibilities, $(\partial V/\partial T)_p$, has been used to

provide calculations of temperature. Calculations of temperature using Richarz's method for average gamma as described by Kassner and Schmitt³⁷ were also used and compared with the results of the preceding method. It is concluded that there is essentially no difference in the results obtained with the two methods.

When immediate calculations are needed and no computing machine is available, the graphical method of temperature determination is useful. This makes the graphical method very adaptable to uses involving Aitken nuclei counters because of the independence from office machines.

The course of a perfectly adiabatic expansion is a vertical line on the entropy diagram. Latent heat is easily accounted for through the definition of entropy $ds=dQ/T$. When using air, there is so little difference in the diagram with a small mole fraction change that small changes in the mole fraction due to droplet growth are negligible.

Use of this technique complete with droplet growth corrections is outlined in detail by Kassner⁵⁹ et al. Referring to the diagram, Fig. 19, the expansion begins at the top of the diagram proceeded straight down to point A where a correction is made for vapor depletion (negligibly small at this time). At points B and C the corrections for latent heat begin to be sizable. An excessively large droplet concentration, 10,000 droplets per cm^3 was assumed in the calculation to make the effects show up vividly. Comparison of this method with the exact integration technique shows essentially no difference in accuracy.

In conclusion, any of the three basic methods of temperature calculations may be used with confidence. Each has its advantages and disadvantages depending upon the situation. Richarz's method for average gamma is most useful where a desk calculator is used and vapor

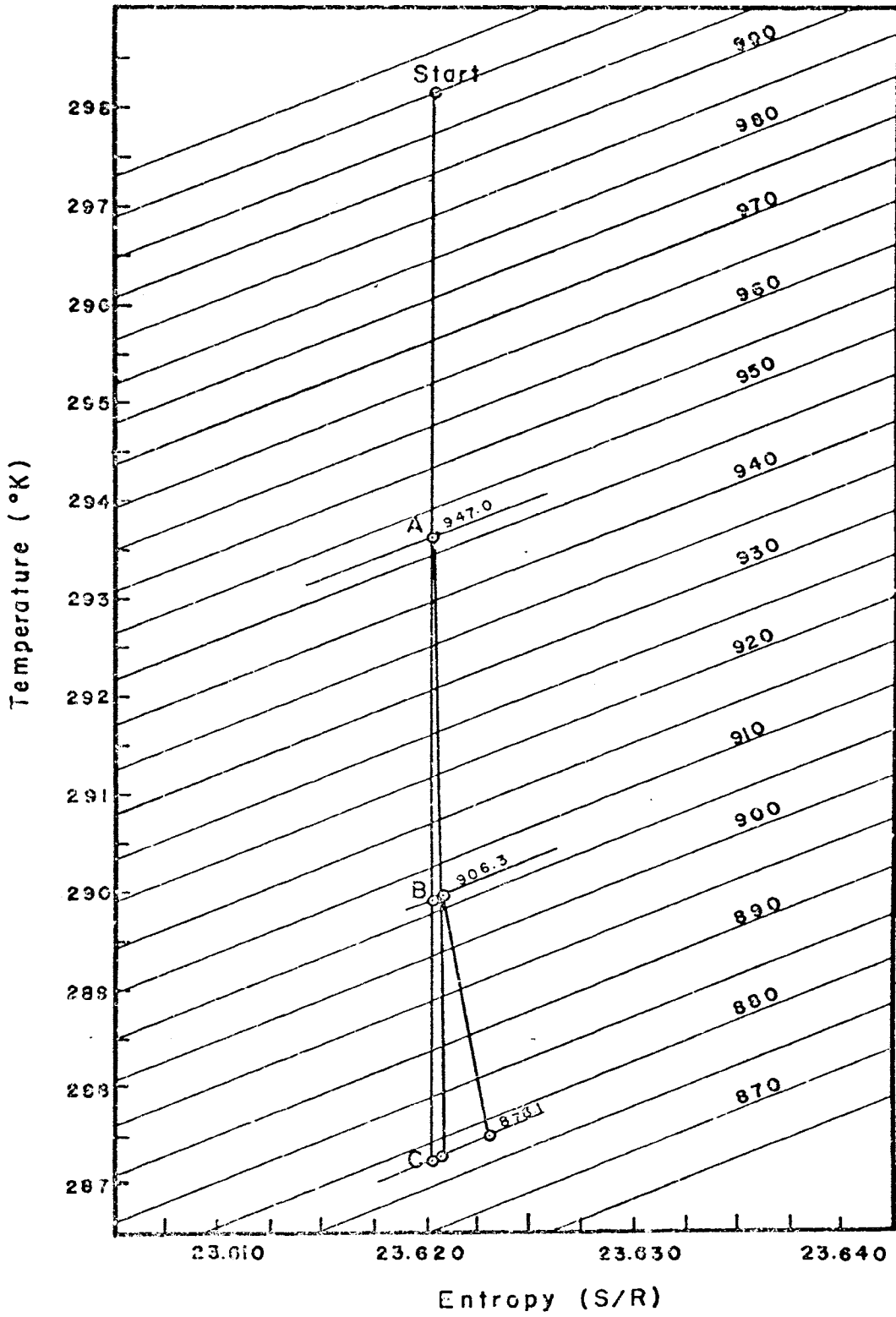


Fig.19. Determination of the True Temperature from the Temperature-Pressure-Entropy Diagram.

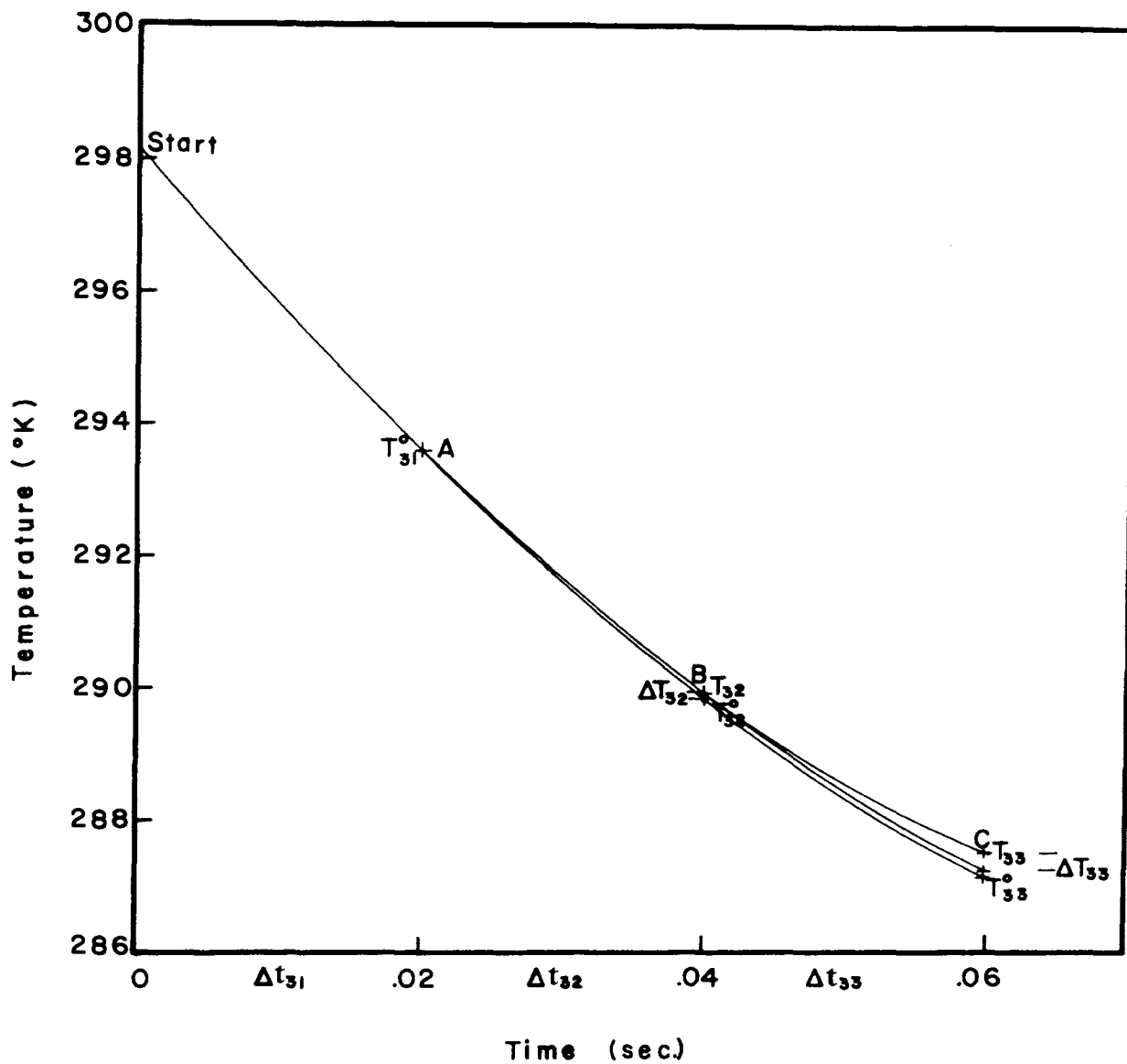


Fig. 20. Determination of the True Temperature by the Entropy Method. The Diagram Corresponds to the Expansion Shown in Fig. 19.

depletion effects are negligible. The graphical technique requires a tedious plotting of a new entropy diagram for each new mole ratio, but is very adaptable where no calculating machines are available and where the same initial conditions are used. The exact numerical integration technique is not adaptable to hand calculations, but is the only method easily programmable for large computing machines when taking all corrections into account. It appears that all three techniques will continue to be used as each has its own range of usefulness making it uniquely adaptable to a given situation.

3-6. Experimental test of equations of state and measuring techniques.

Use of temperature entropy diagrams requires knowledge of entropy values to quite high accuracy. These values have ordinarily been derived by differentiating the equation of state which is risky at best. There is not and has been no doubt that the accuracy of these equations of state is quite good. The following question arises. Since the derived functions such as heat capacity and entropy are obtained by taking first and second order derivatives, just what accuracy is retained in these derived functions? F. Din⁶⁰ most aptly states the problem in his work on argon:

The first differential coefficient was difficult enough to derive even with nominal accuracy whilst values derived for the second differential co-efficient were uncertain in the extreme. It was decided to persevere and values of

$$\left(\frac{\partial r}{\partial t}\right)_p, \quad \left(\frac{\partial^2 r}{\partial T^2}\right)_p \quad \text{and} \quad T \left(\frac{\partial^2 r}{\partial T^2}\right)_p$$

were derived, tabulated and smoothed, values of C_p , entropy and enthalpy were then calculated by integration and it was immediately apparent that they were untenable. They showed

considerable irregularities when plotted and were in no sense systematic.

Considering that the data for argon is perhaps the most accurate and consistent of that for any gas, also that argon is the most ideal of all gases after helium and neon, it is not difficult to imagine inconsistencies arising in the entropy tables.

It was decided that in order to obtain good results with nucleation work, dependable data on the various gases in the cloud chamber must be obtained. The aim was to take sufficient data to check the existing data. It was felt that the accuracy that could be obtained with static measurements was not better than had been obtained by other experimenters, for instance in the case of argon at Leiden by Crommelin and Onnes⁶¹ and coworkers, at Reichsanstalt by Hobborn,⁶² by Masson^{63,64} and coworkers, at the Van der Waals laboratory by Michels⁶⁵ and coworkers and by Bridgman^{66,67}. Therefore, a means was sought to exploit the advantages of the cloud chamber. Data would not be taken recording pressure, volume and temperature, but recording only pressure and temperature during a constant entropy process. Data of this type plotted on a temperature entropy diagram, should yield a vertical line if our results are consistent with the diagram.

The remaining question is, just what sort of accuracy must an experiment provide so that the data obtained is of equal or better quality than the published data. A true error analysis of published data is difficult to carry out. One can judge, however, from the number of significant figures published in a table, the confidence with which an author rates his calculations. This confidence is expressed by publishing one more significant figure than the accuracy of the computations would indicate. This is a necessary evil, however, in order that internal

consistency might be obtained. Using this criterion, the data taken should exceed the accuracy of published data if pressure measurements are maintained to an accuracy of 0.5 mmHg and temperature measurements to 0.05 C°.

With very little modification, the Wilson expansion chamber of this laboratory may be used for making thermodynamic measurements. Temperature and pressure are recorded during an expansion or compression of a gas under conditions of constant entropy. These measurements must be made with extreme accuracy and speed.

3-6.1 Obtaining a pure atmosphere. A new cloud chamber was constructed for this work. It has the advantage of a larger available piston motion so that sizable volume ratios might be obtained without partially filling the sensitive volume with water.

Assembly of the new cloud chamber was done with the greatest care. Every bolt, nut and screw was cleaned with the same care that one would use in a hospital surgical room. The sensitive volume was exposed only to the rubber diaphragm, O-ring seals, stainless steel and glass.

In order that no water vapor or other volatile material enter the chamber, a dry ice and acetone cold trap was installed in the inlet line to the sensitive volume. This cold trap was kept in operation at all times during the period from assembly of the chamber to the completion of the data taking. Each time a new gas or gas mixture was used, a flushing operation was performed which virtually eliminated all traces of the former gas. A vacuum pump was used to remove as much gas as possible. New gas was then run into the chamber so that the final pressure was about three atmospheres. This gives a flushing action whereby three-fourths of the gas is removed each time so that the remaining gas

of the former kind after filling is about twenty-five percent of the total. Usually eight flushing operations of this type were performed for each gas exchange with the result that the purity of the gas as it came from the cylinder was the determining factor in its purity in the cloud chamber.

A pressure transducer such as is used in this laboratory has a natural frequency of 40,000 Hertz. The oscillograph galvanometers have the slowest response of any component in the pressure detection system with a flat response from zero to 240 cycles per second (Heiland type M400-120, 8.62 MV/in, undamped natural frequency 400 cycles per second). Amplifier frequency response is good enough that no difference in gain is noticed for a d.c. signal or a ten kilocycle signal. The net result of the pressure detection system is that pressures are measured to ± 0.02 percent accuracy with a time response which is short compared to anything happening in the cloud chamber.

The thermocouple employed in these measurements was designed to minimize thermal perturbations due to the thermocouple itself while maintaining the lowest possible resistance. The thermocouple is shown in Fig. 21 and its position in the cloud chamber in Fig. 22. It is necessary to maintain the lowest possible resistances for the thermocouple element since the noise level at the output of the amplifier is roughly proportional to the input impedance. In the case of chromel-alumel the output is of the order of forty microvolts per degree centigrade. In order to read a temperature to one-hundredth of a degree, it is therefore necessary to know the voltage coming from the thermocouple to better than one microvolt.

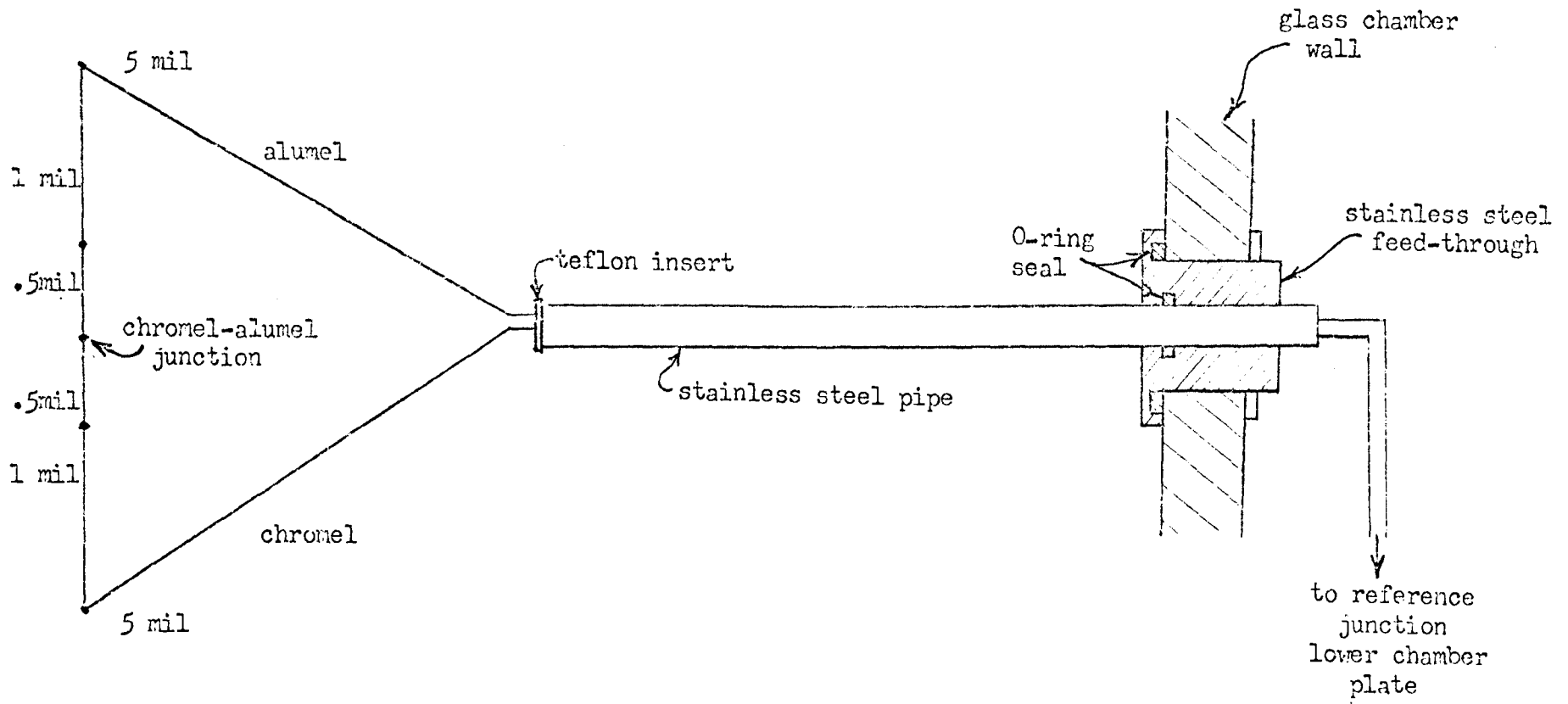


Fig. 21. Thermocouple used for measuring the gas temperature.

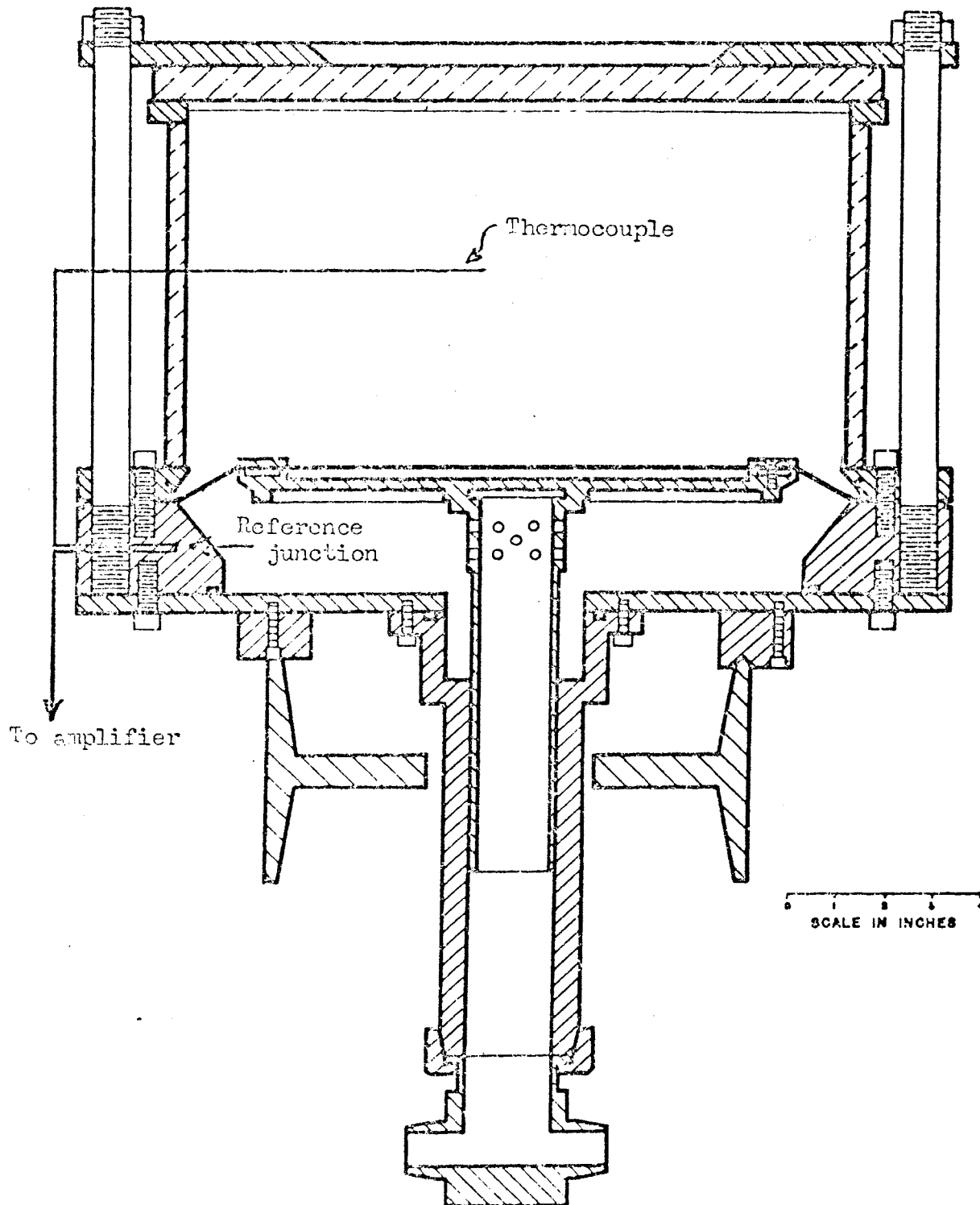


Fig. 22. The cloud chamber used for measuring gas temperature with a thermocouple.

Considering that wide band d.c. amplifiers generally have a noise level referred to the input of the order of tens of microvolts it is easy to see the difficulty in trying to accurately read an output signal to one microvolt. The Model 3101 California Instruments amplifiers used in this laboratory have a rated noise level of seven microvolts referenced to input. Four amplifiers were available so a complete check of each was made to determine which had the lowest noise level in the circuit configuration used with the thermocouple. The amplifiers were run in the potentiometric mode since it showed consistently lower noise levels than the differential mode.

Noise level tests with shorted input were made and recorded for each amplifier. It turned out that two of the amplifiers just met specifications while two were significantly better. Of the other two, one had a noise level of five microvolts peak to peak. The thermocouple used has a resistance of approximately 390 ohms. This value of carbon resistor was then placed across the input of each amplifier and a check made on the noise level. As expected, the noise level was higher, but only by about two microvolts in the case of the lower noise amplifier. A triply shielded twisted pair cable 25 feet long was constructed which has three 95 percent coverage shields. This cable was attached to the amplifier input and shorted, at the other end. Shorted at the end, it gave practically no noise increase, but with the 390 ohm resistor in place, the noise level was intolerable. It was therefore decided that the amplifier must be placed as closely as possible to the thermocouple so that stray capacitive pickup would be minimized.

After the thermocouple was installed and connected to the amplifier, several configurations of grounding the shields were tried. At best, the

noise level referred to the input was down to about eight microvolts peak to peak. This included about five microvolts due to the amplifier, one microvolt due to the bias module and two microvolts due to stray pickup by the thermocouple.

It should also be mentioned that the thermocouple hanging out in the center of the cloud chamber as it did, acted as a very good antenna, picking up signals from every valve and a.c. power line in the vicinity. There was no alternative but to encase all operating valves in a copper-clad one-sixteenth inch iron case. Even the sola transformer operating the amplifier had to be moved from under the chamber. When all these changes were made, the noise level was again down to about eight microvolts peak to peak of mostly sixty cycle noise with some 400 cycle noise from the chopper in the amplifier.

Luckily, the noise peaks from the pressure signal and from the temperature signal were in phase. There also was a flat place in the signal between each peak which corresponded to a period of zero noise level. Because of this, even though noise was present in the signal, readings were taken every $1/120$ second during the quiet period of the noise cycle, thereby achieving the same effect as if the noise were a factor of ten smaller. One disadvantage of this is that in order to get a large number of data points on each run, the expansion or compression time had to be increased almost to the limit. A block diagram of the temperature measuring system is given in Fig. 23.

3-7. Thermal characteristics of fine wire thermocouples. The output response of fine wire thermocouples to a changing environment created by an expanding gas is more complex than many investigators have recognized. The seemingly instantaneous response to a fast expansion

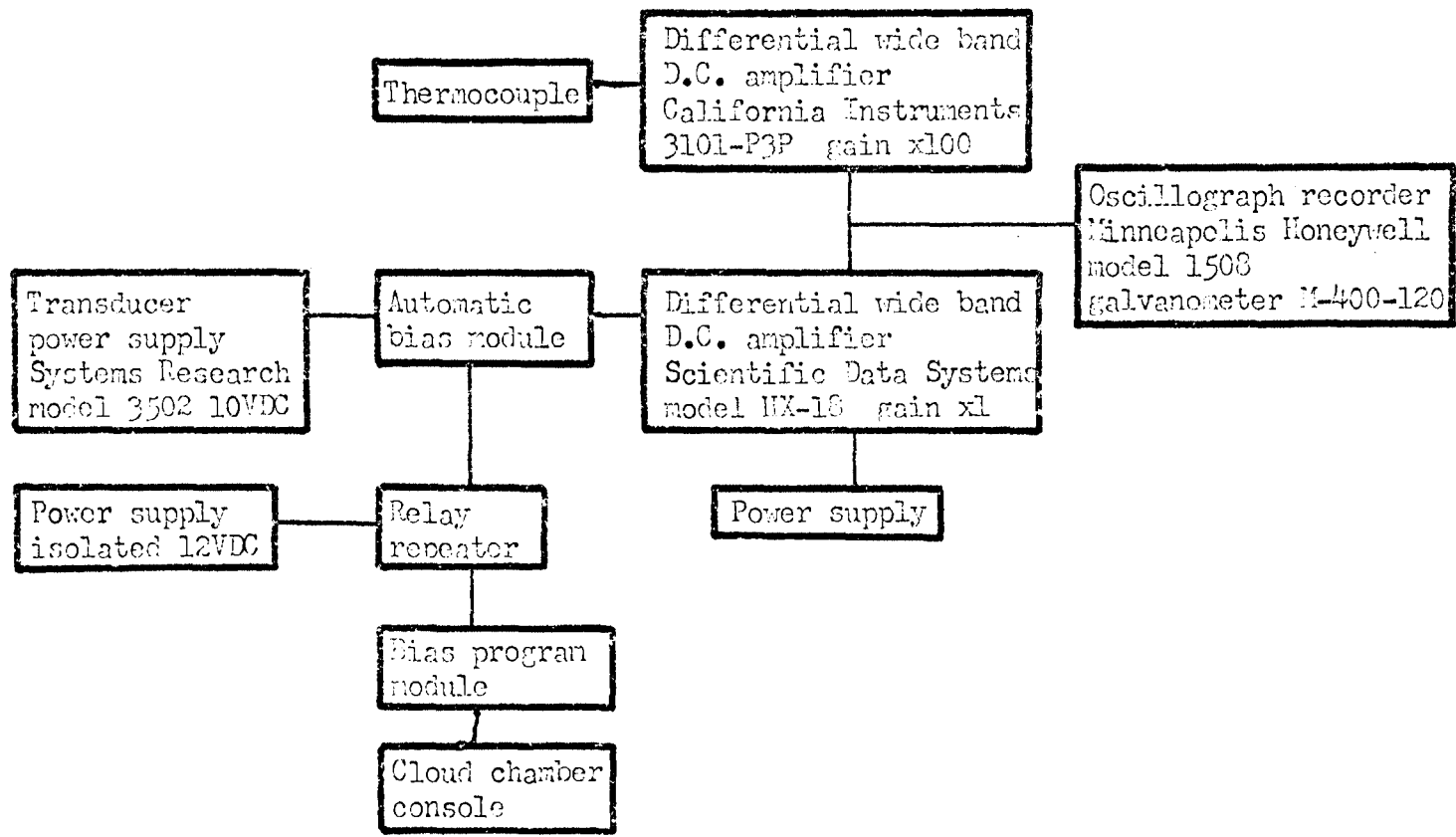


Fig. 23. Block diagram of the temperature measuring system.

has been erroneously assumed to be indicative of the accuracy with which the thermocouple follows the temperature change. It was the purpose of this investigation to place the interpretation of fine wire thermocouple measurements on a sound basis. The commercial availability of 0.0005 in. dia. thermocouple wire and the relative ease with which thermocouples can be fabricated from this size material strongly recommend it for temperature measurements. However, data taken in an expansion cloud chamber with such fine wire thermocouples indicated that the thermal capacity of the thermocouple itself was not negligible.

Let us look briefly at the physical situation. The thermocouple is initially in thermal equilibrium with the gas. Suddenly the gas temperature begins to decrease. The thermocouple wire has a finite thermal capacity and must communicate its excess heat to the surrounding gas by diffusion.

If the expansion proceeds at a constant rate, the temperature of the surrounding medium drops nearly linearly and the thermocouple becomes a steady source of heat just as surely as if it were being heated with an electrical current. Now under these circumstances the rate of diffusion of heat away from the thermocouple will adjust itself so that a steady-state condition exists, i.e. heat diffuses away from the thermocouple just as fast as it is being developed in the thermocouple (to use the electrical analogy). The establishment of the steady-state requires of the order of 10^{-4} sec. and so we see a very fast response to sudden environmental changes. But the temperature being indicated by the thermocouple is not the true temperature of the gas.

The question then arises, how far off are the temperature readings? This point cannot be resolved by experiment alone. First let us determine the speed with which temperature equilibrium is attained within the

thermocouple wire itself. The solution to this problem is given by Churchill.⁶⁸

$$T(r,t) = 1 - 2 \sum_{n=1}^{\infty} \frac{J_0(\alpha_n r/r_0)}{\alpha_n J_1(\alpha_n)} e^{-\left(\alpha_n^2 \frac{\kappa}{C_p} \frac{t}{r_0^2}\right)} \quad (3-11)$$

where κ is the thermal conductivity, C_p is the heat capacity, r_0 is the radius of the thermocouple and the α_n are the zeros of the Bessel functions. $\alpha_1 = 2.405$, $\alpha_2 = 5.520$, $\alpha_3 = 8.654$ and $\alpha_4 = 11.79$. The chromel-alumel thermocouples used were made from 0.005 in. dia. wire. It is seen that a perturbation on the outside of the thermocouple is felt at the center with a half life of 3.0 microsec. After ten microsec. the center is within two percent and after 100 microsec it is within 10^{-8} percent of the outside temperature. Therefore, the relaxation time of the thermocouple itself is completely negligible. This is, of course, one necessary ingredient for fast response.

The calculation of the heat flow from the thermocouple surface out through the gas is much more difficult because the radial symmetry is lost when the gas begins to move past the thermocouple as it does in expansion cloud chambers. However, in this case the gas velocity is small and laminar flow may be assumed.^{69,70}

Since things are everywhere the same in the direction of the axis of the *stretched out* thermocouple wire, the problem reduces to a two dimensional heat flow problem.

$$C_p \frac{\partial T}{\partial t} = \kappa_g \frac{\partial^2 T}{\partial x^2} + \frac{\partial^2 T}{\partial y^2} + f(x,y,\dot{x},t) \quad (3-12)$$

where C_p is the heat capacity of the gas at constant pressure and κ_g is

the thermal conductivity of the gas. ($f(x,y,\dot{x},t)$) is a source function which allows for varying expansion speeds and also allows for the motion of the thermocouple through the gas. Only numerical solutions of this problem were attempted.

Figs. 24 and 25 show the results for an expansion in dry argon. The 0.0005 in. dia. (12 microns) thermocouple was located 3 in. from the top glass. The evacuated chamber was filled with tank argon which was passed through a liquid nitrogen cold trap to insure its dryness. Note that Fig. 25 indicates close agreement between the theoretically predicted thermocouple temperature and the measured thermocouple temperature. The difference is about 1.5 C° after a short time for a gas velocity of 2 cm/sec. Clearly, the fast response of the thermocouple is no indication of the accuracy with which it reads the gas temperature.

A simple calculation shows that the heat capacity of the wire is sufficient to cause a 0.1 C° rise in temperature in a cylinder of gas with a radius of 0.3 cm. This is only misleading since the small gradients make the dispersal of the evolved heat very slow.

Israel and Nix⁷¹ investigated the thermodynamic processes in the Pollak counter by inserting a fine wire thermocouple into the dry chamber, Fig. 26. They reported only a fraction of the temperature change expected from a calculation of the temperature drop by means of the adiabatic law. This result is exactly what one would expect from the foregoing analysis.

Moreover, their Fig. 2 showed a peculiar anomaly at a time of 1.5 sec. One can explain this feature as follows. At the end of the expansion the thermocouple still has a heated gas mass surrounding it and so it reads a temperature which is too high. The heating of the gas adjacent to the walls excites convection currents which take a moment to get

started. At 1.5 sec. after the expansion the convective motion sweeps the heated gas surrounding the thermocouple away, allowing it to read a temperature which more closely approximates the true temperature. The temperature readings from about 2 sec. on should more closely approximate true values and an extrapolation of this part of the curve back to the time immediately after the expansion gives more nearly the temperature drop brought about by the expansion.

In conclusion, we might say that thermocouple measurements of gas temperature present a degree of complexity which has not been generally recognized. The actual response of the fine wire thermocouple (as opposed to the speed with which it responds to a sudden change in its environment) is very slow. Moreover, the equations of state for the gases tested check very well against the data obtained in these experiments.

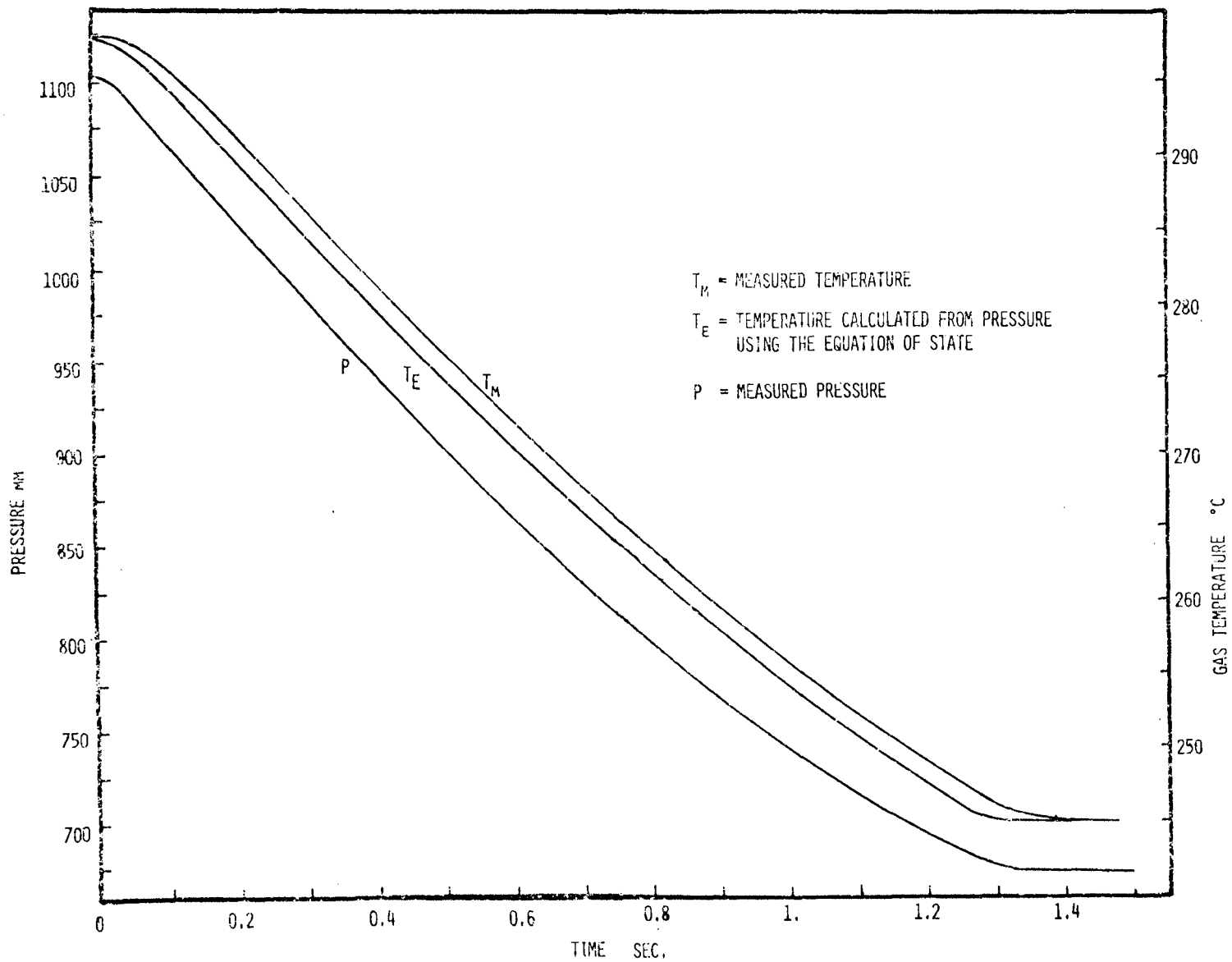


Fig. 24. Measured temperature and pressure in dry argon.

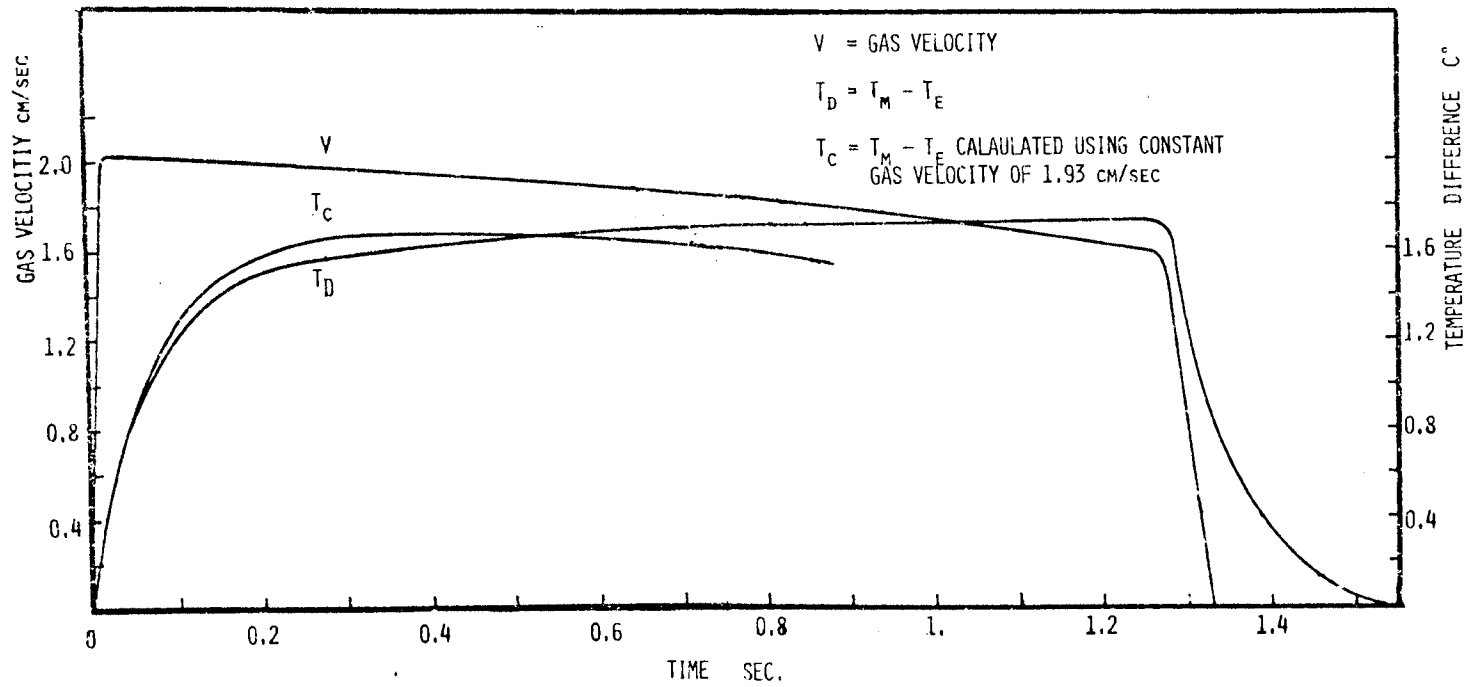


Fig. 25. Temperature difference for the expansion shown in Fig. 24.

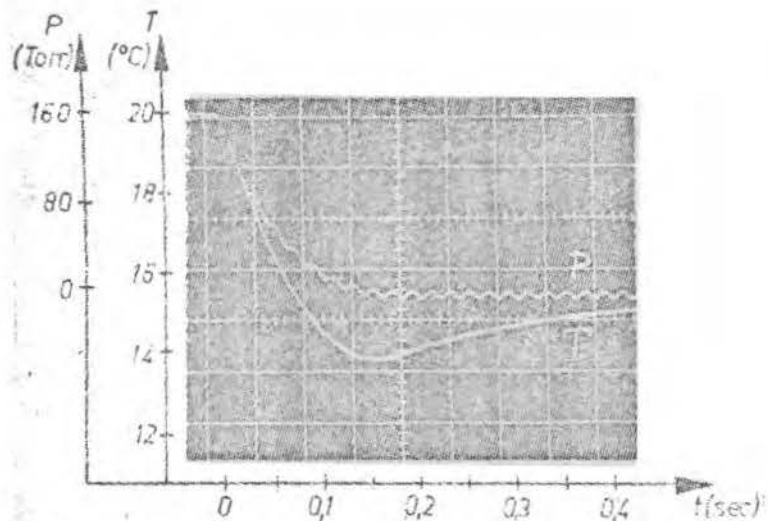


FIG. 1. — Variation of pressure P and temperature T during a dry adiabatic expansion in the condensation nuclei counter of Pollak.

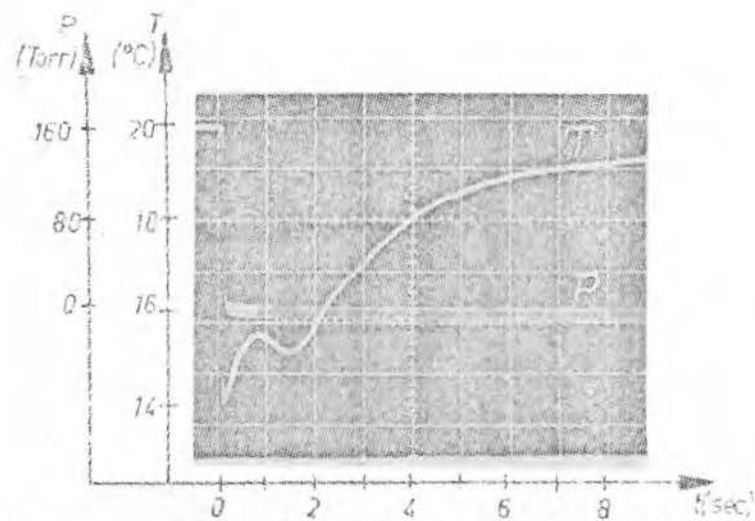


FIG. 2. — Record of the reheating in the condensation nuclei counter.
 P : pressure; T : temperature.

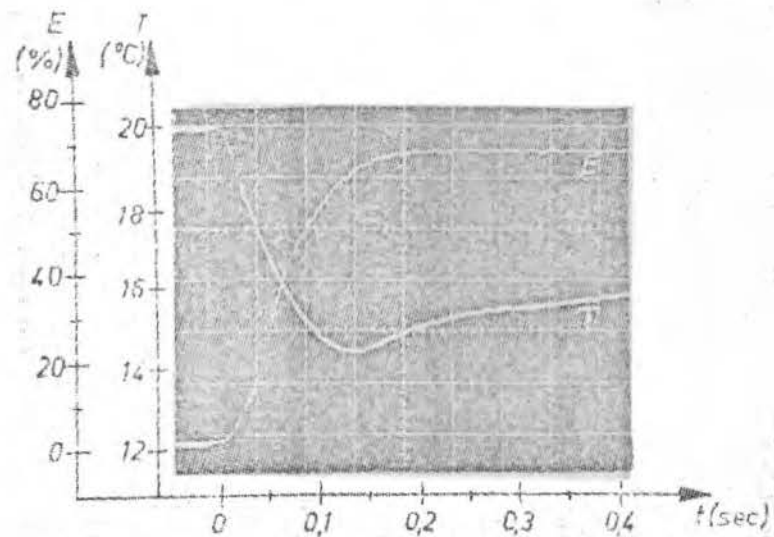


FIG. 3. — Variation of temperature T and extinction E of light.

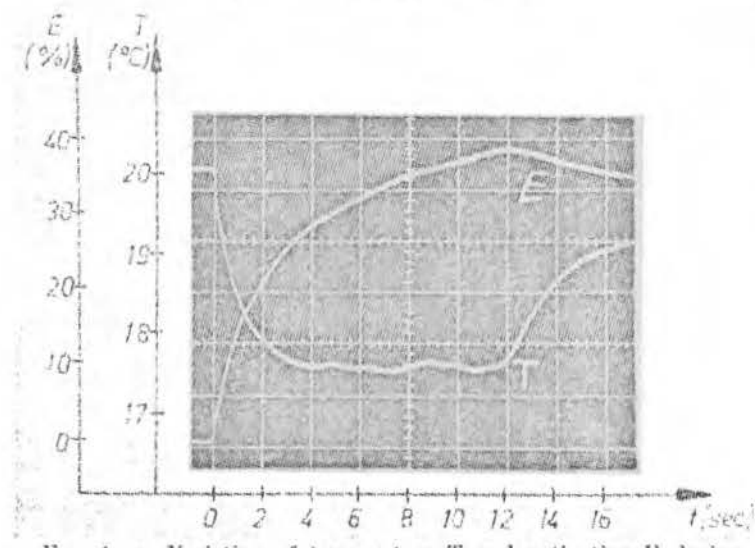


FIG. 4. — Variation of temperature T and extinction E during an extended expansion.

CHAPTER IV

NUCLEATION MEASUREMENTS

The first homogeneous nucleation measurements to be made in this laboratory were made by Allard and Kassner.²⁰ Later, additional measurements were made by Kassner and Schmitt³⁷ with some improvements in technique and data analysis. One of the principal problems was related to the inability to adequately account for the various aspects of droplet growth: bulk depletion of available vapor, effect of diffusion profiles around growing droplets on subsequent nucleation (dead space) and competition for the available vapor supply by closely spaced droplets. Droplet growth measurements are conspicuously lacking and much effort has been expended in studying these effects.

The author has attempted to elucidate the disparity which exists in the literature on the nucleation rate of water vapor by providing comprehensive measurements of the nucleation rate as a function of supersaturation, temperature and sensitive time. Fig. 27 shows data representing the average nucleation rate as a function of average supersaturation for narrow nucleating pulses of sensitive time 0.01 sec. The circles represent data in argon while the crosses represent data in helium, both for an initial starting temperature of 22.5°C. Note that the data in Argon are noticeably and reproducibly higher. Dawbarn⁵² first observed this effect in this laboratory. Classical theory predicts no effect on the nucleation rate due to the nature of the non-condensable gas. This effect might be the manifestation of the alteration in the free energy of the critical cluster due to the inclusion of an argon

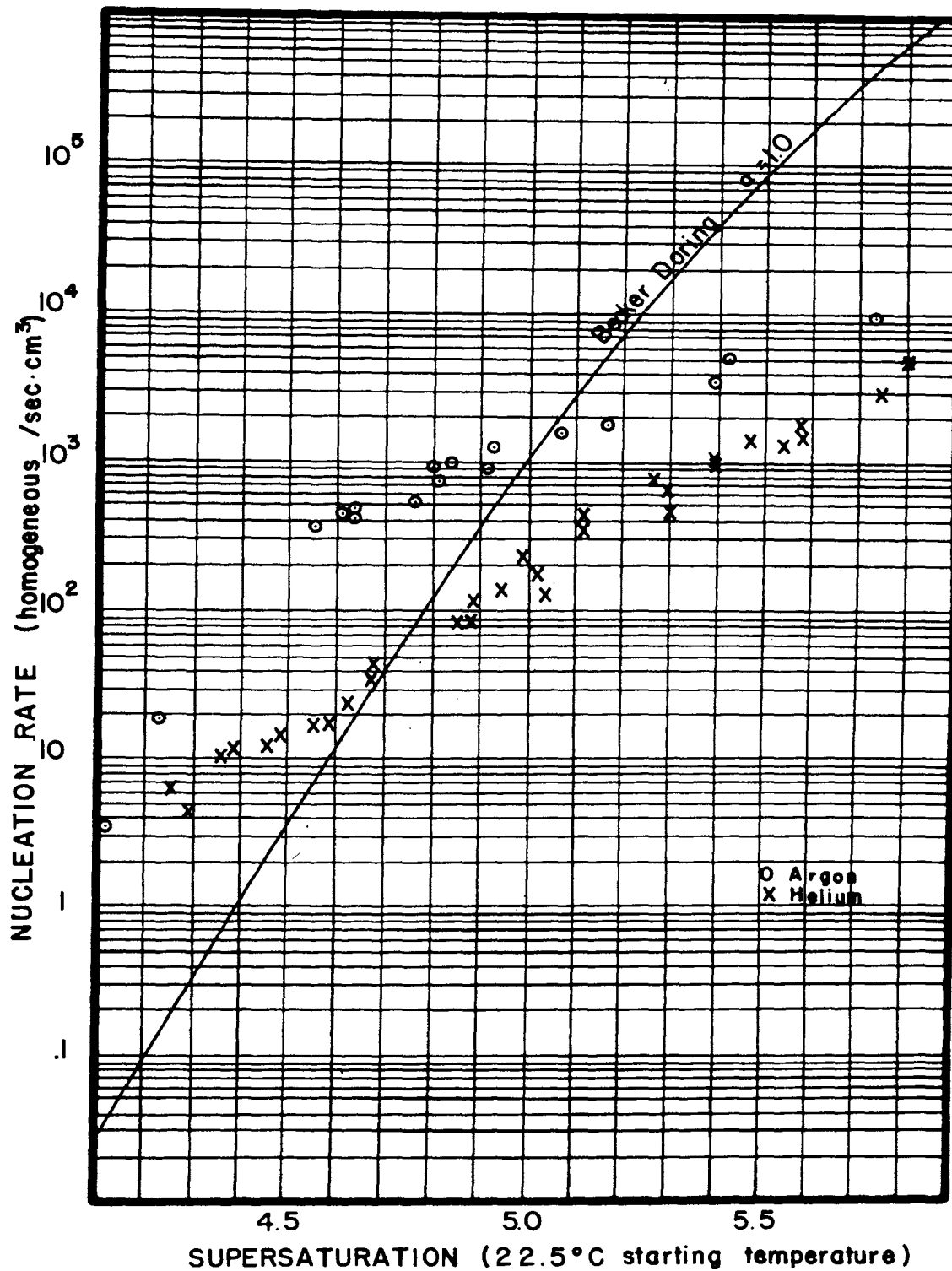


Fig. 27. Comparison of the nucleation rate in argon and helium.

atom in a clathrate like structure of water molecules in the embryo. Pauling^{72,73} has hypothesized such a hydration scheme for xenon in the bulk water structure. Fig. 28 shows a possible arrangement of 20 molecules when an ion is included in the cluster. Fig. 29 shows a possible arrangement of 24 neutral molecules into a clathrate like structure. These two arrangements are dodecahedral and tetrakaidecahedral respectively and are the smallest possible configurations where each oxygen molecule has three hydrogen bonds and the bond angles are maintained near the normal bond angle. If such a configuration actually exists, these structures should be particularly stable and there should be a minimum in the free energy curve for these particular configurations.

Parunge and Lodge⁷⁴ have measured the effect of nonpolar gases upon the freezing point of supercooled water. Their water was of sufficient purity that small droplets normally froze at -16°C . Their data is reproduced in Fig. 30. It is seen that there is a definite ordering of the water molecules due to the presence of the inert gas. Claussen and Polglase⁷⁷ have suggested that the larger voids required in the liquid by krypton and xenon might well be dodecahedral or tetrakaidecahedral, thereby accounting for the discontinuity in the freezing points. If the critical cluster for nucleation of the liquid from the vapor is of the clathrate structure, krypton and xenon might well fit into the critical cluster. This would result in a sizeable lowering of the free energy of the cluster and the nucleation rate of water vapor in these gases would be correspondingly increased.

Fig. 31 shows the number of droplets nucleated per cubic centimeter as a function of peak supersaturation for the narrowest possible pulses. Both the 12.5°C and 22.5°C data exhibit prominent inflections while the 31°C data gives the indication that an inflection may exist

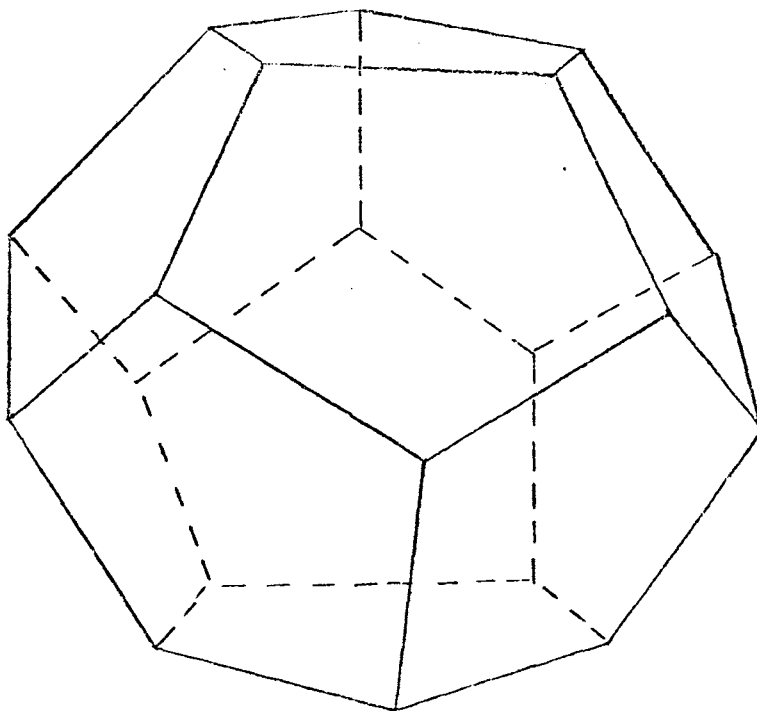


Fig. 28. The arrangement of hydrogen bonds for twenty water molecules in a dodecahedral configuration.

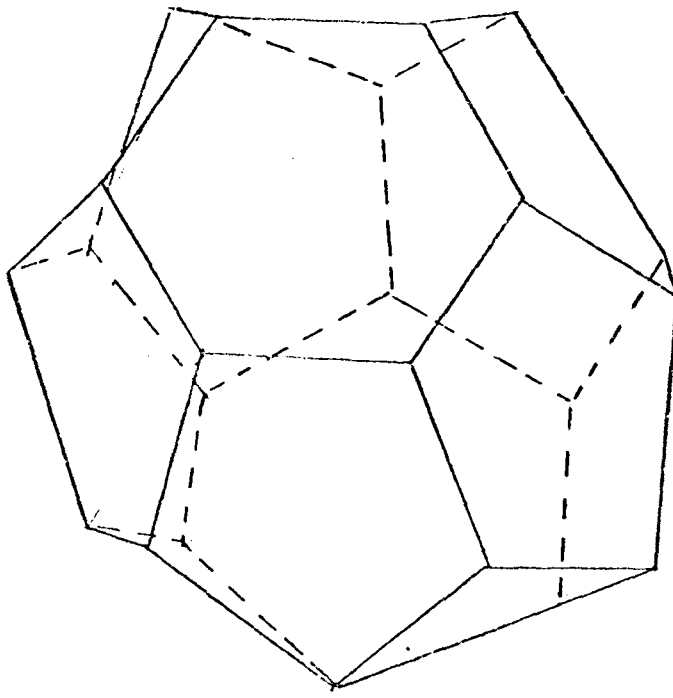


Fig. 29. The arrangement of hydrogen bonds for twenty-four water molecules in a tetrakaidecahedral configuration.

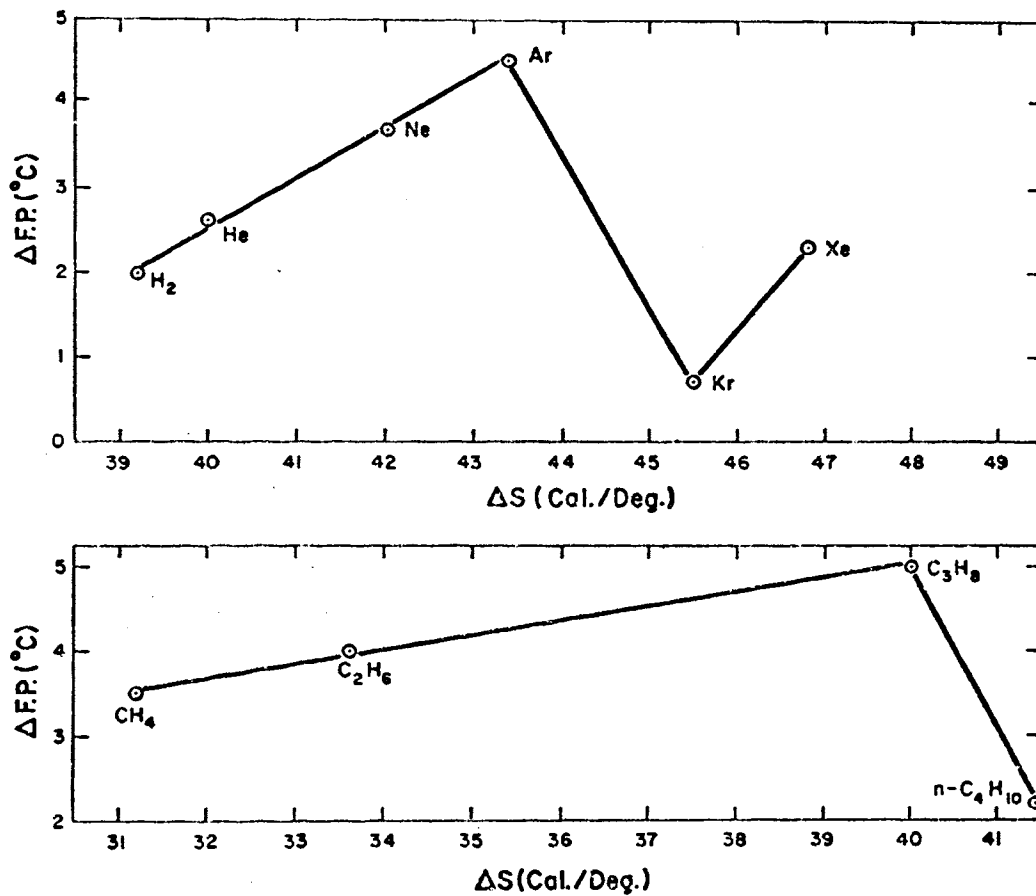


FIG. 1. Increase in the temperature of spontaneous freezing of 0.1-ml drops of solutions of two series of non-polar gases, compared with "pure" water, plotted against the entropies of hydration of the solute gases.

Fig. 30. Data of Parungo and Lodge.

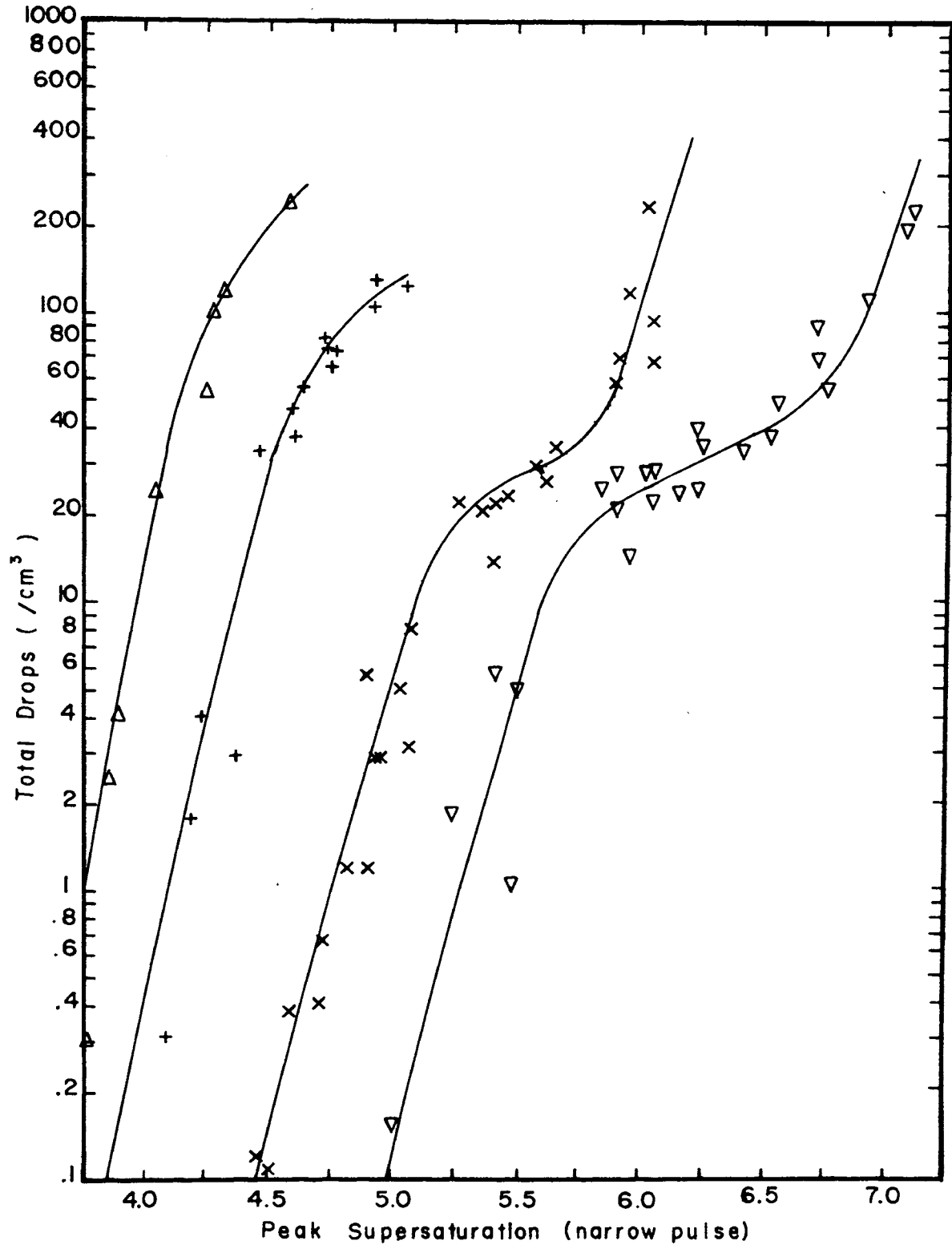


Fig. 31. Number of droplets nucleated as a function of peak supersaturation. The starting temperature is (Δ) 41.5°C, (+) 32.5°C, (x) 22.5°C and (∇) 12.5°C.

for higher droplet densities than could be measured in this experiment. If the number of droplets (corresponding to the plateau of the inflection for the 12.5° and 22.5° curves and the number estimated where the shoulder might lie for the other two helium curves) are compared, it is found that the number is nearly proportional to the initial vapor pressure of water in each case. Schuster⁷⁵ has measured the nucleation rate of water vapor in an argon atmosphere as a function of supersaturation with an initial temperature of 24°C. using light scattering techniques. His data agrees reasonably well with the author's both in slope and magnitude. His data reproduced in Fig. 32 shows slight evidence of an inflection at about the same point as the author's.

Fig. 33 is a correlation of the author's data with temperature dependence data found in the literature. Curve No. 1 is the author's data for an estimated droplet density of 100 drops/cm³ or a nucleation rate of 10,000 drops/cm³sec. Curve No. 2 is the corresponding data for 1 drop/cm³ or a nucleation rate of 100 drops/cm³sec. The dashed lines represent the path of the adiabatic expansion of the cloud chamber for the four sets of data. Curve No. 3 is the data of Volmer and Flood¹⁵ for a rate of 4 drops/cm³sec as estimated by Allard and Kassner.²⁰ The latter corresponds very closely to the author's data for a rate of 1 drop/cm³sec both in magnitude and in slope. The ϕ 's represent Powell's data for an estimated nucleation rate of 10⁵ drops/cm³sec. The author's data, extrapolated to this nucleation rate, agrees reasonably well with that of Powell both in magnitude and in slope. Curve No. 4 represents the homogeneous nucleation rate data of Sander and Damkohler⁷⁶ for their estimated rate of 1 drop/cm³sec. The θ 's are Powell's ion limit data.

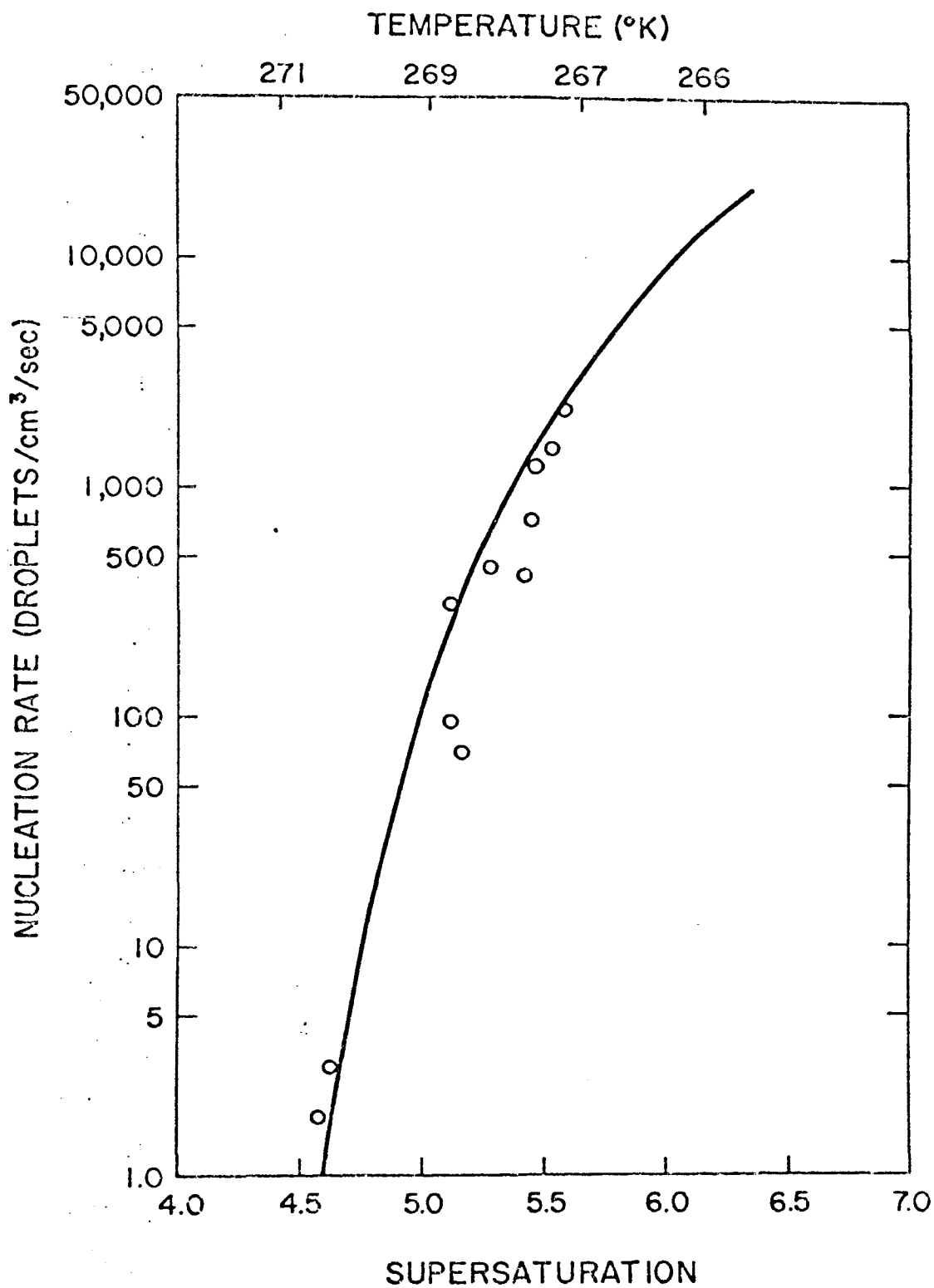


FIGURE 5-5 Variation of Modified Nucleation Rate with Supersaturation and Temperature

Fig. 32. Data of Schuster.

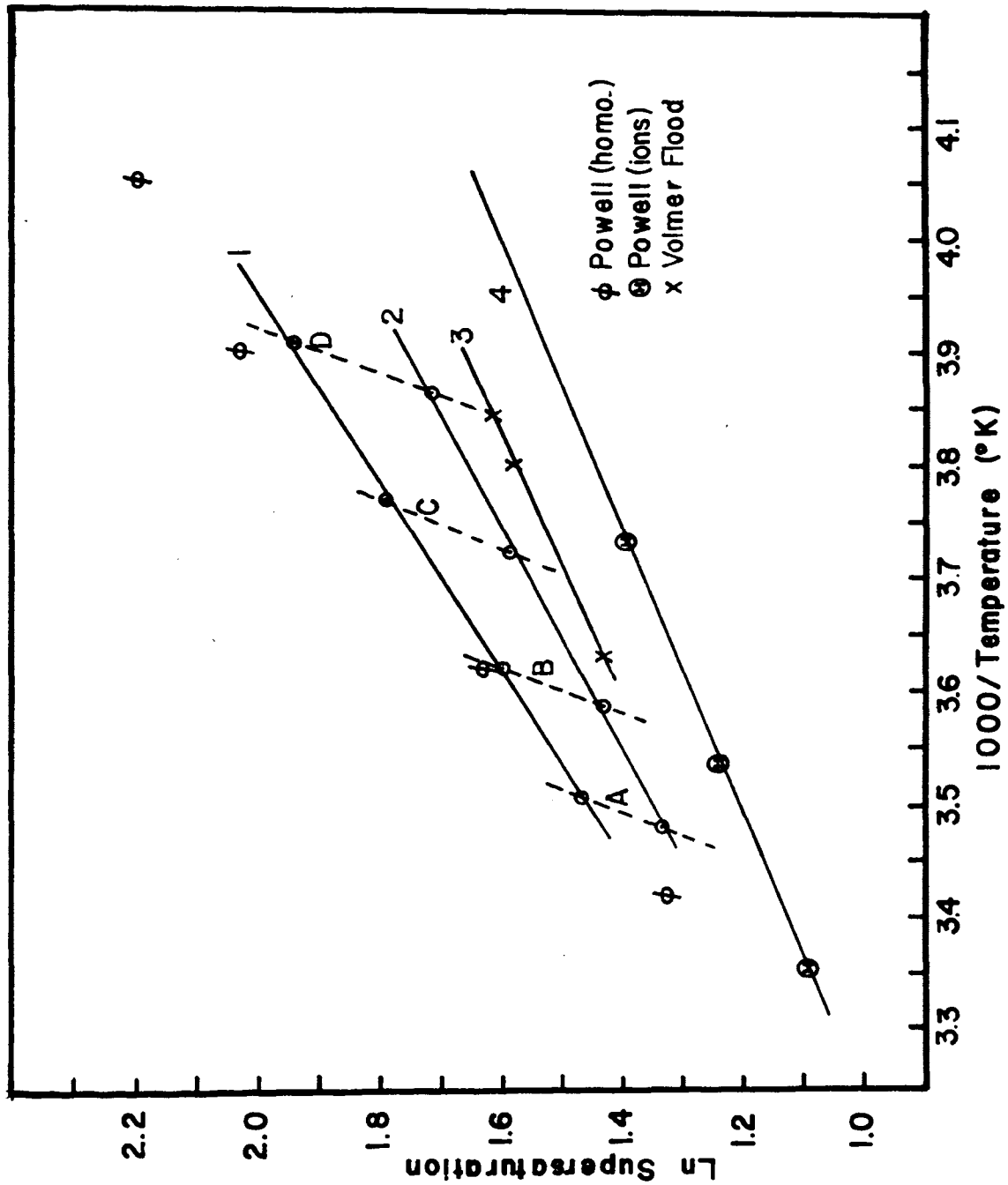


Fig. 33. Temperature dependence of the nucleation rate. The dashed curves are the paths of the adiabatic expansion for starting temperatures of (A) 41.0°C, (B) 32.5°C, (C) 22.5°C and (D) 12.5°C. Line (1) represents the author's data for 10,000 drops/cm³ sec, line (2) is the author's data for 100 drops/cm³ sec, line (3) is the data of Volmer and Flood and line (4) is the homogeneous nucleation data of Sander and Damkohler.

It is impossible to reconcile Sander and Dankohler's consistently low results unless they actually observed nucleation on ions. Curve No. 4 also agrees well with our results for nucleation on ions.

Fig. 34 shows the decrease in the measured nucleation rate as a function of time for supersaturations of 4.4, 4.9, 5.2 and 5.6. The dotted lines are the expected decrease resulting from the effects of droplet growth as calculated using the method given in the following chapter. It is seen that the decrease in the nucleation rate cannot be due to the effects of droplet growth. Moreover, the greatest deviation occurs at the supersaturation corresponding to the inflection in the curve of Fig. 31. In the data where the initial temperature of the cloud chamber was 12.5°C, the cut-off in the nucleation process with increasing sensitive time is even more pronounced. In this case, everything that is going to nucleate does so in the first 0.01 sec. for supersaturations between 6.0 and 6.5. Because of the unexpected nature of this data, both the 12.5°C and 22.5°C data were repeated several weeks after the initial data was taken. There was complete agreement with the previous data for both temperatures so it was felt that the data were accurate.

It is the cut-off phenomenon which indicates the presence of a heterogeneous nucleating agent. This effect is clearly not due to nucleation on ions. A clearing field of 80V/cm is maintained until the beginning of the expansion. Old ions are swept out and ion tracks show clearly at a much lower supersaturation.

Nucleation rate measurements have been carried out in this laboratory since 1960 and the results have all been self-consistent. The purity of the helium-water vapor system used in the experiments has varied widely without any change in the results. Water purification methods

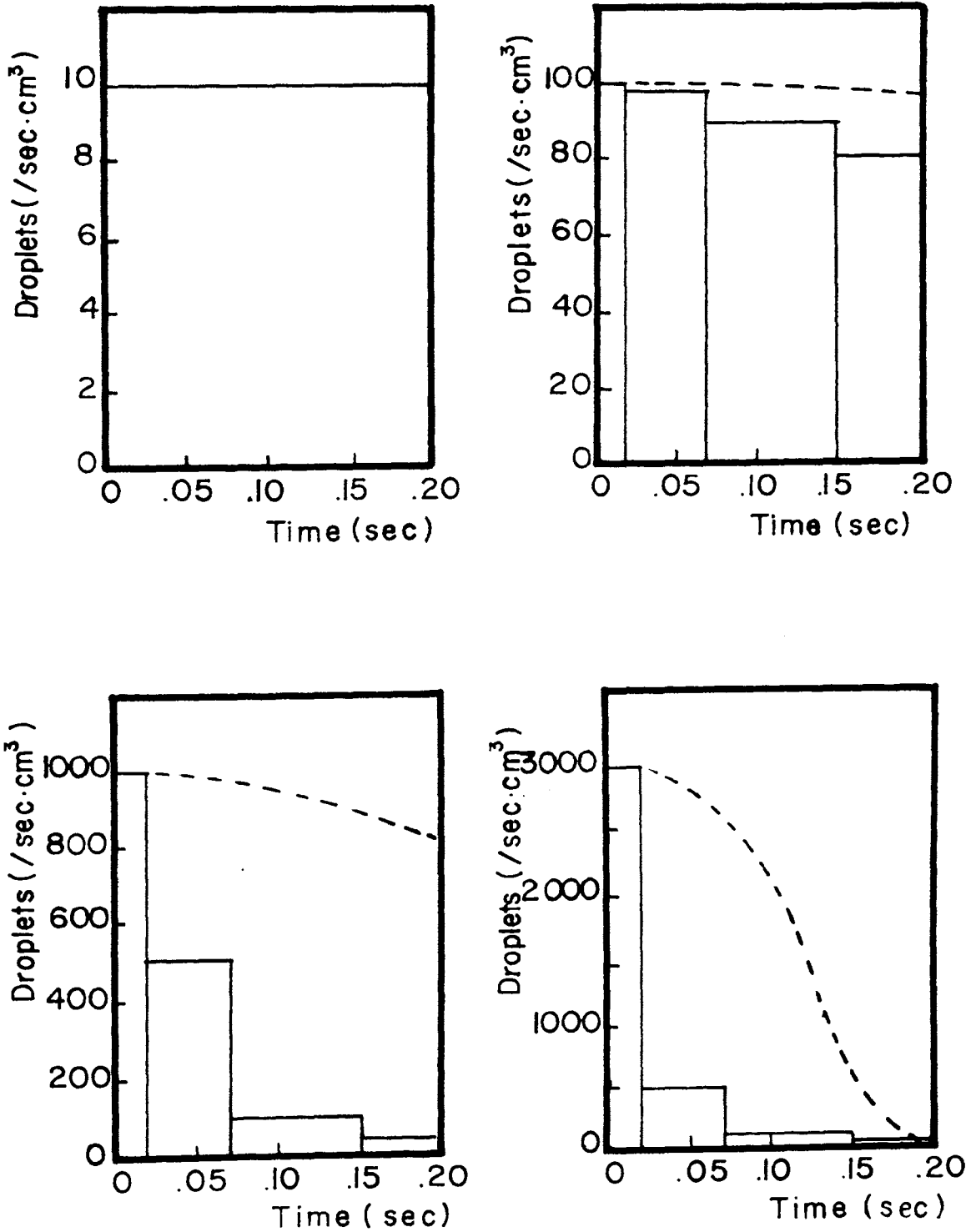


Fig. 34. Nucleation rate as a function of time. The starting temperature is 22.5°C and the supersaturations are left to right respectively 4.4, 4.9, 5.2, and 5.6.

have included deionization columns, ordinary glass distillation systems, distillation columns preceded by a charcoal absorption cell and the method described in Chapter II. None of these have produced any variance in the results. It is difficult to imagine any ordinary impurity which would be present with the observed consistency and in the small concentrations observed in these experiments (30 to 100 molecules/cm³). Because the concentration of the impurity varies in proportion to the initial vapor pressure of the water, it seems likely that this particular nucleating agent is a neutral product formed through the action of ionizing radiation on the water vapor.

The data in the literature seems to be separable into two basic groups. One, such as the data of Volmer and Flood,¹⁵ where measurements have been made yielding very small droplet densities and another, such as the data of Powell,¹⁶ where measurements have yielded large droplet densities, see Fig. 33. Both of these are in good general agreement with the author's results, so it seems likely that the other observations have also recorded the same effect. Moreover, this mode of heterogeneous nucleation retains many of the characteristics of the homogeneous nucleation process and possesses a critical supersaturation limit very close to that predicted by the Becker-Doring theory. The similarity with the homogeneous nucleation process gives a clue as to the nature of the process.

Since the normal rate of ionization is due to both cosmic rays and natural radioactivity, the rate of production of molecules of the nucleating agent would be expected to be fairly constant with the largest fluctuations being due to cosmic ray showers. Cloud chambers cycling at a regular rate would be expected to experience about the same build-up between expansions whereas devices operating with irregular cycle times could easily experience large deviations in results. The scatter

of data points experienced in this work near and below the plateau is reminiscent of that found by Allard⁴⁹ in his data for nucleation on random ionization. It is believed that this may explain the scatter of results displayed by Katz and Ostermier³⁹ for water since they probably cycled their diffusion chamber at irregular intervals.

4-1. Theory. In classical nucleation theory it is assumed that small clusters of water vapor molecules possess the properties of bulk water, i.e. they have a definite temperature and their surface may be characterized by the bulk surface tension for water. When a vapor molecule impinges upon a cluster, a quantity of Gibbs free energy, $kT \ln S$, is released in the transformation from gas to liquid, assuming that the cluster may be considered as bulk water. However, the volume of the cluster must increase with the addition of each molecule so that some of the above energy goes into the creation of new surface, the total surface free energy of the cluster of radius r being $4\pi r^2 \sigma$. Hence, the energy of formation of a homogeneous cluster is

$$\begin{aligned} \Delta G_h &= -NkT \ln S + 4\pi r^2 \sigma & (4-1) \\ &= -4/3 \pi r^2 n_L \ln S + 4\pi r^2 \sigma \end{aligned}$$

where N is the number of molecules in the cluster, k is Boltzmann's constant, T is the absolute temperature of the gas, S is the supersaturation, σ is the surface tension and n_L is the molecular density of liquid water.

Since the volume has an r^3 dependence and the surface has an r^2 dependence, there is always a maximum point in the plot of free energy against radius. The radius to which the maximum free energy belongs

is called the *critical radius* and is found by differentiating the Gibbs free energy. The critical radius

$$r^* = 2\sigma/n_L kT \ln S \quad (4-2)$$

so that the free energy ΔG^* of the critical cluster becomes

$$\Delta G^* = 4/3 \pi r^{*3} n_L kT \ln S + 4\pi r^{*2} \sigma \quad (4-3)$$

$$= \frac{16\pi\sigma^3}{3[n_L kT \ln S]^2} \quad (4-4)$$

where $4/3 \pi r^{*3} n_L$ is the number of molecules in the critical cluster.

It is conjectured that a chemical reaction may take place between a molecule of the heterogeneous nucleating agent and a water molecule. It is also assumed that clustering proceeds upon this complex chemical entity in much the same way that it does upon the clusters in the homogeneous case. The energy of formation of a heterogeneous cluster, i.e. a cluster including the chemical bond of energy ϵ , is

$$\Delta G_\epsilon = -4/3 \pi r^3 n_L kT \ln S + 4\pi r^2 \sigma - \epsilon \quad (4-5)$$

It is seen that because the ϵ term is independent of radius, the critical radius of the heterogeneous cluster is identical with that of the homogeneous cluster (neglecting the size of the single chemically active molecule) so that

$$r^* = 2\sigma/n_L kT \ln S \quad (4-6)$$

and

$$\Delta G_\epsilon^* = \frac{16\pi\sigma^3}{3(n_L kT \ln S)^2} - \epsilon \quad (4-7)$$

The free energy of a cluster as a function of radius is shown in Fig. 35 for both the case of the homogeneous and the heterogeneous clusters.

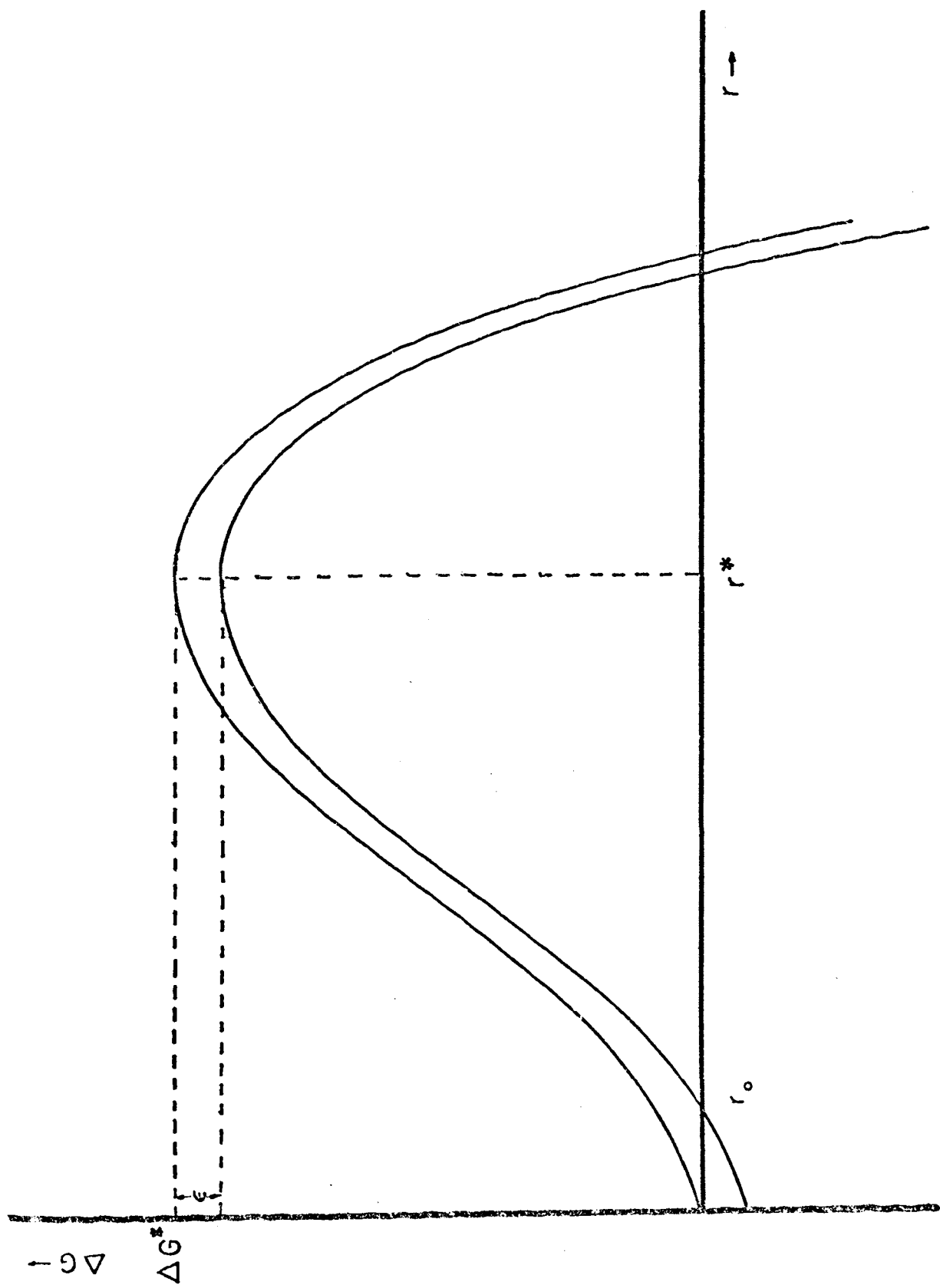


Fig. 35. Gibbs free energy vs. radius.

A small stable cluster of radius r_c exists at saturation which serves to give the heterogeneous clusters a slight head start in the fluctuation process. The author is fully aware of the shortcomings of the classical liquid drop theory and in particular the difficulties which arise when the theory is applied to very small clusters.

The gas is assumed to obey a Boltzmann type distribution law. It is therefore assumed that the probability of occurrence of a process is determined by the energy required to establish the process, i.e.,

$$P = \exp(-\Delta G/kT) \quad (4-8)$$

where P is the probability of occurrence of a cluster whose free energy of formation is ΔG , k is Boltzmann's constant and T is the absolute temperature. If N_0 is the density of monomer water molecules in the gas and N_ϵ is the density of the heterogeneous nucleating centers, the expected density of clusters of size g of both the homogeneous and the heterogeneous types, N_{gh} and $N_{g\epsilon}$, is

$$N_{gh} = N_0 \exp(-\Delta G_h/kT) \quad (4-9)$$

$$N_{g\epsilon} = N_\epsilon \exp(-\Delta G_\epsilon/kT) \quad (4-10)$$

Fig. 36 shows how the number, N_{gh} , of clusters of size g varies with g . The minimum of the curve is the critical cluster size. The distribution is assumed to cut off at a value of g slightly larger than g^* (say about $2g^*$, the exact value is not critical) so that an infinite supply of vapor is not required to maintain the distribution. It is assumed that each cluster which becomes larger than g^* by the acquisition of another vapor molecule becomes a free growing droplet and will continue to grow to macroscopic size. In the classical theory, which is a precatastrophic

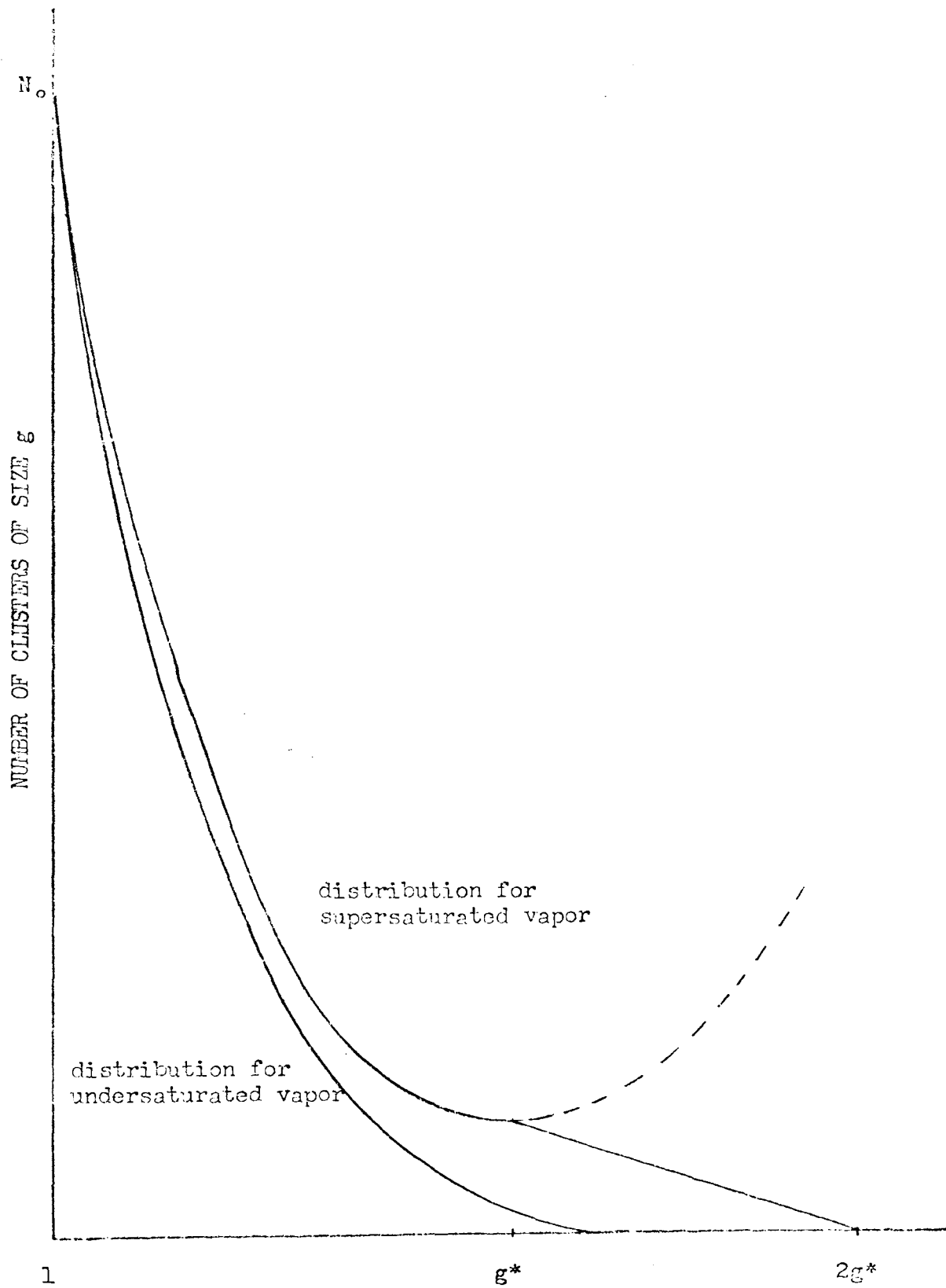


Fig. 36. Distribution of clusters.

theory, these droplets are assumed to be broken up by a Maxwell demon and returned to the vapor as monomers so that a steady state is maintained. The nucleation rate is the number of droplets growing larger than the critical size per unit time. Therefore, the nucleation rate is the product of the number of critical size clusters and the probability of the critical cluster acquiring another molecule. Hence

$$J_h = \frac{p}{(2\pi mkT)^{1/2}} N_0 \exp\left[-\frac{16\pi\sigma^3}{3kT(n_L kT \ln S)^2}\right] \quad (4-11)$$

$$J_\epsilon = \frac{p}{(2\pi mkT)^{1/2}} N_\epsilon \exp\left[-\frac{16\pi\sigma^3}{3kT(n_L kT \ln S)^2} - \frac{\epsilon}{kT}\right] \quad (4-12)$$

where p is the vapor pressure of the water and m is the mass of a water molecule.

It is assumed that the number density of monomer water molecules, N_0 , is so large that its value does not change sensibly during the nucleating process. N_ϵ is much smaller, however, and the supply of these heterogeneous nucleating agents is quickly depleted. Therefore, a situation analogous to that of radioactive decay in nuclear physics exists.

$$-\frac{dN_\epsilon}{dt} = P_\epsilon N_\epsilon \quad (4-13)$$

where $P_\epsilon = J_\epsilon/N_\epsilon$.

This equation is integrated from time $t=0$ to time $t=t$ and from the initial density $N_{\epsilon 0}$ to instantaneous density N_ϵ .

$$\int_{N_{\epsilon 0}}^{N_\epsilon} \frac{dN_\epsilon}{N_\epsilon} = -\int_0^t P_\epsilon dt \quad (4-14)$$

$$N_\epsilon = N_{\epsilon 0} \exp(-P_\epsilon t) \quad (4-15)$$

The total nucleation rate is the sum of the homogeneous and heterogeneous nucleation rates

$$J = J_n + J_e \quad (4-16)$$

$$= \frac{p 4\pi r^*2}{(2\pi m k T)^{1/2}} \left[\exp \frac{16\pi\sigma^3}{3kT [n_L k T \ln S]^2} \right] \left(N_0 + N_{e0} \exp(-P_e t + \frac{\epsilon}{kT}) \right)$$

The second term in the right hand bracket is the heterogeneous contribution to the nucleation rate. Fig. 37 shows how the nucleation rate varies with supersaturation. The dotted line is the path taken by the cloud chamber during an expansion. Depletion of the heterogeneous nucleating centers brings the rate down to that of the purely homogeneous level in a short time.

If the classical liquid drop model is assumed to be valid, one can surmise several things about the free energies and cluster sizes from the data. Putting the free energy into the form of Eq. (4-3) instead of that of Eq. (4-4) brings out the dependence of the critical cluster size and surface energy terms more clearly.

$$J = \frac{p 4\pi r^*2}{(2\pi m k T)^{1/2}} \left[S \left(\frac{4}{3} \pi r^*3 n_L \right) \exp -4\pi r^2 \sigma / kT \right] \left(N_0 + N_{e0} \exp(-P_e t + \frac{\epsilon}{kT}) \right) \quad (4-18)$$

It is seen that the slope of the curve on a plot of $\ln J$ vs. S for constant temperature will give the number of molecules in the critical cluster, $4/3\pi r^*3 n_L$. This would indicate that the critical size may only be 35 and not the 80 predicted by the Kelvin-Thompson equation. This is not surprising since it has been shown⁷⁸ that the surface tension of small drops should be lower than that of the bulk liquid. If this is the case experiments, such as those using nozzles for which it is predicted

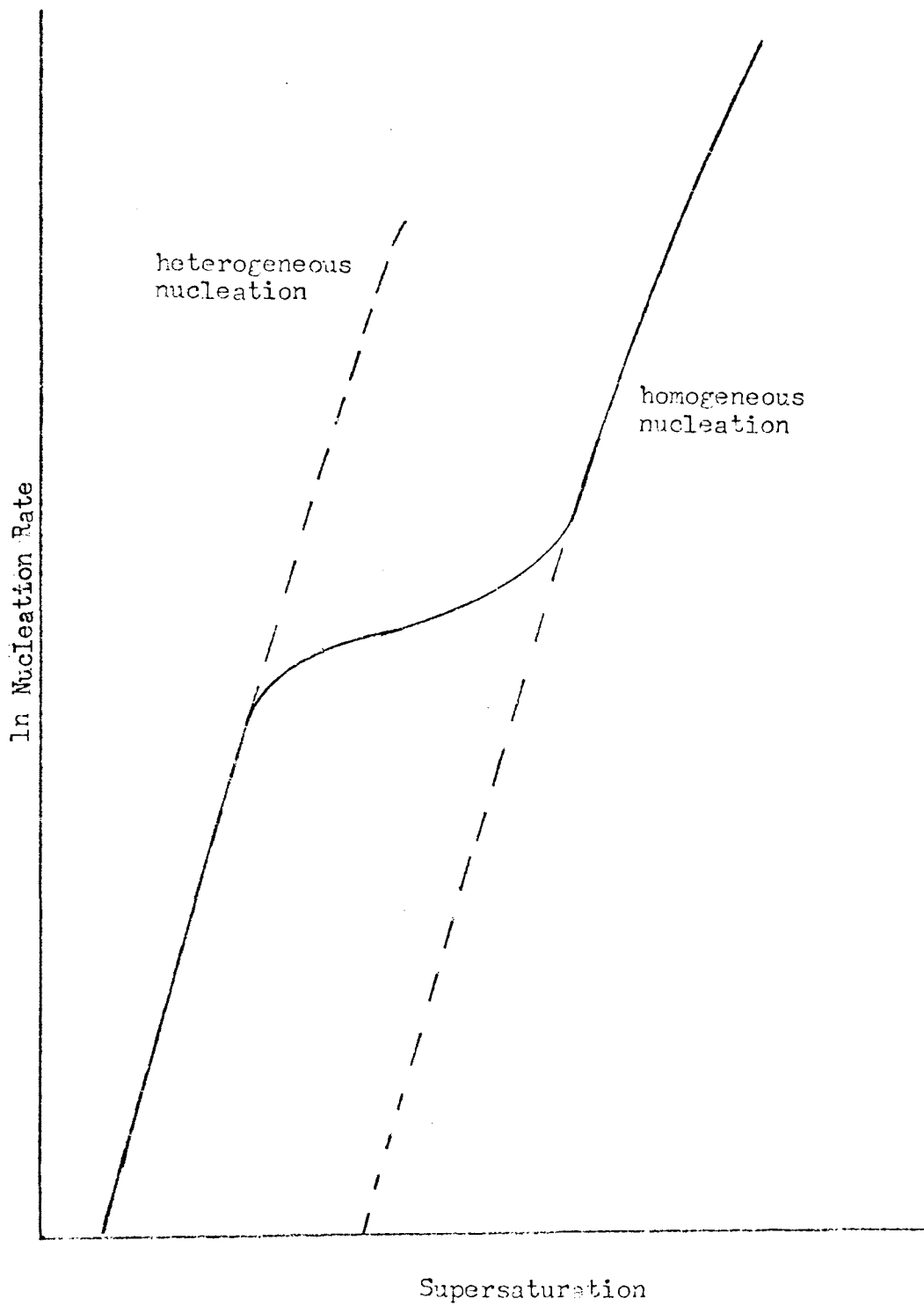


Fig. 37. Comparison of homogeneous and heterogeneous nucleation rates. The solid curve is the total nucleation rate observed in the cloud chamber.

critical cluster sizes are of less than ten molecules, must be re-considered.

It is also seen that the slope of the plot of $\ln S$ vs. $1/T$ gives the surface energy per molecule in the critical cluster which differs in the two cases. The slope of the curves for the homogeneous and heterogeneous nucleation must be different because the heterogeneous slope has included in it an extra $\epsilon/(4/3\pi r^3 n_L)$ term. Moreover, the theory of this chapter predicts a smaller slope for the case of heterogeneous nucleation which is in agreement with experimental data. There is also the additional effect due to the initial vapor pressure of the water vapor which is another temperature dependence which must be included when intercomparing data of different starting temperatures.

CHAPTER V

DROPLET GROWTH

In order to assess the effects of droplet growth upon the nucleating vapor, a detailed calculation is required which accounts for vapor depletion, release of latent heat and the effect of the nonuniform vapor and temperature profiles around the growing drop. An exact calculation is impossible without resorting to the theory of nonuniform gases. Computational complexity of such considerations are discouraging. It is apparent that a simpler version of the theory will be quite adequate for the purposes of this work provided that the depletion of vapor and the evolution of latent heat never become a dominating effect.

The problem of the diffusional growth of liquid droplets from the vapor has been considered by numerous investigators. Frisch and Collins⁷⁹ extended the range of validity down to droplets whose diameter was of the order of magnitude of the mean free path of the gas molecules. They relegated the entire thermal diffusion process to a simple accommodation coefficient which would appear to lose the complex interdependencies of the thermal diffusion process on other physical parameters.

Bagge, Becker and Bekow⁸⁰ formulated a solution for the mass flux which connects continuously to the surface of the drop via a connection with kinetic theory. However, they do not follow similar considerations in the case of thermal transport. Mason⁸¹ takes into account kinetic interactions with the surface by deriving a modified diffusion coefficient. Although it seems to be implicitly implied, he makes no mention of the concept of either a temperature or vapor jump at the surface of the drop.

Beucher⁸² develops a purely kinetic treatment of droplet growth which is valid down to the size of the critical nucleus defined by nucleation theory. He finds that the heat capacity of the droplet accounts for about half as much power as the creation of new surface, both effects dying out simultaneously at about twice the critical radius.

Neiburger and Chien⁸³ calculated droplet growth assuming macroscopic diffusion processes. They accounted for curvature, hygroscopicity and heating caused by the release of latent heat. They, however, neglected the effective modification of the diffusion coefficients at the droplet surface and, hence, did not account for a temperature or vapor density "jump" at the droplet surface.

Schuster⁷⁵ calculated droplet growth taking into account the effects of double diffusion of heat and vapor. He assumes, for simplicity, that the shape of the diffusion profile outside the droplet may be described by the function $1 - \exp(-R_0/r)$ where R_0 is a parameter of the order of the mean free path. This function is used to calculate the vapor density at a point just outside the surface of the droplet. He used kinetic theory to calculate the actual rate of growth of the droplet. His solution is iterated through time in much the same manner as the author's. This technique in conjunction with a series approximation for the above mentioned exponential allows the problem to be solved in closed form.

Carstens⁸⁴ intercompares the predictions of the steady state and the non-steady state versions of the diffusion droplet growth theory. It was found that a cellular approach to the quasi-steady state theory very closely approximates the nonsteady state theory. Reiss and La Mer⁸⁵ demonstrated the effectiveness of the cellular model but only considered

vapor diffusion. More recently the cellular model has been used by Zung⁸⁶ to describe the evaporation of clouds and sprays. Smith⁵³ described the evaporation of very small water droplets utilizing a kinetic connection at the droplet surface. However, he did not use a cellular model.

Carstens and Kassner⁸⁷ discuss in some detail various aspects of droplet growth theory as they apply to cloud chamber measurements. The droplet growth theory utilized in this work is largely based upon their conclusions.

5-1. Droplet growth equations. Most cloud chamber experiments are arranged such that droplet growth occurs in a medium composed of a vapor in dilute solution with an inert gas. Vapor diffusion and thermal diffusion are both controlled by the nature of the inert gas. In the region where droplet radii are much larger than the mean free path of the gas molecules, the quasi-steady state diffusion equations constitute an adequate description of droplet growth.

$$\nabla^2 \rho = K_\rho(t) \quad (5-1)$$

$$\nabla^2 T = K_T(t) \quad (5-2)$$

where ρ and T are the vapor density and temperature and $K_\rho(t)$ and $K_T(t)$ are homogeneous source functions which account for changes in the bulk vapor and temperature of the gaseous system brought about by external means.

Power balance is required at the droplet surface. The latent heat liberated by the condensing flux of vapor molecules must be carried away by the process of thermal diffusion which is accomplished principally by the noncondensable gas under our particular conditions. It is assumed

that the droplet maintains a uniform temperature throughout its interior and that the steady state temperature of the droplet is always maintained.

$$DL \left. \frac{d\rho}{dr} \right|_{r=a} = \kappa \left. \frac{dT}{dr} \right|_{r=a} \quad (5-3)$$

where D and κ are the mass and thermal diffusion coefficients respectively, L is the latent heat of condensation and a is the radius of the drop. The contribution of surface free energy and the thermal capacity of the drop are negligible throughout the region of interest in this work.

The specification of the outer boundary condition requires some physical insight. The principal defect in the steady state theory lies in the fact that the diffusion profiles prematurely extend to infinity. Since we expect to be able to calculate the diffusion profiles outside the droplet for the purpose of calculating the dead space, it is desirable to employ the cellular model. The imposition of an impermeable sphere of radius R which serves as the reservoir for heat and vapor for a droplet, eliminates to a large extent the errors in the diffusion profiles introduced through the use of the quasi-steady state equations.

For a truly isolated drop, R should be chosen so that the integral of the vapor depletion throughout the vapor density profile gives the mass of the drop. Under such a constraint $\rho(R)$ would remain constant throughout droplet growth and R would be moved out indefinitely as growth proceeds. Similar arguments apply to the thermal diffusion process, in general $R(T)$ and $R(\rho)$ being different. However, where a system of droplets exists the period of such isolation is short lived and the R spheres for different droplets begin to overlap. At this point a type of averaged competition for the available vapor becomes active. Strictly speaking, a distribution of R 's should be employed such that the $\left. \frac{d\rho}{dr} \right|_R$ are the

same for all droplets. However, Kassner and Carstens⁸⁸ have shown that the distribution of R's does not appreciably affect droplet growth rates until droplet densities exceed 10^6 drops/cm³. Therefore, it is feasible to use the same size impermeable sphere for all droplets, requiring only that the volume of these spheres fill all space. Fig. 38 illustrates the mechanics of choosing the radius of the impermeable sphere.

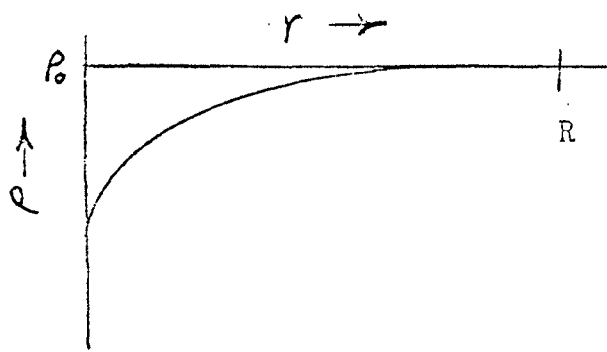
When the drop size is of the order of the mean free path, λ , its growth is dependent upon kinetic theory. A connection may be established between the macroscopic and microscopic regimes by equating the corresponding flux expressions:

$$D \frac{dp}{dr} \Big|_{r=a} = [I_v - I_c] \delta \quad (5-4)$$

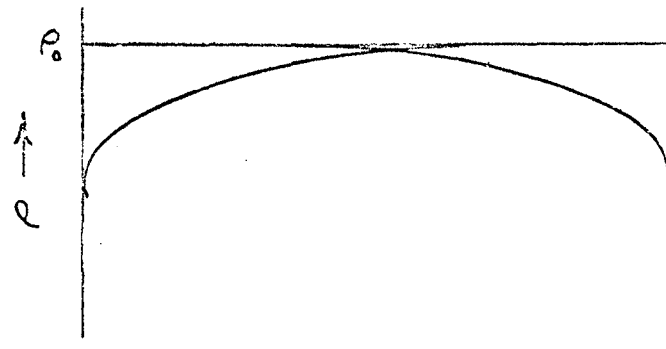
$$\kappa \frac{dT}{dr} \Big|_{r=a} = [I_g C_g \delta_g + I_\rho C_\rho \delta_\rho] \Delta T \quad (5-5)$$

where ΔT = the temperature jump between drop and vapor at the liquid-vapor interface, C_v = the specific heat per molecule of the vapor, C_g = the specific heat per molecule of the non-condensable gas, δ_g = the average proportion of energy transfer between the non-condensable gas and the liquid surface molecules, δ_v = the average proportion of energy transfer between the vapor and the liquid surface molecules, δ = the sticking probability of the vapor molecules on the liquid surface.

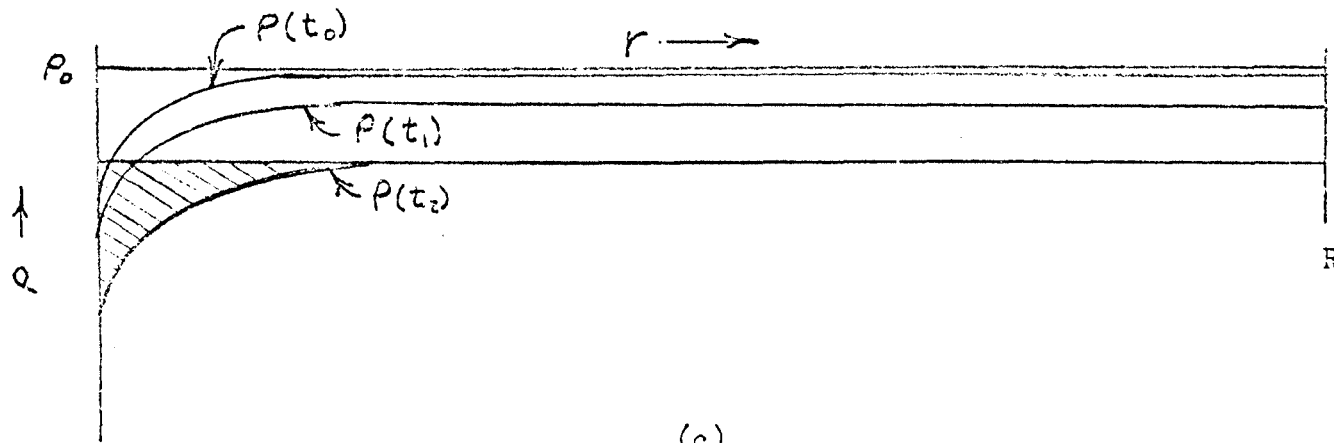
I_g = the flux of non-condensable gas molecules impinging on the drop surface, I_c = the flux of vapor molecules condensing on the surface of the drop as if it were in an equilibrium atmosphere, I_ρ = the flux of vapor molecules impinging on the drop surface.



(a)



(b)



(c)

Fig. 38. Choosing the radius of the impermeable sphere. When droplets do not compete for vapor, the radius R of the impermeable sphere is chosen so that there is no vapor depletion at R . Fig. a. When droplets are closely spaced this is not possible, Fig. b. A practical solution chooses R , not so that $\frac{\partial p}{\partial r}|_R = 0$, but so that $\frac{\partial p}{\partial r}|_R = 0$ and bulk corrections are made for vapor depletion (the error in the correction is the shaded area in Fig. c).

The existence of a temperature jump at the surface of the drop implies that the droplet is unable to maintain the equilibrium vapor pressure immediately outside its surface. Both a temperature jump and a vapor density jump exist.

$$\Delta T = T^{\text{eq}}(a) - T(a) \quad (5-5)$$

$$\Delta \rho = \rho^{\text{eq}}(a) - \rho(a) \quad (5-6)$$

It is assumed that $I_{\rho} C_{\rho} \Delta T$ may be neglected because of the dilutness of the vapor. Then Eq. (5-4) and (5-5) become:

$$D \left. \frac{d\rho}{dr} \right|_{r=a} = 1/4 \{ -\bar{v}_V [T^{\text{eq}}(a)] \rho^{\text{eq}}(a) + \bar{v}_V [T(a)] \rho(a) \} \delta \quad (5-7)$$

$$\kappa \left. \frac{dT}{dr} \right|_{r=a} = 1/4 \rho_g \bar{v}_g [T(a)] \Delta T C_g \delta_g \quad (5-8)$$

where $\bar{v}_g(T)$ = the average molecular velocity of the non-condensable gas at the temperature T , and $\bar{v}_V(T)$ = the average molecular velocity of the vapor at temperature T .

The solutions of Eq. (5-1) and (5-2) in terms of the boundary values are for the steady state:

$$\rho(r) = \frac{R-r}{R-a} \frac{a}{r} [\rho(a) - \rho(R)] + \rho(R) \quad (5-9)$$

$$T(r) = \frac{R-r}{R-a} \frac{a}{r} [T(a) - T(R)] + T(R) \quad (5-10)$$

These solutions substituted into the power balance equation give:

$$\frac{\rho(R) - \rho(a)}{T(a) - T(R)} = \frac{\kappa}{LD} \quad (5-11)$$

The steady state solutions also give for Eqs. (5-7) and (5-8):

$$\rho(a) = \frac{\frac{R}{R-a} \frac{4D}{a} \rho(R) + \bar{v}_v [T^{eq}(a)] \rho^{eq}(a) \delta}{\frac{R}{R-a} \frac{4D}{a} + \bar{v}_v [T(a)] \left[1 + \frac{\Delta T}{T^{eq}(a)}\right]^{1/2} \delta} \quad (5-12)$$

$$T(a) = \frac{\frac{R}{R-a} \frac{4D}{a} T(R) + \bar{v}_g [T^{eq}(a)] \delta_g}{\frac{R}{R-a} \frac{4D}{a} + \bar{v}_g [T(a)] \left[1 + \frac{\Delta T}{T^{eq}(a)}\right]^{1/2} \delta_g} \quad (5-13)$$

To obtain the asymptotic behavior of $\rho(a)$ and $T(a)$

let

$$D = \gamma \bar{v}_v \lambda_v$$

$$K = \gamma' \pi_g \bar{v}_g \lambda_g$$

where γ and γ' are constants of the order unity, λ_v and λ_g are the mean free paths of the vapor and non-condensable gas.

Eqs. (5-12) and (5-13) reduce to

$$\rho(a) = \frac{\frac{R}{R-a} 4\gamma(\lambda_v/a) \rho(R) + \rho^{eq}(a) \delta}{\frac{R}{R-a} 4\gamma(\lambda_v/a) + \left[1 + \frac{\Delta T}{T^{eq}(a)}\right]^{1/2} \delta} \quad (5-14)$$

$$T(a) = \frac{\frac{R}{R-a} \left(\frac{8}{5}\gamma'\right) \frac{\lambda_g}{a} T(R) + T^{eq}(a) \delta_g}{\frac{R}{R-a} \frac{\lambda_g}{a} \left(\frac{8}{5}\gamma'\right) + \left[1 + \frac{\Delta T}{T^{eq}(a)}\right]^{1/2} \delta_g} \quad (5-15)$$

These equations are simplified by the approximation $\left[1 + \frac{\Delta T}{T^{eq}(a)}\right]^{1/2} = 1$ and substitution of n and n' for the remaining variables and constants gives

$$\rho(a) = \frac{n \rho(R) + \rho^{eq}(a)}{1 + n} \quad (5-16)$$

$$T(a) = \frac{n' T(R) + T^{eq}(a)}{1 + n'} \quad (5-17)$$

In the limit that the mean free path is much smaller than the droplet radius:

$$\lim_{a/\lambda_g \rightarrow \infty} T(a) = T_{eq}(R)$$

$$\lim_{a/\lambda_v \rightarrow \infty} \rho(a) = \rho(R)$$

These imply the absence of local vapor depletion.

Another relationship is provided by the Kelvin-Thompson equation which takes into account the change in equilibrium vapor density with drop radius.

$$a = \frac{2\sigma}{\rho RT} / \ln \frac{\rho(a)}{\rho_{eq}(R)}$$

or
$$\frac{\rho(a)}{\rho_{eq}(R)} = \exp\left(\frac{2\sigma}{a\rho RT}\right) = \exp\left(\frac{B}{aT}\right)$$

where σ = the surface tension, ρ = the density of the condensed vapor, R = the gas constant.

This equation when combined with the Clausius-Claperyon equation (integrated for an ideal gas) gives:

$$\rho^{eq}(a) = \frac{\rho^{eq}(R)T(R)}{T^{eq}(a)} \exp\left(a_0 \frac{T^{eq}(a) - T(R)}{T^{eq}(a)T(R)}\right) \exp\left(\frac{B}{aT^{eq}(a)}\right) \quad (5-18)$$

where $a_0 = QM/R$, Q = the latent heat of condensation, M = the molecule weight of the vapor.

There is also the equation relating mass influx to droplet growth.

$$\frac{d}{dt}(\rho \frac{4}{3} \pi a^3) = 4 \pi a^2 D \nabla \rho \Big|_{r=a}$$

or
$$a \frac{da}{dt} = \frac{RD}{R-a} [\rho(R) - \rho(a)] \quad (5-19)$$

The droplet growth process has now been defined in terms of the variables a , $\rho(a)$, $\rho^{eq}(a)$, $T(a)$, and $T^{eq}(a)$ by the Eqs. (5-11), (5-16), (5-17), (5-18), and (5-19).

5-2. Solution of the droplet growth equations. A solution of the droplet growth equations may be obtained as follows. The power balance Eq. (5-11) is combined with the first continuity Eq. (5-16) to eliminate $\rho(a)$.

$$\rho(a) = \frac{n\rho(R) + \rho^{eq}(a)}{n+1} = \rho(R) + \frac{k}{LD}[T(R) - T(a)] \quad (5-20)$$

Now combine Eq. (5-17) with the above to eliminate $T(a)$.

$$T(a) = \frac{LD}{k(n+1)} \rho(R) - \frac{LD}{k(n+1)} \rho^{eq}(a) + T(R) = \frac{n'T(R) + T^{eq}(a)}{n'+1}$$

$$\rho(a)^{eq} = \frac{k}{LD} \frac{n+1}{n'+1} (T(R) - T^{eq}(a)) + \rho(R) \quad (5-21)$$

$$= \frac{\rho^{eq}(R)T(R)}{T^{eq}(a)} \exp\left\{a_0 \frac{T^{eq}(a) - T(R)}{T^{eq}(a)T(R)}\right\} \exp\left\{\frac{B}{aT^{eq}(a)}\right\}$$

$$T^{eq}(a) \left[\rho(R) + \frac{k}{LD} \left(\frac{n+1}{n'+1} \right) T(R) \right] - \frac{k}{LD} \left(\frac{n+1}{n'+1} \right) T^{eq}(a)^2 \rho^{eq}(R) T(R)$$

$$\cdot \exp\left\{\frac{a_0}{T(R)}\right\} \exp\left\{\frac{B}{a} - a_0\right\} = 0 \quad (5-22)$$

Eq. (5-22) gives the relationship between vapor density and temperature at the droplet surface.

The integrated form of Eq. (5-19) is

$$t_1 - t_2 = \int_{a_1}^{a_2} \frac{R^2 - a^2}{RD} \frac{rdr}{[\rho(R) - \rho(r)]} \quad (5-23)$$

Knowing the droplet size at time t_1 , the droplet size at time t_2 is determined as follows. A trial value of radius a_2 is picked and a gaussian-quadrature method of integration is used to evaluate t_2 . If the calculated value of t_2 is not sufficiently close to the real value of t_2 , a new trial value of a_2 , picked by a bisection scheme, is used as the new upper limit of the integration. In the integration, values of $\rho(r)$ are determined from the steady state solutions in conjunction with the connection equations and Eq. (5-22). This process is easily carried out with an electronic computer.

Analysis of an actual data expansion from a cloud chamber is complicated by the fact that the narrowest possible pulse of supersaturation is so long that many different sizes of droplets are growing simultaneously. The procedure used to simplify this situation is to divide the supersaturation pulse into many small time increments. Each time increment is then assumed to have a constant supersaturation which is the actual value of supersaturation in the middle of the time step. Droplets are nucleated all during the time step but are assumed to all be born at the center of the time step so that they all have the same age and size.

5-3. Dead space calculation. A new radius of the impermeable sphere must be calculated after each time increment. This is because the population of droplets increases during each time increment so that a smaller volume is available for the impermeable sphere after each new family of droplets is born.

An approximate family population, AN_i , for the i th time interval is computed for the new family each time by using the bulk values of supersaturation and temperature. The exact population of the new family is computed by integrating the nucleation rate law over the volume

of the impermeable spheres for all the preexisting families. Hence, the number in the i th family, N_i , is

$$N_i = \sum_{j=1}^{i-1} N_j \int_{a_j}^R \text{Rate } 4\pi r^2 dr \Delta t \quad (5-24)$$

where Δt = the duration of the time step.

Knowing N_i , the total droplet population is calculated

$$N_T = \sum_{j=1}^i N_j \quad (5-25)$$

The radius of the impermeable spheres is then calculated for the $(i+1)$ th time step.

$$N_T \frac{4}{3} \pi R^3 = 1 \quad (5-26)$$

A dead space, V_D , is defined to be the volume around the droplets which would have no nucleation if the bulk values are used to calculate the nucleation rate and the total drops nucleated in a step is to be the value calculated using the exact profile, see Eq. (5-24).

$$V_D = 1 - \frac{N_i}{AN_i} \quad (5-27)$$

The average radius of the dead space, r_D , is then defined by the relation

$$\begin{aligned} \frac{4}{3} \pi r_D^3 &= V_D \frac{4}{3} \pi R^3 \\ r_D &= V_D^{1/3} R \end{aligned} \quad (5-28)$$

The concept of dead space is useful as it is an indication of the extent to which the nonuniformity in the vapor and temperature distributions

outside the droplets affects the whole volume. As long as the dead space is small, there is little doubt as to the validity of the droplet growth calculations. When dead space rises to a significant percentage of the total volume, the assumptions made concerning the impermeable spheres must be questioned. Moreover, the dead space is used to correct nucleation rates since no new nucleation occurs within the dead space.

5-4. The computer solution. A computer with moderate storage capacity is required for data analysis using the technique outlined in the preceding sections. A new family of droplets is born each time step and information such as radius, surface temperature, gas temperature at the surface, vapor density at the surface and dead volume must be kept for each family. The actual computer program used in this work follows the procedure outlined above. Numerical integrations and solutions are carried out with sufficient accuracy that errors from this are negligible. Because of the increasing number of families which must be accounted for with each additional time step, computer time rises as the square of the number of time steps in the calculation. Figs. 39-45 are sample plots of values calculated by the computer for one data expansion. A sample computer printout is given in Appendix III.

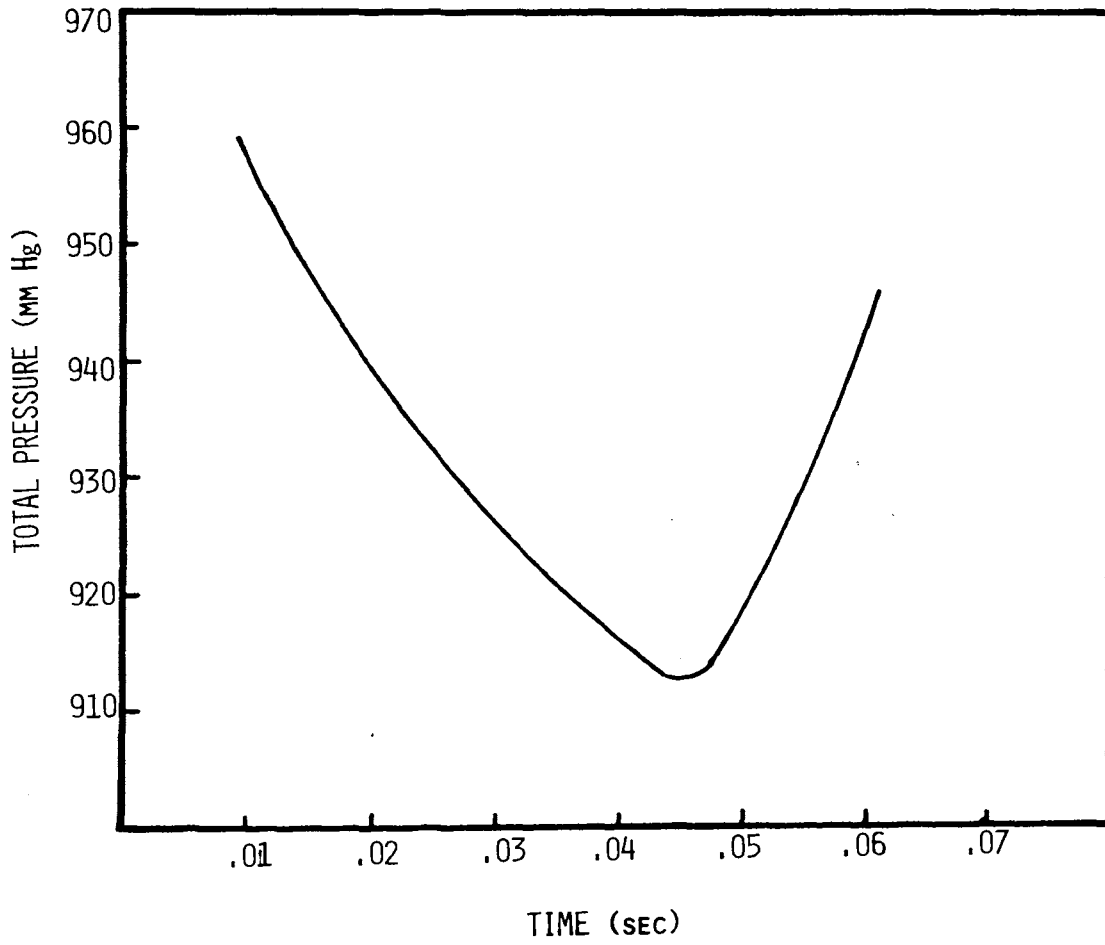


Fig. 39. Pressure vs. time.

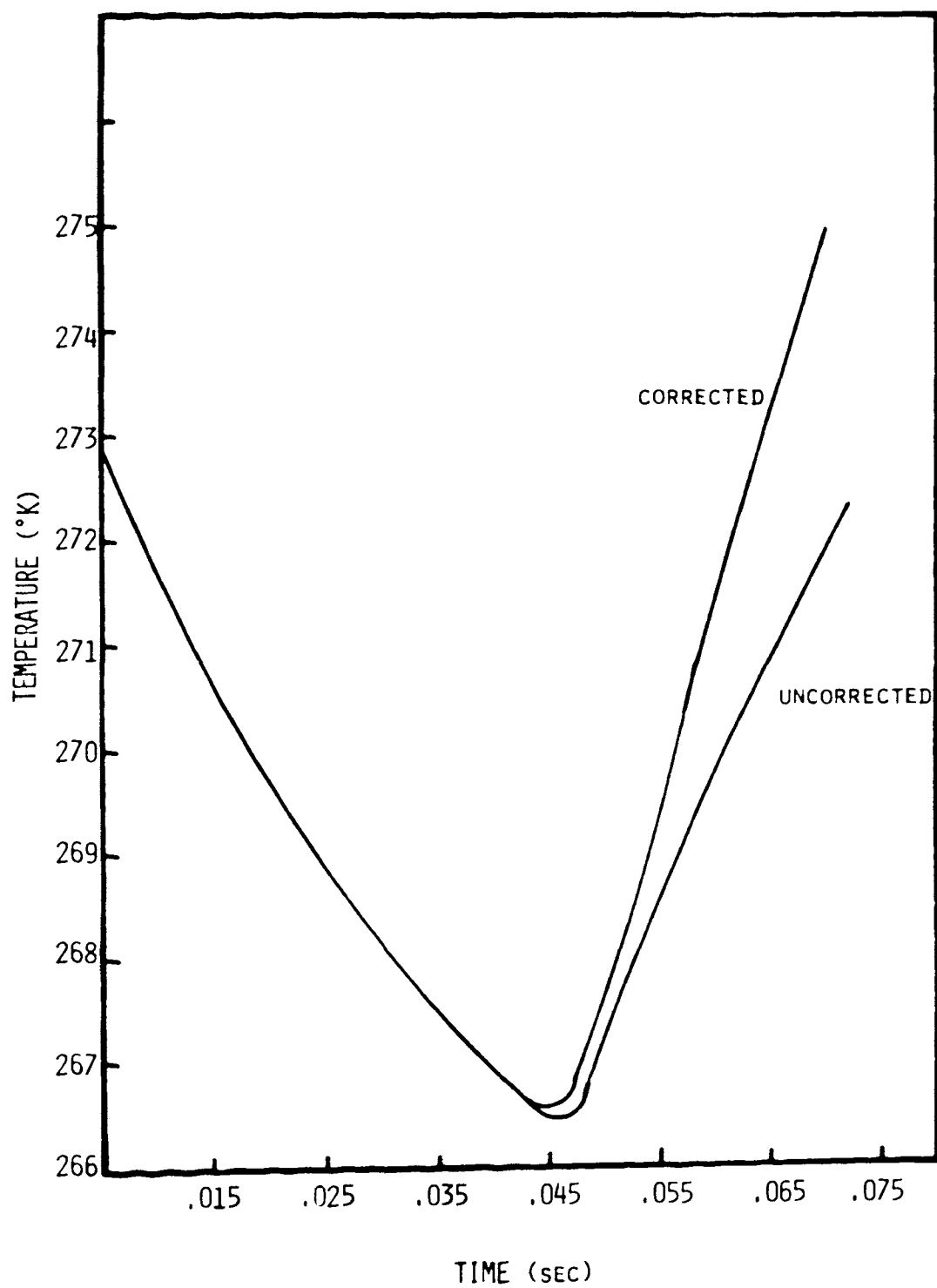


Fig. 40. Temperature vs. time for the expansion of Fig. 39.

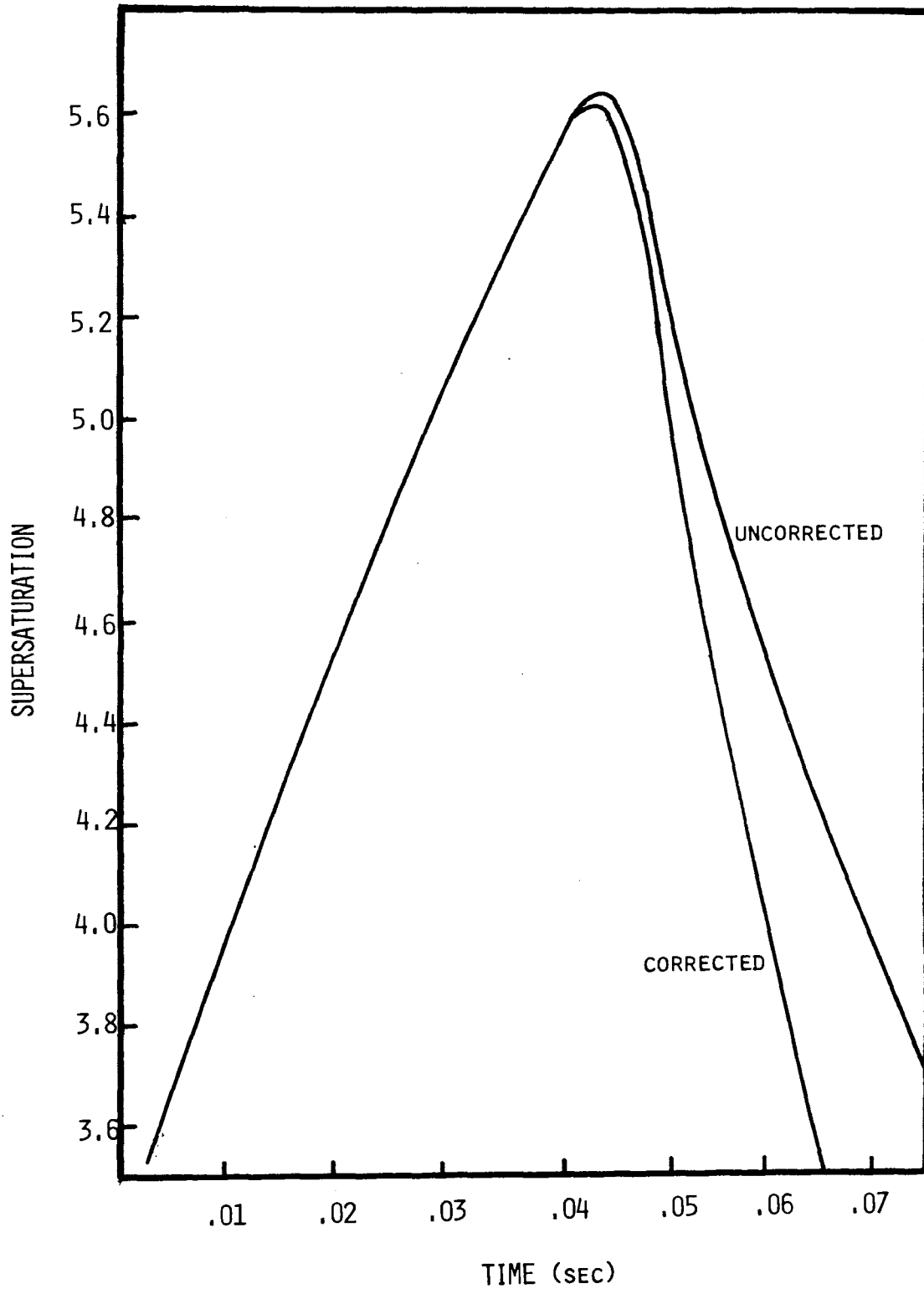


Fig. 41. Supersaturation vs. time for the expansion of Fig. 39.

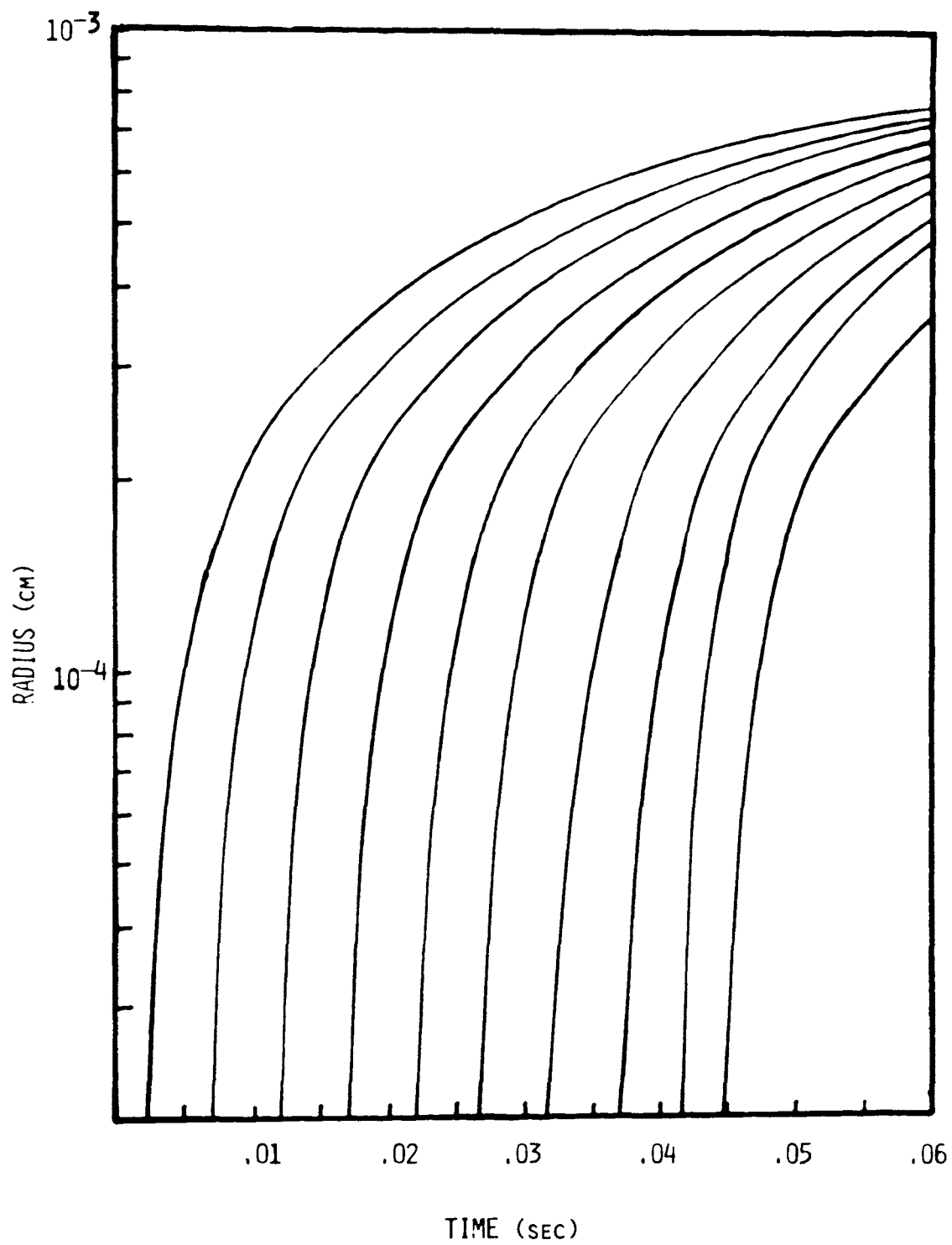


Fig. 42. Radius vs. time for the expansion of Fig. 39.

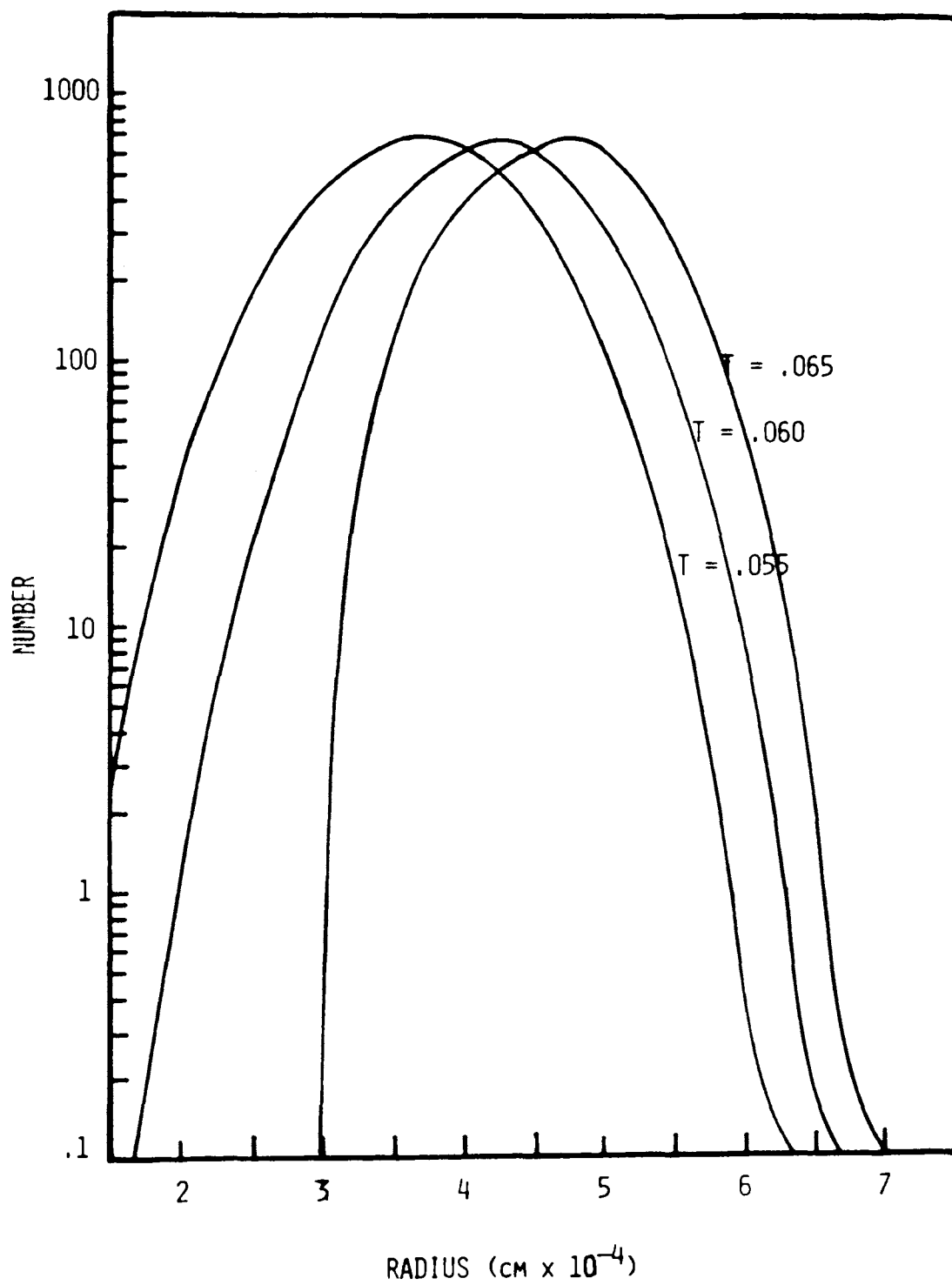


Fig. 43. Number vs. radius for the expansion of Fig. 39.

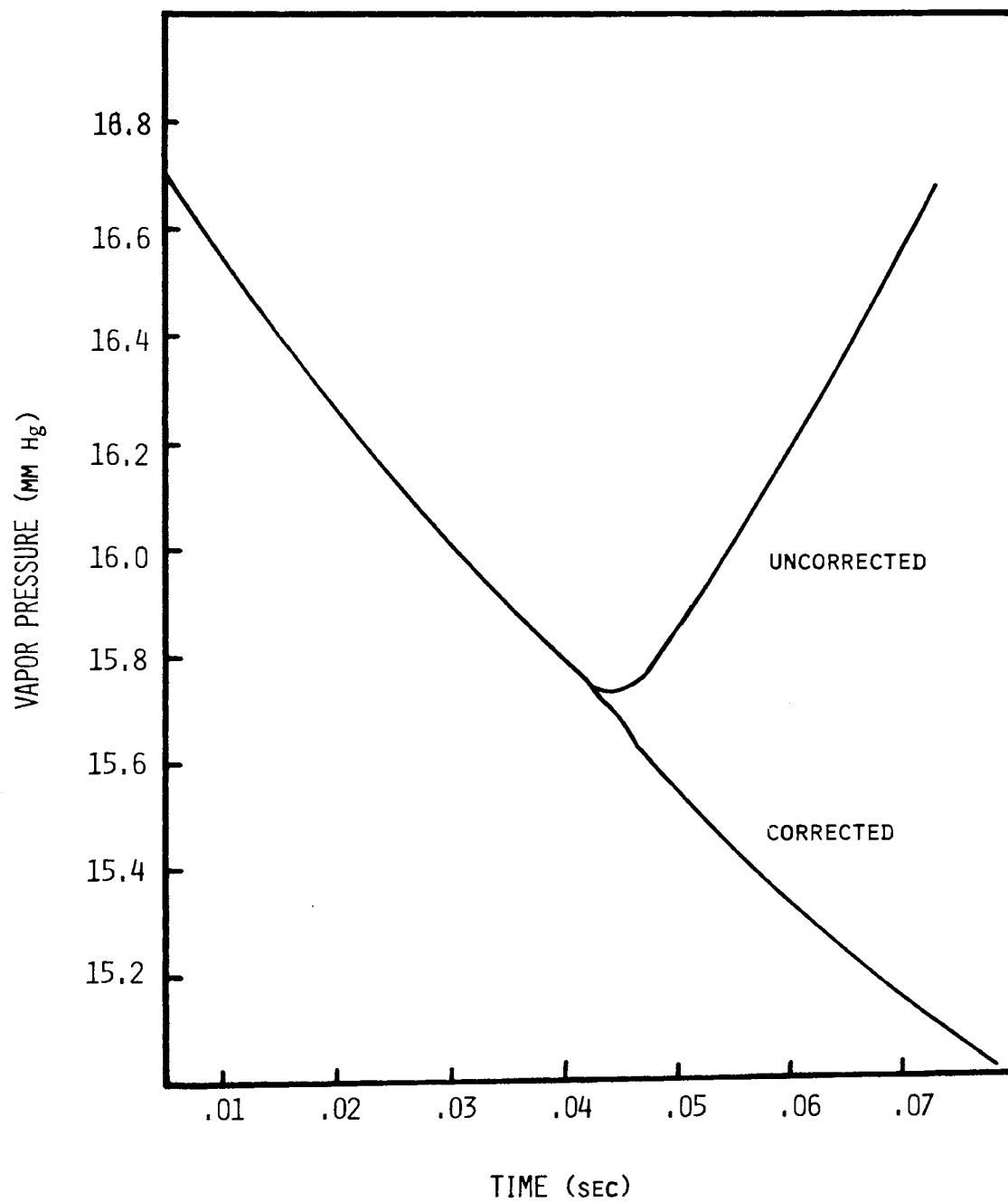


Fig. 44. Vapor pressure vs. time for the expansion of Fig. 39.

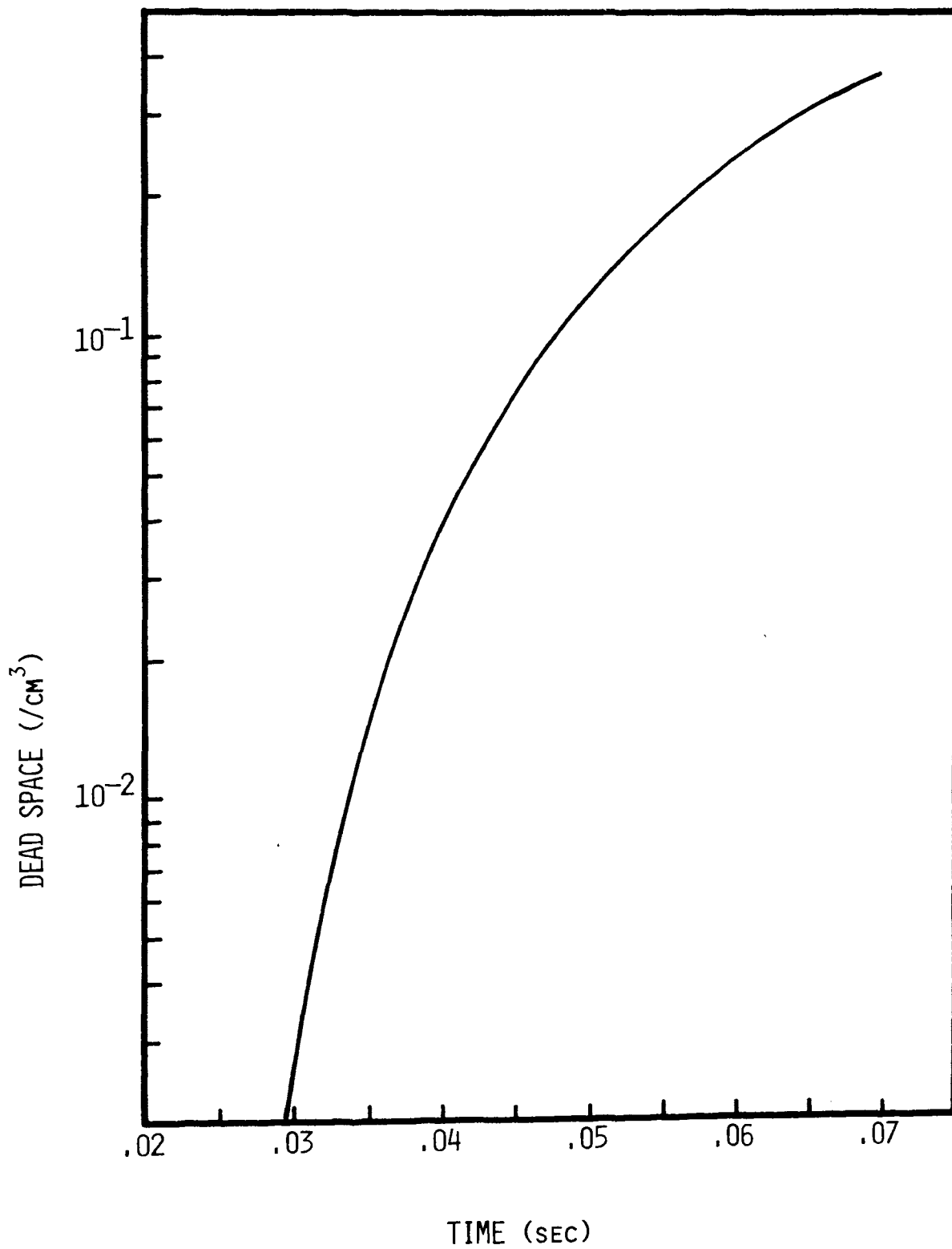


Fig. 45. Dead space for the expansion of Fig. 39.

CHAPTER VI

SUMMARY

The expansion cloud chamber has been developed into a precision instrument, capable of yielding definitive information concerning nucleation and growth of water droplets.

The gas temperature was measured in the dry chamber during the course of an isentropic expansion. It was found that the finite heat capacity is not negligible and must be accounted for. A computer program was developed which solves the problem of heat flow from the thermocouple. When the measured gas temperature is compared with that calculated from the pressure measurement using Eq. (3-1) it is found that there is almost perfect agreement. With some refinement of technique, the expansion chamber, using the same method of measuring temperature and pressure as in this work, could be used to accurately calculate the heat capacity of the gas through the relationship:

$$C_p = T \left(\frac{\partial V}{\partial T} \right)_p \left(\frac{\partial P}{\partial T} \right)_s$$

This method of calculation of the heat capacity is potentially more accurate than any now available.

The nucleation rate was measured as a function of temperature, supersaturation and sensitive time for water vapor in a helium atmosphere. It was found that there exists a form of heterogeneous nucleation occurring above the ion limit at about the supersaturation predicted by the Becker-Doring theory for homogeneous nucleation. This form of heterogeneous nucleation appears to occur upon chemically bonded centers whose

concentration is very low and depends upon the vapor pressure prior to the expansion. The consistency of the number of these nucleating centers indicates that they may be the neutral product of natural radioactivity and cosmic rays. Experiments are planned to test this hypothesis by dosing the cloud chamber with x-rays and checking to see if the number of nucleating centers is increased.

A semiphenomenological theory was developed along the lines of the classical theory but which includes the chemical bond energy of the heterogeneous nucleating center. The theory predicts a different temperature dependence for the heterogeneous and homogeneous nucleation rates and at least qualitatively explains the essential features of the data. Modifications in the photographic technique are under way which will allow an extension of the data to higher and lower droplet densities. If the liquid drop theory satisfactorily describes the nucleation of water vapor, then: (a) the measured temperature dependence of the nucleation rate will yield the free energy per molecule in the critical embryo and (b) the supersaturation dependence will yield the number of molecules in the critical cluster.

A considerable disparity has existed in the temperature dependence of the critical supersaturation as reported by various experimenters. This disparity has been in large part resolved by properly interpreting the data in terms of the theory derived for the heterogeneous nucleation.

It was definitely established that the nucleation rate of water vapor is higher in an argon atmosphere than in a helium atmosphere. This may be related to a disruptive factor due to the higher velocity

of the helium atoms. It is however more likely due to the hydration of the argon atoms into the critical cluster. Such a hydration has been hypcthized for krypton and xenon in liquid water. These two gases have been obtained so that the same nucleation experiment may be performed in an atmosphere of each of these. If such a hydration is involved the nucleation rate will be considerably higher in these gases.

BIBLIOGRAPHY

1. R. G. Fleagle and J. A. Bushinger, Atmospheric Physics, Academic Press, New York, 1963.
2. M. Neiburger and C. W. Chien, Monograph #5, American Geophysical Union, 1960.
3. A. H. Auer, Jr., *Journal de Recherches Atmospherique*, Vol. 3, 91 (1967).
4. S. Coulier, *F. Pharm. Chim.*, Paris, 22, 165, 1875.
5. J. Aitken, (1880-1), *Collected Papers*, 1923, Cambridge, p. 34.
6. C. T. R. Wilson, *Philos. Trans.*, 189, 265 (1897).
7. T. H. Laby, *Philos. Trans.*, A208, 445 (1908).
8. L. Andren, *Ann. Physik*, 52, 1 (1917).
9. Sir Willaim Thompson (Afterward Lord Kelvin), *Proc. Roy. Soc.*, Edinburg, 7, 60-63 (1870).
10. J. Frenkel, Kenetic Theory of Liquids, Dover Publishing Co., Inc., New York, 1946.
11. L. Farkas, *Zeit. Physik Chem.*, A125, 236 (1927).
12. R. Becken and W. Doring, *Ann. Physik*, 24, 719 (1935).
13. J. Zeldovich, *Zh. Eksperim. i. Teor. Fiz.*, 12, 525 (1942).
14. J. Frenkel, *J. Chem. Phys.* 7, 538 (1939).
15. M. Volmer and H. Flood, *Zeit. Physik Chem.*, (Leipzig), 170, 273, (1934).
16. C. F. Powell, *Proc. Roy. Soc. (London)*, A119, 553 (1928).
17. G. M. Pound, L. A. Madonna and C. M. Sciulli, *Conference on Nucleation*.
18. J. P. Hirth and G. M. Pound, *Prog. Mat. Sc.*, 11, 31 (1963).
19. H. Saltzburg, *Dissertation Boston University Grad. School*, *Nucleation in Supersaturated Gaseous Systems*, 1954.
20. E. F. Allard and J. L. Kassner, Jr., *J. Chem. Phys.* 42, 1401 (1965).

21. J. Lothe and G. M. Pound, *J. Chem. Phys.*, 36, 2080 (1962).
22. H. Reiss, *J. Chem. Phys.*, 6, 840 (1950).
23. H. Reiss, *Industrial and Engineering Chemistry*, 44, 1284 (1952).
24. F. C. Goodrich, *Royal Soc. of London Proc.*, 277, Ser. A., 1964, p. 165.
25. R. L. Liboff, *Phys. Rev.*, 131, 2318 (1963).
26. H. Reiss and J. L. Katz, *J. Chem. Phys.* 46, 2496 (1967).
27. J. L. Katz, H. Saltzburg, H. Reiss, *J. Colloid and Interface Science*, 21, 560 (1966).
28. W. G. Courtney, *J. Phys. Chem.*, 72, 421 (1968).
29. L. H. Lund and J. L. Rivers, Private Communication
30. H. Reiss, *Zeit. fur. Electrochemie*, BD56, 5, 459 (1952).
31. F. F. Abraham, *J. Atmospheric Science*, 25, 47 (1968).
32. F. F. Abraham and G. M. Bund, Palo Alto Scientific Center Technical Report #320-3218, 1967.
33. F. F. Abraham and M. S. Montelbano, Palo Alto Scientific Center Technical Report #320-3227, 1968.
34. R. P. Andres, Homogeneous Nucleation in a Vapor, Princeton Univ. (1967).
35. J. E. McDonald, *Amer. J. Phys.*, 30, 870 (1962); 31, 31 (1963).
36. B. J. Mason, *Discussions of the Faraday Society*, #30 (1960).
37. J. L. Kassner, Jr. and R. J. Schmitt, *J. Chem. Phys.*, 44, 4166 (1966).
38. B. G. Schuster and W. B. Good, *J. Chem. Phys.*, 44, 3132 (1966).
39. J. L. Katz and B. J. Ostermier, *J. Chem. Phys.*, 47, 478 (1967).
40. W. G. Courtney, *J. Phys. Chem*, 72, 433 (1968).
41. R. Ruedy, *Canadian J. of Research*, 22, 77 (1944).
42. P. P. Wegener and L. M. Mack, *Advan. Appl. Mech.*, 5, 307 (1958).
43. A. A. Pouring, *Phys. of Fluids*, 8, 1802 (1965).
44. A. Langsdorf, *Rev. Sci. Instr.*, 10, 91 (1939).
45. E. W. Cowan, *Rev. Sci. Instr.* 21, 901, (1950).

46. T. S. Needels and C. E. Nielsen, *Rev. Sci. Instr.*, 21, 976 (1950).
47. R. P. Shutt, *Rev. Sci. Instr.*, 22, 73 (1951).
48. J. P. Frank and H. G. Hertz, *Z. Physik*, 143, 559 (1951).
49. Allard, E. F., A New Determination of the Homogeneous Nucleation Rate of Water in Helium, Ph.D. Dissertation, University of Missouri-Rolla, 1964.
50. D. L. Packwood, Operating Characteristics of a Cloud Chamber Suited for Condensation Measurements, M.S. Thesis, University of Missouri-Rolla, 1965.
51. R. J. Schmitt, A Second Study of Homogeneous Nucleation of Water Vapor in Helium, M.S. Thesis, University of Missouri-Rolla, 1965.
52. R. Dawborn, A Study of Re-evaporation Nuclei, M.S. Thesis, University of Missouri-Rolla, 1965.
53. J. G. Smith, Re-evaporation Nuclei and Evaporation in a Wilson Cloud Chamber, Ph.D. Dissertation, University of Missouri-Rolla, 1966.
54. D. R. White, Private Communication.
55. F. Richarz, *Ann. d. Physik*, 19, 639 (1906).
56. J. B. Hughes, A Preliminary Search for Subionizers, M.S. Thesis, Missouri School of Mines, 1959.
57. F. W. Sears, Thermodynamics, Addison-Wesley Publishing Co., Inc., Reading, Mass., 1953.
58. M. W. Zamansky, Heat and Thermodynamics, McGraw-Hill Book Co., Inc., New York, 1957.
59. J. L. Kassner, Jr., J.C. Carstens, M. A. Vietti, A. H. Biermann, P.C.P. Yue, L. B. Allen, M. R. Eastburn, D. D. Hoffman, H. A. Noble, D. L. Packwood, "Expansion Cloud Chamber Technique for Absolute Aitken Nuclei Counting", paper presented at International Atmospheric Nuclei Instrument Workshop, September 8-23, 1967, Lanneznezan, France.
60. F. Din, Thermodynamic Functions of Gases, Butterworths, London, 1962.
- 61.. H. Onnes and C. Crommelin, *Commun. Phy. Lab. Univ., Luden*, 1186 (1910).
62. L. Holborn and J. Otto, *Z. Physik*, 23, 77 (1924: 30, 320 (1924).
63. I. Masson and L. Dolley, *Proc. Roy. Soc. A*, 103, 524 (1923).

64. I. Masson and C. Tannen, Proc. Roy. Soc. A., 126, 268 (1930).
65. A. Michels, Wyker and Wilker, Physica's Grav., 15, 627 (1929).
66. O. Bridgeman, Phys. Rev., 45, 930 (1934).
67. O. Bridgeman, Proc. Amer. Acad. Arts. Sci. 70, 1 (1935).
68. R. V. Churchill, Operational Mathematics, McGraw-Hill Book Co., Inc., New York, 1958.
69. H. Schlichting, Boundary Layer Theory, McGraw-Hill Book Co., Inc., New York, 1960.
70. W. H. Adams, Heat Transmission, McGraw-Hill Book Co., Inc., New York, 1954.
71. H. Israel and N. Nix, J. de Recherches Atmospheriques, Vol. II, 185 (1966).
72. L. Pauling, The Nature of the Chemical Bond, Cornell University Press, Ithaca, New York, 1960.
73. L. Pauling and R. Hayward, The Architecture of Molecules, W. H. Freeman and Co., San Francisco, Calif., 1964.
74. F. P. Parungo and J. P. Lodge, Jr., J. Atm. Sci. 24, 439 (1967).
75. B. G. Schuster, Observations of Homogeneous Nucleation and Droplet Growth in a Wilson Cloud Chamber by Means of Laser Scattering, Ph.D. Dissertation, New Mexico State University, 1967.
76. A. Sander and G. Damkohler, Naturwissenschaften, 31, 460 (1943).
77. W. F. Claussen and M. F. Polglase, J. Amer. Chem. Soc., 74, 4817 (1952).
78. J. G. Kirkwood and F. P. Buff, J. Chem Phys., 17, 338 (1949).
79. H. L. Frisch and F. C. Collins, J. Chem. Phys., 20, 1797 (1952).
80. V. E. Bagge, F. Becker, and G. Beckow, Z. Ang. Phys., 3, 13 (1951).
81. B. J. Mason, Proc. Phys. Soc., B64, 773 (1952).
82. R. Beucher, Drop Growth in a Supersaturated Atmosphere, M. S. Thesis, University of Missouri-Rolla, 1965.
83. M. Neiburger and C. W. Chien, Computations of the Growth of Cloud Drops by Condensation Using an Electronic Digital Computer, Monograph #5, Amer. Geophys. Union, Phys. of Precipitation, 1960.

84. J. C. Carsten, Diffusion Drop Growth in a Supersaturated Atmosphere, Ph.D. Dissertation, University of Missouri-Rolla, 1966.
85. H. Reiss and V. K. La Mer, *J. Chem. Phys.*, 18, 1 (1950).
86. J. T. Zung, *J. Chem. Phys.*, 46, 2064 (1967).
87. J. C. Carstens and J. L. Kassner, Jr., "Some Aspects of Droplet Growth Theory Applicable to Aitken Nuclei Measurements", paper presented at International Atmospheric Nuclei Instrument Workshop, September 8-23, 1967, Lanneznezan, France.
88. J. L. Kassner, Jr. and J. C. Carstens, Private Communication.
89. Handbook of Chemistry and Physics, 44th ed., Chemical Rubber Co., Cleveland, Ohio, 1961.
90. M. P. Vukalovich, Thermodynamic Properties of Water and Steam, State Publishing House of Scientific-Technical Literature Concerning Mechanical Engineering, Moscow, 1958.
91. International Critical Tables, Vol. 5, McGraw-Hill Book Co., Inc., New York, 1929.
92. W. J. Lick and H. W. Emmons, Transport Properties of Helium, Harvard University Press, Cambridge, Mass., 1965.
93. Tables of Thermal Properties of Gases, National Bureau of Standards Circular #564, U. S. Government Printing Office, Washington, D. C., 1955.
94. J. H. Jeans, The Dynamical Theory of Gases, Dover Publications, New York, 1954.
95. G. E. Forsythe and W. R. Wasow, Finite Difference Methods for Partial Differential Equations, John Wiley and Sons, 1960.
96. F. B. Hildebrand, Introduction to Numerical Analysis, McGraw-Hill Book Co., Inc., New York, 1956.
97. L. Fox, Numerical Solution of Ordinary and Partial Differential Equations, Addison-Wesley Publishing Co., Inc., Reading, Mass., 1962.

APPENDIX I

VARIATION OF PHYSICAL PARAMETERS

Because of the wide variation in the thermodynamic coordinates during the course of these experiments several of the physical parameters which are normally considered to be constant must be included as variables in the calculations in order that sufficient accuracy may be obtained. The variation of some of these parameters are discussed in the following paragraphs.

I-1. Equilibrium vapor pressure of water. A least squares fit was used for the vapor pressure of water⁸⁹, see Fig. 46.

Below 25°C

$$p = 4.58192 + .333075T + .010758T^2 + .196622 \times 10^{-3}T^3 \\ + .216663 \times 10^{-5}T^4 + .211191 \times 10^{-7}T^5$$

Between 20°C and 60°C

$$p = 5.92556 + .139239T + .0215602T^2 - .94144 \times 10^{-4}T^3 \\ + .59993 \times 10^{-5}T^4$$

where p is the vapor pressure in mmHg and T is the temperature in degrees Centigrade.

I-2. Surface tension of water. Data are available for only the temperature dependence of the surface tension of water.⁸⁹ A linear approximation is satisfactory for the range of interest in this work, see Fig. 47.

$$\sigma = 116.459 - .149228T$$

where σ is the surface tension in dynes per centimeter and T is the absolute temperature in degrees Kelvin.

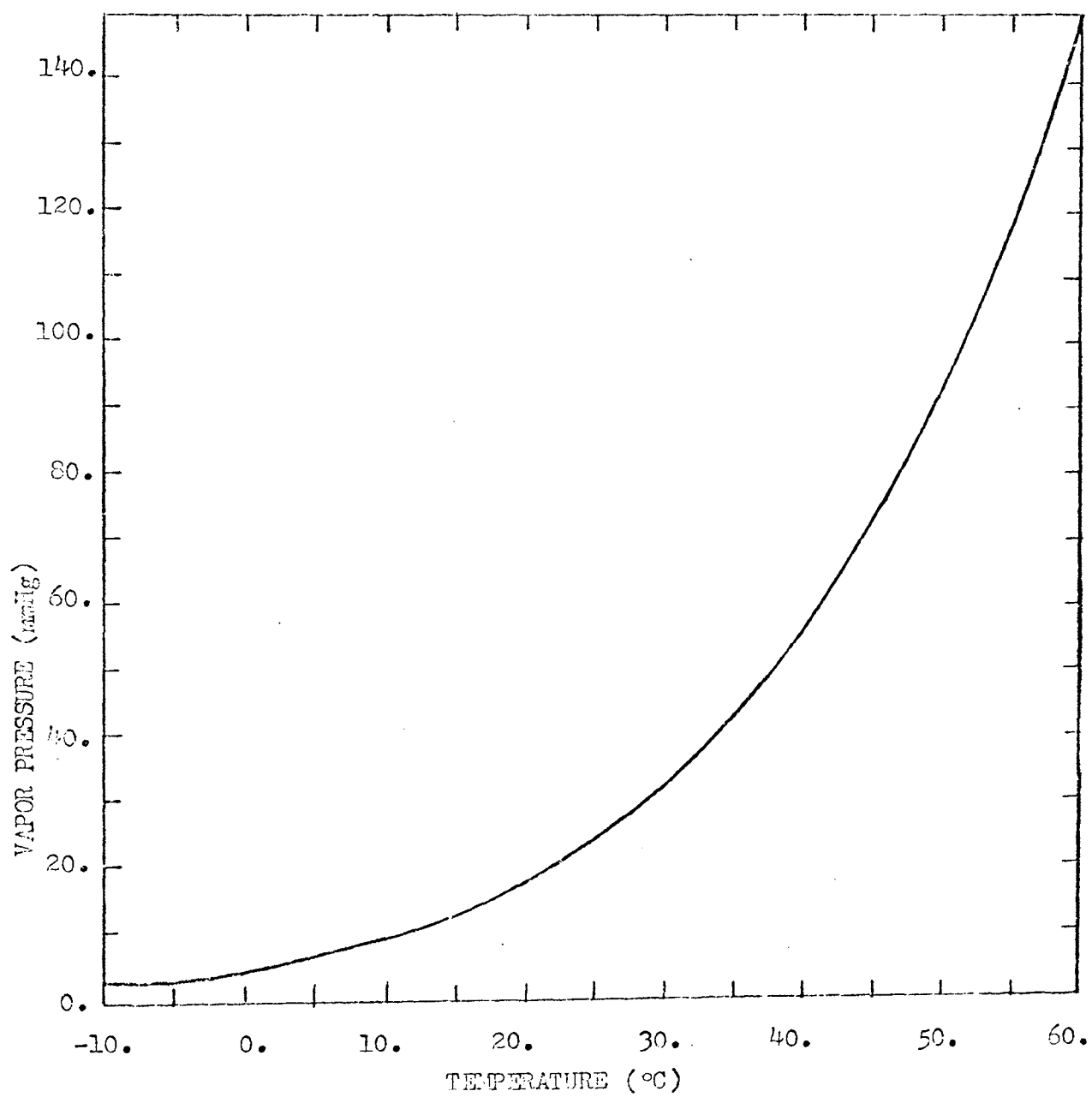


Fig. 46. Equilibrium vapor pressure of water.

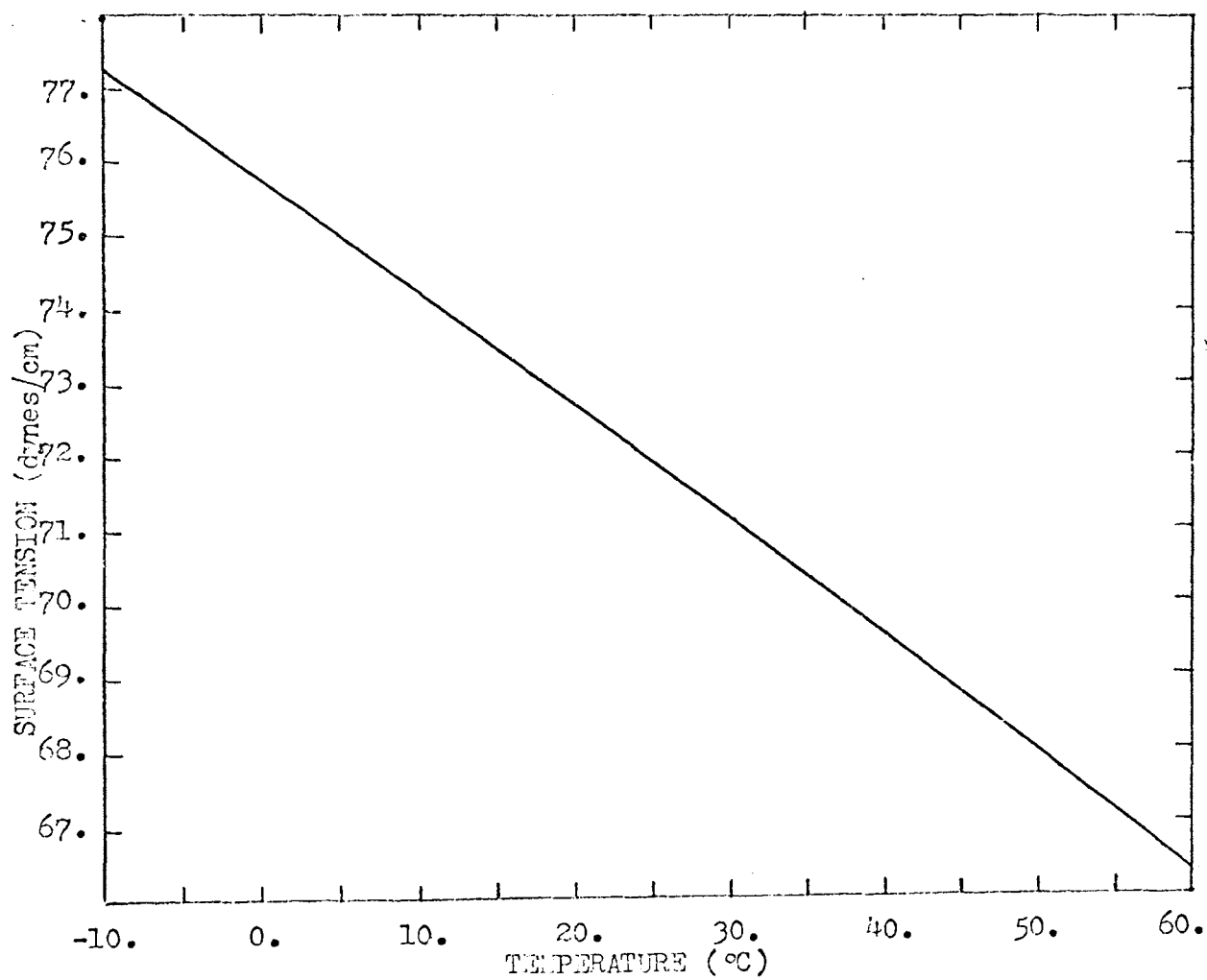


Fig. 47. Surface tension of water.

I-3. Latent heat of vaporization of water. A linear least squares fit was used for the latent heat of vaporization of water⁸⁹, see Fig. 48.

$$Q = 746.1 - .55T$$

where Q is the latent heat in calories per gram and T is the absolute temperature in degrees Kelvin.

I-4. Heat capacity and compressibility of water vapor. The best available compilation of water vapor entropy data is that of Vukalovitch.⁹⁰ The interpolated values of Cp, where Cp is the constant pressure heat capacity divided by the ideal gas constant, are given in Table II. Figs. 49 and 50 show plots of this data. There is a definite discontinuity around 340°K and 23.8 mmHg. Because of this the best curve fit is divided into three expressions.

For any pressure above 340°K

$$C_p = 3.1611$$

Below 23.8 mmHg and below 340°K

$$C_p = 2.9611 + .01201(T-240.)$$

Above 23.8 mmHg and below 340°K

$$C_p = 2.9611 + .01234(T-240.)$$

$$+ \left(\frac{23.2-p}{14.71} \right) [.1958 + .00082(T-240.)]$$

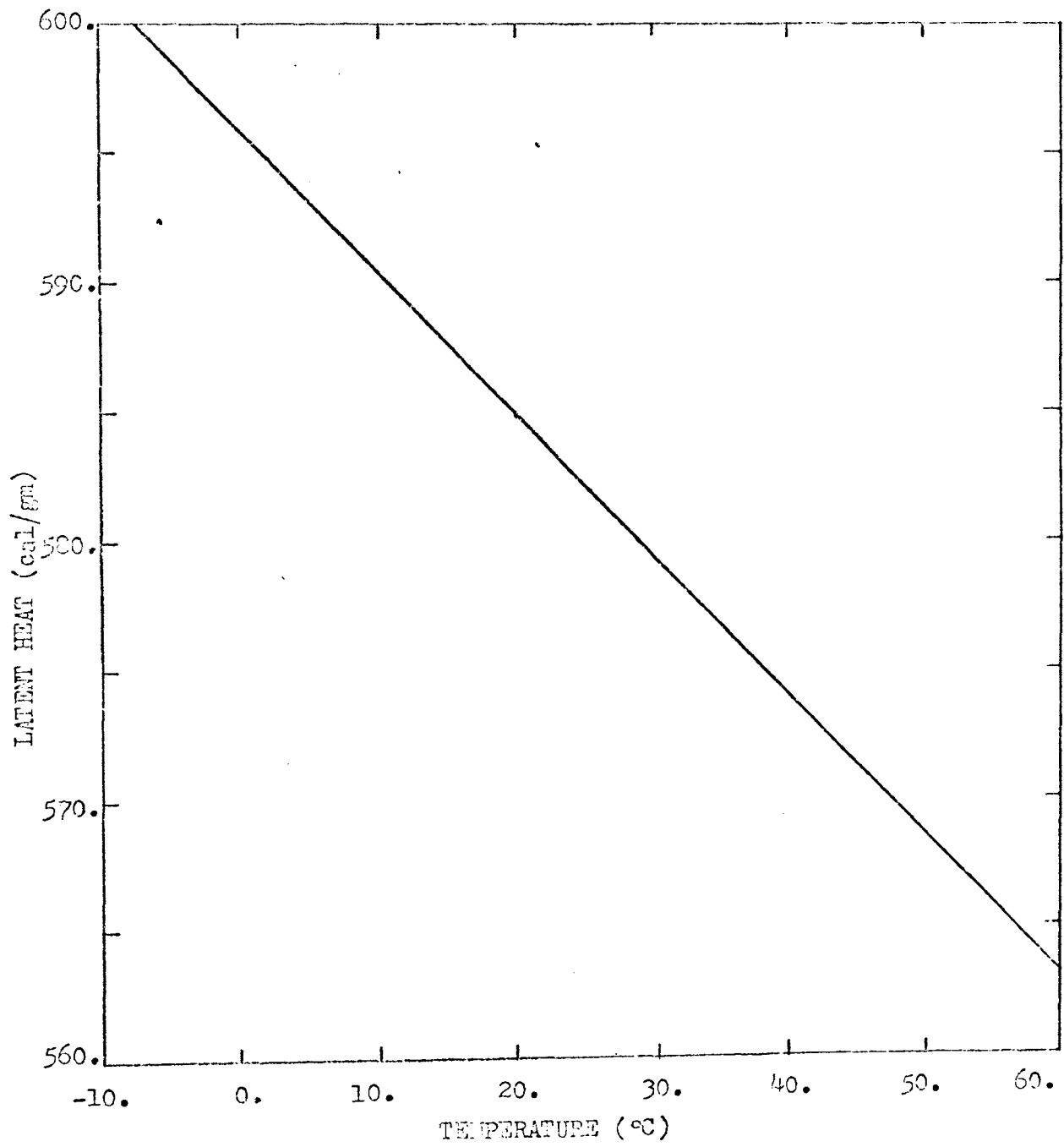


Fig. 48. Latent heat of vaporization of water.

TABLE II. The heat capacity of water vapor.

$T^{\circ}\text{K}$	p mmHg	7.3559	14.71118	22.0667	29.42236	36.778
240		3.1790	3.0919	2.9832	2.9611	2.9611
250		3.3115	3.2207	3.1075	3.0845	3.0845
260		3.4440	3.3496	3.2318	3.2079	3.2079
270		3.5764	3.4784	3.3561	3.3313	3.3313
280		3.7089	3.6072	3.4804	3.4546	3.4546
290		3.8414	3.7361	3.6047	3.5780	3.5780
300		3.9738	3.8649	3.7290	3.7014	3.7014
310		4.1063	3.9937	3.8533	3.8248	3.8248
320		4.2388	4.0646	3.9776	3.9482	3.9482
330		4.3712	4.1019	4.1019	4.0418	4.0418
340		4.5037	4.1337	4.1953	4.1395	4.1395
350		4.1281	4.1279	4.1598	4.1599	4.1279
360		4.3767	4.1479	4.1807	4.1807	4.1479
370		4.0936	4.1288	4.0952	4.0955	4.1288

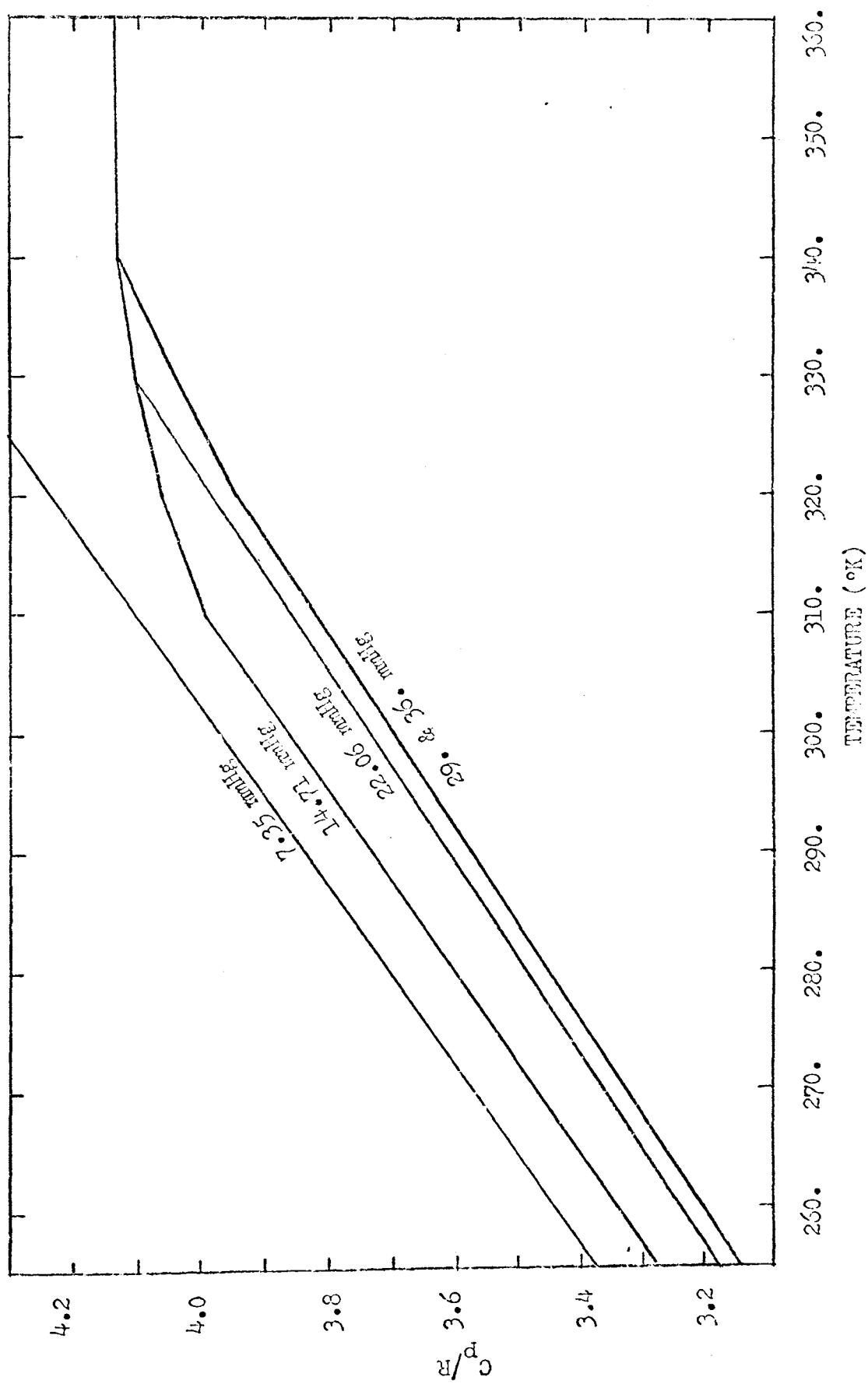


Fig. 49. Heat capacity of water vapor.

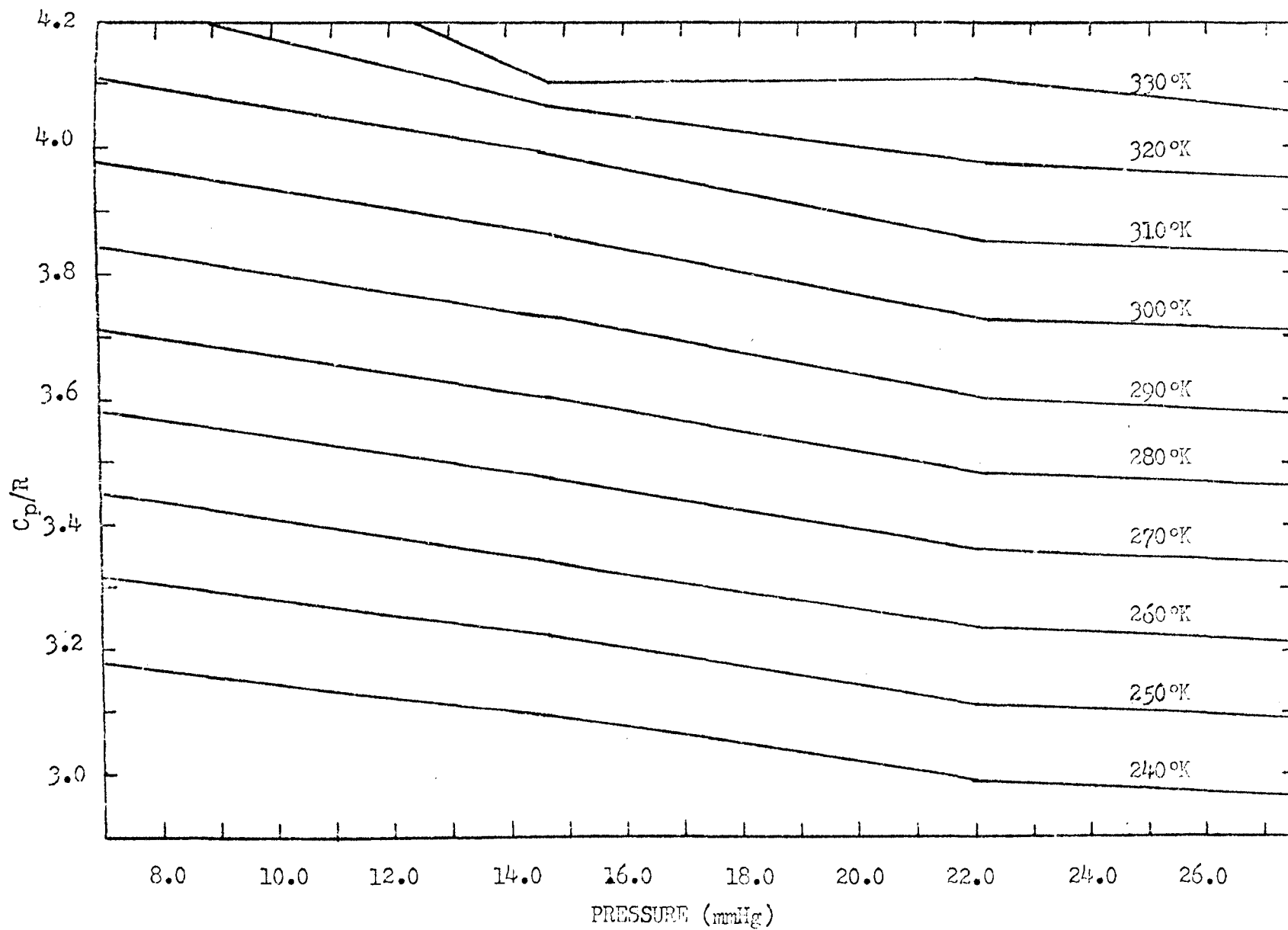


Fig. 50. Heat capacity of water vapor.

The compressibility, $z = (\partial V / \partial T)_p$, is plotted in Fig. 51. There is a negligible pressure dependence.

Below 235°K

$$z = 1.005 + .00054(T-325.)$$

Above 235°K

$$z = 1.005$$

I-5. Thermal conductivity of Helium. A linear relationship was used for the thermal conductivity of Helium as a function of temperature.^{91,92} The pressure variation is insignificant.

$$k = 4300 + 35T$$

where k is the thermal conductivity of helium in ergs per degree second centimeter and T is the absolute temperature in degrees Kelvin.

I-6. Heat capacity and compressibility of Helium, Argon, Nitrogen and Air. In making accurate calculations of temperature as discussed in Chapter 3 it is essential that the heat capacity and compressibility of the atmospheric gases be included as variables in the calculation. For that reason values of heat capacity, compressibility and the constant $(\gamma-1)/\gamma$ which is used in the isentropic ideal gas law, Eq. (3-1), have been tabulated for Argon, Nitrogen and air from data taken from NBS Circular #564.⁹³ Helium is so nearly ideal at the temperature and pressure used in this work that it may be considered ideal for all practical purposes.

The heat capacity is plotted in unitless numbers as C_p/R where R is the ideal gas constant. The compressibility is $PV/RT + T \left(\frac{\partial (PV/RT)}{\partial T} \right)_p$

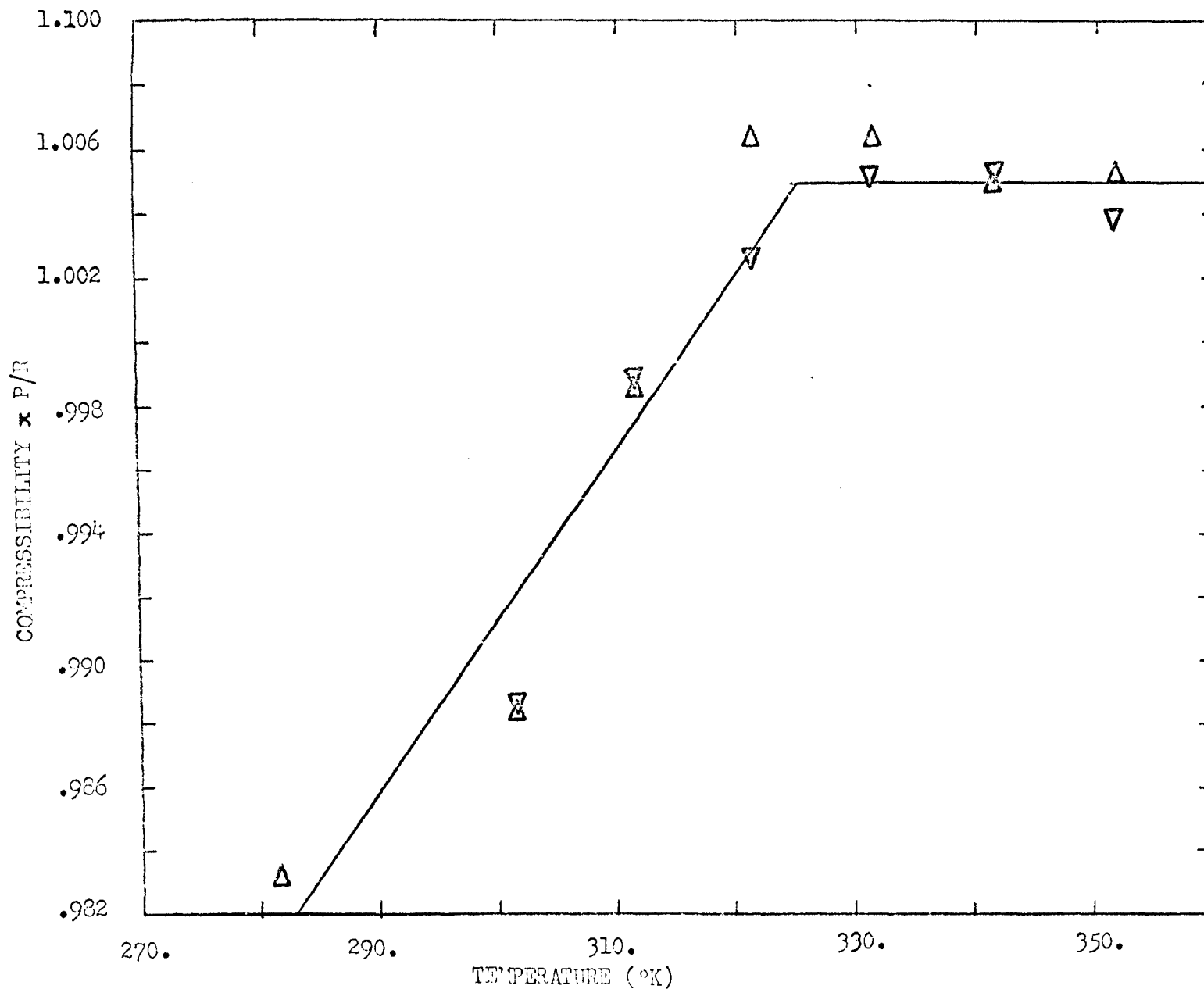


Fig. 51. Compressibility of water vapor. The line is the value of $\left(\frac{P_0 V}{RT}\right)$ used in the calculations. Δ are calculated values for 10 mmHg and ∇ are calculated P values for 22 mmHg.

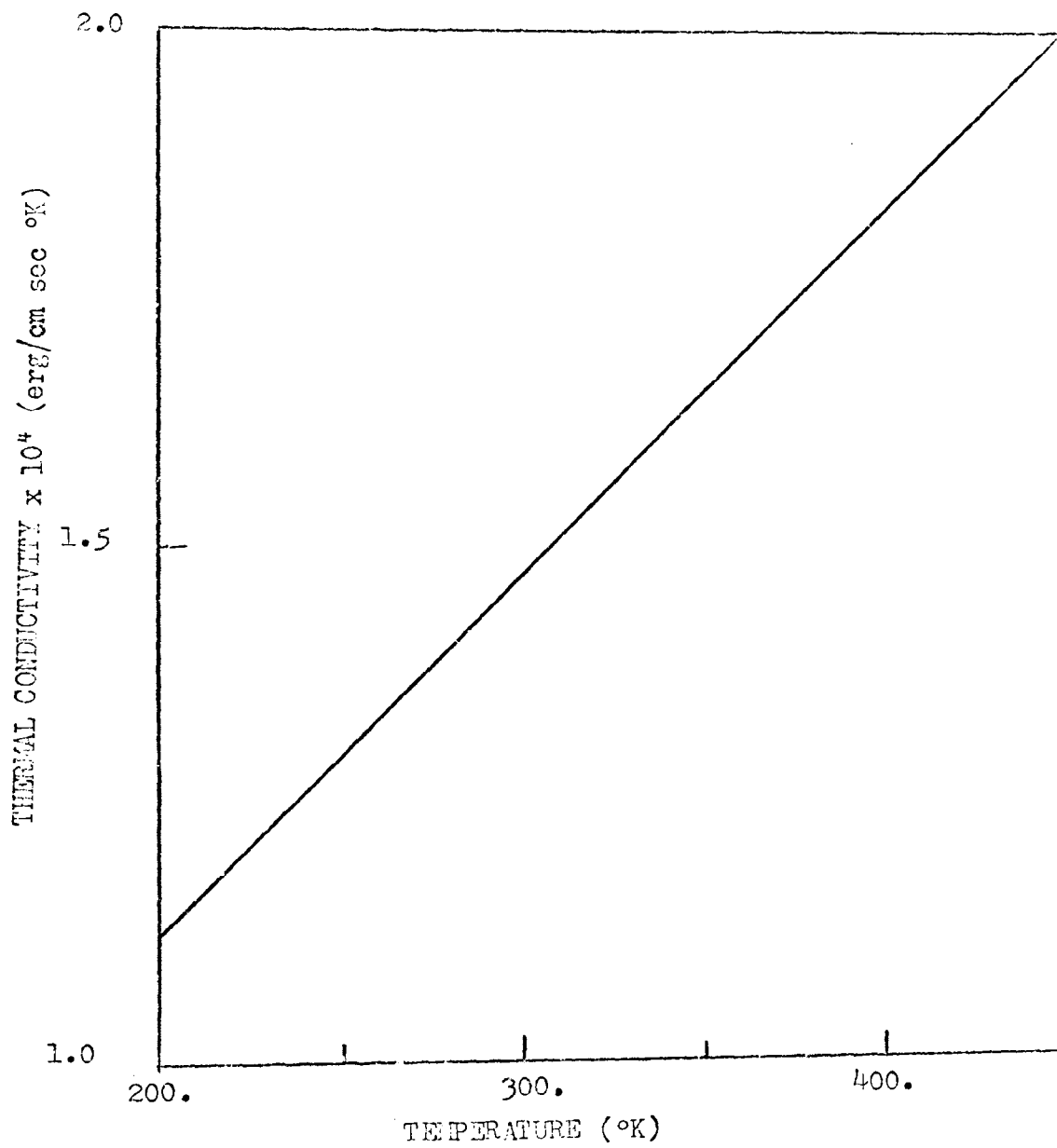


Fig. 52. Thermal conductivity of helium.

where P is pressure, V is volume and T is the absolute temperature. The adiabatic constant is the compressibility divided by the heat capacity.

TABLE III. Compressibility, heat capacity and adiabatic constant of Argon.

$T^{\circ}\text{K}$	<u>Compressibility</u>			
	<u>.7</u>	<u>1.0</u>	<u>1.5</u>	<u>2.0</u>
245	1.00264	1.00391	1.005912	1.00804
295	1.00173	1.00256	1.00390	1.00526
345	1.00119	1.00180	1.00270	1.00360

$T^{\circ}\text{K}$	<u>Heat Capacity</u>			
	<u>.7</u>	<u>1.0</u>	<u>1.5</u>	<u>2.0</u>
245	2.5065	2.5092	2.5139	2.5187
295	2.5042	2.5059	2.5089	2.5119
345	2.5029	2.5042	2.5063	2.5083

$T^{\circ}\text{K}$	<u>Adiabatic Constant</u>			
	<u>.7</u>	<u>1.0</u>	<u>1.5</u>	<u>2.0</u>
245	.40002	.40009	.40014	.40025
295	.40002	.40008	.40013	.40020
345	.40001	.40005	.40007	.40011

TABLE IV. Compressibility, heat capacity and
adiabatic constant of Nitrogen.

p atm T°K	<u>Compressibility</u>			
	<u>.7</u>	<u>1.0</u>	<u>1.5</u>	<u>2.0</u>
245	1.00257	1.00377	1.00578	1.00755
295	1.00161	1.00242	1.00349	1.00486
345	1.00109	1.00181	1.00255	1.00365

p atm T°K	<u>Heat Capacity</u>			
	<u>.7</u>	<u>1.0</u>	<u>1.5</u>	<u>2.0</u>
245	3.5072	3.5098	3.5141	3.5184
295	3.5066	3.5082	3.5110	3.5138
345	3.5098	3.5110	3.5129	3.5149

p atm T°K	<u>Adiabatic Constant</u>			
	<u>.7</u>	<u>1.0</u>	<u>1.5</u>	<u>2.0</u>
245	.28586	.28599	.28621	.28636
295	.28563	.28575	.28581	.28588
345	.28522	.28533	.28539	.28554

TABLE V. Compressibility, heat capacity and
adiabatic constant of Air.

$T^{\circ}\text{K}$	<u>Compressibility</u>			
	<u>.7</u>	<u>1.0</u>	<u>1.5</u>	<u>2.0</u>
245	1.00246	1.00386	1.00579	1.00748
295	1.00182	1.00260	1.00390	1.00520
345	1.00103	1.00172	1.00241	1.00344

$T^{\circ}\text{K}$	<u>Heat Capacity</u>			
	<u>.7</u>	<u>1.0</u>	<u>1.5</u>	<u>2.0</u>
245	3.50015	3.50275	3.50712	3.51148
295	3.50365	3.5053	3.5081	3.5109
345	3.51345	3.5147	3.5163	3.5186

$T^{\circ}\text{K}$	<u>Adiabatic Constant</u>			
	<u>.7</u>	<u>1.0</u>	<u>1.5</u>	<u>2.0</u>
245	.2864	.2866	.2868	.2869
295	.2859	.2860	.2862	.2863
345	.2849	.2850	.2851	.2852

I-7. Diffusion coefficient for water vapor in helium. No experimental data were available for water vapor diffusing through helium. Therefore, a theoretical expression due to Jeans⁹⁴ was used. The resultant equation is approximately a linear function in the region of interest.

$$D = .000946T + .291$$

where D is the diffusion coefficient in cm²/sec and T is the temperature in degrees Kelvin.

APPENDIX II
COMPUTER SOLUTION OF THE HEAT FLOW EQUATION
FOR A CYLINDRICAL WIRE

The heat capacity of a thermocouple is very large in comparison to the heat capacity of a gas. Therefore, when the gas temperature is changing the thermocouple may not be at the same temperature as the gas. For this reason, an exact calculation of the heat flow from the thermocouple must be performed.

Due to the difficulty involved in incorporating a time dependent source term into an analytic solution of the heat flow equation, it was decided to seek only a numerical solution. Moreover, a different analytic solution is required for each set of boundary conditions, whereas the numerical solution, once it is properly programmed, will work for any set of boundary conditions.

In an iterative numerical solution, one assumes that the partial derivative may be approximated by finite differences.^{95,96} Intervals in space and time are picked small enough so that the temperature function may be assumed linear between them. Thus, the x-axis is divided into equal small increments with the points designated as T(1), T(2)···T(N). Stepping forward in time gives a function varying in time. Thus, T(n,1), T(n,2)···T(n,M), where one is looking at the time variation of the function T at the nth point along the x-axis.

The space derivative at the kth point along the x-axis, T(k,r), may be taken in a forward or backward direction.

$$\frac{\partial T(k,t)}{\partial x} = \frac{T(k+1,t) - T(k,t)}{\Delta x} \quad (\text{II-1})$$

is the forward derivative where Δx is the x-distance between lattice points. Similarly,

$$\frac{\partial T(k,t)}{\partial x} = \frac{T(k,t) - T(k-1,t)}{\Delta x} \quad (\text{II-2})$$

is the backward derivative.

Second derivatives are taken in a similar manner.

$$\begin{aligned} \frac{\partial^2 T}{\partial x^2} &= \frac{\partial}{\partial x} \left(\frac{\partial T}{\partial x} \right) = \frac{\frac{T(k+1,t) - T(k,t)}{\Delta x} - \frac{T(k,t) - T(k-1,t)}{\Delta x}}{\Delta x} \quad (\text{II-3}) \\ &= \frac{T(k+1,t) - 2T(k,t) + T(k-1,t)}{(\Delta x)^2} \end{aligned}$$

Before going to the full two dimensional equation, let us simplify by letting $\Delta x = h$, $\Delta y = h$, $\Delta t = k$
 $r = x$ coordinate, $s = y$ coordinate, $t = \text{time coordinate}$. Eq. (3-12) becomes

$$\begin{aligned} \frac{T(r,s,t+1) - T(r,s,t)}{k} &= \frac{K}{C_p h^2} [T(r+1,s,t) + T(r-1,s,t) + T(r,s-1,t) \\ &\quad + T(r,s+1,t) - T(r,s,t)] + f(x,y,x,t) \quad (\text{II-4}) \end{aligned}$$

With the equation cast into this form, it is seen that, if one knows the value of the function T at a point and the points immediately surrounding it at a time t , then the value of the function T may be calculated for a short time Δt in the future. This technique is used at all the points in the region of interest and repeated until the time of interest is reached.

Extreme caution must be exercised in picking the h and k to be used in the approximations. Due to the iterative nature of the solution, when a time interval k (long enough for an equilibrium to be reached in the space interval h) is used, the approximation for short time in the differential equation is invalidated. If a large enough value of k is picked so that there is even a slight error in one time interval, the error tends to compile in successive time intervals. This is known as an exponential instability and the solution diverges exponentially from the true solution.

Fox⁹ has a good treatment of this problem. He shows that for $K/C_p = 1$

$$\frac{\Delta t}{(\Delta x)^2} \leq \frac{5}{2}$$

this is about three times the relaxation time of a square in the lattice.

Argon at room temperature has these possible values of h and k .

TABLE VI. Possible values of h and k for Argon

sec	$.625 \times 10^{-6}$	$.25 \times 10^{-5}$	1×10^{-5}	4×10^{-5}	16×10^{-5}	6.4×10^{-4}	2.56×10^{-3}
cm	.000625	.00125	.0025	.005	.01	.02	.04

Referring to the chart, a square the size of the thermocouple cross section requires time increments of the order of one microsecond. A problem arises when one considers that the mesh must extend outward to 0.3 cm from the thermocouple and the integration must take the time through a period of one second. In order that the problem could be solved with a finite size, finite speed computer, a grid mesh was set up with increasing mesh size as the points recede from the thermocouple, see Fig. 53.

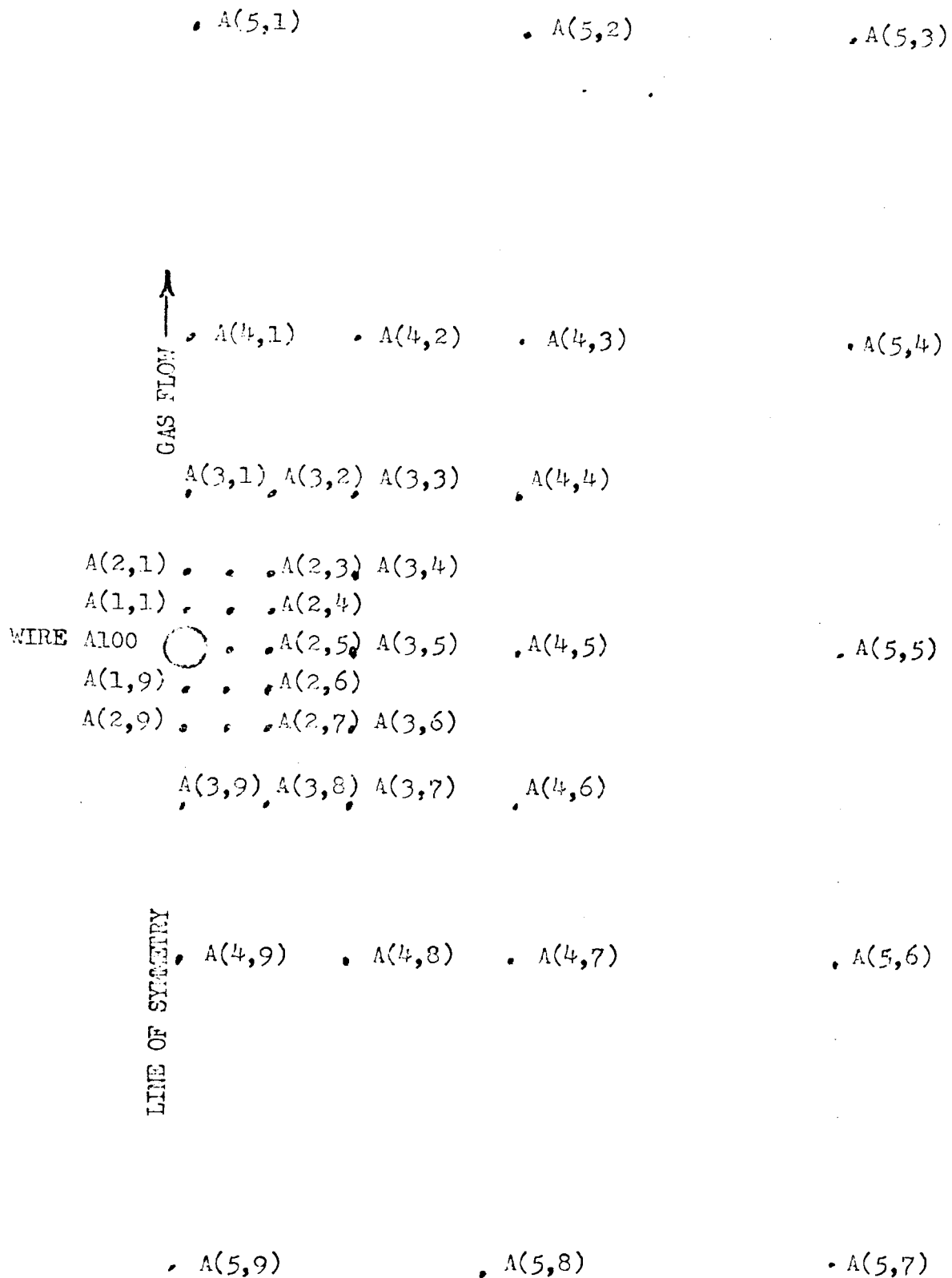


Fig. 53. Mesh used for thermocouple heat flow calculation. The mesh extends outward to the 10th row. The spacing is: row 1-.000675cm, row 2-.000675cm, row 3-.00125cm, row 4-.0025cm.

This technique allows small space intervals near the thermocouple where it is necessary and large space-time intervals in the outlying area. The net result of this technique is that a medium speed, medium capacity computer is sufficient to solve a problem normally suited to a much larger machine. Accuracy is not sacrificed with this technique. Table VII gives a sample of the computer output. Fig. 54 shows the temperature profile around the thermocouple for the expansion shown in Figs. 24 and 25.

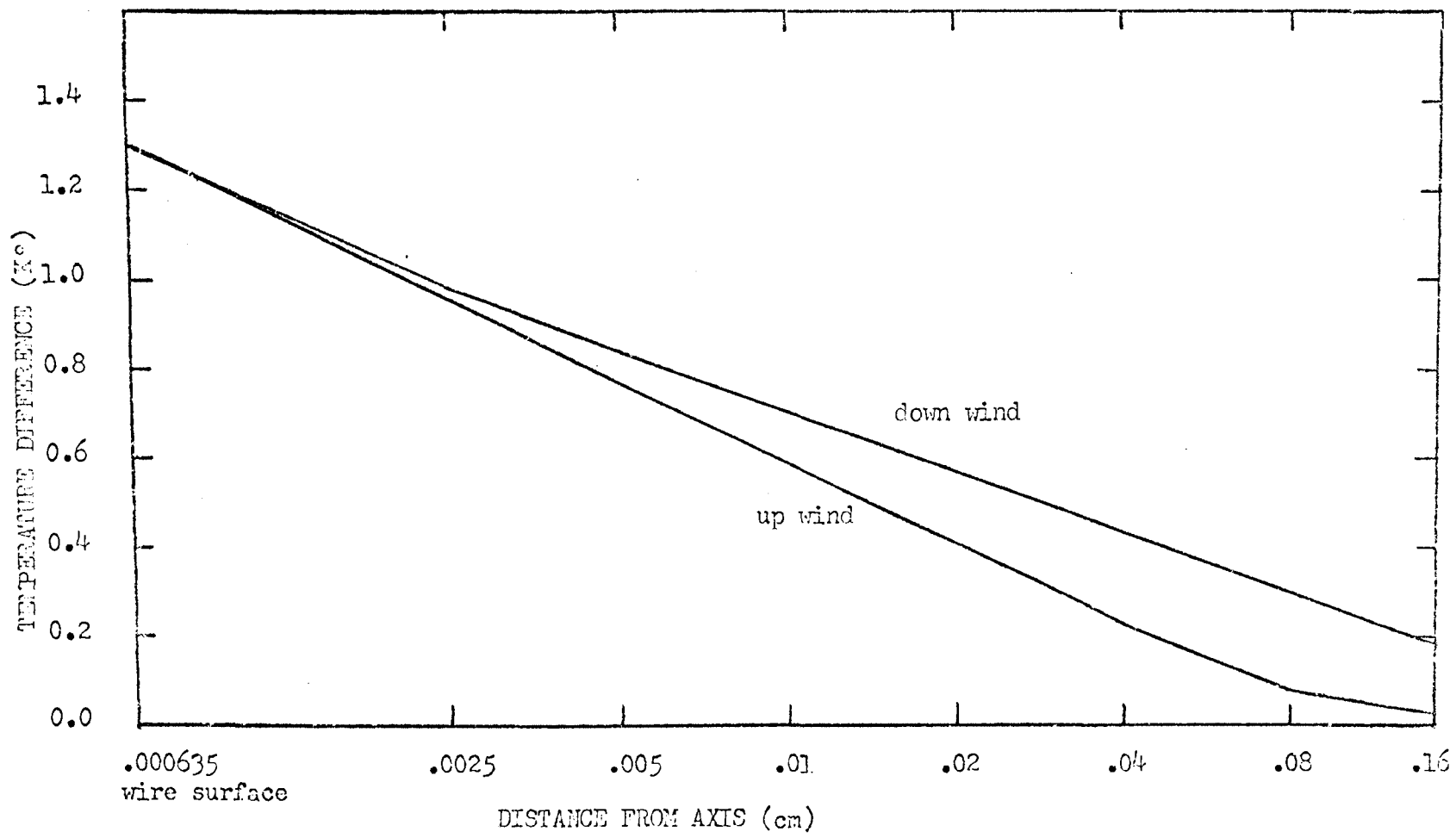


Fig. 54. Temperature profile around the thermocouple.

II-1. Computer program for calculation of the thermal lag of the thermocouple.

```

C PROGRAM FOR CALCULATING THERMAL LAG OF THERMOCOUPLE
  DOUBLE PRECISION A(10,9),DA(10,9),DT,T,P,A100
  DOUBLE PRECISION VC(9),VC1,VC2,VC3,VC4,VC5,VC6
C READ IN INITIAL CONDITIONS
  READ(1,100)P,T
100 FORMAT ( 2E18.8)
  N=0
  A100=T
  DO 99 I=1,10
    DO 99 J=1,9
      A(I,J)=T
  99 DA(I,J)=0.0
  DO 8 I3=1,4
  DO 7 I7=1,4
  DO 6 I6=1,4
  DO 5 I5=1,4
C K, CP (ARGON) DT=1E-5, DX=.0025CM, CPI= HEAT CAPACITY OF WIRE
  CP=(.06032+.000398*P)*P/T
  XK=3.905E-05+(T-273.15)*1.715E-07
  CPI=.18798
  XKH=1.6
  C=(XK/CP)*XKH
  CI=(XK/(CP+CPI))*XKH
  DO 4 I4=1,4
  N=N+1
  VEL=(-(N-1)*(64.E-5)*(0.216)+2.03)*1.E-5
  VC(1)=1.-VEL/0.0025
  DO 15 IX=2,9
15 VC(IX)=1.-2.*(1.-VC(IX-1))
  DO 3 I3=1,4
  DO 2 I2=1,4
  DO 1 I1=1,4
C HEAT FLOW CORRECTION AREA NUMBER ONE
  DA(1,1)=C*(A(2,1)+2*A(1,3)+A100-4*A(1,1))
  DA(1,3)=C*(A(1,1)+A(2,2)+A(2,4)+A(1,5)-4*A(1,3))
  DA(1,5)=C*(A100+A(1,3)+A(2,5)+A(1,7)-4*A(1,5))
  DA(1,7)=C*(A(1,2)+A(1,5)+A(2,5)+A(2,8)-4*A(1,7))
  DA(1,9)=C*(A100+2*A(1,7)+A(2,9)-4*A(1,9))
  A100=C1*(A(1,1)+2*A(1,5)+A(1,9)-4*A100)+A100
  DO 61 I1=1,9,2
61 A(1,I1)=DA(1,I1)+A(1,I1)
C TEMPERATURE CHANGE IN ENTIRE MATRIX DUE TO VOLUME CHANGE
  DT=-.087486*T*VEL
  T=T+DT
  P=P+P*2.49921*DT/T
  A100=A100+CP*DT/CPI
  DO 98 I1=1,9
  DO 98 J1=1,9
98 A(I1,J1)=A(I1,J1)+DT
  VC1=VC(1)
  VC2=1.-VC1
  A(1,1)=VC1*A(1,1)+VC2*A100
  A(1,3)=VC1*A(1,3)+VC2*A(1,5)
  A(1,5)=VC1*A(1,5)+VC2*A(1,7)
  A(1,7)=A(1,7)*VC1+VC2*A(2,8)
  A(1,9)=VC1*A(1,9)+VC2*A(2,9)
1 CONTINUE
  CALL DADEL(DA,A,C,2,VC)
2 CONTINUE
  CALL DADEL(DA,A,C,3,VC)
3 CONTINUE
  CALL DADEL(DA,A,C,4,VC)
4 CONTINUE
  P1=P*760.

```

```

TIME=N*64.F-5
ADEL=A100-A(G,1)
WRITE (3,101)I,P1,A(0,1),TIME,ADEL
WRITE (3,102)A(9,1),A(7,1),A(5,1),A(5,1),A(4,1),
1A(3,1),A(2,1),A(1,1),A100,A(1,0),A(2,0),A(3,0),A(4,0),A(5,0),
2A(6,0),A(7,0),A(8,0)
CALL DADEL(DA,A,C,5,VC)
5 CONTINUE
CALL DADEL(DA,A,C,6,VC)
6 CONTINUE
CALL DADEL(DA,A,C,7,VC)
7 CONTINUE
CALL DADEL(DA,A,C,8,VC)
8 CONTINUE
101 FORMAT(/F7.2,F7.1,F7.2,F7.4,F7.2)
102 FORMAT(17F7.2).
CALL EXIT
END

```

```

C SUBROUTINE DADEL(DA,A,C,I,VC)
TEMPERATURE CORRECTION DUE TO HEAT FLOW BEYOND CENTRAL AREA
DOUBLE PRECISION A(10,9),DA(10,9),D1,T,P,A100
DOUBLE PRECISION VC(9),VC1,VC2,VC3,VC4,VC5,VC6
DA(I,1)=C*(2*A(I,2)+A(I-1,1)+.5*A(I+1,1)-3.5*A(I,1))
DA(I,2)=C*(A(I,1)+A(I,3)+A(I-1,3)+.25*(A(I+1,1)+A(I+1,2))
1-3.5*A(I,2))
DA(I,3)=C*(A(I,2)+A(I,4)+.5*(A(I+1,4)+A(I+1,2))-3*A(I,3))
DA(I,4)=C*(A(I,3)+A(I,5)+A(I-1,3)+.25*(A(I+1,4)+A(I+1,5))
1-3.5*A(I,4))
DA(I,5)=C*(A(I-1,5)+A(I,4)+A(I,6)+0.5*A(I+1,5)-3.5*A(I,5))
DA(I,6)=C*(A(I-1,7)+A(I,5)+A(I,7)+0.25*(A(I+1,5)+A(I+1,6))
1-3.5*A(I,6))
DA(I,7)=C*(A(I,8)+A(I,6)+0.5*(A(I+1,6)+A(I+1,8))-3.0*A(I,7))
DA(I,8)=C*(A(I,9)+A(I-1,7)+A(I,7)+0.25*(A(I+1,8)+A(I+1,9))
1-3.5*A(I,8))
DA(I,9)=C*(A(I-1,9)+2*A(I,P)+0.5*A(I+1,9)-3.5*A(I,9))
DO 10 JA=1,9
10 A(I,JA)=A(I,JA)+DA(I,JA)
VC3=VC(I)
VC4=1.-VC3
VC6=.5*VC4
VC5=1.-VC6
A(I,1)=VC3*A(I,1)+VC4*A(I-1,1)
A(I,2)=VC3*A(I,2)+VC4*A(I-1,3)
A(I,3)=VC3*A(I,3)+VC4*A(I,4)
A(I,4)=VC3*A(I,4)+VC4*A(I,5)
A(I,5)=VC3*A(I,5)+VC4*A(I,6)
A(I,6)=VC3*A(I,6)+VC4*A(I,7)
A(I,7)=VC5*A(I,7)+VC6*A(I+1,P)
A(I,8)=VC5*A(I,8)+VC6*.5*(A(I+1,8)+A(I+1,9))
A(I,9)=VC5*A(I,9)+VC6*A(I+1,9)
RETURN
END

```

TABLE VII

OUTPUT OF THERMOCOUPLE HEAT FLOW COMPUTER PROGRAM

Print out is in this order:

Gas temperature, Pressure, A(9,1), Time, Temperature difference

A(8,1)	A(7,1)	A(6,1)	A(5,1)	A(4,1)	A(3,1)	A(2,1)	A(1,1)	A100	A(1,9)	A(2,9)	A(3,9)	A(4,9)	A(5,9)	A(6,9)	A(7,9)	A(8,9)
289.74	1027.1	289.74	0.1587	1.41												
289.74	289.99	290.15	290.28	290.41	290.55	290.69	290.82	291.14	290.78	290.61	290.42	290.21	290.01	289.85	289.76	289.74
289.61	1025.0	289.61	0.1613	1.41												
289.61	289.86	290.02	290.15	290.29	290.42	290.56	290.69	291.02	290.65	290.48	290.29	290.09	289.88	289.72	289.63	289.61
289.48	1024.8	289.48	0.1638	1.41												
289.48	289.73	289.89	290.03	290.16	290.30	290.43	290.57	290.89	290.52	290.35	290.16	289.96	289.75	289.59	289.50	289.48
289.35	1023.6	289.35	0.1664	1.41												
289.35	289.56	289.77	289.90	290.03	290.17	290.31	290.44	290.75	290.40	290.22	290.04	289.83	289.63	289.46	289.37	289.35
289.22	1022.5	289.22	0.1690	1.42												
289.22	289.53	289.54	289.77	289.91	290.04	290.18	290.31	290.64	290.27	290.10	289.91	289.70	289.50	289.33	289.25	289.22
289.09	1021.4	289.09	0.1715	1.42												
289.09	289.41	289.51	289.65	289.78	289.92	290.05	290.19	290.51	290.14	289.97	289.78	289.58	289.37	289.20	289.12	289.09
288.96	1020.2	288.96	0.1741	1.42												
288.96	289.28	289.38	289.52	289.66	289.79	289.93	290.06	290.38	290.02	289.84	289.66	289.45	289.24	289.07	288.99	288.96
288.83	1019.1	288.83	0.1766	1.42												
288.83	289.15	289.27	289.39	289.53	289.66	289.80	289.93	290.25	289.89	289.72	289.53	289.32	289.12	288.95	288.86	288.84
288.70	1017.9	288.70	0.1792	1.43												
288.70	289.02	289.14	289.27	289.40	289.54	289.67	289.81	290.13	289.76	289.59	289.40	289.20	288.99	288.82	288.73	288.71
288.57	1016.8	288.57	0.1818	1.43												
288.57	288.90	289.01	289.14	289.28	289.41	289.55	289.68	290.00	289.64	289.46	289.28	289.07	288.86	288.69	288.60	288.59
288.45	1015.7	288.45	0.1843	1.43												
288.45	288.77	288.88	289.02	289.15	289.28	289.42	289.56	289.88	289.51	289.34	289.15	288.94	288.73	288.56	288.47	288.45
288.32	1014.5	288.32	0.1869	1.43												
288.32	288.64	288.77	288.89	289.02	289.16	289.29	289.43	289.75	289.38	289.21	289.02	288.82	288.61	288.44	288.34	288.32
288.19	1013.4	288.19	0.1894	1.44												
288.19	288.51	288.64	288.76	288.90	289.03	289.17	289.30	289.63	289.26	289.08	288.90	288.69	288.48	288.31	288.22	288.19
288.06	1012.3	288.06	0.1920	1.44												
288.06	288.38	288.51	288.64	288.77	288.91	289.04	289.18	289.50	289.13	288.96	288.77	288.56	288.35	288.18	288.09	288.06
287.93	1011.2	287.93	0.1946	1.44												
287.93	288.25	288.38	288.51	288.64	288.78	288.91	289.05	289.37	289.00	288.83	288.64	288.44	288.23	288.05	287.96	287.94
287.81	1010.0	287.81	0.1971	1.44												
287.81	288.12	288.26	288.38	288.52	288.65	288.79	288.92	289.25	289.88	288.71	288.52	288.31	288.10	287.93	287.83	287.81
287.68	1008.9	287.68	0.1997	1.44												
287.68	288.00	288.13	288.25	288.39	288.53	288.66	288.80	289.12	288.75	288.58	288.39	288.18	287.97	287.80	287.70	287.68
287.55	1007.8	287.55	0.2022	1.45												
287.55	287.87	288.01	288.13	288.27	288.40	288.54	288.67	288.99	289.62	288.45	288.26	288.06	287.85	287.67	287.57	287.55
287.42	1006.7	287.42	0.2048	1.45												
287.42	287.74	287.88	288.01	288.14	288.27	288.41	288.54	288.87	288.50	288.33	288.14	287.93	287.72	287.55	287.45	287.42
287.29	1005.6	287.29	0.2074	1.45												
287.29	287.61	287.76	287.88	288.01	288.15	288.28	288.42	288.74	288.37	288.20	288.01	287.80	287.59	287.42	287.33	287.30
287.17	1004.4	287.17	0.2099	1.45												
287.17	287.48	287.63	287.76	287.89	288.02	288.16	288.29	288.62	288.25	288.07	287.88	287.68	287.47	287.29	287.20	287.17

APPENDIX III

COMPUTER SOLUTION OF THE DROPLET GROWTH EQUATIONS

100167

IBM OS/360 BASIC FORTRAN IV (F) COMPILATION

```

C      LOUIS R. ALLEN      LIPA NORWOOD HALL
C      GENERALIZED NUCLEATION RATE RATE PROGRAM
C      COPY 2
C      RATE LAW = FARLEY RATE LAW
      REAL K
      DIMENSION AT(54), A1(50), A2(50), CNT(50)
      DIMENSION PT(10), AT(10)
      WRITE(2,1021)
1021  FORMAT(5I10)
1022  FORMAT(5F14.6)
      READ(1,1000) IIC
      READ(1,1001) (CI(I1), I1=1, IIC), (WT(J1), J1=1, IIC)
      READ(1,1001) WTPOS, WTMVP, PI, PGAS, PG, RP, CC, CAMU, PMM, K
      READ(1,1000) IN
      DO 205 L=1, IN
      READ(1,1000) IQ, NEXP
      WRITE(3,1022) NEXP, IQ
1022  FORMAT(4X, 'EXPANSION NUMBER =', I5, 'ION, I5, ' DATA POINTS', //)
      READ(1,1001) PC, TC
      CALL VPREO(TC, VPC)
      READ(1,1001) P1, TIME1
      ATC=TC
      AVPC=VPC
      CT1=TIME1
      CNTCT=0.
      ACNTCT=C.
C      VALUES HEADED BY A ARE UNCORRECTED VALUES
      N1=C
      IO1=IO-2
      DO 200 I=1, IO1
      CALL ICALC(PC, P1, TC, T1, VPC, VPC1)
      CALL ICALC(PC, P1, ATC, AT1, AVPC, AVPC1)
      CALL VPREO(T1, VPREO)
      SUPP=VPC1/VPREO
      CALL VPREO(AT1, VPREO)
      ASUPP=AVPC1/VPREO
      READ(1,1001) P2, TIME2
      CT2=TIME2-TIME1
      CT=(CT1+CT2)*.5
      IF(SUPP-1.0)P6, P6, I10
110  IF(CT1)I11, CT, I11
      96  WRITE(3,1014) SUPP, VPC1, VPREO
1014  FORMAT(7, 'END OF PROGRAM--SUPERSTATION CUT-OFF AT 1,920.4, '
1  VAPOR PRESSURES OF 1,2F10.4)
      92  IO2=IO1-1
      IF(IO2)205, 205, 97
      97  DO 32 I1=1, IO2
      READ(1,1001) P2, TIME2
      WRITE(3,1028)
1028  FORMAT(//, ' THE REMAINING DATA CARDS ARE THE FOLLOWING:', //)
      93  WRITE(3,1020) P2, TIME2
1029  FORMAT(520.2, F15.6)
      WRITE(3,1030)

```

```

1070 FORMAT(////)
1080 GO TO 200
51 CALL RATE (AT1,AVP1,ASUPR,ARATE)
ACM1=ARATE*DT
ACM1OT=ACM1*NT+ACMT
CALL RATE (T1,VP1,SUPR,RATE)
CN1=ARATE*DT
CN1(I)=0
CN=0
WRITE(2,1000) I
1000 FORMAT(' TIME INTERVAL NO.',I4,/)
WRITE(3,1002) O1,DT
1002 FORMAT(4X,10F5.2, ' =1, F10.3, ' 4X, 'MI HG',10X, 'DURATION OF THIS STEP
1 IF(O1*DT=1.128,00.07
99 CN1(I)=(1.-CN1OT)*RATE*DT
WRITE(3,1015) CN1(I)
87 WRITE(3,1008)
1008 FORMAT(5X, 'ASSEMBLY',6X, 'INITIAL RADIUS',6X, 'FINAL RADIUS',6X, 'VP OF
1 DROPS SUP',6X, 'TEMP OF DROP SUP',6X, 'GAS TEMP AT DROPI',6X, 'DROPS F
1 ERMED',/)
1015 FORMAT(' DROPS NUCLEATED IN THE FREE VOLUME =1, F15.6,/)
IV=I
111 DO 20 J=1,I4
C CHECK APPROXIMATION OF A2(J)
IF(I-I) 21,21,20
21 A1(J)=1.-A1(J)
D1J= A1(J)
A2(J)=1.3*A1(J)
GO TO 22
20 DAJ=(A1(J)-A2(J))*0.1
A1(I)=.9*(A1(J)-A2(J))+A1(J)
22 CONTINUE
C=C
N=N+1
MAY=0
DT=0
SUM=0
TEMP=TEMP+1
DO 14 II=1,II0
CN=1.5*((A2(J)-A1(J))*DT(II)+A2(J)+A1(J))
CALL TGRAD(K,PI,PGAS,PG,RN,NT,CAMU,PM,PL,T1,VP1,DU,WTMVP,WTMGS,
1 TEO,TEA,VPA)
CALL CNLAT(TEA,0)
CALL THERM(TEA, THERM, THERM)
14 SUM=SUM+0.5*(A2(J)-A1(J))*WT(II)*DU*Q/(THERM*(TEA-T1))
16 DT=DT2*.5
GO TO 18
17 DT=(DT1+DT2)*.5
18 CONTINUE
C CHECK ERROR, APPLY BISECTION METHOD OF ITERATION
IF(ABS(SUM-DT)-DT/50.110,19,1
1 IF(SUM-DT)2,19,4
2 IF(CK)3,2,7
3 CK=1.
GO TO 8
4 IF(CK)7,5,5
5 CK=-1.
6 N=N+1
7. A2(J)=A2(I)+2.*CK*DAJ/(2.**(N+1))
GO TO 6
19 CALL TGRAD(K,PI,PGAS,PG,RN,NT,CAMU,PM,PL,T1,VP1,A2(J),WTMVP,
1 WTMGS,TEO,TEA,VPA)
IF(N1)114,113,114
114 CN=0.
CN1(I)=0.
RATE=0.
ARATE=0.
GO TO 84
C CALCULATION OF DEAD VOLUME
113 IF(J-I)81,83,83

```



```

02 IF (I-1) 06,04,07
03 CNT=CNTA
04 T1=TA
05 CNT(I)=CNTA
06 TO=04
07 RATIO=A1(J)/(P-A1(J))
08 SUM=C.0
09 DO 11 I=1,110
10 X=.5*(P-A1(J))*T(I) + A1(J)+R
11 TE=RATIO*(TEA-T1)*(P-X)/X+T1
12 CALL VDEFO(TE,VDEFO)
13 VP=(RATIO*(P-X)*(TEA*VDA-T1*VPI)/X+T1*VPI)/TE
14 SC=VP/VDEFO
15 CALL UCALF(TE,VP,SD,PATA)
02 SUM=SUM + 4.*PI*PATA*X*X*(P-A1(J)).5*DT*MT(I)
03 CNT(I)=CNT(I)+CNT
04 CONTINUE
1003 CALL VDEFO(TEQ,VP)
1004 WRITE(3,1003) J,A1(J),A2(J),VQ,TEQ,TEA,CN
1005 FORMAT(I2,F22.8,F12.2,F16.4,F22.4,F22.4,F22.8)
06 CONTINUE
07 IF (CN) 107,115,107
115 CNTDT=CNT(I)+CNTDT
08 IF (CNT(I)/CNTDT - 1.E-10) 04,05,05
04 WRITE(3,1007) CNTDT,CNT(I)
05 N1=1
1007 FORMAT(//,5X,'PROGRAM OUT-OFE SINCE TOTAL DROP COUNT,',F16.6,',
1008 'LEAF EXCEEDS DROP COUNT IN THIS STEP,',F16.6,',')
06 TO 107
05 VQ=1.-CNT(I)/CNTA
06 IF FOR NEXT TIME INTERVAL
1009 WRITE(3,1009) VQ
1010 IF (CNTDT-1.1105,105,106
105 Q=C.62
06 TO 107
104 R=(3./(4.*PI*CNTDT))**(.333333)
107 CONTINUE
08 DRH=C.0
09 DO 15 J=1,110
15 DRH=(4./3.)*PI*CNT(J)*(A2(J)**3-A1(J)**3) + DRH
16 CALL CHLAI(T1,HEAT)
17 Q=DRH*HEAT
18 DTEMP=2.*Q*RGAS*T1/(PI*PAM*5.*1.0872)
19 DVP=DRH*RGAS*T1/(PAM*VPMVP)
20 T1=T1+DTEMP
21 VP1=VP1-DVP
1025 FORMAT(5X,'TEMPERATURE CORRECTION',F16.6,/)
1026 FORMAT(//,5X,'LEAF VOLUME',F16.6)
1027 FORMAT(5X,'VAPOR PRESSURE CORRECTION',F16.6)
1028 FORMAT(5X,'LATENT HEAT RELEASED',F16.6)
1029 FORMAT(5X,'VAPOR DEPLETION',F16.6)
1030 WRITE(3,1024) DRH
1031 WRITE(3,1023) Q
1032 WRITE(3,1026) DVP
1033 WRITE(3,1025) DTEMP
1034 WRITE(3,1004)
1004 FORMAT(20X,'TEMPERATURE',5X,'VAPOR PRESSURE',5X,'SUPERSATURATION',
1005 '14X,'NUCLEATION RATE',5X,'DROPS THIS STEP',5X,'TOTAL DROPS',//)
1005 WRITE(3,1005) A1,AVP1,ASUPR,ARATE,ACNT,ACNTDT
1006 FORMAT(2X,'ADIABATIC',5X,F15.4,F19.4,F20.8,F20.8)
1007 WRITE(3,1006) T1,VP1,SUPR,RATE,CNT(I),CNTDT
1008 FORMAT(2X,'CORRECTED',5X,F15.4,F19.4,F20.6,F20.8,F20.8,F20.8)
1009 WRITE(3,1007)
1007 FORMAT(///,1X,'END OF THIS TIME INTERVAL',///)
1010 TO=T1
1011 VPC=VP1
1012 CC=P1
1013 P1=P2
1014 ATC=A11
1015 AVPC=AVP1
1016 TIME1=TIME2

```

```

      D(1)=D(2)
      DO 100 IY=1,IM
        A1(IY)=A1(IY)
      100 A1(IY)=A2(IY)
      200 CONTINUE
      205 WRITE(2,1021)
      1021 FORMAT(1F11)
      STOP
      END

```

```

SUBROUTINE TCRAD(K,PI,PGAS,PG,PM,MT,CAMU,PMV,P,T,VPR,AP,MTMP,
1  THGS,ICD,TEA,VPA)

```

```

      REAL K
      X=T+10.
      CALL VPREF(T,VPR)
C   DIFFUSION COEFFICIENT(CM**2/SEC) AS A F OF T AND ME PATHS AND MOL WEIGHT
      AD=.000046*T+.001
      CALL THERMO(T,THRM,THRME)
      ETA=4.*AT*SQRT(PI*MT*PI)/(3.*PGAS*T)/AD
      ETAB=4.*T*PI*MT*SQRT(THGS*PI*T)/(3.*PGAS)/((2-VPR)*PM*AD)
      CALL CNLAT(T,D)
      A=(ETA+1.)*THEI/(Q*AD*(ETA+1.))
      B=-MT*VPR*VPR*PI/(PGAS*T)-A*T
      AA=Q*EMV/1.0972
      C=VPR*Q*MT*MT*HYD(AA/T)/PGAS
      CALL SIGMA(T,SIG)
      ETA=2.*SQRT(T*VPR*CAMU/K
      D=ETA/AD-AA
      N=1
      B=A*Y*Y+B*Y+C*EXP(D/Y)
      F0=2.*AB*F0-C*D*EXP(D/X)/(X*X)
      DY=-F/90
      IF (ABS(DY)-.001) 1,1,2
      2 IF(N-2) 4,4,3
      4 X=X+DY
      N=N+1
      GO TO 5
      3 WRITE(2,1000)
      1000 FORMAT(' DID NOT CONVERGE')
      1 TEO=Y
      TEA=(ETA*T+TEO)/(ETA+1.)
      VPA=TEA*(VPR/T+PGAS*THRME*(T-TEA)/(Q*AD*PM*MT*VPR))
      NT=MT+N
      RETURN
      END

```

```

SUBROUTINE VPREF(T,VPR)
C   CALCULATION OF EQUILIBRIUM VAPOR PRESSURE OF WATER
      TC=T-273.15
      VPR=4.58102+TC+.233075+TC**2*.010758+TC**3*1.06622E-4
      1+TC**4*.216463E-5+TC**5*.211191E-7
      RETURN
      END

```

```

SUBROUTINE CNLAT (T,HEAT)
      HEAT=746.1-.55*T
      RETURN
      END

```

```

SUBROUTINE SIGMA(T,SIG)
      SIG=116.450-.149228*T
      RETURN
      END

```

```

SUBROUTINE TCALC (P1,P2,T1,T2,VP1,VP2)
  DOUBLE PRECISION P,1
  REAL THER,MEG,MEG,MEG
  MEG=VP1/PI
  MEG=1-PEG
  MEG=MEG/MEG
  DPTOT=PP-P1
  N=ABS(10.*DPTOT)
  IF (N) 2,2,3
2. DP=DPTOT
  N=1
  GO TO 4
3. DP=DPTOT/N
4. DVP=MEG*DP
  DPC=MEG*DP
  CG=1.0
  CC=2.5
  T=T1
  P=P1
  DO 1 IN=1,N
  P=P+DP
  VP=D*VP
  CG=2*MEG
  T2=T
  CALL HCAP (T2,VP,CG,CM)
1. T=T+(DPC*DP/PC+(DPC*DP*VP/VP)/(CG+MEG*CM))
  T2=T
  RETURN
  END

SUBROUTINE HCAP (T,P2,CP2,CM)
CALCULATION OF H AND CP FOR WATER VAPOR.
  IF (T-240.) 3,4,4
4. CP2=2.1411
  GO TO 7
3. IF (22-22.8) 5,5,6
6. CP2=2.061+(T-240.)*.01201
  GO TO 7
5. CP2=2.0611+(T-240.)*.01234+
1. ((22-P2)/14.71)*(.1253+(T-240.)*.0002)
7. CONTINUE
  IF (T-235.) 8,8,9
9. CP2=1.005+.00057*(T-325.)
  GO TO 10
8. CP2=1.005
10. CONTINUE
  RETURN
  END

```

```

SUBROUTINE THERMC (T,THERM,THERME)
THERMAL CONDUCTIVITY (CAL/DEG SEC CM) AS A FUNCTION OF T (DEG K)
  REAL THER
  THERME=.43E+04+.0035E+04*T
  THERM=THERME/4.186E+07
  RETURN
  END

```

TABLE VIII. OUTPUT OF THE DROPLET GROWTH COMPUTER PROGRAM

Units are: Length-cm, Volume-cm³, Temperature-°K, Pressure-mmHg, Heat-cal, Time-sec.

TIME INTERVAL NO. 6

PRESSURE = 831.700 MM HG

DURATION OF THIS STEP = 0.005000 SECONDS

FAMILY	INITIAL RADIUS	FINAL RADIUS	VF OF DROP SUR	TEMP OF DROP SUR	GAS TEMP AT DROP
1	0.34902502E-03	0.39214152E-03	2.8291	266.6868	265.2322
2	0.30332198E-03	0.35021548E-03	2.2448	266.7595	265.1548
3	0.25266479E-03	0.30776625E-03	2.2653	266.8533	265.0552
4	0.19849994E-03	0.25394979E-03	2.8992	267.0973	264.8906
5	0.04999991E-04	0.18949994E-03	2.9619	267.2878	264.5898
6	0.00999997E-05	0.27499971E-04	3.1465	268.0942	263.7239

DEAD VOLUME	=	0.234604E-02
VAPOR DEPLETION	=	0.760119E-10
LATENT HEAT RELEASED	=	0.459717E-07
VAPOR PRESSURE CORRECTION	=	0.682545E-04
TEMPERATURE CORRECTION	=	0.160180E-03

TOTAL DROPS

ADIABATIC	0.40492125E 01
CORRECTED	0.40402241E 01

	TEMPERATURE	VAPOR PRESSURE	SUPERSATURATION	NUCLEATION RATE	DROPS THIS STEP
ADIABATIC	259.3093	8.5261	5.395782	0.41817090E 03	0.20908537E 01
CORRECTED	259.2093	8.5250	5.395754	0.41813574E 03	0.20857735E 01

END OF THIS TIME INTERVAL

TIME INTERVAL NO. 7

PRESSURE = 827.400 MM HG

DURATION OF THIS STEP = 0.005000 SECONDS

FAMILY	INITIAL RADIUS	FINAL RADIUS	VF OF DROP SUR	TEMP OF DROP SUR	GAS TEMP AT DROP
1	0.39214152E-03	0.42993716E-03	2.7320	266.2312	264.8770
2	0.35021548E-03	0.39355944E-03	2.7437	266.2369	264.8184
3	0.30776625E-03	0.35460223E-03	2.7583	266.3562	264.7458
4	0.25394979E-03	0.30359187E-03	2.7702	266.4546	264.6423
5	0.18949994E-03	0.25629693E-03	2.8121	266.6084	264.4807
6	0.27499971E-04	0.19156237E-03	2.8724	266.8857	264.1868
7	0.00999997E-05	0.27499971E-04	3.0598	267.7153	263.2954

DEAD VOLUME	=	0.237493E-02
VAPOR DEPLETION	=	0.166227E-09
LATENT HEAT RELEASED	=	0.120350E-06
VAPOR PRESSURE CORRECTION	=	0.149988E-03
TEMPERATURE CORRECTION	=	0.351421E-03

TOTAL DROPS

ADIABATIC	0.76828156E 01
CORRECTED	0.76607838E 01

	TEMPERATURE	VAPOR PRESSURE	SUPERSATURATION	NUCLEATION RATE	DROPS THIS STEP
ADIABATIC	259.8216	8.4267	5.585413	0.72672095E 03	0.36336031E 01
CORRECTED	259.8302	8.4264	5.585338	0.72656421E 03	0.36205597E 01

TIME	PRESS	TEMP	SUPR
0.010	045.0	272.42	3.81
0.015	045.2	271.72	4.00
0.020	045.7	271.70	4.17
0.025	045.0	270.56	4.31
0.030	045.0	270.31	4.32
0.031	046.0	270.34	4.38
0.034	046.5	270.40	4.36
0.040	046.5	270.40	4.36
0.041	045.7	270.30	4.30
0.046	045.7	270.30	4.39
0.048	047.6	270.52	4.33
0.050	051.0	270.00	4.22
0.055	064.0	272.59	3.70

EXP. NO. 744 0.1 PRESS/CC

TIME	PRESS	TEMP	SUPR
0.005	1105.7	205.45	1.00
0.010	076.0	272.77	3.51
0.015	048.2	272.80	3.74
0.020	040.1	271.09	3.96
0.025	055.6	271.39	4.09
0.030	040.0	270.74	4.26
0.032	043.6	270.14	4.42
0.035	043.6	270.03	4.47
0.038	043.7	270.04	4.46
0.039	045.2	270.21	4.42
0.041	043.7	270.04	4.46
0.045	058.3	271.35	4.10

EXP. NO. 747 1.0 PRESS/CC

TIME	PRESS	TEMP	SUPR
0.005	1106.0	205.65	1.00
0.010	077.0	272.72	3.52
0.015	049.6	272.70	3.74
0.020	041.1	271.05	3.94
0.025	055.1	271.27	4.12
0.030	050.2	270.72	4.27
0.034	047.0	270.36	4.37
0.035	047.6	270.42	4.35
0.040	046.7	270.32	4.39
0.044	046.0	270.31	4.39
0.045	048.0	270.47	4.34
0.050	049.4	270.52	4.33
0.064	047.1	270.37	4.37
0.066	047.5	270.41	4.36
0.080	048.6	270.54	4.32
0.090	048.6	270.54	4.32
0.100	049.2	270.61	4.30
0.110	049.0	270.58	4.31
0.115	049.0	270.60	4.28
0.120	052.3	270.33	4.20
0.125	063.2	272.18	3.89

EXP. NO. 740 0.6 PRESS/CC

TIME	PRESS	TEMP	SUPR
0.005	1105.5	205.45	1.00
0.010	077.0	272.72	3.52
0.015	070.3	272.04	3.70
0.020	042.0	272.12	3.90
0.025	051.0	271.44	4.00
0.030	049.0	270.00	4.23
0.034	048.1	270.40	4.34
0.038	048.6	270.46	4.34
0.043	047.0	271.52	4.33
0.046	046.0	270.36	4.37
0.052	048.0	270.32	4.38
0.057	049.0	270.45	4.35
0.065	047.0	270.50	4.31
0.075	049.4	270.44	4.35
0.085	048.0	270.63	4.29
0.095	048.0	270.54	4.22
0.105	049.7	270.64	4.20
0.115	051.8	270.64	4.20
0.120	042.0	270.75	4.26
0.125	064.0	271.00	4.20
		272.06	3.87

EXP. NO. 752 0.9 PRESS/CC

TIME	PRESS	TEMP	SUPR
0.005	1105.6	205.65	1.00
0.010	077.0	272.72	3.51
0.015	064.6	272.63	3.70
0.020	050.0	271.72	3.90
0.025	052.0	271.10	4.17
0.030	047.0	270.80	4.33
0.035	042.0	249.04	4.40
0.038	039.5	260.57	4.60
0.043	041.0	260.63	4.50
0.046	041.0	259.72	4.56
0.050	037.0	260.51	4.59
0.054	039.0	260.61	4.59
0.058	041.0	260.76	4.55
0.065	041.0	260.01	4.53
0.075	041.5	260.80	4.54
0.085	042.0	260.80	4.51
0.105	042.0	260.80	4.51
0.115	042.4	260.00	4.51
0.120	044.0	270.00	4.45
0.125	052.0	271.10	4.17

EXP. NO. 754 1.5 PRESS/CC

TIME	PRESS	TEMP	SUPR
0.005	1105.0	205.65	1.00
0.010	076.0	272.75	3.52
0.015	068.0	272.86	3.72
0.020	048.0	271.06	3.94
0.025	054.7	271.27	4.12
0.030	056.0	270.73	4.27
0.035	044.0	270.16	4.43
0.040	041.0	260.71	4.56
0.045	041.6	260.72	4.54
0.050	040.0	260.60	4.57

TIME	DEP. SEC	TEMP	SUPR
0.000	041.7	260.66	4.60
0.007	041.1	260.72	4.56
0.014	041.4	260.77	4.55
0.021	041.0	260.81	4.53
0.028	041.3	260.80	4.52
0.035	042.5	260.80	4.51
0.042	042.2	260.85	4.52
0.049	042.8	260.82	4.50
0.056	042.0	260.80	4.50
0.063	042.4	260.80	4.49
0.070	041.0	270.31	6.37
0.077	041.4	272.02	5.83

EXP. NO.	NO.	742	0.4	DEP. SEC	TEMP	SUPR
0.000	1184.4	205.40	1.00			
0.007	076.4	272.01	3.51			
0.014	067.4	272.00	3.74			
0.021	050.2	271.00	3.95			
0.028	042.2	271.00	4.13			
0.035	049.4	271.00	4.30			
0.042	043.8	271.11	4.44			
0.049	041.1	260.03	4.53			
0.056	041.5	260.77	4.54			
0.063	041.0	260.00	4.53			
0.070	060.0	260.04	4.49			
0.077	045.0	270.00	4.30			
0.084	052.4	271.00	3.99			

EXP. NO. 757 0.7 DEP. SEC

TIME	DEP. SEC	TEMP	SUPR
0.000	1184.0	205.65	1.00
0.007	076.7	272.73	3.52
0.014	071.1	272.00	3.60
0.021	041.7	272.05	2.92
0.028	040.2	271.22	4.11
0.035	070.1	270.75	4.26
0.042	044.7	270.13	4.44
0.049	044.3	260.63	4.53
0.056	020.5	260.54	4.61
0.063	040.0	260.75	4.53
0.070	040.4	260.52	4.49
0.077	040.7	260.52	4.57
0.084	040.2	260.62	4.50
0.091	041.4	260.76	4.55
0.098	041.2	260.72	4.55
0.105	042.0	260.74	4.55
0.112	042.0	260.22	4.53
0.119	045.5	270.22	4.41
0.126	050.1	271.65	4.02

EXP. NO. 744 0.7 DEP. SEC

TIME	DEP. SEC	TEMP	SUPR
0.000	1184.0	205.65	1.00
0.007	076.2	272.77	3.51
0.014	044.6	272.47	3.92
0.021	054.7	271.00	4.04
0.028	050.2	270.05	4.24
0.035	045.0	270.20	4.30
0.042	030.7	260.65	4.53
0.049	024.0	260.50	4.68
0.056	020.0	260.22	4.71
0.063	026.7	260.31	4.69
0.070	027.0	260.35	4.67
0.077	028.2	260.40	4.63
0.084	047.1	270.50	4.33
0.091	041.2	272.00	3.91
0.098	044.1	271.20	4.12
0.105	041.3	272.15	3.90
0.112	055.4	271.46	4.07

EXP. NO. 740 0.6 DEP. SEC

TIME	DEP. SEC	TEMP	SUPR
0.000	1185.2	205.65	1.00
0.007	070.2	272.63	3.54
0.014	066.1	272.60	3.79
0.021	040.5	271.76	3.99
0.028	042.4	271.07	4.13
0.035	047.0	270.55	4.22
0.042	042.6	260.06	4.40
0.049	030.9	260.65	4.50
0.056	040.4	260.71	4.55
0.063	041.4	260.71	4.56
0.070	030.2	260.58	4.60
0.077	030.5	260.60	4.59
0.084	040.4	260.71	4.56
0.091	041.7	260.85	4.52
0.098	045.0	270.45	4.35
0.105	042.0	272.15	3.89

EXP. NO. 747 1.2 DEP. SEC

TIME	DEP. SEC	TEMP	SUPR
0.000	1185.4	205.65	1.00
0.007	070.0	272.60	3.53
0.014	063.0	272.25	3.87
0.021	054.4	271.20	4.12
0.028	042.1	270.56	4.31
0.035	042.3	260.01	4.50
0.042	027.3	260.74	4.67
0.049	023.0	260.00	4.81
0.056	021.7	260.60	4.83
0.063	021.2	260.65	4.89
0.070	022.4	260.77	4.85
0.077	040.3	260.43	4.57
0.084	042.2	270.57	4.31
0.091	053.0	271.77	3.80
0.098	060.1	272.03	3.71

EXP. NO. 770 1,2 DROPS/CC

TIME	PRESS	TEMP	SUPP
1105.6		295.65	1.00
0.005	075.0	272.65	3.54
0.010	062.2	272.25	3.97
0.015	054.9	271.32	4.11
0.020	049.6	271.60	4.39
0.025	042.7	269.93	4.49
0.030	037.4	269.33	4.69
0.035	035.5	269.11	4.74
0.038	034.2	268.92	4.91
0.039	034.5	269.05	4.73
0.041	033.0	269.49	4.66
0.045	046.0	270.41	4.36
0.050	047.2	271.92	3.95

EXP. NO. 770 3,0 DROPS/CC

TIME	PRESS	TEMP	SUPP
1105.6		295.65	1.00
0.005	075.0	272.65	3.54
0.010	061.7	272.14	3.90
0.015	052.0	271.14	4.16
0.020	048.0	271.34	4.37
0.025	040.1	269.40	4.57
0.030	034.0	269.13	4.75
0.034	031.0	269.78	4.24
0.037	031.7	269.73	4.96
0.040	029.0	269.77	4.95
0.044	031.0	269.75	4.96
0.047	030.4	269.40	4.90
0.051	030.3	269.57	4.32
0.053	031.3	269.62	4.32
0.056	024.1	269.01	4.72
0.060	049.4	269.72	4.56
0.065	059.1	271.15	4.13
0.070	061.0	272.14	3.90

EXP. NO. 772 3,2 DROPS/CC

TIME	PRESS	TEMP	SUPP
1105.5		295.65	1.00
0.005	075.6	273.65	3.54
0.010	061.1	272.02	3.93
0.015	049.4	271.04	4.19
0.020	046.5	270.26	4.40
0.025	039.6	269.50	4.60
0.030	035.3	269.10	4.75
0.035	030.0	269.42	4.95
0.037	027.9	269.24	5.02
0.040	027.0	269.15	5.06
0.042	027.4	269.22	5.03
0.044	031.0	269.61	4.99
0.048	041.0	269.85	4.52
0.055	054.3	271.26	4.13
0.060	061.4	272.06	3.92

EXP. NO. 770 5.0 DROPS/CC

TIME	PRESS	TEMP	SUPP
1102.4		295.65	1.00
0.005	074.7	272.74	3.52
0.010	059.0	271.87	3.97
0.015	049.1	270.84	4.23
0.020	043.0	270.17	4.43
0.025	037.4	269.55	4.61
0.030	033.1	269.04	4.77
0.035	029.4	269.41	4.90
0.039	029.0	269.81	4.94
0.040	029.9	269.54	4.92
0.045	023.0	269.75	4.95
0.049	024.0	269.31	5.00
0.051	024.5	269.29	5.01
0.054	027.0	269.40	4.97
0.057	031.1	269.91	4.84
0.060	036.0	269.27	4.66
0.065	042.5	270.70	4.25
0.070	057.0	271.95	3.97

EXP. NO. 774 3.0 DROPS/CC

TIME	PRESS	TEMP	SUPP
1105.0		295.65	1.00
0.005	075.5	273.69	3.53
0.010	061.1	272.07	3.92
0.015	048.1	271.17	4.15
0.020	044.6	270.20	4.42
0.025	041.0	269.63	4.57
0.030	034.0	269.06	4.76
0.034	031.1	269.66	4.89
0.037	030.0	269.54	4.93
0.041	030.0	269.66	4.90
0.043	031.1	269.66	4.90
0.046	029.7	269.62	4.90
0.049	030.1	269.55	4.92
0.051	029.2	269.44	4.96
0.054	029.4	269.58	4.91
0.058	025.2	269.13	4.74
0.062	048.7	270.67	4.29
0.070	044.0	272.30	3.83

EXP. NO. 792 12,4 DROPS/CC

TIME	PRESS	TEMP	SUPP
1104.7		295.45	1.00
0.005	068.6	272.04	3.70
0.010	058.6	271.80	4.04
0.015	047.7	271.52	4.31
0.020	040.9	269.86	4.53
0.025	035.0	269.24	4.70
0.030	031.0	269.70	4.97
0.035	027.0	269.22	5.03
0.039	025.4	269.15	5.05
0.043	027.5	269.29	5.01
0.047	026.7	269.19	5.04
0.051	024.0	267.99	5.11
0.055	025.5	269.05	5.09
0.060	027.3	269.25	5.02

0.005	027.2	244.22	5.23
0.010	027.2	244.67	5.27
0.015	027.2	244.82	5.28
0.020	027.2	244.89	4.83
0.025	027.2	244.97	4.87
0.030	027.2	244.61	4.50
0.035	027.2	271.24	4.13
0.040	027.2	272.22	3.98

0.045	027.2	244.2	4.00
0.050	027.2	244.24	4.00
0.055	027.2	244.24	4.02
0.060	027.2	244.24	4.07
0.065	027.2	244.27	4.03
0.070	027.2	244.30	4.00
0.075	027.2	244.34	4.00
0.080	027.2	244.47	4.05
0.085	027.2	244.51	4.03
0.090	027.2	244.10	4.72
0.095	027.2	272.26	4.25
0.100	027.2	272.14	3.90

EXP. NO. 784 32.0 PPOPS/CC

TIME	PPSS	TEMP	SUPR
0.005	1125.7	238.45	1.00
0.010	027.2	272.72	3.75
0.015	027.2	271.51	4.06
0.020	027.2	270.53	4.32
0.025	027.2	240.75	4.55
0.030	027.2	240.18	4.72
0.035	027.2	248.42	4.00
0.040	027.2	248.18	5.08
0.045	027.2	247.67	5.22
0.050	027.2	247.43	5.29
0.055	027.2	247.41	5.31
0.060	027.2	247.10	5.30
0.065	027.2	247.15	5.40
0.070	027.2	247.31	5.34
0.075	027.2	247.37	5.32
0.080	027.2	247.33	5.34
0.085	027.2	247.24	5.36
0.090	027.2	247.29	5.32
0.095	027.2	247.47	5.20
0.100	027.2	247.32	5.32
0.105	027.2	247.40	5.31
0.110	027.2	247.40	5.28
0.115	027.2	247.50	5.14
0.120	027.2	250.00	4.75
0.125	027.2	270.53	4.32
0.130	027.2	271.65	4.02
0.135	027.2	272.64	3.77

EXP. NO. 782 8.1 PPOPS/CC

TIME	PPSS	TEMP	SUPR
0.005	1124.3	238.45	1.00
0.010	027.2	272.72	3.55
0.015	027.2	271.42	4.03
0.020	027.2	270.30	4.27
0.025	027.2	240.45	4.58
0.030	027.2	240.17	4.70
0.035	027.2	248.45	4.05
0.040	027.2	248.27	5.02
0.045	027.2	248.24	4.00
0.050	027.2	248.28	4.07
0.055	027.2	248.28	4.03
0.060	027.2	248.22	5.03
0.065	027.2	248.15	5.05
0.070	027.2	248.27	5.02
0.075	027.2	248.20	4.85
0.080	027.2	270.01	4.47
0.085	027.2	271.52	4.06

EXP. NO. 784 14.0 PPOPS/CC

TIME	PPSS	TEMP	SUPR
0.005	1135.3	238.45	1.00
0.010	027.2	272.52	3.57
0.015	027.2	270.27	3.84
0.020	027.2	270.25	4.24
0.025	027.2	270.31	4.32
0.030	027.2	240.20	4.65
0.035	027.2	240.06	4.70
0.040	027.2	247.97	4.06
0.045	027.2	247.93	5.12
0.050	027.2	247.43	5.20
0.055	027.2	247.53	5.27
0.060	027.2	248.06	5.00
0.065	027.2	248.70	4.55
0.070	027.2	271.01	4.10
0.075	027.2	272.31	3.86

EXP. NO. 786 16.5 PPOPS/CC

TIME	PPSS	TEMP	SUPR
0.005	1134.4	238.45	1.00
0.010	027.2	272.02	3.71
0.015	027.2	271.78	3.09
0.020	027.2	270.92	4.24
0.025	027.2	270.05	4.46
0.030	027.2	240.35	4.67
0.035	027.2	240.77	4.85
0.040	027.2	248.23	4.00
0.045	027.2	248.21	5.00
0.050	027.2	248.32	5.00
0.055	027.2	248.04	5.00
0.060	027.2	248.07	5.08
0.065	027.2	248.24	5.02
0.070	027.2	248.20	5.04
0.075	027.2	248.07	5.08
0.080	027.2	248.25	5.09
0.085	027.2	248.33	4.09
0.090	027.2	248.23	5.03
0.095	027.2	248.24	5.03

EXP. NO. 707 34.8 DRIPS/CC

TIME	PRESS	TEMP	SUPP
11:05.7	075.7	295.65	1.00
0.005	070.2	272.62	3.69
0.010	080.5	271.82	2.93
0.015	047.0	270.51	4.33
0.020	032.1	269.51	4.62
0.025	030.0	269.23	4.70
0.030	026.7	269.00	5.07
0.035	021.5	267.50	5.28
0.040	016.3	266.35	5.47
0.045	013.0	266.50	5.60
0.050	013.4	266.56	5.64
0.055	010.5	267.26	5.36
0.060	032.0	266.79	4.84
0.065	051.0	270.84	4.52
0.070	041.1	272.00	4.23
			3.93

EXP. NO. 804 29.2 DRIPS/CC

TIME	PRESS	TEMP	SUPP
11:05.2	072.0	299.65	1.00
0.005	060.8	272.41	3.60
0.010	057.8	272.80	3.79
0.015	053.4	271.80	4.01
0.020	048.4	271.10	4.14
0.025	043.5	270.44	4.20
0.030	038.6	269.84	4.46
0.035	034.0	269.50	4.52
0.040	029.0	269.00	4.70
0.045	024.1	268.41	4.97
0.050	024.8	267.02	5.13
0.055	024.4	266.41	5.31
0.060	019.1	266.40	5.40
0.065	013.0	266.60	5.57
0.070	014.2	266.60	5.58
0.075	017.7	267.10	5.42
0.080	020.2	268.44	4.96
0.085	041.2	269.00	4.84
0.090	052.5	271.00	4.17
0.095	043.5	272.00	3.95

EXP. NO. 700 27.0 DRIPS/CC

TIME	PRESS	TEMP	SUPP
11:05.8	075.8	295.65	1.00
0.010	065.8	272.55	3.56
0.015	056.7	272.62	3.73
0.020	045.0	271.40	4.03
0.025	036.3	270.10	4.42
0.030	030.1	269.24	4.70
0.035	024.0	268.40	4.95
0.040	020.1	267.87	5.15
0.045	020.1	267.32	5.34
0.050	017.0	266.97	5.47
0.055	015.6	266.02	5.40
0.060	013.0	266.00	5.46
0.065	022.0	267.10	5.42
0.070	022.0	267.64	5.23
0.075	046.0	269.14	4.74
0.080	050.4	270.26	4.37
0.085	050.4	271.80	4.01

EXP. NO. 807 59. DRIPS/CC

TIME	PRESS	TEMP	SUPP
11:05.2	072.0	295.65	1.00
0.005	064.8	272.36	3.61
0.010	059.0	272.46	3.82
0.015	050.0	271.69	4.01
0.020	042.5	271.07	4.17
0.025	047.2	270.47	4.34
0.030	041.7	269.95	4.52
0.035	036.4	269.24	4.70
0.040	032.1	268.75	4.85
0.045	027.8	268.26	5.03
0.050	022.9	267.76	5.19
0.055	019.0	267.24	5.37
0.060	013.8	266.64	5.59
0.065	010.2	266.23	5.74
0.070	009.1	265.03	5.94
0.075	007.0	265.04	5.36
0.080	009.0	266.06	5.31
0.085	015.8	266.07	5.50
0.090	023.8	267.20	5.10
0.095	032.6	268.00	4.84
0.100	041.0	269.07	4.51
0.105	051.2	270.03	4.21
0.110	062.4	272.10	3.82

EXP. NO. 800 21.7 DRIPS/CC

TIME	PRESS	TEMP	SUPP
11:05.0	074.0	295.65	1.00
0.005	052.0	272.44	3.59
0.010	042.0	270.97	4.20
0.015	035.0	269.04	4.49
0.020	030.4	269.07	4.76
0.025	025.2	268.51	4.94
0.030	025.5	267.00	5.11
0.035	021.5	267.40	5.23
0.040	020.3	267.35	5.33
0.045	020.4	267.36	5.33
0.050	020.7	267.30	5.31
0.055	020.5	267.27	5.32
0.060	021.3	267.46	5.29
0.065	020.4	268.30	4.97
0.070	043.7	270.03	4.47
0.075	054.5	271.25	4.13
0.080	063.4	272.25	3.87

EXP. NO. 800 118. DRIPS/CC

TIME	PRESS	TEMP	SUPP
11:04.1	072.0	295.65	1.00
0.005	064.4	272.47	3.58
0.010	057.2	272.54	3.80
0.015	051.0	271.71	4.01
0.020	046.7	271.11	4.16
0.025	041.3	270.52	4.33
0.030	041.3	269.91	4.50

0.035	076.5	249.27	4.65
0.040	077.4	249.28	4.62
0.045	077.4	249.22	5.00
0.050	078.2	249.25	5.15
0.055	079.0	247.34	5.33
0.060	079.5	264.77	5.54
0.065	080.2	244.21	5.75
0.070	080.2	245.27	5.39
0.075	081.1	245.73	5.24
0.080	081.6	245.91	5.87
0.085	081.4	246.47	5.65
0.090	082.3	245.64	5.22
0.095	082.4	263.61	4.81
0.100	082.2	260.60	4.51
0.105	082.4	271.17	4.15
0.110	081.5	272.19	3.28

0.035	076.5	249.27	4.65
0.040	077.4	249.28	4.62
0.045	077.4	249.22	5.00
0.050	078.2	249.25	5.15
0.055	079.0	247.34	5.33
0.060	079.5	264.77	5.54
0.065	080.2	244.21	5.75
0.070	080.2	245.27	5.39
0.075	081.1	245.73	5.24
0.080	081.6	245.91	5.87
0.085	081.4	246.47	5.65
0.090	082.3	245.64	5.22
0.095	082.4	263.61	4.81
0.100	082.2	260.60	4.51
0.105	082.4	271.17	4.15
0.110	081.5	272.19	3.28

EXP. NO. 212 28.2 DRIPS/CC

TIME	DRIPS	TEMP	SHDR
0.035	1134.5	295.65	1.00
0.040	071.2	272.25	3.63
0.045	032.2	272.25	3.87
0.050	051.2	271.54	4.05
0.055	051.2	271.01	4.19
0.060	046.2	272.42	4.35
0.065	042.2	272.07	4.46
0.070	042.2	249.21	4.71
0.075	038.2	263.67	4.38
0.080	026.2	262.14	5.06
0.085	021.2	267.64	5.23
0.090	017.2	267.14	5.41
0.095	014.1	265.75	5.55
0.100	013.1	266.62	5.60
0.105	013.2	266.71	5.55
0.110	015.7	265.23	5.48
0.115	022.0	247.66	5.22
0.120	022.3	262.42	4.65
0.125	043.7	271.63	4.20
0.130	056.5	271.59	4.04

EXP. NO. 217 30. DRIPS/CC

TIME	DRIPS	TEMP	SHDR
0.035	1125.7	295.45	1.00
0.040	073.7	272.49	3.58
0.045	066.4	272.66	3.77
0.050	060.1	271.56	3.94
0.055	055.6	271.29	4.00
0.060	049.9	270.72	4.25
0.065	044.9	270.23	4.41
0.070	038.4	262.61	4.59
0.075	034.6	262.15	4.75
0.080	029.4	269.60	4.90
0.085	026.1	263.60	5.00
0.090	021.9	267.50	5.25
0.095	019.7	267.15	5.40
0.100	016.5	266.00	5.44
0.105	017.2	267.07	5.43
0.110	016.2	265.24	5.40
0.115	015.9	266.00	5.40
0.120	021.7	267.50	5.25
0.125	024.2	260.02	4.77
0.130	045.1	271.25	4.40
0.135	055.7	271.44	4.07

EXP. NO. 214 263. DRIPS/CC

TIME	DRIPS	TEMP	SHDR
0.035	1124.8	295.65	1.00
0.040	071.2	272.22	3.54
0.045	052.2	272.21	3.88
0.050	051.2	271.52	4.05
0.055	051.2	270.08	4.20
0.060	046.2	270.41	4.35
0.065	040.7	249.75	4.54
0.070	036.0	260.24	4.70
0.075	031.3	268.70	4.97
0.080	026.9	263.20	5.04
0.085	022.5	267.70	5.21
0.090	018.2	247.19	5.39
0.095	013.1	266.60	5.60
0.100	008.7	266.09	5.80
0.105	005.1	265.57	5.97
0.110	003.9	265.53	6.22
0.115	004.1	265.55	6.01
0.120	004.9	265.65	5.98

EXP. NO. 210 53. DRIPS/CC

TIME	DRIPS	TEMP	SHDR
0.035	1125.6	295.65	1.00
0.040	072.7	272.31	3.52
0.045	066.0	272.44	3.72
0.050	059.7	271.74	4.00
0.055	053.2	271.12	4.15
0.060	042.1	270.55	4.32
0.065	043.3	270.00	4.49
0.070	038.7	269.49	4.62
0.075	033.7	269.01	4.81
0.080	029.1	249.39	4.90
0.085	026.6	267.04	5.12
0.090	022.0	267.40	5.30
0.095	016.5	249.23	5.48
0.100	014.0	266.64	5.59
0.105	013.5	266.50	5.61
0.110	014.2	266.44	5.63
0.115	012.2	266.54	5.64
0.120	012.8	266.50	5.64
0.125	012.0	266.52	5.64
0.130	014.5	266.45	5.50
0.135	014.5	266.60	5.57
0.140	013.0	266.62	5.60
0.145	014.1	266.65	5.59

EXP. NO.	DEPTH	TEMP	SUPR
0.110	047.2	267.25	5.37
0.111	047.7	269.64	4.39
0.112	047.7	270.12	4.44
0.113	048.4	271.14	4.15
0.114	044.1	272.55	3.85

EXP. NO.	DEPTH	TEMP	SUPR
0.115	045.1	265.66	1.00
0.116	047.2	273.25	3.61
0.117	048.9	272.79	3.77
0.118	049.1	272.04	3.92
0.119	047.7	271.43	4.08
0.120	047.6	270.95	4.23
0.121	045.0	270.33	4.38
0.122	047.2	269.90	4.54
0.123	045.2	269.21	4.71
0.124	049.2	268.61	4.90
0.125	045.4	268.09	5.08
0.126	045.9	267.64	5.23
0.127	047.3	267.22	5.38
0.128	047.3	267.15	5.40
0.129	047.3	267.23	5.37
0.130	047.3	267.11	5.42
0.131	047.3	267.15	5.40
0.132	047.5	267.29	5.35
0.133	048.5	267.20	5.35
0.134	047.1	267.24	5.37
0.135	047.2	267.35	5.33
0.136	049.4	267.39	5.31
0.137	049.4	267.38	5.33
0.138	049.4	267.39	5.31
0.139	049.4	267.38	5.33
0.140	049.4	267.44	5.30
0.141	049.4	267.74	5.19
0.142	049.4	269.80	4.91
0.143	044.4	270.76	4.40
0.144	054.3	271.38	4.09

EXP. NO.	DEPTH	TEMP	SUPR
0.145	014.6	266.70	5.89
0.146	015.2	266.87	5.58
0.147	015.4	266.91	5.49
0.148	015.4	266.91	5.49
0.149	015.4	266.91	5.49
0.150	016.1	266.92	5.46
0.151	016.0	267.00	5.46
0.152	016.1	266.99	5.46
0.153	016.4	267.02	5.45
0.154	019.2	267.24	5.33
0.155	029.6	268.54	4.92
0.156	040.7	270.84	4.46
0.157	052.5	271.26	4.12

EXP. NO. 927 26. DEEPS/CC

TIME	DEPTH	TEMP	SUPR
0.015	1105.1	295.65	1.00
0.016	045.4	272.57	3.70
0.017	049.2	271.04	3.94
0.018	053.3	271.19	4.15
0.019	049.3	272.73	4.27
0.020	045.7	272.32	4.38
0.021	042.1	269.91	4.50
0.022	036.0	269.21	4.71
0.023	032.2	268.79	4.84
0.024	027.3	269.22	5.03
0.025	024.5	267.90	5.14
0.026	021.3	267.53	5.27
0.027	021.2	267.53	5.27
0.028	022.1	267.62	5.24
0.029	021.3	267.53	5.27
0.030	021.9	267.58	5.25
0.031	022.0	267.70	5.21
0.032	022.8	267.70	5.21
0.033	022.1	267.62	5.24
0.034	022.0	267.72	5.20
0.035	023.0	267.82	5.16
0.036	023.0	267.72	5.20
0.037	022.7	267.60	5.21
0.038	023.9	267.91	5.17
0.039	024.4	267.82	5.14
0.040	023.8	267.91	5.17
0.041	023.8	267.91	5.17
0.042	024.3	267.92	5.13
0.043	024.7	267.92	5.13
0.044	024.4	267.93	5.15
0.045	024.6	267.90	5.14
0.046	025.5	269.01	5.10
0.047	025.2	267.97	5.11
0.048	026.4	269.11	5.07
0.049	023.2	269.99	4.31
0.050	053.9	271.23	4.13

EXP. NO.	DEPTH	TEMP	SUPR
0.051	047.6	272.52	3.57
0.052	047.7	272.85	3.72
0.053	046.6	272.08	3.91
0.054	047.6	271.62	4.03
0.055	045.2	270.90	4.22
0.056	048.8	270.73	4.27
0.057	049.0	269.73	4.55
0.058	049.0	269.16	4.73
0.059	049.0	269.50	4.91
0.060	025.5	263.19	5.04
0.061	022.1	267.68	5.21
0.062	017.5	267.16	5.40
0.063	013.6	266.70	5.57
0.064	013.5	266.69	5.57
0.065	013.6	266.70	5.57
0.066	012.9	266.62	5.60
0.067	013.7	266.71	5.56
0.068	014.6	266.81	5.53
0.069	014.3	266.78	5.54

EXP. NO.	DEPTH	TEMP	SUPR
0.070	051.4	270.44	4.99
0.071	044.6	270.67	4.39
0.072	035.0	269.68	4.57
0.073	031.9	269.22	4.71

0.134	034.5	249.51	4.62
0.134	031.9	249.22	4.71
0.132	032.7	249.31	4.68
0.134	035.5	249.57	4.60
0.134	033.4	249.29	4.65
0.134	034.4	249.50	4.62
0.134	035.3	249.60	4.59
0.132	033.7	249.44	4.64
0.132	035.8	249.46	4.53
0.132	035.0	249.67	4.57
0.134	035.1	249.59	4.60
0.134	036.8	249.78	4.54
0.132	034.0	249.76	4.54
0.130	044.0	270.93	4.21

0.134	026.7	249.74	4.24
0.132	025.3	249.80	4.21
0.132	025.9	249.64	4.80
0.132	026.0	249.77	4.85
0.132	026.2	249.77	4.85
0.132	026.4	249.71	4.87
0.132	026.7	249.74	4.86
0.132	027.2	249.90	4.84
0.132	027.1	249.70	4.85
0.132	026.7	249.74	4.86
0.132	027.1	249.74	4.85
0.132	027.0	249.88	4.82
0.132	028.3	249.83	4.86
0.132	028.7	249.87	4.79
0.132	027.4	249.82	4.82
0.132	027.9	249.87	4.79
0.132	028.6	249.86	4.79
0.132	029.6	249.86	4.79
0.132	028.5	249.85	4.79
0.132	029.2	249.83	4.77
0.132	029.6	249.84	4.73
0.132	029.1	249.82	4.77
0.132	029.9	249.86	4.78
0.132	029.5	249.86	4.76
0.132	029.5	249.85	4.79
0.132	029.0	249.81	4.78
0.132	030.1	249.83	4.74
0.132	030.0	249.82	4.74
0.132	030.8	249.81	4.71
0.132	034.4	249.63	4.59
0.132	044.3	270.98	4.20

EXP. NO. 510 4.0 OP OPS/CC

TIME	PRESS	TEMP	SUPR
0.1173	051.2	295.65	1.00
0.1051	051.4	271.50	4.06
0.1100	045.3	270.91	4.25
0.1115	040.2	270.23	4.41
0.1225	035.2	269.74	4.55
0.1337	032.0	269.91	4.62
0.1335	035.8	269.73	4.56
0.1345	036.2	269.78	4.54
0.1345	034.4	269.58	4.60
0.1345	035.0	269.63	4.53
0.1350	037.8	269.84	4.52
0.1355	027.2	269.96	4.51
0.1345	034.2	269.77	4.54
0.1370	034.5	269.81	4.53
0.1370	037.4	269.91	4.50
0.1375	037.9	269.97	4.49
0.1380	037.7	249.94	4.49
0.1385	036.7	269.83	4.53
0.1390	037.3	269.96	4.51
0.1395	037.9	269.95	4.49
0.1400	038.2	269.96	4.51
0.1405	037.3	269.90	4.51
0.1410	037.4	269.91	4.50
0.1415	038.4	270.02	4.47
0.1420	038.0	270.01	4.49
0.1425	037.7	269.94	4.49
0.1430	043.3	270.58	4.31

EXP. NO. 524 31. OP OPS/CC

TIME	PRESS	TEMP	SUPR
0.1173	051.2	295.65	1.00
0.1051	051.4	271.50	4.06
0.1100	045.3	270.91	4.23
0.1115	040.4	270.25	4.40
0.1225	035.8	269.73	4.56
0.1337	031.1	269.10	4.72
0.1335	026.3	269.79	4.87
0.1345	025.3	249.52	4.83
0.1345	025.5	249.66	4.92
0.1345	025.4	249.55	4.92
0.1345	025.4	249.53	4.93
0.1350	027.0	249.72	4.87
0.1355	027.1	249.72	4.87
0.1355	025.5	249.54	4.92
0.1355	025.5	249.54	4.92
0.1360	027.6	249.72	4.85
0.1365	027.2	249.74	4.86
0.1370	026.4	249.65	4.89
0.1375	027.0	249.71	4.87
0.1380	029.0	249.83	4.83
0.1385	027.0	249.82	4.84
0.1390	027.2	249.74	4.85
0.1395	028.6	249.94	4.83
0.1400	027.0	249.92	4.82
0.1405	029.2	249.84	4.84
0.1410	029.1	249.84	4.83
0.1415	029.0	249.85	4.76
0.1420	028.2	249.85	4.83
0.1425	028.1	249.84	4.83

EXP. NO. 522 21. OP OPS/CC

TIME	PRESS	TEMP	SUPR
0.1173	051.5	295.65	1.00
0.1051	051.4	271.57	4.04
0.1100	046.1	270.97	4.20
0.1115	040.5	270.36	4.37
0.1225	035.7	269.78	4.54
0.1337	031.3	269.27	4.69
0.1335	027.4	268.83	4.83
0.1345	024.8	268.53	4.93
0.1345	026.0	268.66	4.89
0.1345	024.6	268.50	4.94
0.1350	024.6	268.50	4.94
0.1355	024.8	268.53	4.93
0.1360	025.8	268.64	4.89

0.140	020.4	269.00	4.79
0.145	020.7	269.02	4.77
0.170	020.0	269.34	4.80
0.175	020.2	269.07	4.79
0.180	020.1	269.07	4.76
0.185	020.0	269.56	4.76
0.190	020.0	269.05	4.76
0.195	020.1	269.07	4.76
0.200	021.6	269.13	4.74
0.205	026.7	269.62	4.83
0.210	036.0	269.75	4.55

0.050	020.4	269.00	4.79
0.055	020.2	269.02	4.77
0.060	021.0	269.34	4.80
0.065	021.2	269.07	4.79
0.070	021.2	269.07	4.76
0.075	021.2	269.56	4.76
0.080	020.0	269.05	4.76
0.085	020.1	269.07	4.76
0.090	020.7	269.13	4.74
0.095	026.7	269.62	4.83
0.100	036.0	269.75	4.55
0.105	022.4	269.00	4.79
0.110	022.4	269.02	4.77
0.115	023.1	269.34	4.80
0.120	023.1	269.07	4.79
0.125	023.1	269.07	4.76
0.130	023.1	269.56	4.76
0.135	023.1	269.05	4.76
0.140	023.1	269.07	4.76
0.145	023.1	269.13	4.74
0.150	023.1	269.62	4.83
0.155	023.1	269.75	4.55
0.160	024.7	269.00	4.79
0.165	024.7	269.02	4.77
0.170	025.4	269.34	4.80
0.175	025.4	269.07	4.79
0.180	025.4	269.07	4.76
0.185	025.4	269.56	4.76
0.190	025.4	269.05	4.76
0.195	025.4	269.07	4.76
0.200	025.4	269.13	4.74
0.205	025.4	269.62	4.83
0.210	025.4	269.75	4.55

EXP. NO. 527

0.3 DROPS/CC

TIME	DESS	TEMP	SUPR
0.005	1121.2	295.65	1.00
0.010	051.4	271.22	4.11
0.015	047.2	270.85	4.24
0.020	041.9	270.23	4.41
0.025	037.2	269.71	4.55
0.030	035.4	269.59	4.62
0.035	034.1	269.35	4.57
0.040	033.0	269.32	4.69
0.045	033.4	269.29	4.69
0.050	037.8	269.77	4.54
0.055	041.4	270.10	4.42
0.060	045.0	270.70	4.29

EXP. NO. 528

48. DROPS/CC

TIME	DESS	TEMP	SUPR
0.005	1180.4	299.65	1.00
0.010	051.4	271.22	4.11
0.015	046.7	270.85	4.23
0.020	042.2	270.25	4.27
0.025	037.5	269.21	4.53
0.030	032.7	269.26	4.70
0.035	027.5	269.68	4.39
0.040	022.5	269.10	5.07
0.045	020.0	267.80	5.17
0.050	020.6	267.87	5.15
0.055	019.7	267.76	5.10
0.060	018.7	267.45	5.23
0.065	018.5	267.74	5.10
0.070	020.6	267.27	5.15
0.075	020.7	267.90	5.15
0.080	019.7	267.76	5.10
0.085	020.6	267.87	5.15
0.090	021.7	267.09	5.11
0.095	021.3	267.05	5.12
0.100	020.6	267.07	5.15
0.105	021.6	267.00	5.11
0.110	022.3	269.06	5.09
0.115	021.4	267.06	5.12
0.120	020.8	267.80	5.14
0.125	022.0	269.03	5.10
0.130	022.7	268.11	5.09
0.135	022.5	269.00	5.09
0.140	026.7	268.57	4.92
0.145	042.0	270.32	4.28

EXP. NO. 529

5.7 DROPS/CC

TIME	DESS	TEMP	SUPR
0.005	1121.2	295.65	1.00
0.010	051.4	271.22	4.10
0.015	046.9	270.82	4.24
0.020	042.0	270.27	4.40
0.025	036.9	269.69	4.57
0.030	032.4	269.17	4.72
0.035	030.1	269.01	4.81
0.040	028.7	269.75	4.86
0.045	028.1	269.79	4.84
0.050	032.4	269.17	4.72
0.055	035.0	269.47	4.63
0.060	040.7	270.12	4.44

EXP. NO. 534

7.8 DROPS/CC

TIME	DESS	TEMP	SUPR
0.005	1122.2	295.65	1.00
0.010	051.4	271.23	4.13
0.015	046.7	270.70	4.28
0.020	041.9	270.15	4.43
0.025	037.7	269.67	4.57
0.030	033.2	269.16	4.73
0.035	030.0	268.89	4.81
0.040	032.2	269.04	4.77
0.045	031.8	269.00	4.78
0.050	030.0	268.79	4.85

EXP. NO. 542

12.2 DROPS/CC

TIME	DESS	TEMP	SUPR
0.005	1175.5	299.65	1.00
0.010	051.4	271.01	3.99
0.015	047.7	271.20	4.09
0.020	043.0	270.25	4.21
0.025	039.2	270.42	4.36
0.030	034.0	269.92	4.50
0.035	029.2	269.27	4.69

0.121	234.6	267.06	4.49
0.125	232.0	267.43	4.65
0.127	237.7	268.93	4.80
0.134	222.0	268.32	4.82
0.139	212.2	267.95	5.12
0.141	217.8	267.70	5.13
0.142	214.6	267.68	5.21
0.146	217.2	267.72	5.27
0.147	217.2	267.80	5.17
0.150	212.7	268.00	5.11
0.154	234.7	267.59	4.91
0.160	212.2	270.14	4.44

0.125	226.6	267.05	5.12
0.130	226.2	267.01	5.14
0.135	227.1	268.00	5.10
0.140	220.9	268.43	4.96
0.145	243.0	269.22	4.53

EXP. NO. 564

47. DRIPS/CC

EXP. NO. 562

23.4 DRIPS/CC

TIME	DRIPS	TEMP	SUPP
1175.7	295.65	271.65	1.00
0.117	251.4	271.73	4.00
0.118	246.7	271.25	4.14
0.119	241.0	271.45	4.29
0.120	235.0	270.88	4.45
0.124	221.7	269.45	4.64
0.126	226.0	268.03	4.82
0.130	222.0	268.47	4.95
0.134	212.4	267.95	5.12
0.139	216.2	267.71	5.21
0.144	215.4	267.61	5.24
0.146	215.1	267.57	5.25
0.147	215.4	267.60	5.24
0.150	217.2	267.76	5.19
0.154	223.7	268.56	4.92
0.160	228.2	269.66	4.49
0.168	274.2	270.92	4.21

TIME	DRIPS	TEMP	SUPP
1126.2	295.65	270.65	1.00
0.117	251.4	270.86	4.23
0.118	246.7	270.36	4.38
0.119	241.0	269.78	4.54
0.120	237.3	269.25	4.70
0.125	232.7	268.73	4.86
0.130	229.4	268.24	5.03
0.135	223.0	267.72	5.20
0.140	220.1	267.28	5.36
0.145	220.1	267.28	5.36
0.150	212.7	267.23	5.37
0.155	212.6	267.22	5.38
0.160	217.7	267.09	5.46
0.165	212.2	267.17	5.39
0.170	212.5	267.21	5.39
0.175	212.4	267.08	5.43
0.180	212.5	267.09	5.42
0.185	220.3	267.30	5.35
0.190	220.1	267.28	5.35
0.195	219.9	267.13	5.41
0.200	219.7	267.23	5.37
0.205	221.3	267.42	5.31
0.210	220.7	267.35	5.33
0.215	220.2	267.29	5.35
0.220	220.2	267.36	5.33
0.225	221.4	267.45	5.30
0.230	221.4	267.43	5.30
0.235	221.4	267.43	5.30
0.240	217.3	267.01	5.45
0.245	223.6	267.68	5.21

EXP. NO. 562

33.7 DRIPS/CC

TIME	DRIPS	TEMP	SUPP
1107.2	295.65	270.65	1.00
0.117	251.4	270.79	4.26
0.118	247.0	270.29	4.37
0.119	242.0	269.78	4.54
0.120	239.0	269.26	4.70
0.124	223.5	268.74	4.86
0.126	224.0	268.22	5.03
0.130	224.0	267.75	5.19
0.134	224.7	267.73	5.20
0.139	224.7	267.73	5.20
0.144	221.3	267.40	5.31
0.146	222.2	267.44	5.30
0.150	224.4	267.60	5.21
0.154	225.2	267.70	5.18
0.159	223.4	267.53	5.25
0.164	223.3	267.57	5.25
0.169	225.2	267.92	5.17
0.174	225.6	267.93	5.16
0.179	224.3	267.68	5.21
0.184	224.3	267.65	5.23
0.189	225.7	267.84	5.16
0.194	226.2	267.91	5.14
0.199	226.6	267.91	5.14
0.204	226.6	267.75	5.19
0.209	226.6	267.73	5.20
0.214	226.6	267.92	5.13

EXP. NO. 567

61.5 DRIPS/CC

TIME	DRIPS	TEMP	SUPP
1124.4	295.65	270.65	1.00
0.117	251.4	270.95	4.24
0.118	242.0	270.46	4.34
0.119	240.0	269.88	4.51
0.120	239.0	269.33	4.68
0.124	233.5	268.81	4.84
0.126	233.0	268.30	5.01
0.130	229.9	267.78	5.21
0.135	223.2	267.19	5.39
0.140	220.3	266.93	5.46
0.145	217.6	267.07	5.42
0.150	213.4	266.99	5.46
0.155	217.7	266.91	5.40
0.160	217.7	266.91	5.40
0.165	213.3	267.06	5.43
0.170	210.6	267.21	5.39
0.175	210.0	267.14	5.40
0.180	212.2	267.05	5.44
0.185	212.4	267.19	5.39
0.190	212.4	267.19	5.39

EXP. NO. 522 22.0 DRIPS/CC

TIME	DEPRESS	TEMP	SHDR
1138.0	051.4	270.65	1.00
0.005	045.4	270.70	4.28
0.010	046.7	270.17	4.43
0.015	041.5	269.59	4.60
0.020	034.6	269.02	4.77
0.025	032.3	269.53	4.93
0.030	029.1	269.05	5.09
0.035	023.9	267.55	5.26
0.039	021.1	267.24	5.37
0.040	021.7	267.20	5.39
0.042	021.6	267.30	5.35
0.045	026.7	267.81	5.17
0.050	022.6	269.36	4.67

0.110	027.8	268.2	5.10
0.115	027.9	269.17	5.16
0.117	027.4	268.13	5.11
0.118	027.8	269.00	5.11
0.120	029.0	269.14	5.05
0.125	029.1	268.17	5.05
0.130	029.3	269.19	5.02
0.135	030.1	269.29	5.01
0.140	044.1	257.89	4.51

EXP. NO. 524 20.2 DRIPS/CC

TIME	DEPRESS	TEMP	SHDR
1138.0	051.4	270.65	1.00
0.005	045.9	270.00	4.30
0.010	040.5	269.39	4.48
0.015	035.7	268.95	4.63
0.020	031.5	269.37	4.88
0.025	027.5	267.91	5.14
0.030	024.7	267.59	5.25
0.035	025.3	267.65	5.22
0.040	025.6	267.60	5.21
0.041	024.4	267.57	5.25
0.047	023.1	267.40	5.31
0.050	022.1	267.20	5.35
0.055	022.0	267.30	5.32
0.060	024.0	267.53	5.27
0.065	026.1	267.75	5.10
0.070	020.6	269.15	5.06
0.075	045.0	270.01	4.47

EXP. NO. 522 69.0 DRIPS/CC

TIME	DEPRESS	TEMP	SHDR
1138.4	091.4	295.65	1.00
0.005	046.2	270.00	4.31
0.010	040.7	269.36	4.43
0.020	025.9	268.00	4.57
0.025	031.7	268.32	4.34
0.030	027.1	267.81	4.99
0.035	022.0	267.32	5.17
0.040	012.3	266.70	5.34
0.045	013.7	266.26	5.53
0.050	010.1	265.84	5.73
0.055	011.3	265.09	5.90
0.060	011.2	265.07	5.14
0.065	010.1	265.84	5.25
0.070	011.3	265.09	5.00
0.075	012.5	265.12	5.84
0.080	012.1	265.12	5.73
0.085	012.1	266.02	5.21
0.090	011.7	266.02	5.82
0.095	012.0	266.17	5.77
0.100	013.3	266.21	5.75
0.105	013.1	266.19	5.75
0.110	013.0	266.19	5.77
0.115	014.6	266.27	5.73
0.120	014.6	266.27	5.77
0.125	014.1	266.31	5.69
0.130	015.4	266.46	5.72
0.135	012.7	266.53	5.65
0.140	015.4	266.46	5.65
0.145	018.1	266.46	5.66
0.150	023.7	266.77	5.54
0.155	046.7	268.55	4.32
0.160	046.7	270.04	4.46

EXP. NO. 527 20.0 DRIPS/CC

TIME	DEPRESS	TEMP	SHDR
1147.0	051.4	295.65	1.00
0.005	047.1	270.71	4.27
0.010	042.2	270.22	4.41
0.015	036.7	269.67	4.57
0.020	032.7	269.04	4.77
0.025	028.7	268.58	4.91
0.030	025.6	268.13	5.06
0.035	026.3	267.77	5.18
0.040	025.0	267.85	5.16
0.045	024.2	267.70	5.13
0.050	024.8	267.61	5.24
0.055	026.8	267.68	5.22
0.060	026.8	267.91	5.14
0.065	026.8	267.91	5.14
0.070	025.4	267.75	5.19
0.075	027.0	267.81	5.17
0.080	027.5	267.90	5.11
0.085	027.4	267.98	5.11
0.090	026.5	267.97	5.15
0.095	026.9	267.92	5.13

EXP. NO. 524 44.7 DRIPS/CC

TIME	DEPRESS	TEMP	SHDR
1138.0	051.4	295.65	1.00
0.005	045.0	270.00	4.35
0.010	040.5	269.36	4.51
0.015	035.8	268.95	4.69
0.020	031.4	268.75	4.86
0.025	027.4	268.35	5.02
0.030	027.0	267.74	5.19
0.035	027.0	267.27	5.36
0.040	019.2	266.73	5.56
0.045	014.0	266.35	5.70
0.050	015.5	266.43	5.67
0.055	015.4	266.41	5.68
0.060	013.6	266.20	5.76

EXP. NO.	TIME	PRESS	TEMP	SUPP.
0000	005	014.0	267.24	5.71
0000	010	014.0	266.47	5.65
0000	015	015.1	266.40	5.55
0000	020	016.5	266.34	5.75
0000	025	016.4	266.47	5.65
0000	030	017.3	266.64	5.52
0000	035	016.5	266.53	5.63
0000	040	017.0	266.47	5.65
0000	045	017.5	266.65	5.55
0000	050	017.2	266.72	5.55
0000	055	017.7	266.65	5.55
0000	060	017.5	266.65	5.55
0000	065	017.4	266.75	5.55
0000	070	017.1	266.73	5.55
0000	075	017.9	266.90	5.55
0000	080	018.4	266.90	5.55
0000	085	018.6	266.77	5.55
0000	090	018.9	267.14	5.55
0000	095	018.4	266.90	5.55

EXP. NO.	TIME	PRESS	TEMP	SUPP.
507	005	051.4	295.65	1.00
0000	010	044.1	270.57	4.31
0000	015	046.7	269.07	4.40
0000	020	035.0	269.35	4.67
0000	025	021.3	269.91	4.84
0000	030	021.0	269.29	5.01
0000	035	022.6	269.25	5.22
0000	040	019.0	267.29	5.35
0000	045	019.4	266.97	5.51
0000	050	020.0	266.91	5.49
0000	055	020.0	266.92	5.45
0000	060	019.0	266.90	5.50
0000	065	020.7	267.06	5.43
0000	070	020.2	267.12	5.41
0000	075	020.0	267.00	5.46
0000	080	020.6	267.05	5.44
0000	085	021.0	267.20	5.38
0000	090	022.0	267.21	5.38
0000	095	021.1	267.11	5.42
0000	100	021.4	267.14	5.41
0000	105	022.6	267.22	5.36
0000	110	022.5	267.22	5.36
0000	115	022.2	267.24	5.36
0000	120	023.1	267.34	5.34
0000	125	023.0	267.43	5.30
0000	130	023.4	267.27	5.32
0000	135	023.3	267.36	5.33
0000	140	024.2	267.46	5.29
0000	145	024.7	267.52	5.27
0000	150	024.1	267.45	5.29
0000	155	023.2	267.45	5.25
0000	160	023.2	267.50	5.25
0000	165	023.4	267.50	5.24
0000	170	025.2	267.54	5.26
0000	175	024.0	267.50	5.24
0000	180	025.4	267.60	5.24
0000	185	026.0	267.67	5.22
0000	190	026.1	267.68	5.22
0000	195	025.9	267.66	5.21
0000	200	027.7	267.78	5.18
0000	205	027.1	267.79	5.18
0000	210	027.1	267.79	5.18
0000	215	027.7	267.81	5.17
0000	220	030.0	268.22	5.02

EXP. NO.	TIME	PRESS	TEMP	SUPP.
607	005	081.4	311.44	1.00
0000	010	081.4	309.24	4.30
0000	015	082.0	308.24	4.61
0000	020	082.0	308.24	4.69
0000	025	087.6	308.05	4.76
0000	030	087.1	308.04	4.83
0000	035	087.1	308.09	5.02
0000	040	084.3	307.52	5.27
0000	045	085.0	307.04	5.40
0000	050	085.0	306.44	5.46
0000	055	087.0	306.33	5.47
0000	060	087.0	306.33	5.47
0000	065	087.0	306.33	5.47
0000	070	087.0	306.33	5.47
0000	075	087.0	306.33	5.47
0000	080	087.0	306.33	5.47
0000	085	087.0	306.33	5.47
0000	090	087.0	306.33	5.47
0000	095	087.0	306.33	5.47
0000	100	087.0	306.33	5.47
0000	105	087.0	306.33	5.47
0000	110	087.0	306.33	5.47
0000	115	087.0	306.33	5.47
0000	120	087.0	306.33	5.47
0000	125	087.0	306.33	5.47
0000	130	087.0	306.33	5.47
0000	135	087.0	306.33	5.47
0000	140	087.0	306.33	5.47
0000	145	087.0	306.33	5.47
0000	150	087.0	306.33	5.47
0000	155	087.0	306.33	5.47
0000	160	087.0	306.33	5.47
0000	165	087.0	306.33	5.47
0000	170	087.0	306.33	5.47
0000	175	087.0	306.33	5.47
0000	180	087.0	306.33	5.47
0000	185	087.0	306.33	5.47
0000	190	087.0	306.33	5.47
0000	195	087.0	306.33	5.47
0000	200	087.0	306.33	5.47
0000	205	087.0	306.33	5.47
0000	210	087.0	306.33	5.47
0000	215	087.0	306.33	5.47
0000	220	087.0	306.33	5.47
0000	225	087.0	306.33	5.47

EXP. NO.	TIME	PRESS	TEMP	SUPP.
98	005	1101.3	270.65	1.00
0000	010	051.4	270.46	4.36
0000	015	044.1	269.07	4.52
0000	020	046.7	269.35	4.73
0000	025	035.0	269.91	4.91
0000	030	021.3	269.29	5.11
0000	035	021.0	269.25	5.25
0000	040	022.6	267.29	5.43
0000	045	021.0	267.07	5.62
0000	050	021.0	266.91	5.70
0000	055	020.0	266.92	5.78
0000	060	019.0	266.90	5.81
0000	065	020.7	267.06	5.81
0000	070	020.2	267.12	5.81
0000	075	020.0	267.00	5.81
0000	080	021.0	267.20	5.81
0000	085	022.0	267.21	5.81
0000	090	021.1	267.11	5.81
0000	095	021.4	267.14	5.81
0000	100	022.6	267.22	5.81
0000	105	022.5	267.22	5.81
0000	110	022.2	267.24	5.81
0000	115	023.1	267.34	5.81
0000	120	023.0	267.43	5.81
0000	125	023.4	267.27	5.81
0000	130	023.3	267.36	5.81
0000	135	024.2	267.46	5.81
0000	140	024.7	267.52	5.81
0000	145	024.1	267.45	5.81
0000	150	023.2	267.45	5.81
0000	155	023.2	267.50	5.81
0000	160	023.4	267.50	5.81
0000	165	023.4	267.54	5.81
0000	170	025.2	267.54	5.81
0000	175	024.0	267.50	5.81
0000	180	025.4	267.60	5.81
0000	185	026.0	267.67	5.81
0000	190	026.1	267.68	5.81
0000	195	025.9	267.66	5.81
0000	200	027.7	267.78	5.81
0000	205	027.1	267.79	5.81
0000	210	027.1	267.79	5.81
0000	215	027.7	267.81	5.81
0000	220	030.0	268.22	5.81

0.000	015.0	266.24	5.74
0.005	012.2	266.72	5.86
0.010	011.2	266.00	5.88
0.015	014.1	266.14	5.78
0.020	014.2	266.17	5.77
0.025	013.2	266.03	5.92
0.030	013.7	266.13	5.92
0.035	014.0	266.22	5.75
0.040	014.2	266.23	5.75
0.045	013.4	266.14	5.81
0.050	014.1	266.14	5.78
0.055	015.6	266.30	5.72
0.060	015.7	266.32	5.71
0.065	015.0	266.24	5.74
0.070	014.0	266.13	5.79
0.075	015.0	266.24	5.74
0.080	015.2	266.28	5.73
0.085	014.1	266.14	5.78
0.090	014.9	266.00	5.84
0.095	017.2	266.50	5.64
0.100	022.4	267.81	5.17
0.105	040.0	269.11	4.74

0.080	013.3	266.45	5.86
0.085	014.1	266.77	5.83
0.090	014.5	266.71	5.86
0.095	026.0	266.14	5.66
0.100	031.0	266.62	4.80
0.105	041.0	269.80	4.51

EXP. NO. 410 96. DRIPS/CC

TIME	PRESS	TEMP	SUPR
0.000	1101.0	205.65	1.00
0.005	091.4	270.35	4.37
0.010	046.7	269.83	4.53
0.015	041.7	269.25	4.70
0.020	036.7	268.59	4.88
0.025	031.9	268.12	5.06
0.030	027.1	267.59	5.25
0.035	021.7	266.96	5.47
0.040	017.5	266.48	5.65
0.045	013.0	266.06	5.81
0.050	010.3	265.65	5.93
0.055	009.9	265.47	5.95
0.060	009.7	265.44	5.95
0.065	009.2	265.52	5.93
0.070	009.0	265.59	5.91
0.075	009.0	265.50	5.91
0.080	009.0	265.50	5.91
0.085	009.0	265.71	5.95
0.090	009.1	266.79	5.64
0.095	009.1	266.15	5.95
0.100	009.4	269.44	4.64

EXP. NO. 414 194. DRIPS/CC

TIME	PRESS	TEMP	SUPR
0.000	1108.4	205.65	1.00
0.005	091.4	270.35	4.24
0.010	046.7	270.35	4.30
0.015	040.1	269.85	4.61
0.020	035.7	269.06	4.79
0.025	030.8	268.39	4.98
0.030	024.4	267.77	5.18
0.035	020.2	267.26	5.36
0.040	015.0	266.77	5.54
0.045	011.0	266.26	5.74
0.050	007.0	265.77	5.93
0.055	003.0	265.37	6.00
0.060	000.4	264.86	6.26
0.065	000.5	264.86	6.31
0.070	000.6	264.09	6.26
0.075	000.7	264.47	6.55
0.080	015.6	266.73	5.56
0.085	025.4	267.86	5.15
0.090	036.7	269.80	4.75

EXP. NO. 612 69. DRIPS/CC

TIME	PRESS	TEMP	SUPR
0.000	1184.0	205.65	1.00
0.005	091.4	270.35	4.20
0.010	045.9	270.35	4.37
0.015	040.7	269.77	4.54
0.020	035.5	269.18	4.72
0.025	030.5	268.60	4.91
0.030	025.5	268.03	5.10
0.035	021.1	267.52	5.27
0.040	016.5	266.99	5.46
0.045	012.3	266.50	5.64
0.050	008.7	266.08	5.90
0.055	005.2	265.68	5.97

EXP. NO. 300 10.8 DRIPS/CC

TIME	PRESS	TEMP	SUPR
0.000	1182.8	205.65	1.00
0.005	067.4	262.59	3.00
0.010	061.6	262.95	4.17
0.015	055.5	262.29	4.37
0.020	050.1	261.69	4.56
0.025	045.5	261.19	4.72
0.030	040.1	260.59	4.92
0.035	036.2	260.16	5.09
0.040	031.5	259.65	5.27
0.045	026.9	259.39	5.37
0.050	022.9	259.39	5.42
0.055	020.1	259.48	5.23
0.060	018.0	260.35	5.91
0.065	013.0	262.10	4.43

EXP. NO. 312 7.8 DRIPS/CC

TIME	PRESS	TEMP	SUPR
0.000	1182.1	205.65	1.00
0.005	067.4	262.73	3.05
0.010	061.1	262.64	4.15
0.015	055.7	262.45	4.32
0.020	050.0	261.92	4.51
0.025	045.0	261.29	4.69
0.030	040.9	260.72	4.89
0.035	035.5	260.21	5.05
0.040	031.2	259.76	5.22
0.045	029.7	259.58	5.29
0.050	030.5	259.67	5.26
0.055	038.8	260.59	4.92
0.060	053.4	262.20	4.40

EXP. NO. 317 2.9 DRIPS/CC

TIME	PRESS	TEMP	SUPR
	1191.2	285.45	1.00
0.005	067.4	262.86	3.02
0.010	059.0	262.89	4.10
0.015	059.0	262.92	4.30
0.020	040.4	261.83	4.51
0.025	044.2	261.26	4.70
0.030	036.1	262.81	4.85
0.035	036.6	262.42	4.98
0.036	036.0	262.35	5.01
0.037	036.4	262.42	4.92
0.040	037.2	262.55	4.94
0.045	055.2	262.48	4.31

EXP. NO. 319 5.6 DRIPS/CC

TIME	PRESS	TEMP	SUPR
	1195.3	285.65	1.00
0.005	047.4	262.45	4.23
0.010	051.4	262.81	4.21
0.015	055.9	262.18	4.40
0.020	050.4	261.59	4.59
0.025	045.1	261.01	4.73
0.030	037.4	260.38	5.00
0.035	035.6	259.80	5.17
0.036	032.2	259.62	5.27
0.041	033.2	259.71	5.24
0.045	042.0	260.76	4.86
0.050	058.0	262.42	4.33

EXP. NO. 322 9.5 DRIPS/CC

TIME	PRESS	TEMP	SUPR
	1120.0	285.65	1.00
0.005	047.4	262.95	4.17
0.010	061.4	262.20	4.37
0.015	055.2	261.69	4.55
0.020	057.4	261.13	4.75
0.025	044.0	262.50	4.96
0.030	040.0	259.95	5.15
0.035	037.0	259.60	5.24
0.040	037.0	259.72	5.24
0.045	037.0	259.71	5.24
0.050	035.8	259.49	5.32
0.055	035.5	259.46	5.34
0.060	036.2	259.67	5.23
0.045	029.4	259.78	5.22
0.070	037.4	259.60	5.25
0.075	039.3	259.77	5.22
0.080	047.5	260.78	4.86

EXP. NO. 324 24.8 DRIPS/CC

TIME	PRESS	TEMP	SUPR
	1191.5	285.65	1.00
0.005	047.4	262.80	4.10
0.010	052.0	262.51	4.36
0.015	056.2	261.68	4.55
0.020	051.7	261.11	4.74
0.025	045.0	261.52	4.95
0.030	040.1	260.80	5.17
0.035	035.7	259.43	5.35
0.040	031.2	259.92	5.54
0.043	029.2	259.22	5.50
0.044	021.3	259.94	5.54
0.045	023.0	259.13	5.47
0.055	032.7	259.17	5.48
0.060	022.1	259.00	5.51
0.065	021.7	259.00	5.52
0.070	022.0	259.11	5.47
0.075	023.7	259.21	5.44
0.080	023.5	259.18	5.44
0.085	023.2	259.15	5.46
0.090	023.4	259.17	5.45
0.095	024.4	259.28	5.41
0.100	024.5	259.30	5.40
0.105	025.7	259.42	5.35
0.110	044.2	260.36	5.00

EXP. NO. 327 7.6 DRIPS/CC

TIME	PRESS	TEMP	SUPR
	1190.7	285.65	1.00
0.005	047.4	262.12	4.12
0.010	041.3	262.46	4.32
0.015	055.4	261.91	4.52
0.020	057.0	261.22	4.71
0.025	045.2	260.60	4.80
0.030	020.0	260.11	5.00
0.035	026.0	259.73	5.22
0.040	038.3	259.93	5.16
0.045	037.0	259.86	5.18
0.050	035.8	259.66	5.26
0.055	035.3	259.60	5.29
0.060	036.2	259.70	5.25
0.065	037.6	259.96	5.19
0.070	037.6	259.96	5.19
0.075	037.7	259.91	5.20
0.080	036.8	259.77	5.22
0.085	037.8	259.82	5.19
0.090	038.6	259.87	5.15
0.095	033.5	259.85	5.15
0.100	038.7	259.00	5.14
0.105	042.6	261.07	4.76

EXP. NO. 329 33. DRIPS/CC

TIME	PRESS	TEMP	SUPR
	1180.0	285.65	1.00
0.005	047.4	262.12	4.12
0.010	061.0	262.52	4.30
0.015	055.7	261.95	4.51

0.000	055.4	251.27	4.69
0.005	055.3	260.74	4.87
0.010	055.2	260.11	5.09
0.015	055.2	260.55	5.29
0.020	055.1	250.09	5.48
0.025	055.0	250.77	5.61
0.030	055.0	250.06	5.53
0.035	055.0	250.00	5.52
0.040	055.0	250.86	5.57
0.045	055.0	250.82	5.59
0.050	055.0	250.05	5.54
0.055	055.0	250.00	5.49
0.060	055.0	250.00	5.49
0.065	055.0	250.03	5.51
0.070	055.0	250.01	5.51
0.075	055.0	250.10	5.48
0.080	055.0	250.10	5.44
0.085	055.0	250.10	5.45
0.090	055.0	250.10	5.44
0.095	055.0	260.14	5.28
0.100	055.0	261.83	4.51

0.005	015.7	207.46	6.19
0.010	015.4	200.77	5.57
0.015	015.7	207.21	5.74
0.020	015.9	207.20	4.79
0.025	015.1	251.00	4.49

EXP. NO. 332

TIME	TEMP	TEMP	SUPR
0.005	1103.7	285.65	1.00
0.010	067.4	262.15	4.12
0.015	055.1	262.49	4.31
0.020	040.3	251.81	4.52
0.025	044.5	261.17	4.72
0.030	039.5	260.50	4.92
0.035	034.0	250.08	5.14
0.040	020.2	250.48	5.33
0.045	024.5	250.05	5.54
0.050	018.0	250.60	5.76
0.055	015.3	257.92	5.92
0.060	014.4	257.40	5.20
0.065	015.4	257.30	5.25
0.070	026.0	257.41	5.20
0.075	026.0	258.70	5.64
0.080	047.1	260.06	5.11
0.085	053.4	260.03	4.81
0.090	053.4	261.62	4.58

EXP. NO. 337

53, 000PS/CC

TIME	TEMP	TEMP	SUPR
0.005	1198.0	285.65	1.00
0.010	077.4	263.21	4.10
0.015	050.7	260.27	4.34
0.020	052.7	261.60	4.52
0.025	041.2	260.05	4.80
0.030	041.2	260.24	5.01
0.035	035.0	250.75	5.23
0.040	031.0	260.01	5.43
0.045	025.6	250.01	5.67
0.050	022.6	250.06	5.61
0.055	016.2	257.56	5.13
0.060	011.7	257.26	5.36
0.065	007.5	256.56	6.09
0.070	000.0	256.40	6.69
0.075	004.7	256.27	6.75
0.080	005.6	256.37	6.70
0.085	010.5	256.02	6.43
0.090	024.7	256.51	5.72
0.095	029.0	250.45	5.33
0.100	040.1	260.00	5.11
0.105	040.1	261.21	4.71

EXP. NO. 334

49, 000PS/CC

TIME	TEMP	TEMP	SUPR
0.005	1100.0	285.65	1.00
0.010	067.4	262.13	4.12
0.015	050.5	262.27	4.37
0.020	040.4	261.60	4.58
0.025	041.0	261.03	4.77
0.030	036.6	260.34	5.01
0.035	031.9	250.75	5.23
0.040	026.0	250.23	5.42
0.045	022.0	258.65	5.65
0.050	017.0	258.13	5.88
0.055	012.0	257.57	6.12
0.060	009.0	257.11	6.34
0.065	009.0	256.78	6.50
0.070	009.0	256.68	6.55
0.075	009.0	256.78	6.50

EXP. NO. 339

110, 000PS/CC

TIME	TEMP	TEMP	SUPR
0.005	1137.9	285.65	1.00
0.010	067.4	262.22	4.09
0.015	056.0	262.00	4.43
0.020	040.2	261.24	4.70
0.025	040.7	261.52	4.95
0.030	036.0	250.87	5.18
0.035	031.7	250.31	5.40
0.040	027.4	250.83	5.53
0.045	021.7	250.20	5.25
0.050	016.9	257.66	6.20
0.055	012.7	257.10	6.30
0.060	009.5	256.71	6.53
0.065	004.4	256.25	6.76
0.070	001.8	256.06	6.91
0.075	001.4	256.02	6.92
0.080	002.3	256.01	6.88
0.085	004.7	256.28	6.74
0.090	015.7	257.52	6.15
0.095	026.0	250.75	5.61
0.100	030.0	250.46	5.26
0.105	045.0	260.78	4.86
0.110	056.1	261.00	4.46

EXP. NO. 342 40, DRIPS/CC

TIME	PRESS	TEMP	SUPR
1187.5	285.65	1.00	
0.005	067.4	262.25	4.09
0.010	067.1	262.46	4.32
0.015	053.5	261.78	4.53
0.020	047.2	261.11	4.74
0.025	042.8	260.56	4.93
0.030	037.6	260.00	5.14
0.035	032.6	259.42	5.35
0.040	027.3	258.94	5.50
0.045	022.7	258.23	5.70
0.050	017.7	257.77	6.03
0.055	014.2	257.29	6.21
0.060	012.7	257.32	6.24
0.065	014.4	257.40	6.23
0.070	014.3	257.42	6.10
0.075	023.0	258.47	5.74
0.080	028.0	247.06	5.11
0.085	040.5	261.20	4.68
0.090	058.2	262.25	4.39

EXP. NO. 343 48, DRIPS/CC

TIME	PRESS	TEMP	SUPR
1187.5	285.65	1.00	
0.005	067.4	262.22	4.10
0.010	060.2	260.82	4.27
0.015	056.2	261.00	4.40
0.020	050.2	261.25	4.47
0.025	045.1	260.78	4.56
0.030	039.4	260.14	5.08
0.035	034.0	259.65	5.26
0.040	028.7	259.00	5.49
0.045	024.7	258.52	5.71
0.050	019.5	257.92	5.95
0.055	015.0	257.52	6.15
0.060	012.4	257.14	6.32
0.065	013.3	257.25	6.27
0.070	013.0	257.21	6.24
0.075	012.6	257.17	6.21
0.080	012.0	267.10	6.34
0.085	013.1	257.32	6.20
0.090	014.7	257.40	6.20
0.095	014.4	257.37	6.22
0.100	014.7	257.40	6.20
0.105	014.0	257.41	6.20
0.110	014.6	257.39	6.21
0.115	015.5	257.40	6.16
0.120	015.5	267.40	6.16
0.125	016.4	257.61	6.11
0.130	027.5	258.83	5.50
0.135	043.7	260.42	4.91
0.140	054.3	261.70	4.53

EXP. NO. 344 26, DRIPS/CC

TIME	PRESS	TEMP	SUPR
1187.6	285.65	1.00	
0.005	067.4	262.24	4.09
0.010	052.0	262.75	4.23
0.015	052.4	262.15	4.41
0.020	047.4	261.61	4.58
0.025	047.2	261.24	4.77
0.030	041.1	260.37	5.00
0.035	036.5	260.06	5.19
0.040	031.5	259.30	5.40
0.045	025.0	258.68	5.65
0.050	022.5	258.20	5.89
0.055	021.4	258.18	5.86
0.060	021.0	258.34	5.78
0.065	027.0	259.00	5.56
0.070	029.4	260.19	5.07
0.075	051.0	261.54	4.60
0.080	057.0	262.21	4.39

EXP. NO. 352 28, DRIPS/CC

TIME	PRESS	TEMP	SUPR
1189.0	285.65	1.00	
0.005	067.4	262.14	4.12
0.010	061.0	262.52	4.30
0.015	055.7	261.26	4.50
0.020	050.5	261.28	4.63
0.025	045.5	260.75	4.87
0.030	039.8	260.12	5.00
0.035	035.1	259.60	5.23
0.040	030.1	259.04	5.50
0.045	024.7	258.44	5.75
0.050	019.0	257.91	5.97
0.055	015.2	257.72	6.06
0.060	012.7	257.80	6.08
0.065	023.7	258.50	5.56
0.070	045.0	260.70	4.95
0.075	054.4	261.72	4.55

EXP. NO. 347 29, DRIPS/CC

TIME	PRESS	TEMP	SUPR
1187.6	285.65	1.00	
0.005	067.4	262.24	4.09
0.010	062.0	262.66	4.26
0.015	055.7	261.97	4.47
0.020	050.3	261.39	4.66
0.025	045.4	260.24	4.84
0.030	039.8	260.22	5.05
0.035	035.0	259.40	5.25
0.040	030.0	259.14	5.46
0.045	024.7	258.55	5.70
0.050	020.0	258.02	5.92
0.055	017.8	257.78	6.03
0.060	019.1	257.92	5.97
0.065	025.7	258.46	5.66
0.070	041.2	260.45	4.97
0.075	051.6	261.52	4.61
0.080	058.6	262.28	4.37

EXP. NO. 354 5,1 DRIPS/CC

TIME	PRESS	TEMP	SUPR
1189.0	285.65	1.00	
0.005	067.4	262.21	4.10
0.010	062.0	262.60	4.25
0.015	057.1	262.00	4.43
0.020	051.0	261.52	4.61
0.025	047.2	261.00	4.78

0.020	041.6	247.30	5.60
0.025	037.7	250.84	5.10
0.040	031.0	250.21	5.20
0.043	030.1	250.11	5.47
0.045	030.5	250.05	5.50
0.046	030.1	250.11	5.47
0.048	030.4	250.01	5.22
0.050	044.2	257.00	7.32
0.055	057.7	263.15	4.41

EXP. NO. 360	26,	DRIPS/CC	
TIME	DRPSS	TEMP	SUPR
0.015	1108.0	285.65	1.00
0.018	067.4	263.13	4.12
0.019	062.4	262.58	4.20
0.020	054.7	261.04	4.47
0.021	051.4	261.20	4.65
0.022	046.7	260.07	4.83
0.023	040.0	260.22	5.06
0.024	034.2	250.72	5.24
0.025	031.0	250.10	5.44
0.026	027.7	250.40	5.64
0.027	026.0	250.67	5.65
0.028	029.2	250.83	5.58
0.029	027.0	250.70	5.41
0.030	026.0	250.67	5.65
0.031	027.2	253.71	5.63
0.032	020.0	250.24	5.52
0.033	020.0	250.00	5.56
0.034	020.5	250.04	5.52
0.035	020.5	250.04	5.50
0.036	020.4	250.04	5.54
0.037	021.1	250.03	5.50
0.038	026.4	250.71	5.24
0.039	023.4	261.60	4.50

EXP. NO. 357	1.3	DRIPS/CC	
TIME	DRPSS	TEMP	SUPR
0.005	1100.2	285.65	1.00
0.010	067.4	263.10	4.10
0.015	055.5	262.56	4.20
0.020	050.1	261.00	4.40
0.025	045.4	261.20	4.60
0.030	040.1	260.70	4.86
0.035	034.6	260.20	5.06
0.036	035.2	250.01	5.21
0.038	036.0	250.77	5.22
0.041	028.5	250.05	5.10
0.045	044.4	260.02	5.13
		260.70	4.80

EXP. NO. 420	20.9	DRIPS/CC	
TIME	DRPSS	TEMP	SUPR
0.005	1104.1	285.65	1.00
0.008	052.5	263.02	4.15
0.010	042.0	261.07	4.47
0.016	043.8	260.07	4.70
0.024	035.5	260.05	5.11
0.032	027.7	250.10	5.44
0.036	022.0	250.55	5.70
0.040	019.0	250.22	5.80
0.044	017.7	250.07	5.90
0.048	021.3	250.47	5.73
0.052	023.4	250.02	5.20
0.056	040.7	261.51	4.61

EXP. NO. 350	28,	DRIPS/CC	
TIME	DRPSS	TEMP	SUPR
0.005	1100.3	285.65	1.00
0.010	067.4	263.10	4.11
0.015	061.0	262.50	4.23
0.020	054.0	261.01	4.52
0.025	040.3	261.21	4.71
0.030	044.5	260.60	4.80
0.035	030.7	260.04	5.12
0.040	022.7	250.40	5.33
0.045	020.2	250.00	5.56
0.050	021.0	250.04	5.54
0.055	022.0	250.07	5.00
0.060	022.0	250.27	5.32
0.065	022.4	250.34	5.79
0.070	021.5	250.17	5.86
0.075	022.4	250.13	5.83
0.080	022.0	250.23	5.84
0.085	022.0	250.40	5.76
0.090	023.4	250.40	5.76
0.095	022.0	250.34	5.70
0.100	022.0	250.20	5.81
0.105	024.7	250.26	5.78
0.110	025.0	250.48	5.73
0.115	035.0	250.42	5.67
0.120	050.0	261.20	4.60

EXP. NO. 430	14.5	DRIPS/CC	
TIME	DRPSS	TEMP	SUPR
0.005	1104.4	285.65	1.00
0.010	050.1	263.02	4.30
0.015	052.2	261.00	4.46
0.020	047.7	261.07	4.56
0.025	042.7	260.00	4.54
0.030	037.1	260.20	5.06
0.035	031.7	250.40	5.24
0.040	027.1	250.00	5.48
0.045	021.6	250.40	5.73
0.047	019.1	250.00	5.80
0.048	016.0	250.04	5.96
0.049	019.5	250.11	5.90
0.052	022.0	250.60	5.64
0.055	031.4	250.67	5.20
0.060	043.3	260.80	4.80

EXP. NO. 434 37.5 DRIPS/CC

TIME	PRESS	TEMP	SUPR
1187.0	062.5	235.65	1.00
0.015	056.0	262.04	4.15
0.015	049.0	262.31	4.36
0.020	044.1	261.65	4.57
0.025	039.1	261.02	4.79
0.030	033.7	260.47	4.97
0.035	027.6	259.74	5.22
0.040	022.0	259.19	5.44
0.045	017.0	258.47	5.65
0.050	012.0	258.10	5.80
0.055	009.4	257.47	6.17
0.060	010.6	257.15	6.32
0.065	011.2	257.20	6.25
0.070	011.1	257.35	6.22
0.075	011.0	257.34	6.23
0.080	011.5	257.32	6.24
0.085	012.3	257.20	6.21
0.090	012.0	257.48	6.17
0.095	012.0	257.44	6.18
0.100	014.0	257.67	6.28
0.105	014.7	258.79	5.60
0.110	056.6	260.75	4.87
		262.30	4.34

0.015	064.3	236.32	5.20
0.020	023.0	259.05	5.42
0.025	020.0	257.40	5.44
0.030	012.0	257.08	5.61
0.035	016.2	257.00	5.62
0.040	015.7	257.76	5.65
0.045	017.2	257.02	5.67
0.050	021.7	258.41	5.76
0.055	024.6	258.26	5.53
0.060	043.6	261.04	4.84
0.065	057.2	262.21	4.25

EXP. NO. 437 33.5 DRIPS/CC

TIME	PRESS	TEMP	SUPR
1185.0	065.0	235.65	1.00
0.015	062.5	262.04	4.18
0.020	057.3	262.37	4.34
0.025	051.3	261.72	4.55
0.030	045.0	261.12	4.74
0.035	040.2	261.40	4.96
0.040	034.2	259.95	5.19
0.045	029.2	259.23	5.43
0.050	023.5	258.64	5.66
0.055	019.3	258.05	5.91
0.060	013.7	257.84	6.14
0.065	014.0	257.58	6.12
0.070	015.4	257.72	6.05
0.075	015.0	257.60	6.07
0.080	015.2	257.71	6.06
0.085	016.0	257.80	6.02
0.090	016.0	257.80	6.02
0.095	018.0	258.05	5.91
0.100	021.9	259.57	5.20
0.105	045.6	261.20	4.72

EXP. NO. 442 23.5 DRIPS/CC

TIME	PRESS	TEMP	SUPR
1184.7	086.6	236.40	1.00
0.015	062.5	262.07	4.17
0.020	057.0	262.27	4.35
0.025	050.0	261.71	4.55
0.030	044.7	261.02	4.73
0.035	039.1	260.40	4.90
0.040	032.4	259.77	5.22
0.045	028.4	259.17	5.45
0.050	022.2	258.50	5.40
0.055	017.0	258.03	5.62
0.060	014.1	257.61	6.11
0.065	013.1	257.50	6.16
0.070	014.1	257.41	6.11
0.075	020.2	258.29	5.80
0.080	023.6	259.70	5.21
0.085	045.2	261.19	4.72

EXP. NO. 439 22.5 DRIPS/CC

TIME	PRESS	TEMP	SUPR
1185.3	065.0	235.65	1.00
0.005	062.5	262.01	4.18
0.010	057.0	262.31	4.36
0.015	051.8	261.74	4.54
0.020	045.5	261.06	4.76
0.025	039.0	260.43	4.98

EXP. NO. 444 38.0 DRIPS/CC

TIME	PRESS	TEMP	SUPR
1182.0	065.0	235.65	1.00
0.005	062.5	262.04	4.15
0.010	056.0	262.42	4.33
0.015	050.7	261.75	4.54
0.020	044.7	261.10	4.75
0.025	039.6	260.41	4.99
0.030	033.5	259.80	5.10
0.035	029.1	259.25	5.42
0.040	022.6	258.64	5.67
0.045	017.0	258.10	5.80
0.050	012.5	257.50	6.16
0.055	012.0	257.10	6.34
0.060	007.7	256.05	6.41
0.065	000.1	257.01	6.30
0.070	013.8	257.65	6.00
0.075	025.1	259.01	5.35
0.080	041.1	260.60	4.80
0.085	050.2	261.60	4.56

EXP. NO. 447

75, 000PS/CC

TIME	DEPRESS	TEMP	SUPR
0.005	1184.6	285.65	1.00
0.010	082.5	262.52	4.14
0.015	085.2	262.18	4.40
0.020	040.2	261.52	4.41
0.025	043.5	258.90	4.82
0.030	037.9	257.27	5.03
0.035	022.7	256.70	5.25
0.040	027.4	259.11	5.47
0.045	021.7	259.47	5.73
0.050	013.5	257.91	5.97
0.055	011.5	257.33	6.24
0.060	007.2	256.84	6.47
0.065	005.5	256.60	6.50
0.070	004.5	256.76	6.50
0.075	005.5	256.80	6.49
0.080	006.7	256.79	6.49
0.085	007.0	256.82	6.49
0.090	007.6	256.89	6.44
0.095	007.6	256.89	6.44
0.100	007.5	256.89	6.45
0.105	007.7	256.90	6.44
0.110	008.5	256.90	6.40
0.115	009.4	257.00	6.35
0.120	010.2	259.10	5.25
0.125	020.4	250.33	5.30
0.130	051.0	261.81	4.52

EXP. NO. 448

47, 000PS/CC

TIME	DEPRESS	TEMP	SUPR
0.005	1182.6	285.64	1.00
0.010	062.5	262.52	4.14
0.015	062.5	262.46	4.32
0.020	040.2	261.76	4.53
0.025	044.7	261.11	4.74
0.030	030.2	260.51	4.95
0.035	024.0	258.02	5.16
0.040	020.1	259.20	5.37
0.045	022.3	259.74	5.62
0.050	013.4	257.19	5.84
0.055	013.4	257.03	6.10
0.060	008.1	257.14	6.32
0.065	007.0	256.91	6.43
0.070	006.0	257.12	6.23
0.075	006.0	257.17	6.31
0.080	006.0	257.13	6.22
0.085	006.2	257.16	6.20
0.090	006.5	257.20	6.20
0.095	010.3	257.20	6.25
0.100	010.3	257.20	6.25
0.105	010.4	257.20	6.25
0.110	011.0	257.24	6.22
0.115	011.6	257.42	6.10
0.120	016.0	259.01	5.03
0.125	037.1	259.42	5.32
0.130	044.9	261.34	4.67

EXP. NO. 449

78, 000PS/CC

TIME	DEPRESS	TEMP	SUPR
0.005	1182.7	285.55	1.00
0.010	062.5	263.05	4.14
0.015	055.0	262.33	4.35
0.020	044.0	261.73	4.54
0.025	030.0	261.13	4.74
0.030	034.0	260.52	4.95
0.035	028.0	259.92	5.16
0.040	024.0	259.35	5.39
0.045	012.0	259.75	5.62
0.050	012.5	259.10	5.35
0.055	009.0	257.63	6.10
0.060	005.3	257.11	6.34
0.065	004.4	256.71	6.53
0.070	007.1	256.23	6.47
0.075	004.0	256.91	6.43
0.080	004.0	256.28	6.45
0.085	003.6	256.90	6.44
0.090	007.4	256.94	6.42
0.095	007.0	257.02	6.30
0.100	003.2	257.02	6.37
0.105	003.2	257.05	6.37
0.110	009.4	257.06	6.35
0.115	009.0	257.11	6.34
0.120	012.0	257.15	6.32
0.125	024.1	259.04	6.11
0.130	044.1	261.04	4.77

EXP. NO. 457

348, 000PS/CC

TIME	DEPRESS	TEMP	SUPR
0.005	1182.1	285.65	1.00
0.010	042.5	262.11	4.12
0.015	040.4	262.66	4.26
0.020	062.1	261.97	4.47
0.025	046.0	261.40	4.65
0.030	041.5	260.80	4.85
0.035	034.5	260.25	5.04
0.040	031.2	259.67	5.26
0.045	025.0	259.00	5.42
0.050	020.0	258.35	5.72
0.055	016.7	257.70	5.96
0.060	012.3	257.02	6.24
0.065	008.1	256.34	6.52
0.070	008.0	256.74	6.81
0.075	008.0	256.15	7.12
0.080	008.0	256.55	7.40
0.085	008.2	255.92	7.54
0.090	008.0	255.30	7.40
0.095	008.0	255.68	7.31
0.100	008.0	255.02	7.24
0.105	008.0	255.41	7.15
0.110	008.0	255.75	7.03
0.115	008.0	255.02	6.93
0.120	008.0	256.20	6.85
0.125	008.7	256.64	6.77
0.130	013.1	257.24	6.00
0.135	025.5	259.04	5.50
0.140	037.0	260.40	4.90
0.145	050.2	261.77	4.53

EXP. NO. 450 69, DRIPS/CC

TIME	DRIPS	TEMP	SUPR
1191.0	285.65	1.00	
0.005	264.21	4.10	
0.010	262.22	4.30	
0.015	261.46	4.63	
0.020	260.22	4.84	
0.025	260.22	5.05	
0.030	259.66	5.26	
0.035	259.14	5.46	
0.040	259.52	5.71	
0.045	257.97	5.95	
0.050	257.39	6.21	
0.055	256.01	6.43	
0.060	256.46	6.66	
0.065	256.24	6.71	
0.070	256.46	6.66	
0.075	256.86	6.46	
0.080	259.71	5.64	
0.085	260.12	5.27	
0.090	261.62	4.58	
0.095	262.45	4.32	

0.100	264.21	4.10	
0.105	262.22	4.30	
0.110	261.46	4.63	
0.115	260.22	4.84	
0.120	260.22	5.05	
0.125	259.66	5.26	
0.130	259.14	5.46	
0.135	259.52	5.71	
0.140	257.97	5.95	
0.145	257.39	6.21	
0.150	256.01	6.43	
0.155	256.46	6.66	
0.160	256.24	6.71	
0.165	256.46	6.66	
0.170	256.86	6.46	
0.175	260.12	5.27	
0.180	261.62	4.58	
0.185	262.45	4.32	

EXP. NO. 457 37, DRIPS/CC

TIME	DRIPS	TEMP	SUPR
1197.4	285.65	1.00	
0.005	262.72	4.24	
0.010	261.94	4.48	
0.015	261.26	4.66	
0.020	260.70	4.88	
0.025	259.05	5.12	
0.030	259.45	5.33	
0.035	259.03	5.54	
0.040	259.25	5.78	
0.045	257.96	6.00	
0.050	257.27	6.26	
0.055	256.01	6.44	
0.060	256.76	6.51	
0.065	256.07	6.45	
0.070	257.20	6.30	
0.075	259.24	5.82	
0.080	260.72	5.24	
0.085	260.92	4.84	
0.090	261.69	4.55	

EXP. NO. 452 228, DRIPS/CC

TIME	DRIPS	TEMP	SUPR
1197.0	285.65	1.00	
0.005	262.76	4.23	
0.010	261.90	4.52	
0.015	261.00	4.78	
0.020	259.31	5.02	
0.025	259.67	5.26	
0.030	259.13	5.46	
0.035	259.61	5.68	
0.040	259.01	5.93	
0.045	257.40	6.20	
0.050	256.76	6.51	
0.055	256.20	6.74	
0.060	259.71	7.05	
0.065	259.54	7.14	
0.070	255.71	7.05	
0.075	259.02	6.32	
0.080	259.55	6.70	
0.085	260.23	6.25	
0.090	261.25	4.70	
0.095	262.12	4.42	

EXP. NO. 460 89, DRIPS/CC

TIME	DRIPS	TEMP	SUPR
1196.6	285.65	1.00	
0.005	262.90	4.22	
0.010	262.12	4.42	
0.015	261.51	4.61	
0.020	260.86	4.83	
0.025	259.23	5.03	
0.030	259.69	5.26	
0.035	259.09	5.49	
0.040	259.50	5.72	
0.045	259.00	5.94	
0.050	257.41	6.20	
0.055	256.91	6.43	
0.060	256.47	6.55	
0.065	256.61	6.63	
0.070	256.49	6.64	
0.075	256.25	6.64	
0.080	256.40	6.58	
0.085	256.47	6.65	
0.090	256.55	6.61	
0.095	256.53	6.62	
0.100	256.56	6.61	
0.105	256.64	6.57	
0.110	256.64	6.57	
0.115	256.64	6.57	
0.120	256.64	6.57	
0.125	256.70	6.53	

EXP. NO. 464 198, DRIPS/CC

TIME	DRIPS	TEMP	SUPR
1197.6	285.65	1.00	
0.005	262.71	4.24	
0.010	261.75	4.54	
0.015	260.96	4.80	
0.020	259.73	5.22	
0.025	259.65	5.27	
0.030	259.09	5.48	
0.035	259.54	5.71	
0.040	259.00	5.93	
0.045	257.42	6.19	
0.050	256.79	6.49	

0.135
0.145
0.145
0.155
0.155
0.165
0.165
0.175
0.175

007.7
007.7
008.1
008.5
008.4
012.3
024.6
042.3
054.0

256.72
256.72
256.77
256.92
256.92
256.90
257.24
259.62
259.59
261.06
5.52
5.52
5.53
5.43
5.43
5.22
5.67
4.93
4.47

0.045
0.055
0.055
0.065
0.070
0.075
0.085
0.085
0.095
0.095
0.105
0.105
0.115
0.115
0.125
0.125
0.135
0.135
0.145
0.145
0.155
0.155
0.165
0.165

257.13
257.13
257.16
257.22
257.22
257.27
257.27
257.35
257.35
257.41
257.41
257.44
257.44
257.47
257.47
257.54
257.54
257.56
257.56
257.58
257.58
259.59
260.59

EXP. NO. 472

44, DRIPS/CC

TIME	DEFS	TEMP	SUPR
0.005	062.5	285.65	1.00
0.010	059.2	262.77	4.22
0.015	059.2	262.30	4.26
0.020	046.7	261.66	4.57
0.025	046.7	261.24	4.77
0.030	036.4	260.40	4.99
0.035	036.5	259.92	5.20
0.040	025.0	259.25	5.42
0.045	025.5	258.64	5.66
0.050	015.2	257.14	5.87
0.055	011.6	257.14	5.14
0.060	011.0	257.14	5.32
0.065	011.6	257.07	6.36
0.070	009.7	257.14	6.32
0.075	009.7	256.93	6.43
0.080	010.0	256.93	6.43
0.085	010.0	256.96	6.41
0.090	010.5	257.02	6.38
0.095	011.0	257.07	6.36
0.100	011.0	257.05	6.37
0.105	010.9	257.06	6.36
0.110	010.9	257.06	6.36
0.115	011.5	257.14	6.32
0.120	011.5	257.12	6.33
0.125	012.1	257.12	6.33
0.130	012.1	257.18	6.30
0.135	012.1	257.20	6.30
0.140	012.5	257.20	6.30
0.145	012.7	257.24	6.26
0.150	012.7	257.27	6.26
0.155	013.3	257.26	6.27
0.160	012.2	257.23	6.24
0.165	031.2	259.30	5.99
0.170	040.4	261.24	5.67

EXP. NO. 477

36, DRIPS/CC

TIME	DEFS	TEMP	SUPR
0.005	066.7	285.65	1.00
0.010	062.5	262.77	4.22
0.015	056.0	262.30	4.43
0.020	044.0	261.42	4.64
0.025	044.0	260.84	4.83
0.030	034.6	260.22	5.01
0.035	020.0	259.72	5.24
0.040	020.0	259.22	5.43
0.045	024.4	259.50	5.63
0.050	014.4	259.04	5.92
0.055	010.7	257.47	6.17
0.060	010.2	257.06	6.36
0.065	011.2	257.06	6.39
0.070	011.6	257.26	6.36
0.075	011.6	257.16	6.32
0.080	011.6	257.16	6.32
0.085	012.5	257.26	6.27
0.090	012.4	257.27	6.26
0.095	013.6	257.27	6.26
0.100	013.3	257.34	6.24
0.105	013.3	257.35	6.23
0.110	013.2	257.35	6.23
0.115	013.7	257.30	6.21
0.120	013.7	257.30	6.21
0.125	014.0	257.40	6.20
0.130	014.0	257.46	6.18
0.135	014.2	257.46	6.18
0.140	014.5	257.42	6.17
0.145	015.0	257.46	6.17
0.150	020.5	258.15	6.97
0.155	027.7	260.06	5.11

EXP. NO. 474

36, DRIPS/CC

TIME	DEFS	TEMP	SUPR
0.005	062.5	285.65	1.00
0.010	057.0	262.72	4.42
0.015	050.0	262.13	4.63
0.020	045.3	260.84	4.84
0.025	040.5	260.31	5.02
0.030	035.2	259.72	5.24
0.035	030.0	259.15	5.46
0.040	024.6	258.54	5.70

EXP. NO. 470 21, DRIPS/CC

TIME	TEMP	SS	TEMP	SUPR
1106.4	285	65	1.00	
0067.5	262	22	4.21	
0068.1	262	23	4.30	
0069.0	261	61	4.58	
0070.0	261	11	4.75	
0071.0	260	54	4.94	
0072.0	259	27	5.14	
0073.0	259	44	5.34	
0074.0	258	26	5.57	
0075.0	258	31	5.80	
0076.0	257	22	5.99	
0077.0	257	22	6.07	
0078.0	257	79	6.23	
0079.0	257	94	6.40	
0080.0	257	94	6.55	
0081.0	257	97	6.70	
0082.0	258	90	6.83	
0083.0	259	90	6.99	
0084.0	259	91	7.11	
0085.0	259	97	7.26	
0086.0	259	97	7.40	
0087.0	259	99	7.55	
0088.0	259	99	7.70	
0089.0	259	99	7.84	
0090.0	259	99	7.99	
0091.0	259	99	8.14	
0092.0	259	99	8.29	
0093.0	259	99	8.44	
0094.0	259	99	8.59	
0095.0	259	99	8.74	
0096.0	259	99	8.89	
0097.0	259	99	9.04	
0098.0	259	99	9.19	
0099.0	259	99	9.34	
0100.0	259	99	9.49	
0101.0	259	99	9.64	
0102.0	259	99	9.79	
0103.0	259	99	9.94	
0104.0	259	99	10.09	
0105.0	259	99	10.24	
0106.0	259	99	10.39	
0107.0	259	99	10.54	
0108.0	259	99	10.69	
0109.0	259	99	10.84	
0110.0	259	99	10.99	
0111.0	259	99	11.14	
0112.0	259	99	11.29	
0113.0	259	99	11.44	
0114.0	259	99	11.59	
0115.0	259	99	11.74	
0116.0	259	99	11.89	
0117.0	259	99	12.04	
0118.0	259	99	12.19	
0119.0	259	99	12.34	
0120.0	259	99	12.49	
0121.0	259	99	12.64	
0122.0	259	99	12.79	
0123.0	259	99	12.94	
0124.0	259	99	13.09	
0125.0	259	99	13.24	
0126.0	259	99	13.39	
0127.0	259	99	13.54	
0128.0	259	99	13.69	
0129.0	259	99	13.84	
0130.0	259	99	13.99	
0131.0	259	99	14.14	
0132.0	259	99	14.29	
0133.0	259	99	14.44	
0134.0	259	99	14.59	
0135.0	259	99	14.74	
0136.0	259	99	14.89	
0137.0	259	99	15.04	
0138.0	259	99	15.19	
0139.0	259	99	15.34	
0140.0	259	99	15.49	
0141.0	259	99	15.64	
0142.0	259	99	15.79	
0143.0	259	99	15.94	
0144.0	259	99	16.09	
0145.0	259	99	16.24	
0146.0	259	99	16.39	
0147.0	259	99	16.54	
0148.0	259	99	16.69	
0149.0	259	99	16.84	
0150.0	259	99	16.99	
0151.0	259	99	17.14	
0152.0	259	99	17.29	
0153.0	259	99	17.44	
0154.0	259	99	17.59	
0155.0	259	99	17.74	
0156.0	259	99	17.89	
0157.0	259	99	18.04	
0158.0	259	99	18.19	
0159.0	259	99	18.34	
0160.0	259	99	18.49	
0161.0	259	99	18.64	
0162.0	259	99	18.79	
0163.0	259	99	18.94	
0164.0	259	99	19.09	
0165.0	259	99	19.24	
0166.0	259	99	19.39	
0167.0	259	99	19.54	
0168.0	259	99	19.69	
0169.0	259	99	19.84	
0170.0	259	99	19.99	
0171.0	259	99	20.14	
0172.0	259	99	20.29	
0173.0	259	99	20.44	
0174.0	259	99	20.59	
0175.0	259	99	20.74	
0176.0	259	99	20.89	
0177.0	259	99	21.04	
0178.0	259	99	21.19	
0179.0	259	99	21.34	
0180.0	259	99	21.49	
0181.0	259	99	21.64	
0182.0	259	99	21.79	
0183.0	259	99	21.94	
0184.0	259	99	22.09	
0185.0	259	99	22.24	
0186.0	259	99	22.39	
0187.0	259	99	22.54	
0188.0	259	99	22.69	
0189.0	259	99	22.84	
0190.0	259	99	22.99	
0191.0	259	99	23.14	
0192.0	259	99	23.29	
0193.0	259	99	23.44	
0194.0	259	99	23.59	
0195.0	259	99	23.74	
0196.0	259	99	23.89	
0197.0	259	99	24.04	
0198.0	259	99	24.19	
0199.0	259	99	24.34	
0200.0	259	99	24.49	

EXP. NO. 492 22, DRIPS/CC

TIME	TEMP	SS	TEMP	SUPR
1106.4	285	65	1.00	
0067.5	262	22	4.21	
0068.1	262	23	4.30	
0069.0	261	61	4.58	
0070.0	261	11	4.75	
0071.0	260	54	4.94	
0072.0	259	27	5.14	
0073.0	259	44	5.34	
0074.0	258	26	5.57	
0075.0	258	31	5.80	
0076.0	257	22	5.99	
0077.0	257	22	6.07	
0078.0	257	79	6.23	
0079.0	257	94	6.40	
0080.0	257	94	6.55	
0081.0	257	97	6.70	
0082.0	258	90	6.83	
0083.0	259	90	6.99	
0084.0	259	91	7.11	
0085.0	259	97	7.26	
0086.0	259	97	7.40	
0087.0	259	99	7.55	
0088.0	259	99	7.70	
0089.0	259	99	7.84	
0090.0	259	99	7.99	
0091.0	259	99	8.14	
0092.0	259	99	8.29	
0093.0	259	99	8.44	
0094.0	259	99	8.59	
0095.0	259	99	8.74	
0096.0	259	99	8.89	
0097.0	259	99	9.04	
0098.0	259	99	9.19	
0099.0	259	99	9.34	
0100.0	259	99	9.49	
0101.0	259	99	9.64	
0102.0	259	99	9.79	
0103.0	259	99	9.94	
0104.0	259	99	10.09	
0105.0	259	99	10.24	
0106.0	259	99	10.39	
0107.0	259	99	10.54	
0108.0	259	99	10.69	
0109.0	259	99	10.84	
0110.0	259	99	10.99	
0111.0	259	99	11.14	
0112.0	259	99	11.29	
0113.0	259	99	11.44	
0114.0	259	99	11.59	
0115.0	259	99	11.74	
0116.0	259	99	11.89	
0117.0	259	99	12.04	
0118.0	259	99	12.19	
0119.0	259	99	12.34	
0120.0	259	99	12.49	
0121.0	259	99	12.64	
0122.0	259	99	12.79	
0123.0	259	99	12.94	
0124.0	259	99	13.09	
0125.0	259	99	13.24	
0126.0	259	99	13.39	
0127.0	259	99	13.54	
0128.0	259	99	13.69	
0129.0	259	99	13.84	
0130.0	259	99	13.99	
0131.0	259	99	14.14	
0132.0	259	99	14.29	
0133.0	259	99	14.44	
0134.0	259	99	14.59	
0135.0	259	99	14.74	
0136.0	259	99	14.89	
0137.0	259	99	15.04	
0138.0	259	99	15.19	
0139.0	259	99	15.34	
0140.0	259	99	15.49	
0141.0	259	99	15.64	
0142.0	259	99	15.79	
0143.0	259	99	15.94	
0144.0	259	99	16.09	
0145.0	259	99	16.24	
0146.0	259	99	16.39	
0147.0	259	99	16.54	
0148.0	259	99	16.69	
0149.0	259	99	16.84	
0150.0	259	99	16.99	
0151.0	259	99	17.14	
0152.0	259	99	17.29	
0153.0	259	99	17.44	
0154.0	259	99	17.59	
0155.0	259	99	17.74	
0156.0	259	99	17.89	
0157.0	259	99	18.04	
0158.0	259	99	18.19	
0159.0	259	99	18.34	
0160.0	259	99	18.49	
0161.0	259	99	18.64	
0162.0	259	99	18.79	
0163.0	259	99	18.94	
0164.0	259	99	19.09	
0165.0	259	99	19.24	
0166.0	259	99	19.39	
0167.0	259	99	19.54	
0168.0	259	99	19.69	
0169.0	259	99	19.84	
0170.0	259	99	19.99	
0171.0	259	99	20.14	
0172.0	259	99	20.29	
0173.0	259	99	20.44	
0174.0	259	99	20.59	
0175.0	259	99	20.74	
0176.0	259	99	20.89	
0177.0	259	99	21.04	
0178.0	259	99	21.19	
0179.0	259	99	21.34	
0180.0	259	99	21.49	
0181.0	259	99	21.64	
0182.0	259	99	21.79	
0183.0	259	99	21.94	
0184.0	259	99	22.09	
0185.0	259	99	22.24	
0186.0	259	99	22.39	
0187.0	259	99	22.54	
0188.0	259	99	22.69	
0189.0	259	99	22.84	
0190.0	259	99	22.99	
0191.0	259	99	23.14	
0192.0	259	99	23.29	
0193.0	259	99	23.44	
0194.0	259	99	23.59	
0195.0	259	99	23.74	
0196.0	259	99	23.89	
0197.0	259	99	24.04	
0198.0	259	99	24.19	
0199.0	259	99	24.34	
0200.0	259	99	24.49	

0.005	014.0	257.45	5.17
0.010	015.0	257.47	5.17
0.015	015.4	257.51	5.15
0.020	015.6	257.53	5.15
0.025	015.6	257.53	5.15
0.030	015.9	257.55	5.13
0.035	016.0	257.53	5.12
0.040	016.0	257.53	5.12
0.045	016.0	257.53	5.12
0.050	016.0	257.53	5.12
0.055	016.0	257.53	5.12
0.060	016.0	257.53	5.12
0.065	016.0	257.53	5.12
0.070	016.0	257.53	5.12
0.075	016.0	257.53	5.12
0.080	016.0	257.53	5.12
0.085	016.0	257.53	5.12
0.090	016.0	257.53	5.12
0.095	016.0	257.53	5.12
0.100	016.0	257.53	5.12
0.105	016.0	257.53	5.12
0.110	016.0	257.53	5.12
0.115	016.0	257.53	5.12
0.120	016.0	257.53	5.12
0.125	016.0	257.53	5.12
0.130	016.0	257.53	5.12
0.135	016.0	257.53	5.12
0.140	016.0	257.53	5.12
0.145	016.0	257.53	5.12
0.150	016.0	257.53	5.12
0.155	016.0	257.53	5.12
0.160	016.0	257.53	5.12
0.165	016.0	257.53	5.12

0.005	010.0	280.76	3.70
0.010	011.0	280.00	3.74

EXP. NO. 824 38, PROPS/CC

TIME	PROPS	TEMP	SUPR
0.005	1100.6	305.65	1.00
0.010	091.5	282.22	3.27
0.015	075.5	282.53	3.40
0.020	063.8	281.76	3.55
0.025	063.5	281.15	3.69
0.030	058.1	280.53	3.83
0.035	043.1	279.39	4.10
0.040	044.1	278.00	4.22
0.045	029.2	278.29	4.29
0.050	034.2	277.74	4.33
0.055	022.2	277.50	4.60
0.059	022.2	277.55	4.58
0.061	023.2	277.63	4.56
0.065	027.4	278.11	4.43
0.070	050.0	279.64	4.04
0.075	064.7	281.20	3.66
0.080	073.2	282.27	3.46

EXP. NO. 822 131, PROPS/CC

TIME	PROPS	TEMP	SUPR
0.005	1125.2	305.65	1.00
0.015	091.5	282.73	3.13
0.015	075.9	282.24	3.30
0.020	063.0	282.24	3.45
0.025	053.1	281.61	3.59
0.030	057.9	281.00	3.72
0.035	052.1	280.34	3.87
0.035	047.5	279.80	4.00
0.040	045.1	279.29	4.13
0.045	032.5	279.75	4.25
0.050	022.0	279.10	4.43
0.055	028.2	277.54	4.58
0.060	023.6	276.80	4.74
0.065	020.7	276.43	4.85
0.070	018.7	276.40	4.90
0.075	010.7	276.49	4.89
0.080	004.1	277.05	4.73
0.085	034.2	279.24	4.30
0.090	045.2	279.31	4.12
0.095	040.0	280.08	3.93
0.100	042.1	281.40	3.62
0.105	072.5	282.70	3.37

EXP. NO. 827 51, PROPS/CC

TIME	PROPS	TEMP	SUPR
0.005	1100.2	305.65	1.00
0.010	091.5	283.26	3.26
0.015	076.7	282.71	3.37
0.020	070.4	281.98	3.51
0.025	066.0	281.51	3.61
0.030	059.0	280.77	3.77
0.035	053.0	280.04	3.94
0.040	049.2	279.54	4.06
0.045	044.0	279.03	4.19
0.050	039.0	278.44	4.34
0.055	035.0	277.98	4.49
0.055	031.7	277.43	4.60
0.056	031.3	277.43	4.62
0.060	031.7	277.48	4.60
0.062	032.2	277.55	4.58
0.065	035.0	277.89	4.49
0.070	045.0	279.13	4.15

EXP. NO. 800 124, PROPS/CC

TIME	PROPS	TEMP	SUPR
0.005	1185.0	305.65	1.00
0.010	091.5	283.58	3.20
0.015	075.1	282.92	3.34
0.020	067.0	282.02	3.51
0.025	061.3	281.31	3.65
0.030	057.1	280.77	3.78
0.035	051.6	280.12	3.92
0.040	047.2	279.47	4.03
0.045	043.0	279.16	4.16
0.050	039.0	279.34	4.20
0.055	033.2	277.97	4.47
0.060	029.1	277.37	4.63
0.065	023.5	276.93	4.79
0.070	019.2	275.32	4.94
0.075	016.3	275.97	5.05
0.080	017.0	276.16	4.90
0.085	024.0	277.12	4.70
0.090	030.0	279.45	4.20
0.095	045.5	279.42	4.00
0.100	056.5	281.70	3.70
0.105	069.0	283.20	3.47

TIME	PPHSS	TEMP	SUPR
0.005	075.2	283.22	3.30
0.010	069.2	283.42	3.42
0.015	064.2	281.87	3.54
0.020	059.2	281.22	3.68
0.025	053.2	280.52	3.82
0.030	047.2	280.12	3.92
0.035	041.2	279.62	4.05
0.040	035.2	279.26	4.18
0.045	029.2	278.55	4.31
0.050	023.2	278.11	4.43
0.055	017.2	278.05	4.45
0.060	011.2	273.20	4.32
0.065	005.2	270.62	4.04
0.070	000.2	281.22	3.65
0.075	000.2	282.44	3.42

EXP. NO.	PPHSS	TEMP	SUPR
114	095.5	305.65	1.00
0.005	091.5	292.75	3.17
0.010	076.1	292.23	3.46
0.015	071.0	290.91	3.74
0.020	066.0	280.26	3.89
0.025	059.0	279.78	4.00
0.030	054.4	279.33	4.12
0.035	048.2	278.72	4.27
0.040	043.2	278.15	4.41
0.045	037.5	277.51	4.57
0.050	032.0	277.09	4.72
0.055	026.0	276.92	4.76
0.060	020.0	277.14	4.70
0.065	014.0	278.52	4.32
0.070	008.0	279.01	3.97
0.075	002.0	280.85	3.76
0.080	000.0	282.18	3.47

EXP. NO. 009 75, PPHSS/CC

TIME	PPHSS	TEMP	SUPR
0.005	1185.0	305.65	1.00
0.010	081.5	282.75	3.17
0.015	074.2	282.92	3.31
0.020	068.2	282.23	3.46
0.025	063.0	281.62	3.59
0.030	058.0	280.91	3.74
0.035	051.3	280.26	3.89
0.040	047.2	279.78	4.00
0.045	043.2	279.33	4.12
0.050	038.1	278.72	4.27
0.055	033.4	278.15	4.41
0.060	028.7	277.51	4.57
0.065	024.2	277.09	4.72
0.070	020.0	276.92	4.76
0.075	016.7	277.14	4.70
0.080	013.4	278.52	4.32
0.085	010.3	279.01	3.97
0.090	007.4	280.85	3.76
0.095	004.0	282.18	3.47

EXP. NO. 017 3.0 PPHSS/CC

TIME	PPHSS	TEMP	SUPR
0.005	1185.0	305.65	1.00
0.010	091.5	292.75	3.17
0.015	077.2	292.23	3.27
0.020	067.1	290.92	3.49
0.025	061.5	281.46	3.63
0.030	056.5	280.87	3.75
0.035	051.7	280.31	3.88
0.040	047.0	279.76	4.01
0.045	043.0	279.39	4.12
0.050	039.4	278.99	4.23
0.055	035.2	278.59	4.35
0.060	031.7	278.14	4.46
0.065	028.6	277.71	4.57
0.070	025.2	281.19	3.63
0.075	022.0	282.66	3.38

EXP. NO. 012 67, PPHSS/CC

TIME	PPHSS	TEMP	SUPR
0.005	1184.0	305.65	1.00
0.010	091.5	282.76	3.17
0.015	074.9	282.92	3.31
0.020	068.2	282.23	3.46
0.025	063.1	281.64	3.59
0.030	057.0	281.04	3.72
0.035	052.5	280.41	3.86
0.040	047.6	279.84	3.99
0.045	043.7	279.28	4.10
0.050	039.3	278.81	4.25
0.055	035.0	278.32	4.40
0.060	031.2	277.89	4.54
0.065	028.2	277.42	4.68
0.070	025.2	276.93	4.75
0.075	023.3	277.35	4.64
0.080	021.4	277.31	4.37
0.085	019.6	279.72	4.02
0.090	018.0	280.79	3.79
0.095	016.4	282.02	3.51

EXP. NO. 010 0.3 PPHSS/CC

TIME	PPHSS	TEMP	SUPR
0.005	1184.0	305.65	1.00
0.010	091.5	282.76	3.17
0.015	077.5	282.31	3.25
0.020	072.3	282.70	3.37
0.025	067.4	282.14	3.48
0.030	062.5	281.57	3.60
0.035	058.0	280.91	3.74
0.040	053.0	280.36	3.87
0.045	048.1	280.60	3.81
0.050	043.5	280.50	3.84
0.055	039.1	280.25	3.80
0.060	035.0	280.36	3.87
0.065	031.0	280.57	3.82
0.070	027.0	280.50	3.84
0.075	023.0	280.40	3.86
0.080	019.0	280.54	3.83
0.085	015.0	280.91	3.74
0.090	011.0	282.17	3.48

EXP. NO. 022		1,2 DRIPS/CC		EXP. NO. 023		1,2 DRIPS/CC	
TIME	PRESS	TEMP	SUPR	TIME	PRESS	TEMP	SUPR
0.005	1193.6	305.65	1.00	0.005	1192.0	305.65	1.00
0.010	091.5	284.89	3.15	0.010	091.5	283.69	3.14
0.015	074.3	283.11	3.29	0.015	057.2	281.15	3.59
0.020	070.1	282.57	3.40	0.020	070.0	282.63	3.39
0.025	066.3	282.12	3.48	0.025	065.6	282.12	3.40
0.030	061.1	281.53	3.61	0.030	062.2	281.74	3.57
0.035	056.2	280.85	3.75	0.035	062.5	281.76	3.56
0.040	051.0	280.34	3.87	0.040	062.4	281.75	3.56
0.045	046.6	279.84	3.99	0.045	061.0	281.61	3.59
0.050	043.5	279.42	4.09	0.050	061.5	281.64	3.59
0.055	044.5	279.65	4.04	0.055	062.0	281.31	3.55
0.060	044.5	279.65	4.05	0.060	062.4	281.26	3.54
0.065	043.1	279.42	4.00	0.065	062.2	281.74	3.57
0.070	044.3	279.59	4.05	0.070	063.7	281.99	3.53
0.075	045.6	279.73	4.02	0.075	074.5	281.99	3.51
0.080	044.0	279.65	4.04	0.080	063.0	281.82	3.55
0.085	046.7	279.86	3.99	0.085	062.0	281.81	3.55
0.090	061.0	281.52	3.61	0.090	064.7	282.01	3.51
0.095	075.2	283.16	3.28	0.095	064.6	282.00	3.51
				0.100	063.4	281.96	3.54
				0.105	063.8	282.02	3.51
				0.110	064.6	282.00	3.51
				0.115	064.2	281.95	3.52
				0.120	064.7	282.01	3.51
				0.125	070.6	282.69	3.37
				0.130			
				0.135			
				0.140			
				0.145			

EXP. NO. 024		0,2 DRIPS/CC		EXP. NO. 025		0,2 DRIPS/CC	
TIME	PRESS	TEMP	SUPR	TIME	PRESS	TEMP	SUPR
0.005	1193.0	305.65	1.00	0.005	1192.0	305.65	1.00
0.010	091.5	284.01	3.12	0.010	091.5	283.69	3.14
0.015	077.0	283.52	3.21	0.015	057.2	281.15	3.59
0.020	072.2	282.05	3.32	0.020	070.0	282.63	3.39
0.025	066.7	282.21	3.45	0.025	065.6	282.12	3.40
0.030	061.1	281.66	3.52	0.030	062.2	281.74	3.57
0.035	056.7	281.09	3.71	0.035	062.5	281.76	3.56
0.040	052.0	280.60	3.79	0.040	062.4	281.75	3.56
0.045	047.8	280.70	3.82	0.045	061.0	281.61	3.59
0.050	043.0	280.52	3.91	0.050	061.5	281.64	3.59
0.055	038.1	280.55	3.82	0.055	062.0	281.31	3.55
0.060	033.6	280.59	3.80	0.060	062.4	281.26	3.54
0.065	029.2	280.70	3.77	0.065	062.2	281.74	3.57
0.070	025.7	280.60	3.70	0.070	063.7	281.99	3.53
0.075	022.3	280.64	3.80	0.075	074.5	281.99	3.51
0.080	019.6	280.79	3.77	0.080	063.0	281.82	3.55
0.085	017.1	280.95	3.76	0.085	062.0	281.81	3.55
0.090	015.0	280.72	3.79	0.090	064.7	282.01	3.51
0.095	013.4	280.77	3.78	0.095	064.6	282.00	3.51
0.100	012.6	280.91	3.74	0.100	063.4	281.96	3.54
0.105	012.5	280.91	3.75	0.105	063.8	282.02	3.51
0.110	012.5	280.91	3.77	0.110	064.6	282.00	3.51
0.115	012.5	281.06	3.71	0.115	064.2	281.95	3.52
0.120	012.5	282.02	3.47	0.120	064.7	282.01	3.51
0.125				0.125			
0.130				0.130			

EXP. NO. 027		0,3 DRIPS/CC		EXP. NO. 032		0,3 DRIPS/CC	
TIME	PRESS	TEMP	SUPR	TIME	PRESS	TEMP	SUPR
0.005	1192.0	305.65	1.00	0.005	1195.6	305.65	1.00
0.010	091.5	284.03	3.12	0.010	091.5	283.69	3.18
0.015	075.0	283.39	3.24	0.015	077.8	283.27	3.26
0.020	071.3	282.86	3.34	0.020	072.4	282.65	3.38
0.025	066.5	282.31	3.45	0.025	069.0	282.14	3.48
0.030	060.7	281.64	3.59				
0.035	055.8	281.07	3.71				

TIME	PRSS	TEMP	SUPR
0.005	062.5	281.51	3.61
0.010	057.0	281.00	3.75
0.015	055.0	281.73	3.72
0.020	056.0	281.85	3.76
0.025	055.5	280.60	3.70
0.030	054.0	280.62	3.81
0.035	054.0	280.78	3.77
0.040	057.0	280.90	3.75
0.045	064.0	281.70	3.77
0.050	055.0	280.74	3.79
0.055	057.1	280.82	3.75
0.060	058.0	280.82	3.73
0.065	057.0	280.87	3.75
0.070	064.0	280.70	3.77
0.075	059.0	281.00	3.73
0.080	059.0	281.08	3.71
0.085	057.0	281.04	3.74
0.090	058.0	281.00	3.75
0.095	058.0	281.08	3.71
0.100	058.0	281.11	3.70
0.105	058.0	281.02	3.71
0.110	061.0	281.06	3.73
0.115	061.0	281.33	3.65
0.120	071.4	282.53	3.40

EXP. NO.	PRSS	TEMP	SUPR
189	065.0	314.15	1.00
0.005	070.0	291.02	3.13
0.010	070.0	290.20	3.27
0.015	064.0	290.45	3.41
0.020	059.0	290.01	3.51
0.025	054.0	291.23	3.55
0.030	049.0	297.53	3.79
0.035	043.0	294.02	3.91
0.040	037.0	294.20	4.07
0.045	033.0	295.74	4.23
0.050	031.0	295.40	4.26
0.055	029.0	295.62	4.22
0.060	031.0	295.46	4.26
0.065	030.0	295.25	4.20
0.070	032.0	295.50	4.23
0.075	033.0	295.71	4.20
0.080	032.0	295.62	4.22
0.085	032.0	295.63	4.22
0.090	035.0	295.06	4.14
0.095	044.0	297.12	3.98
0.100	059.0	299.69	3.65
0.105	060.0	290.02	3.61

EXP. NO. 934 114, PRSS/CC

TIME	PRSS	TEMP	SUPR
0.005	1138.0	305.65	1.00
0.010	091.0	283.57	3.21
0.015	075.0	283.06	3.24
0.020	060.0	282.19	3.47
0.025	044.0	281.56	3.60
0.030	050.0	280.03	3.73
0.035	047.0	280.25	3.88
0.040	043.0	279.67	4.03
0.045	039.0	279.15	4.16
0.050	033.0	279.63	4.29
0.055	029.0	279.00	4.46
0.060	024.0	277.40	4.75
0.065	020.0	276.47	4.00
0.070	020.0	276.40	4.02
0.075	021.0	276.50	4.06
0.080	021.0	276.61	4.05
0.085	021.0	276.51	4.02
0.090	021.0	276.50	4.06
0.095	022.0	276.76	4.81
0.100	022.0	276.71	4.82
0.105	021.0	276.61	4.85
0.110	022.0	276.85	4.78
0.115	024.0	276.05	4.76
0.120	023.0	276.84	4.79
0.125	024.0	276.91	4.77
0.130	025.0	277.10	4.71
0.135	025.0	277.11	4.71
0.140	026.0	277.03	4.72
0.145	027.0	277.15	4.70
0.150	027.0	277.20	4.66
0.155	027.0	277.23	4.67
0.160	027.0	277.28	4.66
0.165	032.0	277.82	4.50
0.170	044.0	279.26	4.13
0.175	055.0	281.61	3.81
0.180	064.0	281.65	3.59
0.185	074.0	282.73	3.37

EXP. NO. 907 245, PRSS/CC

TIME	PRSS	TEMP	SUPR
0.005	1189.0	314.15	1.00
0.010	079.0	291.04	3.12
0.015	073.0	290.50	3.22
0.020	068.0	290.76	3.35
0.025	062.0	290.10	3.46
0.030	054.0	290.54	3.62
0.035	050.0	297.84	3.72
0.040	045.0	297.27	3.85
0.045	040.0	296.40	3.99
0.050	040.0	296.40	4.13
0.055	031.0	295.50	4.25
0.060	027.0	295.22	4.37
0.065	024.0	294.44	4.51
0.070	022.0	294.21	4.59
0.075	020.0	294.40	4.51
0.080	020.0	295.00	4.16
0.085	024.0	297.21	3.94
0.090	030.0	298.10	3.65
0.095	054.0	290.50	3.40

EXP. NO. 900 112, PRSS/CC

TIME	PRSS	TEMP	SUPR
0.005	1190.0	314.15	1.00
0.010	079.0	291.04	3.12
0.015	073.0	290.45	3.23
0.020	067.0	290.77	3.35
0.025	061.0	290.14	3.47
0.030	056.0	290.54	3.59
0.035	052.0	297.08	3.70
0.040	046.0	297.37	3.83
0.045	041.0	296.71	3.97
0.050	036.0	296.17	4.09

0.005	020.1	285.60	4.23	0.035	045.0	287.22	3.36
0.010	023.1	285.24	4.31	0.040	046.0	287.21	3.24
0.015	021.0	285.47	4.25	0.043	046.2	286.41	4.04
0.020	024.4	285.80	4.16	0.046	047.3	286.62	3.00
0.025	040.0	287.61	3.78	0.050	042.5	287.02	3.00
0.030	050.6	288.88	3.52	0.055	053.0	288.25	3.44
0.035	071.0	290.22	3.27	0.060	066.0	289.77	3.35

EXP. NO. 2 105, DROPS/CC				EXP. NO. 0 2,5 DROPS/CC			
TIME	PRESS	TEMP	SUPR	TIME	PRESS	TEMP	SUPR
0.005	1180.0	314.15	1.00	0.005	1128.0	314.15	1.00
0.010	072.0	291.06	3.12	0.010	072.0	290.47	3.23
0.015	066.4	290.70	3.36	0.015	067.0	290.30	3.34
0.020	060.5	289.20	3.49	0.020	062.2	289.22	3.45
0.025	055.5	289.41	3.61	0.025	057.4	288.65	3.56
0.030	050.1	287.77	3.74	0.030	052.1	288.22	3.60
0.035	044.2	287.37	3.89	0.035	047.8	287.51	3.80
0.040	038.0	286.44	4.03	0.039	046.3	287.27	3.82
0.045	034.2	285.97	4.16	0.042	047.5	287.47	3.90
0.049	031.6	285.56	4.24	0.044	043.1	287.54	3.70
0.050	030.4	285.42	4.27	0.047	049.6	287.63	3.77
0.053	028.0	285.61	4.23	0.050	050.2	288.02	3.59
0.056	026.0	286.20	4.09	0.055	065.0	289.65	3.37
0.060	047.5	287.46	3.81				
0.065	060.4	288.99	3.50				

EXP. NO. 4 55, DROPS/CC				EXP. NO. 12 4,3 DROPS/CC			
TIME	PRESS	TEMP	SUPR	TIME	PRESS	TEMP	SUPR
0.005	1180.5	314.15	1.00	0.005	1128.0	314.15	1.00
0.010	072.0	291.11	3.12	0.010	072.0	290.27	3.24
0.015	066.4	290.75	3.36	0.015	066.5	290.70	3.35
0.020	061.0	289.11	3.47	0.020	061.2	289.11	3.47
0.025	056.4	289.57	3.59	0.025	056.2	288.51	3.50
0.030	051.0	287.92	3.71	0.030	051.1	287.00	3.71
0.035	045.4	287.26	3.85	0.035	046.7	287.25	3.82
0.040	040.0	286.66	3.92	0.040	044.0	287.13	3.88
0.045	031.0	285.61	4.23	0.045	044.6	287.26	3.89
0.049	030.0	285.65	4.21	0.049	044.6	287.12	3.88
0.051	031.4	286.50	4.23	0.045	047.0	287.52	3.70
0.055	042.0	286.86	3.84	0.050	058.0	288.02	3.53
0.060	053.0	288.27	3.64				
0.065	066.6	289.77	3.35				

EXP. NO. 7 25, DROPS/CC				EXP. NO. 14 2,9 DROPS/CC			
TIME	PRESS	TEMP	SUPR	TIME	PRESS	TEMP	SUPR
0.005	1188.7	314.15	1.00	0.005	1100.0	314.15	1.00
0.010	078.0	291.09	3.12	0.010	078.0	290.26	3.14
0.015	066.7	290.76	3.35	0.015	072.4	290.21	3.25
0.020	061.6	290.16	3.46	0.020	067.2	290.70	3.36
0.025	056.0	288.50	3.59	0.025	062.5	290.14	3.47
0.030	050.1	287.80	3.74	0.025	057.0	289.50	3.50
				0.030	052.0	288.00	3.70
				0.035	050.0	287.67	3.76
				0.040	057.7	287.75	3.75
				0.045	050.0	287.67	3.76
				0.050	060.6	287.50	3.80

0	0	049.2	287.58	3.78
0	0	050.9	287.74	3.74
0	0	051.1	287.80	3.74
0	0	050.6	287.62	3.77
0	0	051.1	287.58	3.76
0	0	051.2	287.90	3.72
0	0	052.7	287.08	3.75
0	0	050.0	288.84	3.53

EXP. NO. 17 5.4 DROPS/CC

TIME	DROPS	TEMP	SUPR
00.00	1190.2	314.15	1.00
00.05	079.0	201.06	3.12
00.10	072.0	200.54	3.21
00.15	049.7	200.97	3.21
00.20	044.0	200.42	3.42
00.25	050.0	200.00	3.53
00.30	052.7	200.00	3.65
00.35	049.0	200.75	3.75
00.40	049.2	200.55	3.73
00.45	049.0	200.64	3.77
00.50	047.6	200.48	3.80
00.55	047.0	200.40	3.80
01.00	049.2	200.55	3.79
01.05	049.7	200.72	3.75
01.10	049.6	200.50	3.78
01.15	047.5	200.47	3.80
01.20	040.0	200.49	3.75
01.25	050.6	200.92	3.73
01.30	040.1	200.65	3.77
01.35	049.7	200.60	3.78
01.40	050.3	200.70	3.74
01.45	051.1	200.80	3.72
01.50	053.5	200.17	3.66
01.55	049.1	200.00	3.33

EXP. NO. 18 1.2 DROPS/CC

TIME	DROPS	TEMP	SUPR
00.00	1190.2	314.15	1.00
00.05	079.0	201.06	3.12
00.10	072.0	200.54	3.24
00.15	067.5	200.91	3.34
00.20	062.3	200.00	3.45
00.25	057.2	200.00	3.57
00.30	052.0	200.00	3.68
00.35	051.1	200.47	3.72
00.40	057.2	200.50	3.57
00.45	051.1	200.87	3.72
00.50	051.1	200.67	3.70
00.55	053.0	200.10	3.67
01.00	053.2	200.08	3.70
01.05	052.0	200.05	3.68
01.10	053.8	200.10	3.66
01.15	053.8	200.19	3.66
01.20	052.7	200.06	3.67
01.25	054.5	200.00	3.64
01.30	050.7	200.88	3.52

EXP. NO. 22 0.6 DROPS/CC

TIME	DROPS	TEMP	SUPR
00.00	1190.2	314.15	1.00
00.05	079.0	201.06	3.12
00.10	072.0	200.54	3.22
00.15	069.0	200.97	3.21
00.20	062.0	200.42	3.42
00.25	050.0	200.00	3.53
00.30	056.4	200.00	3.50
00.35	057.0	200.75	3.55
00.40	057.6	200.64	3.57
00.45	056.4	200.50	3.50
00.50	057.0	200.57	3.55
00.55	058.0	200.71	3.55
01.00	059.7	200.00	3.54
01.05	057.0	200.68	3.56
01.10	057.0	200.47	3.56
01.15	050.0	200.91	3.53
01.20	050.0	200.00	3.51
01.25	050.0	200.78	3.54
01.30	050.0	200.00	3.52
01.35	040.3	200.06	3.50
01.40	050.0	200.24	3.53
01.45	050.0	200.88	3.53
01.50	067.0	200.75	3.26
01.55	060.7	200.01	3.40
02.00	068.0	200.06	3.33

EXP. NO. 24 0.3 DROPS/CC

TIME	DROPS	TEMP	SUPR
00.00	1190.2	314.15	1.00
00.05	079.0	201.06	3.12
00.10	074.0	200.60	3.20
00.15	060.0	200.01	3.31
00.20	062.7	200.00	3.42
00.25	059.0	200.00	3.52
00.30	054.0	200.00	3.62
00.35	052.0	200.00	3.66
00.40	054.0	200.75	3.64
00.45	052.0	200.13	3.67
00.50	052.7	200.00	3.69
00.55	054.0	200.00	3.63
01.00	053.0	200.27	3.64
01.05	053.0	200.13	3.67
01.10	055.0	200.23	3.65
01.15	055.4	200.41	3.61
01.20	055.0	200.00	3.62
01.25	054.0	200.24	3.65
01.30	055.0	200.00	3.63
01.35	055.5	200.42	3.61
01.40	055.0	200.00	3.62
01.45	056.4	200.27	3.60
01.50	061.5	200.13	3.47

TABLE X

ARGON DATA

EXP. NO. 849				EXP. NO. 854			
65.00 DIPS/CC				29.00 DIPS/CC			
TIME	PRESS	TEMP	SUPR	TIME	PRESS	TEMP	SUPR
C.005	1194.1	295.65	1.00	C.005	1127.1	295.65	1.00
C.010	095.5	274.82	3.28	C.010	085.5	274.60	3.24
C.015	091.0	274.24	3.28	C.015	081.2	274.12	3.44
C.020	078.2	272.74	3.52	C.020	074.9	272.41	3.50
C.025	069.9	272.14	3.66	C.025	070.4	272.82	3.73
C.030	065.4	272.66	3.77	C.030	064.6	272.27	3.86
C.035	060.5	272.09	3.91	C.035	059.2	271.66	4.02
C.040	055.7	271.54	4.05	C.040	054.3	271.09	4.17
C.045	051.4	270.96	4.18	C.045	049.7	270.50	4.31
C.050	046.1	270.46	4.34	C.050	044.4	269.93	4.48
C.055	040.0	269.95	4.52	C.055	039.0	269.35	4.67
C.060	034.0	269.20	4.69	C.060	035.1	268.92	4.80
C.065	031.7	268.81	4.84	C.065	034.4	268.85	4.83
C.070	029.5	268.44	4.96	C.070	034.5	268.94	4.82
C.075	029.6	268.97	4.92	C.075	033.4	268.74	4.86
C.080	029.5	268.56	4.92	C.080	030.7	268.45	4.84
C.085	029.2	268.41	4.97	C.085	028.0	270.04	4.20
C.090	029.2	268.78	4.95	C.090	024.6	272.27	3.37
C.095	029.3	268.65	4.89	C.095	023.0	273.31	3.62
C.100	029.7	268.58	4.91				
C.105	029.9	268.48	4.95				
C.110	029.0	268.62	4.90				
C.115	029.6	268.69	4.88				
C.120	029.0	268.73	4.86				
C.125	047.4	269.90	4.53				
C.130	055.0	271.46	4.07				
C.135	065.1	272.60	3.79				
C.140	072.3	273.81	3.57				
EXP. NO. 852				EXP. NO. 857			
45.00 DIPS/CC				6.7 DIPS/CC			
TIME	PRESS	TEMP	SUPR	TIME	PRESS	TEMP	SUPR
C.005	1182.8	295.65	1.00	C.005	1187.3	295.65	1.00
C.010	085.8	274.04	3.27	C.010	085.5	274.50	3.24
C.015	082.0	274.20	3.40	C.015	082.6	274.26	3.41
C.020	074.2	272.65	3.54	C.020	078.9	272.51	3.57
C.025	069.0	272.06	3.67	C.025	070.6	272.82	3.71
C.030	064.0	272.50	3.81	C.030	065.6	272.24	3.84
C.035	059.0	271.95	3.94	C.035	060.4	271.78	3.90
C.040	054.0	271.38	4.09	C.040	055.2	271.10	4.14
C.045	049.1	270.82	4.24	C.045	050.0	270.71	4.27
C.050	043.8	270.22	4.41	C.050	045.0	270.12	4.44
C.055	039.3	269.59	4.60	C.055	040.2	269.40	4.63
C.060	034.1	268.91	4.74	C.060	039.5	269.41	4.65
C.065	031.4	268.90	4.84	C.065	040.4	269.52	4.62
C.070	032.6	268.99	4.80	C.070	038.5	270.36	4.25
C.075	032.1	268.76	4.85	C.075	034.0	272.23	3.36
C.080	031.9	268.94	4.82	C.080	031.5	273.02	3.68
C.085	032.6	268.88	4.82				
C.090	032.1	268.83	4.83				
C.095	031.5	268.98	4.79				
C.100	035.8	269.31	4.63				
C.105	045.0	270.36	4.37				
C.110	050.4	271.00	3.94				
C.115	059.4	272.11	3.66				
C.120	069.4	274.12	3.44				
C.125	078.5						
EXP. NO. 859				EXP. NO. 859			
				8.5 DIPS/CC			
TIME	PRESS	TEMP	SUPR	TIME	PRESS	TEMP	SUPR
C.005	1185.2	295.65	1.00	C.005	1185.2	295.65	1.00
C.010	085.5	274.77	3.30	C.010	085.5	274.77	3.30
C.015	080.2	274.19	3.42	C.015	080.2	274.19	3.42
C.020	074.9	273.58	3.55	C.020	074.9	273.58	3.55
C.025	070.5	272.90	3.69	C.025	070.5	272.90	3.69
C.030	064.6	272.44	3.82	C.030	064.6	272.44	3.82
C.035	059.8	271.90	3.96	C.035	059.8	271.90	3.96
C.040	054.4	271.38	4.11	C.040	054.4	271.38	4.11
C.045	050.4	270.84	4.24	C.045	050.4	270.84	4.24
				C.045	045.5	270.20	4.30

0.005	940.0	260.66	4.58
0.010	938.0	260.42	4.64
0.015	937.2	260.35	4.67
0.020	937.7	260.40	4.65
0.025	944.6	270.18	4.42
0.030	948.0	270.23	4.41
0.035	941.3	272.07	3.91
0.040	948.7	272.80	3.71
0.045	974.6	273.78	3.51

0.010	978.7	273.93	3.48
0.015	972.5	273.24	3.62
0.020	969.5	272.70	3.74
0.025	968.0	272.53	3.80
0.030	967.3	272.71	3.76
0.035	969.0	272.75	3.74
0.040	967.0	272.62	3.78
0.045	966.2	272.64	3.80
0.050	967.2	272.71	3.76
0.055	968.0	272.82	3.73
0.060	968.3	272.77	3.74
0.065	967.1	272.83	3.78
0.070	967.2	272.65	3.77
0.075	969.4	272.85	3.74
0.080	969.8	272.92	3.73
0.085	969.4	272.73	3.74
0.090	967.2	272.71	3.76
0.095	969.5	272.73	3.75
0.100	969.3	272.89	3.72
0.105	969.7	272.89	3.71
0.110	972.1	272.20	3.62

EXP. NO. 864 0.4 DROPS/CC

TIME	PRESS	TEMP	SUPR
1185.6	295.65	1.00	
0.005	985.5	274.74	3.31
0.010	980.5	274.18	3.42
0.015	975.1	272.58	3.56
0.020	977.7	273.02	3.67
0.025	965.2	272.49	3.81
0.030	967.4	271.94	3.95
0.035	959.7	271.41	4.09
0.040	951.0	270.87	4.23
0.041	950.2	270.78	4.25
0.042	949.6	270.72	4.27
0.045	950.4	270.81	4.25
0.050	960.3	271.92	3.95
0.055	971.8	273.21	3.64
0.060	978.4	273.95	3.47

EXP. NO. 874 0.1 DROPS/CC

TIME	PRESS	TEMP	SUPR
1185.8	295.45	1.00	
0.005	985.5	274.72	3.31
0.010	979.3	274.02	3.46
0.015	977.2	273.86	3.51
0.020	978.4	273.93	3.48
0.025	978.4	273.23	3.48
0.030	977.7	273.65	3.50
0.035	979.7	274.07	3.45
0.040	978.4	273.23	3.48
0.045	978.5	274.05	3.45
0.050	978.7	274.07	3.45
0.055	978.5	274.06	3.45
0.060	980.5	274.16	3.43
0.065	979.0	274.10	3.44
0.070	980.2	274.13	3.44
0.075	980.2	274.13	3.44

EXP. NO. 860 0.3 DROPS/CC

TIME	PRESS	TEMP	SUPR
1185.5	295.65	1.00	
0.005	985.5	274.79	3.29
0.010	980.7	274.26	3.41
0.015	975.0	272.63	3.55
0.020	969.8	272.04	3.68
0.025	964.2	272.48	3.81
0.030	960.1	271.96	3.94
0.035	956.0	271.40	4.06
0.040	953.0	271.17	4.15
0.045	953.0	271.26	4.12
0.050	954.5	271.32	4.11
0.055	952.0	271.14	4.16
0.060	952.6	271.11	4.16
0.065	954.2	271.30	4.11
0.070	954.9	271.36	4.10
0.075	952.5	271.21	4.14
0.080	953.8	271.24	4.13
0.085	959.6	271.80	3.96
0.090	976.2	273.76	3.52

EXP. NO. 877 14.1 DROPS/CC

TIME	PRESS	TEMP	SUPR
1185.5	295.65	1.00	
0.005	985.5	274.75	3.30
0.010	980.0	274.14	3.43
0.015	974.0	273.47	3.58
0.020	969.2	272.84	3.70
0.025	964.3	272.29	3.84
0.030	959.2	271.81	3.98
0.035	954.5	271.28	4.12
0.040	949.3	270.69	4.28
0.045	943.8	270.07	4.46
0.050	938.0	269.54	4.61
0.055	936.9	269.29	4.69
0.060	937.0	269.29	4.66
0.065	938.8	269.50	4.63
0.070	942.1	269.95	4.48
0.075	957.5	271.65	4.02
0.080	970.5	273.07	3.67
0.085	978.6	273.98	3.47

EXP. NO. 872 0.2 DROPS/CC

TIME	PRESS	TEMP	SUPR
1186.2	295.65	1.00	
0.005	985.5	274.68	3.32

EXP. NO. 070 49, DRIPS/CC

TIME	PRESS	TEMP	SUPR
0.005	1184.2	295.65	1.00
0.010	095.5	274.48	3.32
0.015	089.4	274.12	3.44
0.020	075.3	272.55	3.56
0.025	060.9	272.95	3.70
0.030	064.9	272.37	3.84
0.035	069.7	271.84	3.97
0.040	065.7	271.25	4.10
0.045	055.4	270.75	4.25
0.050	045.1	270.15	4.43
0.055	047.0	269.57	4.60
0.060	035.2	269.02	4.77
0.065	031.0	269.54	4.92
0.070	026.0	268.07	5.08
0.075	024.1	267.75	5.19
0.080	023.2	269.53	4.93
0.085	043.2	269.03	4.49
0.090	050.4	270.75	4.26
0.095	059.7	271.69	4.01
0.100	070.7	273.03	3.68

0.040	043.3	270.24	4.37
0.045	030.1	269.80	4.51
0.050	034.4	269.35	4.67
0.055	029.9	268.92	4.84
0.060	025.0	269.27	5.01
0.065	021.5	267.26	5.15
0.070	025.0	269.27	5.09
0.075	036.8	269.62	4.59
0.080	047.7	272.96	4.23
0.085	054.0	271.00	3.96
0.090	048.5	272.21	3.64
0.095	077.0	274.26	3.41

EXP. NO. 002 56, DRIPS/CC

TIME	PRESS	TEMP	SUPR
0.005	1182.7	295.65	1.00
0.010	099.5	274.91	3.27
0.015	070.3	274.10	3.42
0.020	070.4	272.45	3.53
0.025	049.5	272.02	3.68
0.030	044.2	272.54	3.80
0.035	059.9	271.84	3.95
0.040	054.0	271.39	4.09
0.045	049.6	270.78	4.26
0.050	043.3	270.17	4.43
0.055	039.0	269.62	4.57
0.060	035.0	269.23	4.71
0.065	030.2	269.68	4.88
0.070	025.0	268.99	5.08
0.075	019.9	267.49	5.29
0.080	019.2	267.29	5.35
0.085	019.6	267.45	5.29
0.090	020.2	269.56	4.92
0.095	041.0	270.01	4.47
0.100	050.7	271.01	4.19
0.105	060.0	272.06	3.92
0.110	070.4	272.23	3.64
0.115	080.3	274.33	3.39

EXP. NO. 007 71, DRIPS/CC

TIME	PRESS	TEMP	SUPR
0.005	1184.7	295.65	1.00
0.010	095.5	272.90	3.48
0.015	090.0	272.29	3.62
0.020	075.0	272.74	3.75
0.025	049.5	272.13	3.90
0.030	044.6	271.58	4.04
0.035	059.0	270.04	4.21
0.040	053.5	270.23	4.38
0.045	048.3	269.75	4.55
0.050	042.0	269.13	4.74
0.055	039.2	268.71	4.87
0.060	035.5	269.20	5.01
0.065	031.0	267.78	5.19
0.070	026.0	267.21	5.38
0.075	024.3	267.01	5.45
0.080	024.3	267.01	5.45
0.085	025.5	267.26	5.36
0.090	033.0	268.11	5.07
0.095	040.6	268.97	4.82
0.100	051.8	270.14	4.44
0.105	062.2	271.31	4.11
0.110	072.1	272.41	3.83

EXP. NO. 004 49, DRIPS/CC

TIME	PRESS	TEMP	SUPR
0.005	1191.6	295.65	1.00
0.010	095.5	275.11	3.23
0.015	076.7	274.13	3.44
0.020	070.0	273.38	3.60
0.025	064.1	272.72	3.76
0.030	058.6	272.10	3.91
0.035	053.1	271.48	4.07
0.040	047.9	270.89	4.22

EXP. NO. 000 182, DRIPS/CC

TIME	PRESS	TEMP	SUPR
0.005	1196.0	295.65	1.00
0.010	095.5	273.70	3.53
0.015	077.3	272.90	3.74
0.020	070.6	272.05	3.92
0.025	064.5	271.37	4.10
0.030	058.5	270.70	4.28
0.035	053.1	270.00	4.45
0.040	048.1	269.53	4.62
0.045	042.9	269.04	4.80
0.050	038.0	268.39	4.98
0.055	034.0	267.93	5.13
0.060	029.6	267.42	5.30
0.065	024.4	266.93	5.52
0.070	019.3	266.24	5.74
0.075	014.5	265.93	5.86
0.080	023.7	264.75	5.55
0.085	035.8	269.13	5.06
0.090	046.4	269.33	4.69
0.095	055.0	270.40	4.36
0.100	065.3	271.46	4.07
0.105	074.8	272.51	3.81

EXP. NO. 892 146, DROPS/CC

TIME	PRESS	TEMP	SUPR
0.005	1100.8	295.65	1.00
0.010	085.5	272.53	3.57
0.015	077.9	272.68	3.77
0.020	066.1	272.05	3.92
0.025	041.1	271.39	4.09
0.030	056.7	270.92	4.24
0.035	052.9	270.32	4.38
0.040	048.7	269.89	4.51
0.045	044.6	269.42	4.65
0.050	040.1	268.96	4.79
0.055	034.4	268.45	4.95
0.060	028.4	267.80	5.17
0.065	023.8	267.12	5.41
0.070	022.4	266.50	5.61
0.075	022.4	266.45	5.66
0.080	021.2	266.52	5.63
0.085	031.6	267.48	5.28
0.090	042.4	268.71	4.87
0.095	051.5	269.74	4.55
0.100	062.1	270.03	4.21
0.095	074.0	272.35	3.84

0.040	080.0	270.92	4.24
0.045	047.4	270.44	4.35
0.050	043.1	240.73	4.50
0.055	030.6	260.52	4.62
0.060	026.5	260.18	4.72
0.064	025.9	260.10	4.75
0.067	036.2	260.15	4.73
0.070	030.5	260.52	4.62
0.075	042.6	270.54	4.32
0.080	057.1	271.52	4.26
0.085	062.1	272.10	3.99
0.090	075.0	272.52	3.57

EXP. NO. 894 97, DROPS/CC

TIME	PRESS	TEMP	SUPR
0.005	1100.1	295.65	1.00
0.010	085.5	274.41	3.37
0.015	077.2	273.51	3.57
0.020	070.5	272.75	3.75
0.025	074.8	272.11	3.90
0.030	050.4	271.50	4.06
0.035	054.0	270.90	4.22
0.040	040.1	270.24	4.38
0.045	042.2	269.67	4.57
0.050	039.4	269.15	4.73
0.055	034.7	268.70	4.87
0.060	030.7	268.25	5.02
0.065	026.5	267.77	5.18
0.070	021.1	267.14	5.40
0.075	015.9	266.53	5.63
0.080	015.4	266.49	5.65
0.085	015.9	266.53	5.63
0.090	020.3	267.25	5.44
0.095	033.3	268.54	4.92
0.100	042.4	269.58	4.60
0.095	051.1	270.57	4.31
0.090	062.2	271.52	3.93
0.100	071.4	272.55	3.73

EXP. NO. 890 88 DROPS/CC

TIME	PRESS	TEMP	SUPR
0.005	1105.6	295.65	1.00
0.010	095.5	274.74	3.31
0.015	070.0	273.01	3.69
0.020	065.0	272.45	3.82
0.025	040.2	271.01	3.95
0.030	048.6	270.60	4.13
0.035	044.6	270.15	4.43
0.040	041.2	269.76	4.55
0.045	029.2	269.42	4.64
0.050	024.0	269.04	4.75
0.053	023.2	268.85	4.83
0.056	025.7	268.12	4.74
0.060	032.5	268.77	4.85
0.065	044.8	270.17	4.43
0.070	047.3	270.45	4.24
0.075	053.1	271.11	4.16
0.080	050.2	271.00	3.98
0.085	060.3	272.02	3.71

EXP. NO. 897 15,4 DROPS/CC

TIME	PRESS	TEMP	SUPR
0.005	1106.1	295.65	1.00
0.010	085.5	274.69	3.32
0.015	078.4	273.90	3.48
0.020	071.6	273.15	3.66
0.025	066.4	272.56	3.79
0.030	062.5	272.13	3.90
0.030	057.6	271.57	4.04

EXP. NO. 892 88 DROPS/CC

TIME	PRESS	TEMP	SUPR
0.005	1106.0	295.65	1.00
0.010	085.5	274.70	3.31
0.015	070.6	274.05	3.45
0.020	074.1	273.43	3.59
0.025	049.2	272.90	3.71
0.030	064.2	272.23	3.85
0.035	050.6	271.81	3.98
0.040	034.8	271.27	4.12
0.045	048.6	270.73	4.29
0.050	045.9	270.25	4.40
0.052	042.2	269.84	4.52
0.055	041.5	269.74	4.55
0.058	043.1	269.04	4.49
0.060	052.1	270.06	4.20
0.065	060.7	272.16	3.89
0.070	070.2	273.00	3.60

EXP. NO.	984	DEGRS/CC		
TIME	PRESS	TEMP	SUPR	
	1184.2	295.65	1.00	
0.005	985.5	274.63	3.32	
0.010	979.9	274.05	3.45	
0.015	974.9	272.40	3.53	
0.020	969.2	272.93	3.70	
0.025	964.5	272.34	3.85	
0.030	960.1	271.55	3.97	
0.035	955.9	271.37	4.09	
0.040	952.2	270.80	4.25	
0.045	946.4	270.20	4.39	
0.050	942.0	269.37	4.51	
0.053	941.0	269.70	4.54	
0.055	942.1	269.92	4.59	
0.060	954.0	271.16	4.15	
0.065	954.0	272.29	3.86	
0.070	970.0	272.96	3.70	

VITA

The author was born on October 5, 1940 in Forbes, Missouri, the eldest son of Mr. and Mrs. Louis B. Allen, Sr. He graduated from the Public High School in Savannah, Missouri in 1958 and entered the Missouri School of Mines where he held a Harry Kessler Scholarship for two years. He worked for the Missouri State Highway Department for a year, then reentered the Missouri School of Mines. He graduated with a B.S. in Physics in June 1963, a M.S. in Physics in June 1964 and has continued work toward the doctorate. He has held a teaching assistantship, a three year National Defense Education Act fellowship and a National Science Foundation Research Fellowship.

The author is married to the former Miss Barbara Leonard of St. Joseph, Missouri. They have three daughters, Trina, Wendy and Laura.